
THE UNIVERSITY of ADELAIDE

# Investigation of the formation and interaction of solids and renewable crude during hydrothermal liquefaction

**Md Arafat Hossain**

Thesis submitted for the degree of Doctor of Philosophy

School of Chemical Engineering
Faculty of Sciences, Engineering and Technology
The University of Adelaide, Australia

February 2024

**Table of Contents**

**Abstract**

The hydrothermal liquefaction (HTL) is a highly promising method for converting biomass into renewable crude (RNC) oil using subcritical water. Near the critical point, water exhibits unique properties such as lower viscosity and higher solubility of organic materials, making it an excellent medium for efficient and homogeneous reactions. However, during HTL, the co-products of aqueous phase, hydrochar, and gases are formed alongside the renewable crude. The solid and renewable crude mixture is challenging to separate, even with solvent extraction methods. As a result, the actual yield of renewable crude is lower than expected. The reasons for oil trapping and how experimental parameters affect product yields and oil trapping in hydrochar were not well understood.

This study aims to re-evaluate the HTL process of biomass, with a focus on the formation and interaction between solid and renewable crude. Published data were analysed to gather additional information that could shed light on the solid-renewable crude interaction. Understanding the influence of experimental parameters on product yields and the trapping of renewable crude in solids during HTL reactions is crucial. In this investigation, pure carbohydrate was chosen as the raw material. The parameters examined included temperature (260-350°C), residence time (10-25 minutes), and biomass-to-water ratio (0.25-1), which were analysed to determine their effect on the trapping of renewable crude into solids and the overall product yields.

Dichloromethane (DCM) was utilised as a solvent to identify the recovered renewable crude from the solid phase. The Source Rock Analyser (SRA) was employed to identify the light and heavy oils trapped in the solids before and after solvent extraction. The optimal conditions for higher renewable crude yields were found to be 350°C, 10 minutes residence time, and a 0.5 biomass-to-solvent ratio. However, increasing the residence time and biomass-to-water ratio resulted in decreased yields of renewable crude by 37% and 7%, respectively. Maximum

biocrude trapping in solids was observed at 320°C, and solvent extraction was able to extract up to 58% of the crude oil, with a higher extraction efficiency for light oil compared to heavy oil.

Furthermore, the study investigated the fundamental reasons behind the interaction between solid and renewable crude using a mixture of model compounds (cellulose, lignin, protein, and lipid) and real biomass (pine wood, sludge, and microalgae). Mixtures such as 50% cellulose + 50% protein, 50% cellulose + 50% lipid, 50% lignin + 50% protein, and 50% lignin + 50% lipid were prepared to ensure sufficient renewable crude production, as cellulose and lignin primarily produced solid, while lipid and protein mainly produced crude.

HTL of binary mixtures of model compounds generally resulted in higher yields of renewable crude at higher temperatures, except for cases where secondary cracking occurred, leading to decreased yields. For the cellulose (50%) and lipid (50%) mixture, 57% to 71% of RNC was trapped in the hydrochar, with maximum and minimum yields recorded at 350°C and 260°C, respectively. Similarly, the cellulose (50%) and protein (50%) mixture trapped 64% to 77% of RNC, with maximum and minimum yields observed at 290°C and 350°C. The lignin (50%) and lipid (50%) mixture trapped 64% to 77% of RNC, with maximum and minimum yields at 320°C and 260°C. Lastly, the lignin (50%) and protein (50%) mixtures trapped 60% to 66% of RNC, with maximum and minimum yields at 350°C and 260°C.

In terms of real biomass, pine wood resulted in maximum and minimum RNC yields of 14% and 8% at 320°C and 350°C, respectively, due to secondary cracking occurring at 350°C. Sludge exhibited maximum and minimum RNC yields of 20% and 14% at 350°C and 260°C, while microalgae showed maximum and minimum RNC yields of 21% and 12% at 260°C and 350°C, indicating that the secondary cracking of oil started from the beginning and resulted in decreased RNC yields at higher temperatures for microalgae. The analysis with source rock

analyser (SRA) suggested that a significant amount of RNC was trapped in the hydrochar, with 42% to 61% for pine wood, 50% to 67% for sludge, and 48% to 71% for microalgae.

During the investigation of the fundamental reasons for solid-oil interaction, it was found that the functional groups of hydrochar, acid value, wettability capability, and viscosity of the renewable crude were responsible for the interaction between solid and renewable crude.

**Declaration**

I certify that this work contains no material which has been accepted for the award of any other degree or diploma in my name, in any university or other tertiary institution and, to the best of my knowledge and belief, contains no material previously published or written by another person, except where due reference has been made in the text. In addition, I certify that no part of this work will, in the future, be used in a submission in my name, for any other degree or diploma in any university or other tertiary institution without the prior approval of the University of Adelaide and where applicable, any partner institution responsible for the joint award of this degree.

The author acknowledges that copyright of published works contained within the thesis resides with the copyright holder(s) of those works.

I give permission for the digital version of my thesis to be made available on the web, via the University's digital research repository, the Library Search and also through web search engines, unless permission has been granted by the University to restrict access for a period of time.

I acknowledge the support I have received for my research through the provision of an Australian Government Research Training Program Scholarship.

Md Arafat Hossain Date: 01/02/2024

**Acknowledgements**

The compilation of this thesis would not have been achieved without the support, guidance, instruction, advice and contribution of many people. I would like to acknowledge and thank the following people.

I would firstly like to thank my supervisors Dr Philip van Eyk, Professor David Lewis and Dr Jason Connor. I thank Dr. Philip for his constant support and always being present to help solve any problem at any time. I thank Prof. David for constantly helping me improve my work with his insightful ideas and suggestions. Dr. Philip and Prof. David also helped me a lot for the concept developments. I thank Dr Jason Connor for contributing his great knowledge and ideas in the area of hydrothermal liquefaction.

I acknowledge the support I have received for my research through the provision of an Australian Government Research Training Program Scholarship.

I would like to Dr Tony Hall from the School of Physics, Chemistry and Earth Sciences, the University of Adelaide for his assistance in the analytical techniques used during my PhD which allowed me to gather many of essential data.

I would like I would like to thank the members of the Faculty of Sciences, Engineering and Technology infrastructure team especially the members of the analytical lab for their training and ideas.

I would like to thank my fellow PhD candidates in the HTL research group, Reem Obeid, Jasim Al-Juboori, Benjamin Keiller, Sylvia Edifor, Thomas Scott, Andres Chacon Parra and Robran Cock for always being present to discuss ideas and provide support.

Finally, I owe my deepest gratitude to my parents and wife for their understanding, encouragement, affection, constant support and patience even on the most challenging time.

## Preface

This thesis has been prepared and submitted as a portfolio of publications according to the 'Specifications for Thesis 2023' of the University of Adelaide. The main body of this thesis includes four manuscripts that were prepared for publication. The four manuscripts form a series of work that focused on the HTL condition of products yields and the fundamental reason of solid-renewable crude interaction. The main body of this work contains the following manuscripts which were prepared ready for submission to appropriate journals.

1. Re-evaluation of hydrothermal liquefaction of biomass focusing on solid-biocrude formation and interaction

Md Arafat Hossain, David Lewis, Jason Connor, Philip van Eyk

2. Influence of HTL processing parameters on solid-renewable crude formation and interaction during the HTL of relevant feed focusing on carbohydrate.

Md Arafat Hossain, David Lewis, Tony Hall, Philip van Eyk

3. Investigation of the fundamental reasons of solid- Renewable crude interaction during the HTL of mixture of model compounds.

Md Arafat Hossain, David Lewis, Philip van Eyk

4. Study of the fundamental causes of solid-renewable crude interaction during the hydrothermal liquefaction of actual biomass

Md Arafat Hossain, David Lewis, Philip van Eyk

**List of Abbreviations and symbols**

| Abbreviations | Meaning | Abbreviations | Meaning |
|---|---|---|---|
| HTL | Hydrothermal liquefaction | SRA | Source rock analyser |
| TOC | Total organic carbon | vol.% | Percentage of volume |
| wt.% | Percentage of weight | $H_2$ | Hydrogen |
| $H_2O$ | Water | $N_2$ | Nitrogen |
| RNC | Renewable crude | CL50% | 50% cellulose and 50% lipid mixture |
| CP50% | 50% cellulose and 50% protein mixture | LL50% | 50% lipid and 50% lipid mixture |
| LP50% | 50% lipid and 50% protein mixture | BET | Brunauer-Emmett-Teller surface area analysis |
| FTIR | Fourier-transform infrared spectroscopy | CO | Carbon monoxide |
| $CO_2$ | Carbon dioxide | mg | Milligram |
| mL | Millilitre | HTP | Hydrothermal Process |
| HTC | Hydrothermal carbonisation | DOT | Degree of Trapping |
| AV | Acid value | TAGs | Triacylglycerides |
| DCM | Dichloromethane | FID | Ionisation Detector |
| ASTM | American Society for Testing and Materials | | |
| | | | |
| | | | |
| | | | |
| | | | |

# CHAPTER 1 - INTRODUCTION

## 1.1 Background

Global energy demand is increasing because of the growing population, industrial activity and advances in developing and developed countries. This growing energy demand mostly depends on the fossil fuels, such as petroleum, natural gas and coal. One of the significant environmental problems linked with fossil fuel use is greenhouse gas (GHGs) emissions, leading to global warming and creating problems related to climate change [1].

Biomass can be considered the most plentiful renewable energy source and can be a vital part of a sustainable future energy system. Several thermochemical processes can be applied for biomass conversion into energy. Hydrothermal liquefaction (HTL) is an effective technique for converting biomass into energy because of the wet nature of the biomass. During the HTL conversion, wet biomass can be used directly, and there is no need for drying, which can save money and time and allows for a huge amount of low-quality feedstocks in HTL [2]. HTL is also less corrosive to reactor than the other thermochemical techniques [3]. HTL is generally carried out at 370 °C and with a reaction pressure until 280 bar [4].

Water at subcritical conditions performs as both catalyst and reactant, which helps biomass conversion efficiently without using any other catalyst. A decreased dielectric constant and density of water can be found at higher temperatures and pressure, which allows high solubility in the water [5]. Though hydrochar, aqueous phase and gases are the by-products of HTL, HTL is mostly focused on producing the renewable crude produced through the several stages of the reaction, for instance, depolymerisation, decomposition and recombination [6, 7]. The renewable crude's lower oxygen ($O_2$) and nitrogen ($N_2$) content was found from and had a higher calorific value. This renewable crude can also be upgraded into fuel as transportation fuels (diesel and gasoline) and products, including aromatics, polymers, asphalt, and lubricants [8].

Several pilot plants are operating worldwide, producing renewable crude though some limitations exist [9]. In the products mixture in the HTL reactor, hydrochar and renewable crude mix together so that renewable crude cannot be extracted easily. Even the solvent extraction method cannot recover the renewable crude fully though various researchers have tested several solvents. Though researchers have investigated the multiple aspects of the HTL of biomass, including investigations of the products yields, characterisation of the products, solvent extraction and kinetics, there is no particular study which focuses on how the reaction parameters can affect the hydrochar and renewable crude interaction and the investigation of the fundamental reason of this interaction.

The principal objectives of this work are to gain insight into the hydrochar and renewable crude interaction. The work has been done in four stages. Firstly, the published data has been re-evaluated to understand the influence of processing parameters on renewable crude and hydrochar yields during HTL of different types of biomass, i.e. non-lignocellulosic and lignocellulosic biomass. The previous study also provides information that may influence hydrochar and renewable crude interaction or attachment. All the clues have been considered to find fundamental reasons for hydrochar and renewable crude interaction. Secondly, a study has been conducted to know the influence of HTL processing parameters on solid-renewable crude formation and interaction during the HTL of relevant feed focusing on carbohydrates. Thirdly, an investigation has been carried out the understanding the fundamental reasons for solid-renewable crude interaction during the HTL of mixture of model compounds. Fourthly, real biomass, i.e., pine wood, sludge and microalgae, have been considered for the investigation of fundamental reasons for solid-renewable crude interaction during the HTL.

## 1.2 Scope and structure of a thesis

Chapter 2 comprises a comprehensive literature review based on a scientific study of HTL of biomass to establish familiarity with and understanding current research in bio-energy, thermochemical process and HTL reaction. This charter aims to provide a solid background of biomass conversion through HTL, which can provide a good foundation for this topic. This chapter discusses the various aspects of biomass as a renewable energy source and the HTL of biomass. The structure of biomass has been studied, along with the advantages and disadvantages of using biomass. The reaction pathways and comparison of HTL reaction with other popular thermochemical processes have been discussed broadly. The review discusses relevant literature on HTL products and uses. Depending on the literature, the gap is identified, and the scope of the present work has been finalised.

The first journal article produced from "a study of re-evaluation of the previous data to know the effect of HTL reaction parameters on renewable crude and hydrochar yields during HTL of different types of biomass; i.e. non-lignocellulosic and lignocellulosic biomass" and it is presented in chapter 3. The other factors or properties that possibly cause the hydrophobicity (oil attraction) of the solids have been considered for re-evaluation.

In Chapter 4, the second journal article was introduced. This article discusses a study that examined how temperature, residence time, and biomass/solvent ratio affected the yields of the main products, including renewable crude, hydrochar, flue gas, and aqueous substances. Additionally, the article explored the impact of these parameters on the interaction between hydrochar and renewable crude.

In Chapter 5, the third journal article is presented, which examines the fundamental reasons for the attachment of hydrochar and renewable crude in the HTL reaction of model compounds. Specifically, the study focuses on mixtures of 50% cellulose + 50% protein, 50% cellulose + 50% lipid, 50% lignin + 50% protein, and 50% lignin + 50% lipid.

In Chapter 6, the fourth journal article is introduced, which investigates the underlying reason for the attachment of hydrochar and renewable crude during the HTL process of actual biomass, such as pine wood, sludge, and microalgae.

Chapter 7 summarises the conclusions from this body of work and recommendations for future work.

Finally, references are provided for Chapters 1, 2 and 7, while the references for Chapters 3, 4, 5 and 6 are provided in their respective journal papers.

# CHAPTER 2 – LITERATURE REVIEW

## 2.1 Introduction

hydrothermal Process (HTP) is a promising method for converting biomass into valuable products. Researchers have shown significant interest in hydrothermal Process (HTP) technology over the years due to its potential to produce renewable fuels, chemicals, and hydrochar from biomass. HTP is considered an appealing alternative to conventional fossil fuels, especially with the growing demand for sustainable energy sources. At a specific temperature and pressure, biomass and water are combined in this technique to generate gas, liquid or renewable crude, and solid products without any pre-treatment [10, 11]. HTP is considered a more suitable method than pyrolysis and gasification [12]. During the hydrothermal conversion process, there is no restriction on the moisture content of biomass. In subcritical and supercritical conditions, solubility and crystallisation occur, which eliminates challenges such as agglomeration that are typically encountered in traditional pyrolysis processes [10]. In HTP, thermal decomposition of biomass happens in water and affects the physicochemical properties of water [13]. For instance, the dielectric constant of water is decreased at high temperatures. Consequently, while organic substances are insoluble in water under normal conditions, water can act as a solvent for the organic substances. An increase in the ionic character of water can facilitate acid–base-catalysed reactions [14]. Hydrothermal Processing (HTP) can be conducted under two distinct reaction conditions: subcritical and supercritical water. These conditions are determined by the critical point of water, which is at 374°C and 22.1 MPa. The two conditions offer varying benefits in terms of target product yields, with the supercritical condition being more suitable for gas production [14].

HTP can quickly transform biomass into carbonaceous material and/or value-added chemicals under various hydrothermal conditions applied at different temperatures and pressure [15]. This conversion process can be classified into three categories according to the operating condition and target products, i.e; (1) hydrothermal carbonation (HTC) which occurs at temperature of

180 – 250 °C and produce hydrochar[16, 17], (2) hydrothermal gasification (HTG) which occurs at near-critical temperatures to around 350 to 700 °C and generates the syngas or hydrogen rich gas [10, 18, 19] and (3) HTL which occurs at temperature of 250 – 370 °C with a pressure between 4 – 20 MPa and produce Renewable crude (RNC) or bio-crude. The hydrothermal process reaction stages are depicted in Figure 2.1 which shows that hydrothermal carbonisation, liquefaction and gasification happens with a series of reaction which mainly depends on different reaction parameter like temperature and pressure.

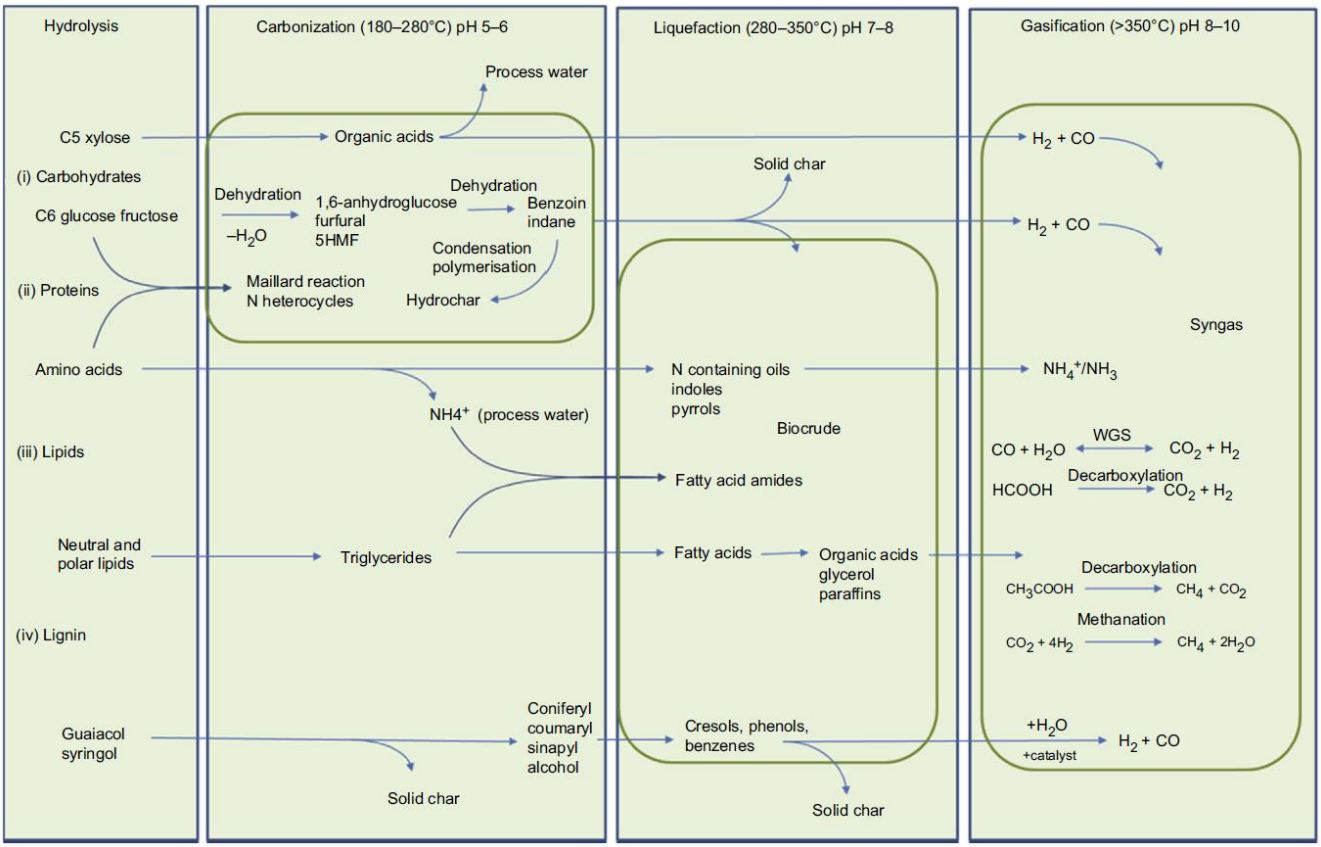


Figure 2.1: Various reaction steps of HTP. Reproduced from Biller et at [20].

## 2.2 Hydrothermal carbonisation

Hydrothermal carbonisation (HTC) is recognised as one of the alternative methods for biomass processing to get biofuel [21]. It has been carried out at a relatively lower temperature (180 – 250 °C) which produces the solid product called hydrochar [16, 17]. During the HTC, biomass is decomposed in an oxygen absence condition in the presence of subcritical water and pressure

in the range of 2 to 10 MPa [17, 22]. In other thermochemical process like pyrolysis, feedstocks with a higher moisture content produce lower amounts of char after drying. But, the main advantage of HTC is that a variety of biomass could be used for processing to produce hydrochar since drying the biomass is not compulsory for HTC [23]. However, larger particle sizes in HTC needs severe reaction conditions to reach similar carbonisation to smaller biomass particle size [20]. Therefore, the feedstock requires pre-treatment to reduce particle size for getting higher efficiency of HTC. Figure 2.2 shows the process layout of HTC. HTC utilises water as a medium for a complex sequence of reactions that involve the removal of hydroxyl groups through dehydration, the elimination of carboxyl and carbonyl groups via decarboxylation, and the cleavage of numerous ester and ether bonds via hydrolysis [20].

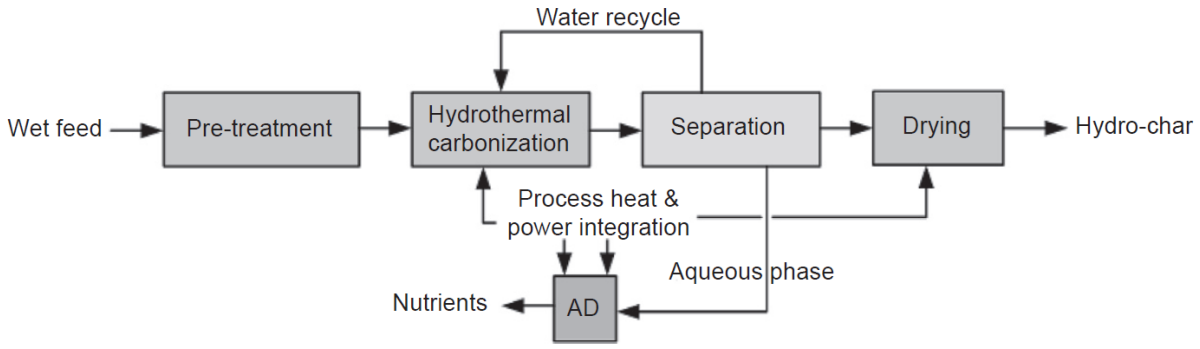


Figure 2.2. Schematic layout of hydrothermal carbonisation. Reproduced from Biller et at. [20].

Hydrothermal carbonation is mainly effective for the production of solid, coal-type products which have high carbon percentages [16]. At the lower temperature, the decomposition rate of biomass can be slow and the volatiles inside the biomass can't pass out easily. Therefore, gas formation is low and higher yield of hydrochar can be expected from the hydrothermal carbonation of biomass [24].

### 2.3 Hydrothermal gasification

Hydrothermal gasification (HTG) generally targets gaseous products. It occurs at super critical temperatures of around 350 to 700 $^{o}$C and generates syngas which includes but not limited to

$H_2$, $CH_4$, and $CO_2$ [25-28]. Thus, gasification can be employed for hydrogen ($H_2$) production since syngas contains $H_2$. An investigation into the gasification of various biomass sources can help identify which ones yield a higher proportion of $H_2$, considering that different types of biomass produce varying amounts of $H_2$. The reaction temperature is much higher in HTG. Therefore, complete decomposition of biomass occurs. This is a specific feature of HTG in comparison with other hydrothermal conversion processes [25].

The utilisation of thermal conversion processes, such as pyrolysis and also partial oxidation, for the gasification of biomass is widely recognised as a means to generate a fuel gas or synthesis gas, consisting of carbon oxides and hydrogen. Hydrothermal gasification can be conducted across various operating temperatures and pressures. Research has highlighted supercritical water as a crucial operating medium, with the supercritical condition being the predominant parameter [29].

### 2.4 Hydrothermal liquefaction process and its mechanism

Figure 2.3 shows the schematic layout of the HTL for lignocellulose. HTL is a promising conversion technique from biomass to renewable crude (RNC), that is carried out in the water at moderate temperature (250 – 370 $^{o}$C) and high pressure (4 – 20 MPa). Renewable crude is the main product together with the hydrochar, gaseous, and aqueous phase by-products [30]. The separation of phases happens spontaneously after the reaction resulting in a $CO_2$ rich gaseous phase, solid residue, aqueous phase, and renewable crude. In HTL, the process water in a reaction can be recycled to reduce the water requirements which can increase the renewable crude yield [20].

On the other hand, under elevated pressure as well as temperature, especially when it exceeds the critical point (374.3 °C and 22.1 MPa) of water, some properties like density, static dielectric constant and ion dissociation constant of water drop considerably, which accelerate

the reaction rate significantly [31]. At the supercritical condition, biomass is gasified that produces the syngas which is mainly a mixture of $H_2$, $CO_2$ and $CH_4$ [2]. Therefore, supercritical condition is not suitable for renewable crude production in HTL reaction.

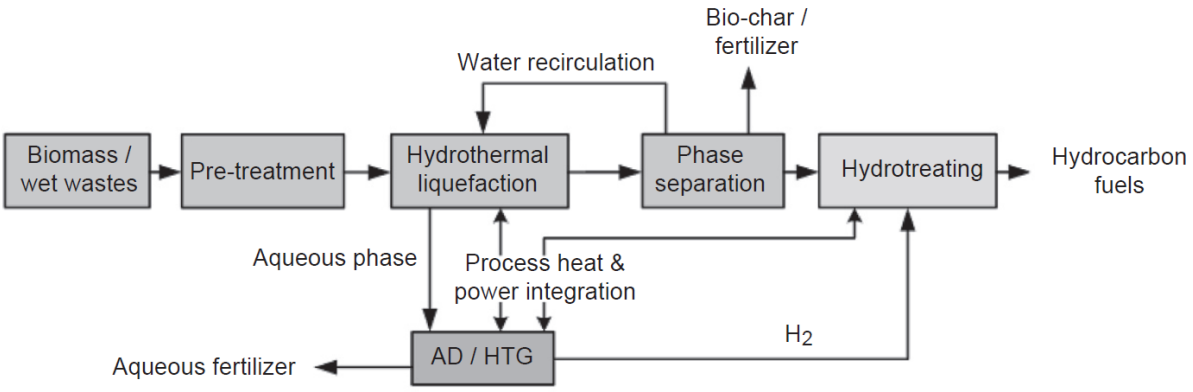


Figure 2.3. Schematic layout of the hydrothermal liquefaction of lignocellulose. Reproduced from Biller et al. [20].

Table 2.1: Properties of water at normal temperature, subcritical and supercritical conditions [2, 34-36].

| Properties | Normal water | Subcritical water | Supercritical water |
|---|---|---|---|
| Density, $\rho$ (g/cm$^3$) | 1 | 0.6 - 0.8 | 0.17 – 0.58 |
| Dielectric constant, $\varepsilon$ (F/m) | 78.5 | 14.07 – 27.1 | 5.9 – 10.5 |
| Ionic product, p$K_w$ | 14.0 | 11.2 – 12 | 11.9 – 19.4 |
| Heat capacity $C_p$ (kJ/kg K) | 4.22 | 4.86 – 10.1 | 6.8 – 13.0 |
| Dynamic viscosity, η (mPa s) | 0.89 | 0.064 – 0.11 | 0.03 – 0.07 |

Water exhibits favourable behaviour for the reaction of biomass at subcritical temperatures. It becomes an outstanding reaction medium, reactant and solvent for biomass conversion during HTL [32, 33]. In case of HTL, water can perform as a reactant and also catalyst. This makes HTL considerably different from other thermochemical techniques like pyrolysis. At conditions near the critical point, water shows some interesting properties, for instance, lower

viscosity and higher solubility of organic materials that can make the subcritical water an excellent medium for the fast, efficient and homogenous reaction [34-39]. The liquid medium (water) staying at the subcritical condition can also increase the renewable crude yield by minimising the gas and solid formation [2]. Therefore, throughout the last decade, a strong interest has grown to use subcritical water as a reaction medium or solvent for biomass conversion. Table 2.1 shows various properties of subcritical and supercritical water.

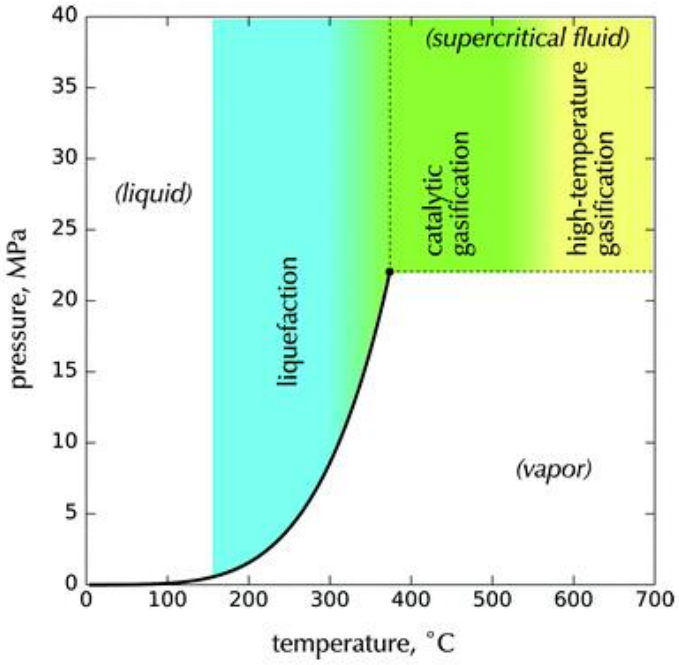


Figure 2.4: HTP in three different regions of water; i.e; properties of water in subcritical, near-critical, and supercritical conditions at 22.1 MPa. Reproduced from Petersonab et al. [19].

Several important factors need to be considered to convert a large amount of different biomass. For instance, conversion techniques can be varied depending on the biomass composition and low-quality feedstock. Effective conversion techniques should also demonstrate the capability to convert cheaply. The HTL technique has the potential to fulfill both criteria and to do so sustainably. For example, dry feed is not required for the HTL reaction, a large amount of low-quality feedstocks which also have a high moisture content can be considered for HTL reactions [40]. Therefore, appropriate use of the HTL technology can produce biofuel by

utilising biomass which can be a big contribution to the biofuel sector. The reaction pathways of HTL include three major steps, i.e; depolymerisation, decomposition and recombination [2].

### 2.4.1 Depolymerisation of the biomass

In this stage of HTL, biomass polymers transform to monomers because of entropy increase at high temperatures. Not only temperature but also high pressure alters the long chain polymers consisting of carbon, hydrogen and oxygen to shorter chain hydrocarbon [41]. Therefore, biomass depolymerisation is a significant dissolving of macromolecules through the use of their physical as well as chemical properties. The general hemicellulose and also cellulose biopolymers contribute certainly to the thermal stability of the biofuel in this stage [42].

### 2.4.2 Decomposition of the Biomass

Biomass monomers are broken down further through several mechanisms, including cleavage of chemical bonds, dehydration (elimination of water molecules), decarboxylaisation (elimination of carboxyl groups) and loss of $CO_2$ gas, and deamination which is the elimination of amine (nitrogen attaching) groups [43]. Normally Oxygen molecules are removed in form of $CO_2$ and $H_2O$ respectively. $H_2O$ at high pressure and temperature can break down the hydrogen-bonded structures of cellulose and can cause the development of glucose monomers [44].

### 2.4.3 Recombination and polymerisation of biomass

The broken monomer fragments are gone through recombination and polymerisation to make various oily products and gases, liquid and solid residues. This recombination or polymerisation is the reverse of the initial processing steps that are happening because of the unavailability of the hydrogen compound [2]. If there is hydrogen available in the organic matrix during HTL process, the free radicals can be stopped to yield a stable molecule. But, in absence of hydrogen or the concentration of free radicals are extremely large, the fragments can be recombined or repolymerised to procedure high molecular weight char compounds [45].

### 2.4.4 Comparison of Hydrothermal Liquefaction to General Pyrolysis

Hydrothermal Liquefaction and pyrolysis are two popular thermochemical conversion techniques of biomass that can produce the bio-based fuel named renewable crude or biocrude. These two technologies can be compared to picking the economically variable technology and for selection of biomass. However, significant differences can be noticed between the two conversion techniques.

Table 2.2: Comparison of HTL and General Pyrolysis for biomass conversion [2, 47, 49-51].

| | Hydrothermal Liquefaction | Pyrolysis |
|---|---|---|
| Operating Pressure (MPa) | 5-20 | 0.1-0.5 |
| Operating Temperature ($^oC$) | 250 – 370 $^oC$ | Around 500 $^oC$ |
| Drying | Not required | Required |
| Catalysts | Yes | No |
| Heating value | High (~30 MJ/Kg) | Low (~17 MJ/Kg) |
| Oxygen content | Low | High |
| Water content | Low | High |
| Viscosity (Renewable crude) | High | Low |
| Upgrade | Easy | hard |

In case of the pyrolysis process, biomass drying is required, while it is not mandatory for the HTL process which holds a great economic value for fuel production because of the wet nature of the various biomass feedstock [46]. Furthermore, the use of catalysts in pyrolysis is not common in most cases, but the solvent (water) employed in the HTL reaction acts as a catalyst in the subcritical condition. It can produce high-quality products as compared to pyrolysis products [47]. Finally, Lower oxygen and moisture contents and higher heating values can be observed in HTL products in comparison to the pyrolysis products. It reduces the fixed and operative costs of handling equipment and storage [48] which makes the HTL technology more suitable to convert biomass into fuel [47]. Yet, it can be noted that the high operating pressure

increases the investment costs in the HTL biomass conversion. Table 2 shows the comparison of HTL and general Pyrolysis.

### 2.5 Biomass Feedstock for HTL reaction

Hydrothermal conversion utilised biomass with high moisture content and can save the high cost of drying. Therefore, a wide range of biomass including wood waste, algae, agricultural residue and biosolids can be considered for HTL.

A heterogeneous mixture of organic and a small amount of inorganic substances is considered biomass. Lignocellulosic biomass refers to biomass that contains cellulose, hemicellulose, and lignin. Algae and sludge have been categorised as non-lignocellulosic biomass. Algae mostly contains lipids and proteins and sludge holds mostly inorganic substances. Therefore, cellulose, hemicellulose, lignin, lipid and protein are considered the model compounds of biomass [14]. The amount of each of the model compounds in biomass varies on various factors for example biomass, growth stage, growing conditions tissue, or preparation methods [52, 53]. Biomass holds a high oxygen content than fossil fuels. Generally, 30 - 60% carbon, 30 - 40% oxygen, and 5 - 6% hydrogen are found in biomass in dry wet. Sulfur (S), Nitrogen (N), and chlorine (Cl) make up less than 1% of the biomass and can be found in the structure of some types of biomass [53]. In order of reducing the percentage of amounts of these biomass elements, are C, O, H, N, Ca, K, Si, Mg, and Al [52]. Inorganic substances of biomass are held in the ash content. The carbohydrate portion of biomass consists of cellulose, hemicellulose and starch whereas the non-carbohydrate portion consists of lignin [54]. Carbohydrate portion, i.e, cellulose and hemicellulose are responsible for the structural and mechanical strength of the plant, while lignin, a non-carbohydrate, maintain the stability of these structures [55]. Figure 2.1 explains the various reaction steps of major compounds to form biofuel during the hydrothermal conversion techniques.

### 2.5.1 Carbohydrates

Cellulose, hemicellulose and starch are the plentiful carbohydrates in biomass. Carbohydrates undergo rapid hydrolysis to form glucose and other saccharides which further degrade to produce the biofuel. The rate of the hydrolysis reaction can vary for different carbohydrates depending on their crystalline structure [56].

#### 2.5.1.1 Cellulose

Cellulose can be considered the natural polymer which is most abundant in nature. $1.5\times10^{12}$ tons of annual production of cellulose throughout the world has been estimated each year and is considered to be an unlimited source of biomass raw material [57]. Cellulose is represented by the common formula $(C_6H_{10}O_5)_n$, which is a long chain polysaccharide with a high degree of polymerisation (approximately 10,000), and a high molecular weight (approximately 500,000) [14]. Cellulose in biomass consists of glucose units that are connected by β-(1→4)-glycosidic bonds. The formation of glucose units is in straight chains in cellulose which makes the formation of strong intra-and inter-molecule hydrogen bonds [58]. A high degree of crystallinity can be observed in cellulose. This crystallinity makes it insoluble in water and resistant to attack by enzymes. However, at subcritical conditions, cellulose is rapidly solubilised and hydrolysed to its constituents. Cellulose plays a vital role in hydrothermal conversion as it is the main component of plant cell walls and is present in most biomass, imparting mechanical strength and stability to the plant structure. The significance of cellulose lies in its potential as a sustainable and environmentally friendly substitute for fossil fuels and petroleum-based products. Figure 2.5 shows the structure of cellulose.

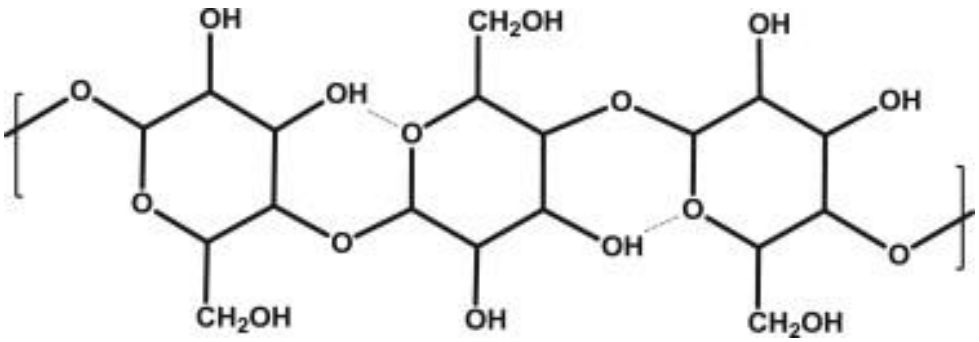


Figure 2.5: Structure of cellulose. Reproduce from Tekin et. al. [14].

### 2.5.1.2 Hemicellulose

Hemicellulose makes up 20 to 40% of dry wet of most wood species. Generally, the amounts of hemicellulose in wood and woody biomass are larger than those in agricultural and herbaceous biomass [59]. It is a heteropolymer composed of different monosaccharides including mannose, xylose, glucose and galactose [60]. All these compositions differ significantly between different plat types, for instance, grass hemicellulose is mostly consisted of xylan, whereas wood hemicelluloses consist of mannan, galactan and glucan. Because of having a less uniform structure and plenty of side-groups in hemicellulose, it has a much lower degree of crystallinity than cellulose. It makes it more unstable and degrades easily when subjected to heat treatment [14]. At a temperature above 180 °C, it is easily solubilised and hydrolysed in water and it can be hydrolysed in both acid and base-catalysed. It is also hydrolysed much faster than cellulose [56]. Figure 2.6 and 2.7 shows the basic constituents of hemicellulose and the structure of xylan (a typical hemicellulose) respectively.

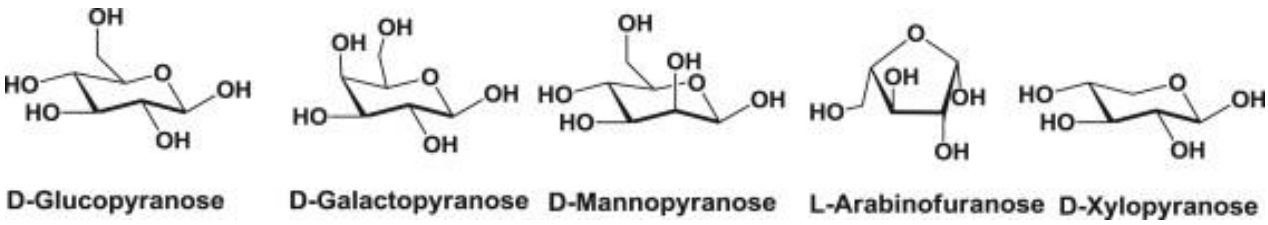


Figure 2.6: Basic constituents of hemicellulose. Reproduced from Tekin et. al. [14].

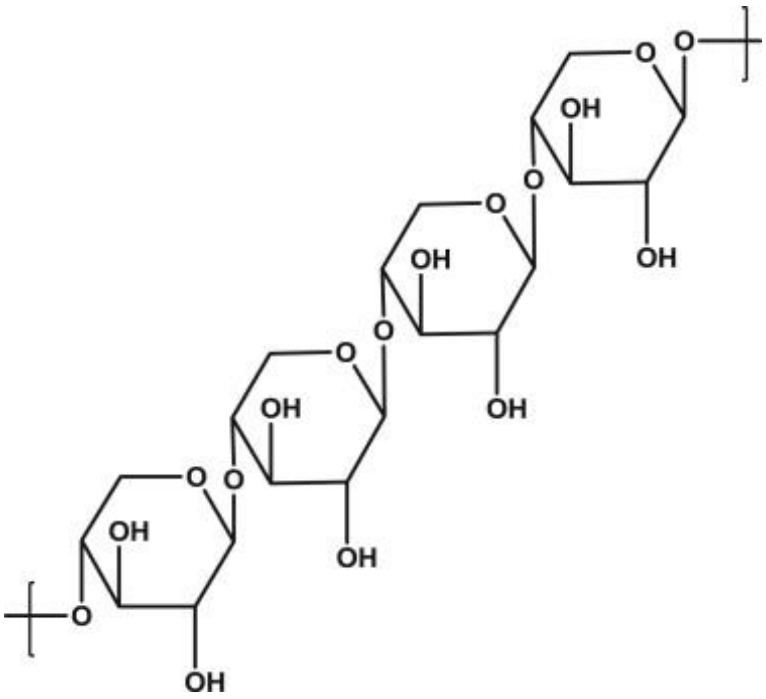


Figure 2.7: Molecular structure of xylan. Reproduced from Tekin et. al. [14].

#### 2.5.1.3 Starch

Starch is another major biomass component, which is a polysaccharide consisting of glucose monomers connected with β-(1→4) and α-(1→6) bonds [19]. In contrast to cellulose, starch can consist of a linear structure and a more branched structure. Starch is also relatively more hydrolysed than cellulose [56].

### 2.5.2 Lignin

Lignin is in common with cellulose and hemicellulose and the main component of plant biomass. It is an aromatic heteropolymer consisting of p-hydroxyphenylpropanoid units held together by C–C or C–O–C bonds. Lignin is found 18 to 25% in hardwoods and 25 to 35% in softwoods [61]. Lignin's solubility in water is very low. It is a hydrophobic and amorphous material. It assists to strengthen their structure, control the flow of fluids, and defend against the micro-organisms and stock energy in biomass on plants [61, 62]. It is comparatively resistant to chemical and enzymatic decomposition [60]. It is also thought to be relatively intact at low temperatures but starts to degrade at higher temperatures (above 250 $^{o}$C) [20].

Hydrothermal conversion techniques especially HTC and HTL of lignin produce a significant amount of solid products called hydrochar. Figure 2.8 and 2.9 shows the basic monomers and Structure of a sample fraction of lignin respectively.

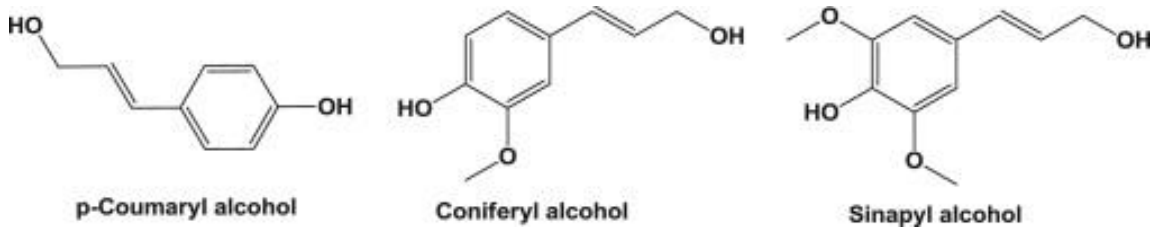


Figure 2.8: Basic monomers of lignin. Reproduced from Tekin et. al. [14].

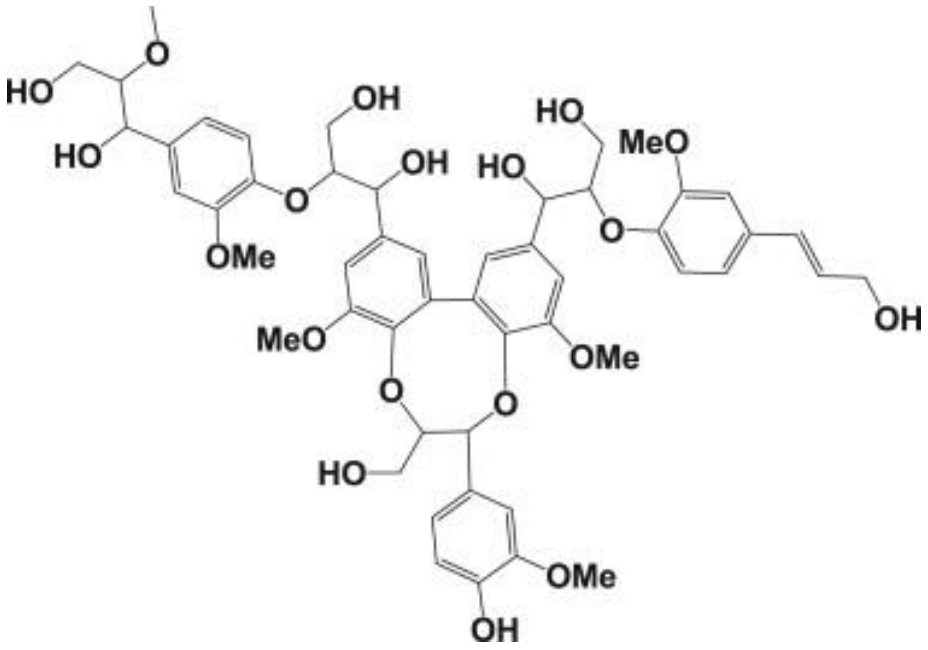


Figure 2.9: Structure of a sample fraction of lignin. Reproduced from Tekin et. al. [14].

### 2.5.3 Lipid

Lipid contains a group of naturally occurring molecules which include fats and oils. These fats and oils are nonpolar compounds with mostly aliphatic character. They are known as triacylglycerides (TAGs), i.e.; triesters of fatty acids and glycerol. In case of HTC and HTL, the dielectric constant of water is pointedly lower at the subcritical conditions, allowing greater miscibility [19, 63]. TAGs are willingly hydrolysed in hot compressed water and catalysts are

not required. On the other hand, the produced free fatty acids are relatively stable in subcritical water [56]. Lipids are also almost completely fractionated to the produced renewable crude as fatty acids and alkanes [20]. During the hydrolysis of triglyceride, glycerol is found as one of the products. Therefore, it is one of the major co-products of bio-diesel production. Glycerol can't be converted to an oily phase during HTL reaction, but rather to water-soluble compounds. Therefore, only glycerol is not an appropriate substrate for hydrothermal production of renewable crude or bio-oil [56].

### 2.5.4 Protein

Proteins are also considered major biomass constituents, found mostly in animal and microbial biomass. Proteins are composed of one or many peptide chains. The structural blocks of protein link the amino acids together in peptide bond and also amide bond between the carboxyl and amine groups of the amino acids. The bonds in a peptide of proteins are found to be more firm than bonds in glycosidic in cellulose and starch, and consequently, only slow hydrolysis happens below the temperature of 230 °C. A significant fraction of nitrogen (N) can be found in proteins that normally be included in renewable crude in HTL process and also affects various properties like smell [56]. The glycosidic bonds in starch and cellulose are less stable than the peptide bonds of proteins [13, 64]. The amino acids represent the main structure of proteins; however, they are heterogeneous [44].

## 2.6 Biomass composition

Several elements make biomass more unique to consider it as a feedstock to produce bio based fuels. Carbon (C) and Hydrogen (H) are the major elements that create a long chain to make the biomass compound. This long chain also holds the Nitrogen (N), Sulphur (S) and Oxygen (O) [44].

### 2.6.1 Carbon

Carbon (C) is considered the most important element of biomass. During Photosynthesis, atmospheric $CO_2$ becomes a part of the plant. This carbon represents the key contribution to the overall heating value [44]. Normally the heat converts this carbon into $CO_2$ which is also discharged into the atmosphere [65]. Normally, the carbon content of biofuel is assessed via the composition of lignin, hemicellulose and cellulose respectively. Such as the more lignin content the biomass has, it can produce more char during the thermochemical reaction. The carbon content can normally vary from 27 to 76 wt% depending on the various biomass [44].

### 2.6.2 Hydrogen

Hydrogen ($H_2$) is considered another key constitute of biomass that can be estimated from the chemical structure of carbohydrate and phenolic polymers. During the thermal conversion, it is converted into $H_2O$ which contributes to the overall heating value [66]. The hydrogen weight content is a little lower in herbaceous biomass (5.5 to 6 wt%) than the woody biomass (6 to 8 wt%) on a dry basis [44].

### 2.6.3 Nitrogen

Nitrogen (N) is the key nutrient form for plants. It is the vital constitute that accelerates the growth and yield of the plants. Sometimes, Nitrogen is externally used in plants for growth. Some plants get nitrogen directly from the atmosphere. Nitrogen is also a crucial component of proteins; consequently, algae and other high-protein biomass will exhibit a high nitrogen concentration. In the present agricultural era, a higher amount of nitrogen is applied to herbaceous biomass. Therefore, herbaceous biomass species obtain a higher amount of nitrogen ranging from 0.4 to 1.0 wt% (dry basis) compared to any woody biomass [67]. Nitrogen present in the biomass does not oxidise during the thermal conversion and therefore it contributes to the overall heating values.

### 2.6.4 Sulphur

Sulphur (S) is also considered one of the nutrients in the structure and of proteins, amino acids and enzymes for substantial plant growth. The higher growth rate of many herbaceous plants indicates that the concentration of sulphur is naturally higher than the woody biomass. The woody biomass can have the sulphur concentration as low as 0% (that generally means that it is below the detection level of most laboratory devices) and can reach up to 0.1% on a dry basis in exceptional cases. 0 to 0.2% or even higher sulphur concentration can be noticed in herbaceous plants [68].

### 2.6.5 Oxygen

Oxygen ($O_2$) organises the vital elements in the chemical composition of any biomass which is obvious from nature through the photosynthetic process. The concentration of oxygen in biomass controls the heating value of bio-crude that can be found via any thermal processing techniques [69]. Most of the Bio-crudes are limited to use due to the excess oxygen concentration. It is obvious that oxygen concentration in the structure of the phenolic compound is complex enough to break into the form of water which can increase the heating values.

## 2.7 Reaction pathways for hydrothermal liquefaction of biomass

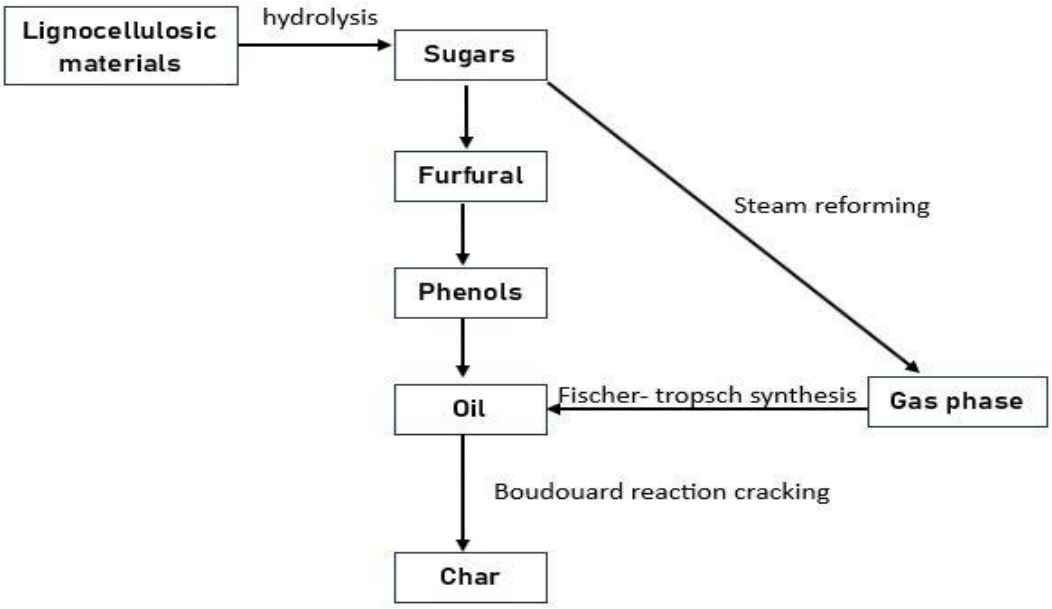


Figure 2.10: Reaction pathways of lignocellulosic biomass. Adapted from Toor et. al. [56].

Figure 2.10 shows the reaction pathways of lignocellulosic biomass. As biomass mainly holds a significant amount of cellulose, hemicellulose and lignin, these are of main attention to understanding the degradation. At the high pressure and temperature in HTL, water establishes a reaction media and because of reaching the critical point, the auto-dissociation of water (reaction 1) is considered [56].

$H_2O \rightarrow H^+ + OH^-$ (1)

The auto-dissociation of water at the critical point is almost 3 orders of magnitude higher than that at ambient conditions [27]. This indicates that an increased number of ions from $H_2O$ makes the acid and base-catalysed reactions.

The higher HTL temperature in the process increases the thermal cracking. Hydrochar can be formed from the thermal cracking of the reaction (reaction 2) or Boudouard reactions (reactions 3 and 4) [56].

$C_nH_{2n} \rightarrow C_n + nH_n$ (2)

$2CO \rightarrow CO_2$ (3)

$CH_4 \rightarrow C + 2H_2$ (4)

Reactions 5 to 7 are the steam reforming reactions where hydrocarbons are converted to hydrogen. Reaction 6 also indicates the water-gas shift as reaction. These reactions are usually found at high temperatures [27, 70]. Therefore, they are considered in HTL process [56].

$C_nH_m + nH_2O \rightarrow nCO + (n + m/2)\ H_2$ (5)

$CO + H_2O \rightarrow CO_2 + H_2$ (6)

$CO + 3H_2 \rightarrow CH_4 + H_2O$ (7)

During the processing of a higher amount of hydrocarbons or biomass, CO formation increases by following the reaction 5. This also can increase the hydrochar yields through the Boudouard reactions (reaction 3) which are by observations in steam reforming [70]. Hydrolysis, hydrogenation and decarboxylation are considered with reactions 8, 9 and 10. During the HTL of lipids, hydrolysis is of interest as this is part of the transesterification of lipids into carboxylic acids [56].

$R_1{-}O{-}R_2{+}H_2\ O \rightarrow R_1{-}OH{+}R_2{-}OH$ (8)

$H_2C = CH_2 + H_2 \rightarrow H_3C{-}CH_3$ (9)

$R - COOH \rightarrow RH + CO_2$ (10)

These reactions can also lead to alcohol and $CO_2$ formation. The hydrogenation reaction is possible to happen because of the formation of hydrogen from the steam reforming reactions and thermal cracking [56].

Fischer-Tropsch process can occur because of the formation of a larger amount of hydrogen and CO. Fischer–Tropsch process is a group of chemical reactions which converts a mixture

of CO and $H_2$ or water gas into liquid hydrocarbons like renewable crude. Through reaction 11, $H_2$ and CO react to form the alkanes and water.

$$nCO + (2n+1)\,H_2 \rightarrow C_nH_{(2n+2)} + nH_2O \quad (11)$$

It is noted that HTL is not a Fischer-Tropsch process though it can happen in HTL reaction. Other aspects of the HTL reaction are that furfurals can be formed from sugars of hydrolysed cellulose. It is possible that furfurals are produced and it can subsequently be converted into phenols and higher molecular weight components at below critical temperature [71, 72]. But this cannot occur at supercritical temperature (gasification) where radical reactions dominate and promote gas production [56, 71]. As lignin contains the structure of a significant amount of benzene rings, it can produce a large number of aromatics during HTL [56]. The hydrolysis of lignocellulosic biomass can produce a larger amount of sugars which can either remain or be converted into renewable crude via thermal decomposition and cracking or through the formation of furfurals and phenols (Figure 2.10).

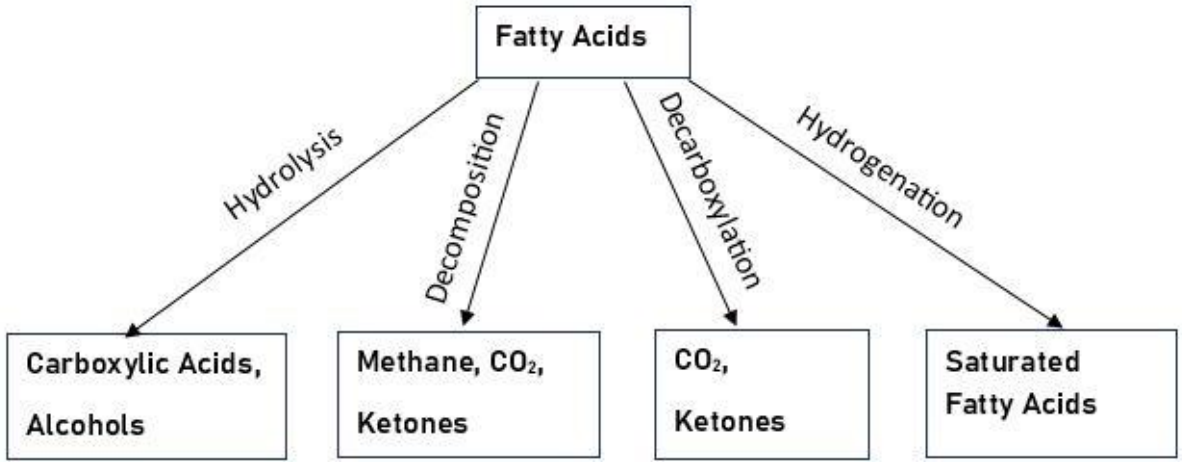


Figure 2.11: Reaction pathways of fatty acid. Adapted from Toor et. al. [56].

Besides the lignocellulosic biomass, conversion of lipid through HTL should be considered. Figure 2.11 demonstrated the possibilities when fatty acids are converted via HTL reaction. In the case of hydrolysis of triglycerides, the ether bonds are likely to form glycerol and free fatty acids. Decarboxylation reactions assist to produce some $CO_2$ and ketones while hydrogenation can saturate any unsaturated bonds in the molecule. Finally, there is a chance of simple thermal decomposition which can produce $CO_2$, methane and possibly some ketones.

### 2.8 Importance of renewable crude produced from HTL

Renewable crude (RNC) or renewable crude is considered a liquid fuel which is described as the solubilised fraction of biomass after subcritical water treatment in HTL [73]. It is a promising substitution for fossil fuel which can be produced from HTL treatment of biomass. It can be used as a substitution for conventional fuels after it is upgraded [74] as RNC has a higher heating value (HHV) and has a considerable percentage of C, H, O and S. Biomass conversion through HTL is focused on the RNC production as the other hydrothermal conversion techniques produce gas or hydrochar. Renewable crude (RNC) has close properties to petroleum and oxygen from biomass contributes chemical functionality to the RNC. Therefore, RNC is relatively stable over time and when exposed to moderate temperature [75].

The various chemical composition of renewable crude (RNC) can affect the economic value, combustion performance, upgrading response and storage stability [76]. RNC generally contains various chemical compounds including carboxylic acids, nitrogenous ring structures, aromatics and phenolic derivatives, straight and branched aliphatic compounds and esters [77-81]. The class of chemical compounds found in RNC is influenced by the ratio of lipid, carbohydrates and protein fraction of the biomass feed [81]. Renewable crude oils are frequently characterised by high heteroatom contents. These heteroatom contents are primarily found in the form of oxygenated and nitrogenous compounds. The high heteroatom content is the key distinguishing feature separating RNC from petroleum [19, 76, 82] and causes in

unwanted RNC qualities for instance acidity, higher viscosity, polymerisation and high-boiling distribution [83, 84]. Therefore, the RNC needs to be upgraded before the use. C, H, N, O and S contribute on the energy value of the RNC as the percentage of C and H seem to be higher in the RNC. Table 3 presents the Elemental composition of renewable crude including the HHV from HTL of different biomass.

Table 2.3: Elemental composition of renewable crude from HTL of different biomass.

| **S.N** | ***HTL Feedstock*** | **Elemental composition of RNC after HTL** | | | | | | | | **Ref.** |
|---|---|---|---|---|---|---|---|---|---|---|
| | | **C (%)** | **H (%)** | **N (%)** | **O (%)** | **S (%)** | **Ash (%)** | **HHV** | **% Yield** | |
| 1 | *Nannochloropsis Salina* | 55.16 | 6.87 | 2.73 | 33.97 | 1.27 | 2.48 | 25.4 | | [85] |
| 2 | *Spirulina algae* | 68.9 | 8.9 | 6.5 | 14.9 | 0.86 | – | 33.2 | 32.6 | [84] |
| 3 | *Swine manure* | 71.2 | 9.5 | 3.7 | 15.6 | 0.12 | – | 34.7 | 30.2 | [84] |
| 4 | *Anaerobic sludge* | 66.6 | 9.2 | 4.3 | 18.9 | 0.97 | – | 32 | 9.4 | [84] |
| 5 | *Arthrospira platensis* | 74.5 | 10.2 | 6.8 | 7.5 | 1 | – | 38.65 | 30 | [86] |
| 6 | *Tetraselmis* | 71.4 | 9.5 | 5.7 | 12.3 | 1.1 | – | 35.58 | 29 | |
| 7 | *Nannochloropsis gaditana* | 76.1 | 10.3 | 4.5 | 8.8 | 0.4 | – | 38 | | [87] |
| 8 | *Scenedesmus almeriensis* | 74.9 | 9.1 | 5.9 | 9.6 | 0.7 | – | 36.2 | | [87] |
| 9 | *Nannochloropsis Sp* | 77.2 | 9.9 | 4.7 | 8.2 | 0.5 | – | 39 | | [87] |
| 10 | *Almeriansis* | 73.2 | 9.3 | 5.1 | 0.8 | 11.7 | 35.8 | – | 42.6 | [87] |
| 11 | *Gaditana* | 74.2 | 9.3 | 4 | 0.6 | 11.8 | 36.2 | – | 50.8 | [87] |
| 12 | *Nannochloropsis Oceana* | 77.6 | 4.9 | 3.4 | – | 0.3 | – | 37.7 | 54.2 | [88] |
| 13 | *Derbesia* | 73 | 7.5 | 6.5 | 10.6 | 0.7 | – | 33.2 | | [89] |
| 14 | *Ulva* | 72.6 | 8.2 | 5.8 | 11 | 0.4 | – | 33.8 | | [89] |
| 15 | *Chaetomorpha* | 70.9 | 7.7 | 6.8 | 11.4 | 0.1 | – | 32.5 | | [89] |
| 16 | *Cladophora* | 71.6 | 8 | 7.1 | 10.6 | 0.9 | – | 33.3 | | [89] |
| 17 | *Oedogonium* | 72.1 | 8.1 | 6.3 | 10.4 | 1.3 | – | 33.7 | | [89] |
| 18 | *Cladophora FW* | 71.1 | 8.3 | 6.8 | 10.6 | 1.3 | – | 33.5 | | [89] |
| 19 | *Aspen wood* | 75.2 | 8.2 | 0.5 | 15.8 | 0.3 | 0.48 | 34.3 | | [90] |
| 20 | *Scenedesmus* | 72.6 | 9 | 6.5 | 10.5 | 1.35 | – | 35.5 | | [91] |
| 21 | *Defatted scene* | 72.2 | 8.9 | 7.8 | 10.5 | 0.9 | – | 35.3 | | [91] |
| 22 | *Spirulina* | 72.2 | 9.1 | 8.1 | 9.2 | 1.41 | – | 35.8 | | [91] |
| 23 | *Nutrient depleted Oedogonium* | 65.8 | 8.5 | 1.5 | 18.3 | – | – | | | [92] |
| 24 | *Spent coffee grounds* | 71.2 | 7.1 | 3 | 18.7 | – | – | 31 | | [93] |
| 25 | *Pinus* | 60.1 | 6 | 1.2 | 32.7 | 0.1 | – | 23.1 | | [94] |
| 26 | *Cupressus funebris* | 62 | 6.6 | 1.6 | 29.8 | 0.1 | – | 25.1 | | [94] |
| 27 | *Platanus* | 70 | 6.3 | 0.7 | 23 | 0.01 | – | 28.6 | | [94] |

| S.N | *HTL Feedstock* | Elemental composition of RNC after HTL | | | | | | | | Ref. |
|---|---|---|---|---|---|---|---|---|---|---|
| | | C (%) | H (%) | N (%) | O (%) | S (%) | Ash (%) | HHV | % Yield | |
| 28 | *Cinnamomum Camphora* | 74 | 8.4 | 1.5 | 16.1 | 0.01 | – | 34.2 | | [94] |
| 29 | *Pittosporum tobira* | 71 | 8.5 | 1.5 | 19 | 0.01 | – | 32.9 | | [94] |
| 30 | *Distylium racemosum* | 64.1 | 6.8 | 0.7 | 28.4 | 0.01 | – | 26.3 | | [94] |
| 31 | *Viburnum odoratissimum* | 71.7 | 8.1 | 1.2 | 19 | 0.01 | – | 32.5 | | [94] |
| 32 | *Salix alba* | 73.7 | 9.2 | 3.1 | 14.1 | 0.01 | – | 35.6 | | [94] |
| 33 | *Algal waste of Indiana polis* | 71.4 | 8.36 | 4.92 | 15.4 | – | – | 33.3 | | [95] |
| 34 | *Swine manure* | 71 | 8.9 | 4.1 | 0.21 | 14.2 | 35 | – | 61 | [2] |
| 35 | *Garbage* | 73.6 | 9.1 | 4.6 | | 12.7 | 36 | – | 21 | [2] |
| 36 | *Indonesian biomass residue* | 67–80 | 6–8 | 0–2 | | 11–23 | 30 | – | 21–36 | [2] |
| 37 | *Sawdust, rice husk, lignin* | | | | | | – | – | 8 | [2] |
| 38 | *Beech wood* | 76.7 | 7.1 | 0.1 | | 16.1 | 34.9 | – | 28 | [2] |
| 39 | *Phytomass* | 76.6 | 7.6 | 2.1 | 0.1 | 13.6 | – | – | | [2] |
| 40 | *Algae Dunaliella tertiolecta* | 63.55 | 7.66 | 3.71 | | 25.8 | 30.7 | – | 25.8 | [2] |
| 41 | *Porphyridium* | 66–83 | 5–11 | 0–12 | 0–1 | 8–27 | 22.8–36.9 | – | 5–25 | [2] |
| 42 | *Nannochloropsis* | 51 | 7 | 9 | 0.6 | 28.8 | | – | 46 | [96] |
| 43 | *Acid mine drainage* | 68.8 | 7.9 | 7.1 | | | – | 29.7 | | [97] |
| 44 | *Cyanobacteria sp.* | 76.02 | 9.1 | 6.29 | 7.44 | 1.15 | – | 36.51 | | [98] |
| 45 | *Bacillariophyta sp.* | 76.09 | 9.11 | 5.6 | 8.28 | 0.92 | – | 36.45 | | |
| 46 | *Seaweed* | 75.54 | 9.16 | 3.65 | 11.66 | 0.62 | – | 35.97 | | [99] |
| 47 | *L.digitata* | 70.5 | 7.8 | 4 | 17 | 0.7 | – | 32 | 17.6 | [100] |
| 48 | *L.hyperbore* | 72.8 | 7.7 | 3.7 | 14.9 | 0.8 | – | 33 | 9.8 | [100] |
| 49 | *L.saccharina* | 74.5 | 7.9 | 3 | 14 | 0.6 | – | 33.9 | 13 | [100] |
| 50 | *A.esculenta* | 73.8 | 8 | 3.8 | 14 | 0.8 | – | 33.8 | 17.8 | [100] |
| 51 | *L.Saccharina* | 31.3 | 3.7 | 2.4 | 26.3 | 0.7 | 24.2 | 12 | | [100] |
| 52 | *Taihu cyanophyta* | 77.3 | 12.08 | 1.1 | 9.01 | | – | 41.73 | | [101] |
| 53 | *Pond water algae biomass* | 46.09 | 6.22 | 9.7 | 37.35 | 0.64 | | | | [102] |
| 54 | *Spirulina* | 48.1 | 6.97 | 10.14 | 34.13 | 0.66 | | | | [102] |
| 55 | *Chlorella* | 51.33 | 7.9 | 9.8 | 30.38 | 0.59 | | | | [102] |
| 56 | *Pond water algae oil* | 59.94 | 11.57 | 0.11 | 28.37 | 0.31 | | | | [102] |
| 57 | *Spirulina oil* | 66.73 | 12.4 | 0.5 | 20.21 | 0.16 | | | | [102] |
| 58 | *Almeriensis* | 41.78 | 6.81 | 7.94 | 42.93 | 0.55 | 14.5 | 17.6 | | [103] |
| 59 | *U.fasciata* | 25.64 | 5.75 | 3.13 | | 5.52 | 16 | | | [104] |
| 60 | *E.grandis* | 47.19 | 5.77 | 0.21 | 46.59 | 0.24 | 0.09 | 18.07 | | [105] |
| 61 | *Dunaliella tertiolecta* | 53.3 | 5.2 | 9.8 | 31.7 | – | | 19.8 | | [106] |
| 62 | *Chlorella vulgaris* | 52.6 | 7.1 | 8.2 | 32.2 | 0.5 | | 23.2 | | [81] |
| 63 | *Nannochloropsis oculata* | 57.8 | 8 | 8.6 | 25.7 | – | | 17.9 | | [81] |

| S.N | *HTL Feedstock* | Elemental composition of RNC after HTL | | | | | | | | Ref. |
|---|---|---|---|---|---|---|---|---|---|---|
| | | C (%) | H (%) | N (%) | O (%) | S (%) | Ash (%) | HHV | % Yield | |
| 64 | *Fucus vesiculosus* | 32.88 | 4.77 | 2.53 | 35.63 | 2.44 | 11.8 | 15 | | [107] |
| 65 | *Chorda filum* | 39.14 | 4.69 | 1.42 | 37.23 | 1.62 | 9.9 | 15.55 | | [107] |
| 66 | *Laminaria digitata* | 31.59 | 4.85 | 0.9 | 34.16 | 2.44 | 10 | 17.6 | | [107] |
| 67 | *Fucus Serratus* | 33.5 | 4.78 | 2.39 | 34.44 | 1.31 | 18.6 | 16.66 | | [107] |
| 68 | *Laminaria hyperborea* | 34.97 | 5.31 | 1.12 | 35.09 | 2.06 | 11.2 | 16.54 | | [107] |
| 69 | *Macrocystis pyrifera* | 27.3 | 4.08 | 2.03 | 34.8 | 1.89 | 18.5 | 16 | | [107] |
| 70 | *Miscanthus* | 46.32 | 5.58 | 0.56 | 41.79 | 0.2 | 2.1 | 19.08 | | [107] |
| 71 | *Synechococcus/Anabaena* | 42.78 | 7.74 | 7.91 | | | 38.1 | 9.61 | | [108] |
| 72 | *Synechocystis* | 46.12 | 7.98 | 3.52 | | | 11.2 | 15.37 | | [108] |
| 73 | *Chlorella.sp* | 47.54 | 7.1 | 6.73 | 38.63 | | 5.93 | 18.59 | | [109] |
| 74 | *E.prolifera* | 35.2 | 5.2 | 2.1 | 32.98 | | 15.91 | 13.4 | | [110] |
| 75 | *Datura Stramonium L* | 43.55 | 5.98 | 0.77 | 49.7 | | 6.38 | 14.39 | | [111] |
| 76 | *E.Spectabilis* | 39.27 | 6.54 | 1.28 | 52.91 | | 4.6 | 13.17 | | [112] |

## 2.9 Renewable crude extraction from hydrothermal liquefaction of biomass

The renewable crude (RNC) produced from HTL of biomass stays with the hydrochar in a way that it is really difficult to extract the RNC if no solvent is used. Gaseous products from HTL can be released or collected in a bag according to the desired study [113]. Extraction of RNC with solvents includes several techniques or steps. Generally, the reactor is washed properly (twice) with extraction solvent, confirming that all the components are extracted. The whole mixture, consisting of solvent extracts, solid residue, and aqueous phase are put in the beaker and are separated using filter paper with a funnel. After filtration, the solid residue and the filter paper are dried in an oven to get the hydrochar [114].

During the solvent extraction of RNC, RNC is called the water-insoluble portion extracted using the given extraction agent. The aqueous phase is defined as the water-soluble portion that passed through the filter [113]. Water insoluble portions can be separated in different ways; i.e, using a pipette or separation funnel. This insoluble portion is then put in the oven at a certain temperature (depending on the solvent) so that solvent can be vaporised and only RNC was found.

## 2.10 Method selection

In this study, no statistical analysis has been conducted since the primary focus is on finding the fundamental reasons behind the attachment of hydrochar and renewable crude. The study of these fundamental reasons involves analysing the properties of hydrochar and solids. Conducting experiments with more than two repetitions posed a significant challenge due to the multitude of samples, model compound and their mixtures, several real biomass, renewable crude extraction with and without solvent involved in this study. The experiments also took into account a comprehensive range of parameters, including temperature (260-350 $^{o}$C), residence time (10-25 minutes), and biomass/water ratio (0.25-1). Given the specific emphasis on understanding the attachment mechanisms, the HTL experiment for every condition was limited to only two repetitions.

Our primary goal was to generate samples that could pinpoint the specific conditions associated with lower and higher trapping of renewable crude (RNC) in solids. In the following step, we conducted an analysis of the characteristics of hydrochar and renewable crude (RNC).

By employing Source Rock Analyser (SRA), this study identified conditions associated with lower and higher trapping of renewable crude in hydrochar. The subsequent stage of the research involved a detailed analysis of the properties of hydrochar and renewable crude under these specific conditions (lower and higher trapping) to identify the fundamental reasons behind the attachments.

Due to the small sample size of only two repetitions, the statistical findings have the risk of error and might not accurately represent the entire population [115]. Therefore, this limitation can result in less stable and less accurate estimates of population parameters. For instance, when dealing with only two sets of data, the mean and median values will be identical, making it challenging to detect true effects or differences. Despite these limitations, the standard

deviation has been represented on the graph as an error bar, providing a visual representation of the variability in the data.

Statistical analysis typically focuses on assessing the variability within a sample population, identifying trends, and determining the significance of differences in replicated results. However, these objectives do not align with the primary focus of our study. As our emphasis lies in understanding the conditions affecting the attachment of RNC in solids, statistical analysis has not been incorporated into this research.

### 2.11 Implication of the current study

HTL of biomass has been widely studied to produce renewable crude (RNC), although other products (such gaseous products, hydrochar and aqueous phase) are also generated during the conversion. The aqueous phase is easy to separate as it makes a distinct layer in the mixture of the products. But RNC and hydrochar stay in a way that it is difficult to extract the whole RNC from hydrochar. The hydrochar obtained from HTL is hydrophobic, i.e, attracts the oil (RNC) which makes the mixture attach. Polar groups destruction of biomass (generally –OH and –COO–) during the HTL reaction reduces the ability of products to attract water by hydrogen bonding, making it hydrophobic [69]. As the researchers used different solvents to extract the crude, they were able to extract a portion of RNC from hydrochar. This solid oil interaction can very depend on various factors and properties. Therefore, the challenge was to extract the RNC from the RNC and hydrochar mixture. The solvent extraction process can extract some RNC. Different solvents can result the different RNC yields. Most of the RNC can still be trapped in hydrochar. During the comparison of acetone, dichloromethane, and toluene as a solvent, dichloromethane results higher RNC yields for *Chlorella* sp., acetone results higher RNC yields for *Enteromorpha* pr., and toluene results higher RNC yields for *Nannochloropsis* sp. [113]. Therefore, different solvents can be beneficial for different biomass for RNC extraction. Knowing the reasons of RNC and hydrochar attachment can be helpful in a way

that the reason for the solid-RNC attachment can be eliminated to extract more RNC. But there is no particular study that focuses on the investigation of the fundamental reasons of solid-RNC interaction during the HTL of biomass. Based on the above limitation, the thesis is focused on the formation of the products along with investigation of the fundamental reasons of the interaction of RNC and hydrochar.

### 2.12 Objectives of the thesis

This study aims to investigate the influence of experimental parameters and the fundamental reasons of hydrochar and renewable crude interaction and product yields for model compounds and real biomass. These aims have been achieved by completing the following objectives.

1. Re-evaluation of published data to investigate the solid-renewable crude formation and interaction.
2. To investigate the influence of HTL processing parameters on solid- renewable crude formation and interaction during the HTL of relevant feed focusing on the carbohydrate.
3. To investigate the fundamental reasons of solid renewable crude interaction during HTL of the model compound mixture.
4. To investigate the fundamental reasons of solid renewable crude interaction during HTL of real biomass (pine wood, microalgae and sludge).

# Chapter 3: Re-evaluation of hydrothermal liquefaction of biomass focusing on solid-renewable crude formation and interaction.

# Statement of Authorship

| | |
|---|---|
| Title of Paper | Re-evaluation of hydrothermal liquefaction of biomass focusing on solid-renewable crude formation and interaction |
| Publication Status | ☐ Published ☐ Accepted for Publication ☐ Submitted for Publication ☑ Unpublished and Unsubmitted work written in manuscript style |
| Publication Details | |

## Principal Author

| | |
|---|---|
| Name of Principal Author (Candidate) | Md Arafat Hossain |
| Contribution to the Paper | Concept developments<br>Gathering and re-evaluating the published data<br>Method developments for analysis of the data<br>Drafting the manuscript |
| Overall percentage (%) | 80 % |
| Certification: | This paper reports on original research I conducted during the period of my Higher Degree by Research candidature and is not subject to any obligations or contractual agreements with a third party that would constrain its inclusion in this thesis. I am the primary author of this paper. |
| Signature | Date 14/07/2023 |

## Co-Author Contributions

By signing the Statement of Authorship, each author certifies that:

i. the candidate's stated contribution to the publication is accurate (as detailed above);

ii. permission is granted for the candidate in include the publication in the thesis; and

iii. the sum of all co-author contributions is equal to 100% less the candidate's stated contribution.

| | |
|---|---|
| Name of Co-Author | David Lewis |
| Contribution to the Paper | Concept developments<br>Assistance with the re-evaluation and reviewing the manuscript<br>Supervise the overall work |
| Signature | Date 19/7/2023 |

| | |
|---|---|
| Name of Co-Author | Jason Connor |
| Contribution to the Paper | Concept developments<br>Assistance with the data collection<br>Assistance with the re-evaluation and reviewing the manuscript<br>Supervise the overall work |
| Signature | Date 30/8/22 |

Please cut and paste additional co-author panels here as required.

| | | | |
|---|---|---|---|
| Name of Co-Author | Philip van Eyk | | |
| Contribution to the Paper | Concept developments<br>Assistance with the data collection<br>Assistance with the re-evaluation and reviewing the manuscript<br>Supervise the overall work | | |
| Signature | | Date | 18/7/2023 |

# Re-evaluation of hydrothermal liquefaction of biomass focusing on solid-renewable crude formation and interaction

[a]Md Arafat Hossain, [a]David Lewis, [b]Jason Connor, [a]Philip van Eyk

[a]School of Chemical Engineering, The University of Adelaide, Adelaide, South Australia 5005, Australia

[b]Stanwell Power Station, Switchyard road, Stanwell QLD 4702

**Abstract**

Hydrothermal liquefaction (HTL) provides a promising method for converting biomass to renewable crude (biocrude) as a fossil fuel alternative. One important advantage of HTL is the feed can have any moisture content. The products are typically made up of aqueous phase, crude phase or renewable crude (RNC), gaseous and solid components. Under ideal conditions, separation of the renewable crude from the aqueous and solid components can be achieved using decantation. However, in the presence of solid particles it has been noted that the actual renewable crude yield in the liquid phase is less than expected. Subsequent investigation has shown that the solid material traps some of the renewable crude. The nature of the trapping has received very little attention; however, there is considerable data in the literature that contains clues about the interaction between the oil and solids formed during HTL processing. We have therefore revaluated the published literature to gain further insight into the conditions that affect the interaction between the oil and solids. The re-evaluation has been carried out for lignocellulosic and non-lignocellulosic biomass to consider how these two categories of biomass behave during HTL. A key observation is that the experimental parameters for forming renewable crude and hydrochar have an influence on the outcome. A higher temperature, lower residence time and a lower biomass to solvent ratio were favourable for the renewable crude yields. The co-solvents acted differently for different biomass, such as pine wood. The solvent efficiency for oil yields can be sequenced as: ethanol > Acetone > water; however, for oil palm from an empty fruit bunch, the solvent efficiency is sequenced as: ethylene glycol > water >

ethanol > acetone > toluene. Several properties of hydrochar and renewable crude such as pores, the non-polar functional group, wettability, charge or ions in the oil and viscosity could be responsible for interactions with the solid-renewable crude; therefore, the related properties that can be relevant to describe the interactions for solid-renewable crude, have been reported. Based on a re-evaluation of data, a recommendation has been suggested for higher renewable crude and hydrochar. The relevant properties of the interactions between solid-renewable crude have also been noted, to understand the interaction more effectively.

Keywords: Hydrothermal liquefaction, Renewable crude, hydrochar, solid-renewable crude attachment, Solvent

### 3.1 Introduction

Biomass is being considered as a promising source of renewable energy like renewable crude (RNC) or gaseous fuels because of the hydrocarbon (C-H) groups that build up the biomass. Carbon (C) is considered the most important element of biomass. Carbon represents the key contribution to the overall heating value [1, 2]. Hydrogen (H) is considered another key constitute of biomass that can be estimated from the chemical structure of carbohydrate and phenolic polymers. $H_2$ has an energy value of 120 MJ/Kg, which is the highest when compared with other conventional fuels [3, 4]. Nitrogen (N), Sulphur (S) and Oxygen (O) are also vital elements of biomass. Herbaceous biomass species obtain a higher amount of nitrogen (0.4 to 1.0 wt%) and sulphur than any woody biomass [5, 6]. Nitrogen present in the biomass does not oxidise during thermal conversion and therefore it contributes to the overall heating values. Biomass offers various advantages, with a key benefit being its non-depletable nature compared to fossil fuels. Given the abundance of plants on Earth, biomass has the potential to serve as a main source of renewable energy, offering a sustainable alternative to fossil fuels. Converting the biomass into fuel using thermochemical methods raises some problems because of the diverse moisture content of different biomass.

For most of the thermochemical processes, like pyrolysis, biomass drying is required. It is not mandatory for the HTL process, which holds great economic value for fuel production because of the wet nature of the various biomass feedstock [7] [8]. As dry feed is not required for an HTL reaction, a large amount of low-quality feed stocks, which also have a high moisture content, can be considered for HTL reactions [9]. Furthermore, use of catalysts in pyrolysis is common in most cases, but the solvent (water) employed in the HTL reaction acts as a catalyst in subcritical conditions. It can produce high quality products when compared with pyrolysis products [10]. Finally, lower oxygen and moisture contents and higher heating values can be observed in HTL products in comparison with pyrolysis products. The HTL process reduces both fixed and the operative costs associated with handling equipment and storage and also saves time [11], which makes HTL technology more suitable for conversion of biomass into fuel [10]. HTL occurs at subcritical conditions (250 – 370 $^{o}$C with a pressure between 4 – 20 MPa) and produces bio-oil or renewable crude. This process blends the biomass with water to produce gas, liquid or renewable crude and solid products without pre-treatment at specific temperatures and pressures [12-14]. Although Hydrothermal carbonation (HTC) happens at comparatively low temperatures (180 - 250 $^{o}$C, 2 - 10 MPa), HTC is mainly focused on the production of hydrochar [15-20], with some renewable crude being produced. The oil produced from this technique can be upgraded by using standard refining techniques to produce gasoline, diesel oil or naphtha [21]. The reaction pathways of HTL include three major steps: depolymerisation, decomposition and recombination [22]. In the depolymerisation stage, long chain polymers consisting of carbon, hydrogen and oxygen are converted into shorter chain hydrocarbons [23]. The general hemicellulose and cellulose biopolymers contribute to the thermal stability of the biofuel at this stage [24]. In the decomposition stage, Biomass monomers are broken down further through several mechanisms, including cleavage of chemical bonds, dehydration (elimination of water molecules), decarboxylaisation (elimination

of carboxyl groups) and loss of $CO_2$ gas, and deamination, which is the process for elimination of amine (nitrogen attaching) groups [25]. Normally, oxygen molecules are removed in the form of $CO_2$ and $H_2O$, respectively. $H_2O$ at high pressure and temperature can break down the hydrogen bonded structures of cellulose and can cause the development of glucose monomers [1]. In the final or recombination stage, the broken monomer fragments go through recombination and polymerisation to make various oily products and gases, liquids and solid residues. The depolymerisation, decomposition and recombination stages are controlled by the different reaction conditions, such as temperature, residence time, and biomass and solvent ratios [26]. As different biomass has different compositions and moisture contents, the HTL process parameters can be different for different biomass [22, 26]. Lignocellulosic biomass refers to biomass that contains cellulose, hemicellulose, and lignin. HTL process parameters can have different effects on both non-lignocellulosic and lignocellulosic biomass. Algae and sludge have been categorised as non-lignocellulosic biomass [27-43]. Though wood [44] or woody biomass, [45, 46] and pinewood [47] a considered of the major sources of lignocellulosic biomass. But, generally all other biomass, biomass, including wood, can be considered lignocellulosic biomass [29, 31, 44-46, 48-64]. Different catalysts and co-solvents can also influence product yields during the HTL of biomass [27-32, 34, 38-40, 42-46, 49-52, 55, 56, 59, 61-63, 65-81]. There is no particular study which focuses on the influence of HTL process parameters on product yields during HTL of diverse types of non-lignocellulosic and lignocellulosic biomass. The nature of the catalysts and co-solvents still need to be studied in detail for better understanding of the process.

Though the aqueous phase stays separate, after the HTL of any carbohydrates, the solid and renewable crude mixture remains together as a mixture. The demolition of polar groups in the actual biomass (mainly –OH and –COO–) during the reaction decreases the capability of resulting products to attract water through hydrogen bonding, making it hydrophobic [82]. The

hydrophobic nature of the solids attracts the renewable crude. Therefore, a strong interaction between solids and renewable crude makes product extraction difficult. Unfortunately, there is insufficient data to understand the solid-renewable crude interaction, although there are some clues in previous data, which may explain the solid-renewable crude interactions in HTL reactions.

Based on the above limitations, the aim of the present study is to re-evaluate the published data to understand the influence of processing parameters on renewable crude and hydrochar yields during HTL of different types of biomass; i.e non-lignocellulosic and lignocellulosic biomass. Co-solvents and catalysts have also been taken into account to explain the yields. It is also very important to know which other factors or properties can possibly cause the hydrophobicity (oil attraction) of the solids. A re-evaluation has also been carried out to consider if there is any relationship between the interaction and information available from previous investigations.

### 3.2 Methodology

#### 3.2.1 Data selection

In this study, data from previous research on the HTL of various biomass sources was selected for analysis. Specifically, the investigation focused on the effects of different experimental parameters, including temperature, residence time, biomass/solvent ratios, catalysts, and co-solvents, as reported in relevant literature on HTL of diverse biomass. The data was extracted and categorised based on these parameters. Non-lignocellulosic biomass, such as algae and sludge, were classified separately for analysis purposes [27-43]; However, it should be noted that the majority of other biomass sources, such as wood, can be categorised as lignocellulosic biomass. [29, 31, 44-46, 48-64]. Furthermore, a set of data from catalytic HTL has been included to explore the impact of catalysts on the HTL of biomass [28, 31, 34, 38, 40, 44, 45, 50, 52, 55, 59, 61, 62, 65-72]. Given the significant impact of co-solvents on the HTL process,

a collection of data on various co-solvents has also been included in the re-analysis [27-32, 38-40, 42, 43, 45, 46, 49, 51, 55, 56, 59, 61-63, 73-81].

### 3.2.2 Data re-analysis

The extracted data and information have been categorised into two groups: lignocellulosic and non-lignocellulosic biomass. Within each category, the data has been analysed to investigate the influence of different parameters on the yields of renewable crude and hydrochar. The parameters have been classified into two categories: major parameters (such as temperature, residence time, biomass/solvent ratio, and co-solvents) and additional parameters (including reactors, catalysts, pressure, and oil extraction methods). In order to isolate the specific impact of each parameter, researchers often held other parameters constant while varying a particular parameter of interest. Consequently, all the other parameters, such as catalysts, co-solvents, pressure, reactor size and type, and separation techniques/solvents, have also been documented for each category.

### 3.2.3 Finding relationships between the previous data and solid-renewable crude attachment

Various researchers have used different solvents to extract renewable crude from solid-oil mixtures obtained through the HTL of biomass. While the investigation of renewable crude trapping in solids was not explicitly conducted, there are indications suggesting that solids could retain a portion of the renewable crude. As a result of the attachment between solids and renewable crude, the recovered yields of renewable crude were found to be lower than expected. These attachments are influenced by specific properties of both the solids and renewable crude. Thus, by examining the available clues from various studies, the relevant properties associated with these attachments have been identified and discussed. Additionally, the mechanisms by which these properties contribute to the attachment of oil in solids have also been recognised.

### 3.3 The influence of process parameters

#### 3.3.1 The influence of temperature on product yields

Figure 3.1 presents an evaluation of the impact of temperature on HTL of both non-lignocellulosic and lignocellulosic biomass. In the context of non-lignocellulosic biomass, the direct liquefaction of *D. tertiolecta* was conducted in a 50 ml autoclave without the use of any catalyst. The process was carried out for 30 minutes, resulting in a significant increase in renewable crude yields. Specifically, at a temperature of 320°C, the yields reached 64 wt.% [27]. This happens because of the higher decomposition of biomass at high temperatures [83, 84]. Consequently, as temperatures rise, the solid residue (hydrochar) decreases while the production of renewable crude increases. Nevertheless, at 340 °C, the yield of renewable crude experiences a slight decrease, reaching 58 wt.%. When temperatures surpass 320 °C, additional reactions (secondary reactions) can occur, such as tar cracking and shifting reactions. These reactions have the potential to decrease the production of specific products and increase gas formation. [85, 86]. Hence, the yield of renewable crude exhibits a slight decline beyond the temperature of 320 °C. In the experimental study involving *D. tertiolecta* in a 100 ml conventional autoclave, a catalyst (Na2CO3) was introduced during a 60-minute process. Surprisingly, the highest yield of renewable crude (43.2 wt.%) was achieved at a comparatively lower temperature of 250 °C. Subsequently, the yield of renewable crude decreased once the temperature exceeded 250 °C [28]. This can happen if secondary cracking starts earlier from using a longer residence time. Jin et al. [29], Aysu et al. [30] and Brown et al. [32] obtained a similar temperature effect, as higher temperatures favour higher yields of renewable crude and lower the hydrochar yields, even when using a mixture of two different algae; i.e, *Spirulina platensis* + *Entermorpha prolifera* (EP) [29]. Two kinds of microalgae (*Spirulina and C.vulgaris*) have been used for HTL reactions to consider the outcome of using a fixed temperature (350 °C) [40]. During the investigation, all other variables remained constant,

including the catalyst (KOH), solvent (water), reaction time (60 minutes), and reactor. When comparing the HTL of C. vulgaris and Spirulina, it was observed that *C. vulgaris* exhibited a higher yield of renewable crude (13.6 wt.%) than Spirulina.

In another study examining the HTL of *Botryococcus braunii*, water as a solvent was employed in a 300 ml autoclave for a duration of 60 minutes. The investigation revealed that the maximum yield of renewable crude recorded was 57 wt.% at a temperature of 300 $^{o}$C. [33]. As the temperature increased to 350 $^{o}$C, a decrease in the yield of renewable crude was observed, indicating the initiation of secondary cracking reactions. Similar reactions were observed when a different catalyst, $Na_2CO_3$, was employed. However, the use of $Na_2CO_3$ aided in further biomass decomposition. Consequently, the maximum yield of renewable crude (64 wt.%) was achieved at a temperature of 300 $^{o}$C when utilising this catalyst.

Regarding lignocellulosic biomass (depicted in Figure 1 (c and d)), during the HTL of C. lanceolate with and without a catalyst, a small influence from temperature could be noticed [44]. The HTL reaction used water as the solvent and $K_2CO_3$ as the catalyst. As the temperature increased, there was a corresponding increase in the yields of renewable crude due to the enhanced decomposition of biomass at higher temperatures. At a temperature of 320 $^{o}$C, the maximum yield of renewable crude reached 23.78 wt.%. However, beyond 320 $^{o}$C, the yields of renewable crude started to decrease. This decrease could be attributed to either secondary cracking or re-polymerisation taking place.

Additionally, the hydrochar yields decreased with rising temperatures, primarily due to the increased decomposition of biomass. The used of the catalyst $K_2CO_3$ resulted the higher yields of renewable crude (with a maximum yield of 32.34 wt.% observed at 340 $^{o}$C) and reduced hydrochar yields. Secondary cracking was observed to commence after 340 $^{o}$C when using the $K_2CO_3$ catalyst.

Consequently, the HTL reactions conducted on various lignocellulosic biomass samples, including Jack Pine powder, Pine Sawdust, Paulownia, Pinewood, Paper sludge, Corn stover, Grassland perennials, and *O. heteracanthum*, exhibited similar trends. Higher temperatures generally led to increased yields of renewable crude, but very high temperatures occasionally triggered secondary cracking, resulting in a reduction of the renewable crude yield. Thus, the influence of temperature strongly indicates that the range of 320 to 350 °C is most favourable for achieving optimal yields of renewable crude, except in the case of HTL of paper sludge.

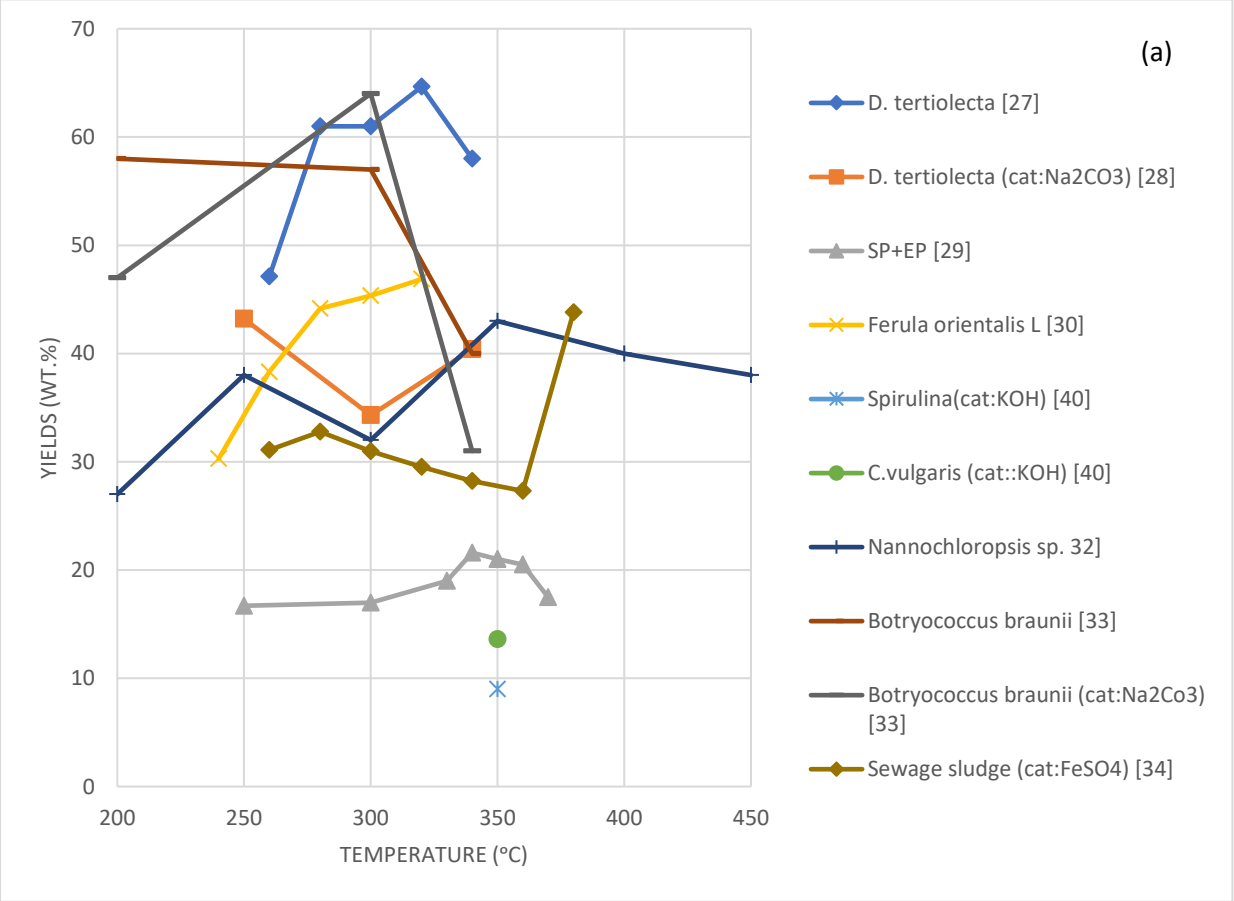

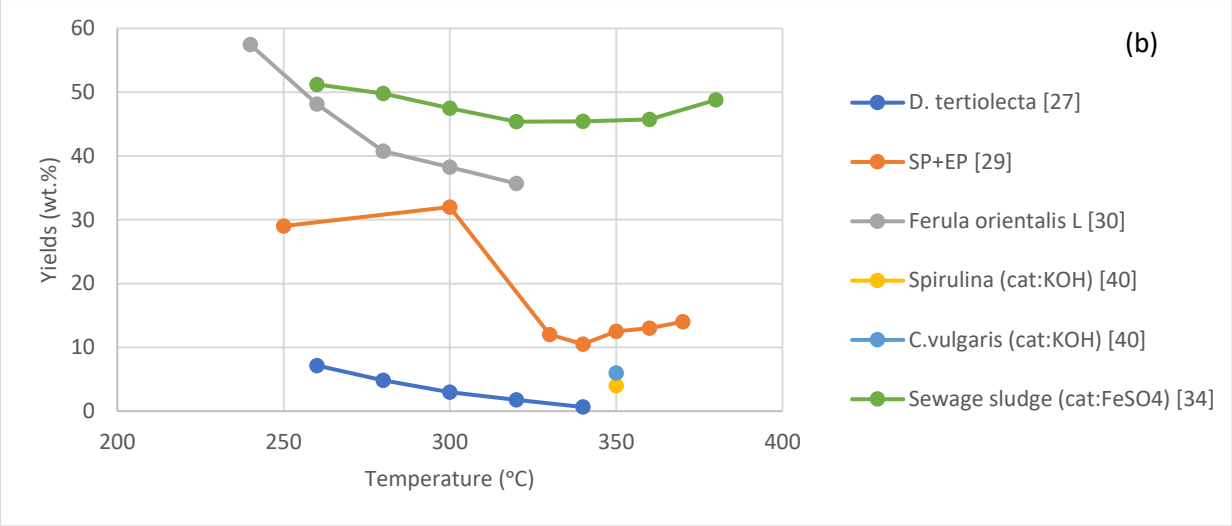
(b)
Yields (wt.%)
Temperature (°C)
D. tertiolecta [27]
SP+EP [29]
Ferula orientalis L [30]
Spirulina (cat:KOH) [40]
C.vulgaris (cat:KOH) [40]
Sewage sludge (cat:FeSO4) [34]

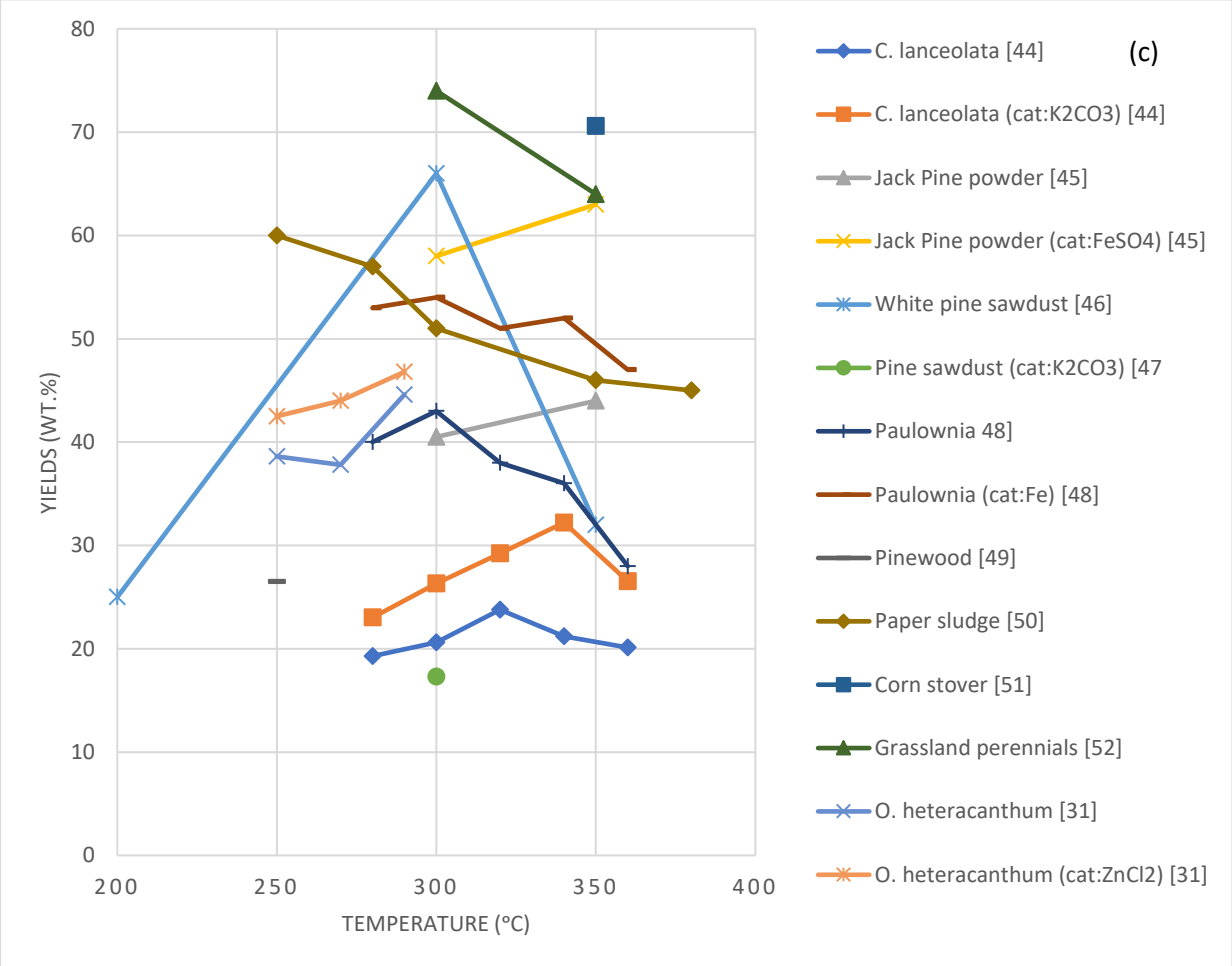
(c)
YIELDS (WT.%)
TEMPERATURE (°C)
C. lanceolata [44]
C. lanceolata (cat:K2CO3) [44]
Jack Pine powder [45]
Jack Pine powder (cat:FeSO4) [45]
White pine sawdust [46]
Pine sawdust (cat:K2CO3) [47
Paulownia 48]
Paulownia (cat:Fe) [48]
Pinewood [49]
Paper sludge [50]
Corn stover [51]
Grassland perennials [52]
O. heteracanthum [31]
O. heteracanthum (cat:ZnCl2) [31]

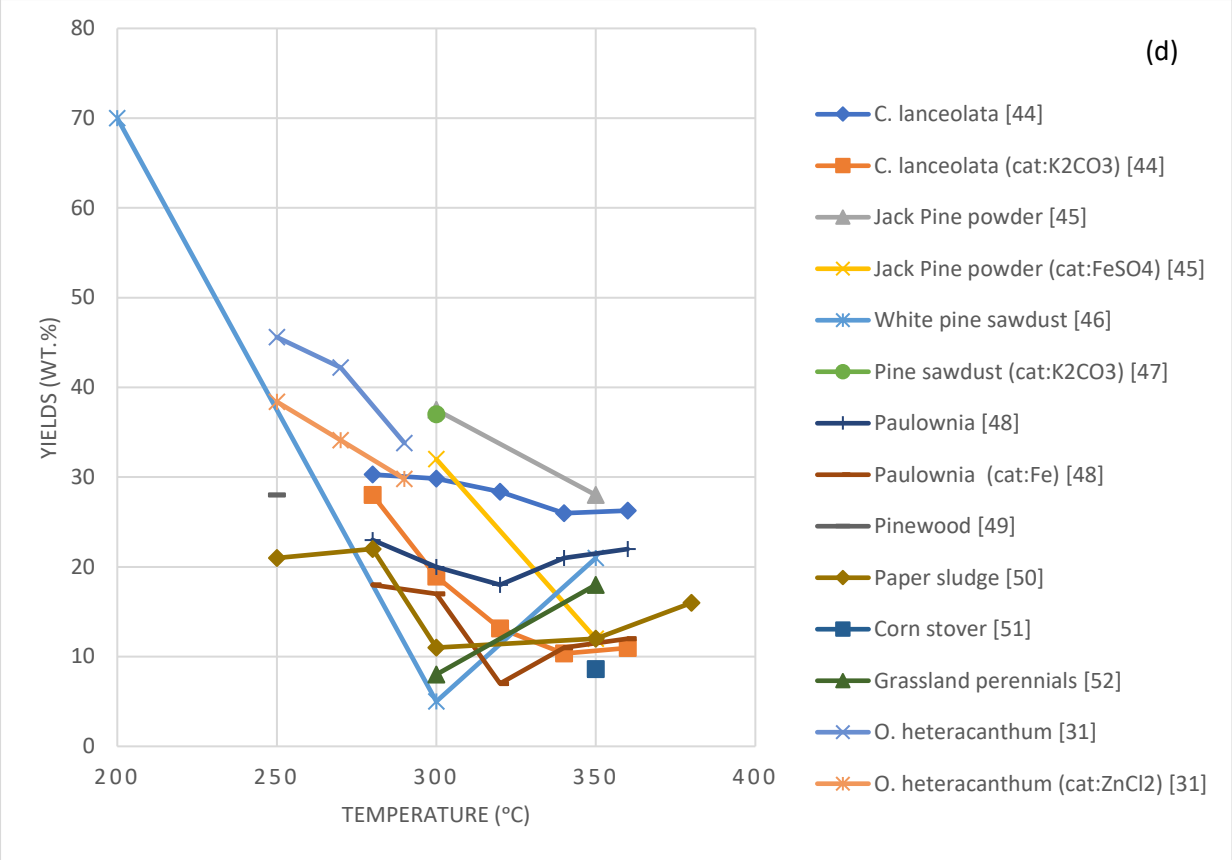


Figure 3.1: Influence of temperature for non-lignocellulosic biomass on (a) renewable crude, (b) hydrochar yields; for lignocellulosic biomass on (c) renewable crude, (d) hydrochar yields.

### 3.3.2 Influence of residence time on product yield

The impact of residence time during HTL of both non-lignocellulosic and lignocellulosic biomass is depicted in Figure 3.2. Various non-lignocellulosic biomass, including *L. Saccharina* [35], a mixture of *Spirulina platensis* and *Entermorpha prolifera* [29] and sewage sludge [34] showed a preference for lower residence time in order to achieve higher yields of renewable crude. Additionally, higher yields of hydrochar were observed at relatively lower temperatures. This phenomenon can be attributed to secondary cracking or re-polymerisation reactions, which lead to further decomposition of the renewable crude and hydrochar, resulting in increased production of other byproducts such as gas. Hence, a longer residence time at higher temperatures can stimulate additional reactions, like secondary cracking or re-

polymerisation. A study on *D. Tertiolecta* [27] showed that a residence time of 30 minutes produced a higher yield of renewable crude (64 wt.%), but a significantly lower yield of hydrochar (1.76 wt.%). Therefore, it can be concluded that a 30-minute residence time is considered relatively short and suitable for *D. tertiolecta*. However, in most studies conducted on HTL of non-lignocellulosic biomass, such as L. Saccharina, SP+EP (mixture of *Spirulina platensis* and *Entermorpha prolifera*), swine manure (SW), mixed-culture algal, and sewage sludge (with cat: FeSO4), a lower residence time favours the production of renewable crude, while a higher residence time favours the yield of hydrochar. Similar results were reported by Yin et al. [87] supporting the notion that re-condensation occurs during longer residence times. Moreover, *Nannochloropsis oceanica* [36], *Dunaliella tertiolecta* [27], Swine manure (SW) and mixed-culture algae [37] also showed higher yields of renewable crude with shorter residence times.

The HTL of different lignocellulosic biomass, including grassland perennials [52], cherry stones [53], and *C. lanceolata* [56] showed a decrease in overall renewable crude yields as the residence time increased. It appears that re-polymerisation and re-condensation reactions start to occur after reaching a minimum residence time. In certain cases, such as rice stalk [58], re-condensation began to take place after 60 minutes of residence time, resulting in a decline in renewable crude yield. Meryemoğlu et al. [55], investigated the HTL of Kenaf, Sorghum, and wheat straw and found that after 60 minutes of residence time, they produced renewable crude yields of 77.2 wt.%, 75.1 wt.%, and 72.1 wt.%, respectively, which were similar. Similarly, Chan et al. [57] examined the HTL of palm waste for 60 minutes at 360 $^{o}$C, but despite the high temperature, the renewable crude yield was only 27.54, which was not significant. This could be attributed to the longer residence time. At high temperatures and longer residence times, secondary cracking or re-polymerisation reactions may occur, leading to a reduction in renewable crude yield and an increase in hydrochar or gas production. Consequently, HTL of

Pine sawdust [46], paulownia [48], corn stover [51], beech wood [54] and pine wood [49] also showed substantial renewable crude yields at shorter residence times, while pinewood sawdust [47] demonstrated a lower yield due to the longer residence time.

The hydrochar yields also gradually decreased for grassland perennials [51], cherry stones [52], switchgrass [60] and rice stalk [58] with increasing residence time. In these cases, further decomposition of biomass resulted in re-polymerisation, predominantly producing other products such as gas or the aqueous phase. Conversely, a slight increase in hydrochar was observed for *C. lanceolate* [56] with a longer residence time, as re-polymerisation or re-condensation produced more hydrochar by reducing the amount of renewable crude.

The hydrochar yields also gradually decreased for grassland perennials [51], cherry stones [52], switchgrass [59], and rice stalk [57] with increasing residence time. In these cases, further decomposition of biomass resulted in re-polymerisation, predominantly producing other products such as gas or the aqueous phase. Conversely, a slight increase in hydrochar was observed for *C. lanceolate* [55] with a longer residence time, as re-polymerisation or re-condensation produced more hydrochar by reducing the amount of renewable crude.

In brief, the HTL of various lignocellulosic biomass, such as cherry stones, beech wood, Kenaf, Sorghum, wheat straw, pine sawdust, pinewood, pinewood sawdust, Heteracanthum stalks, paulownia, palm waste, corn stover, rice stalk, oil palm shell, coconut shell, EFB, and grassland perennials, demonstrated that a shorter residence time is favourable for achieving higher yields of renewable crude and lower yields of hydrochar.

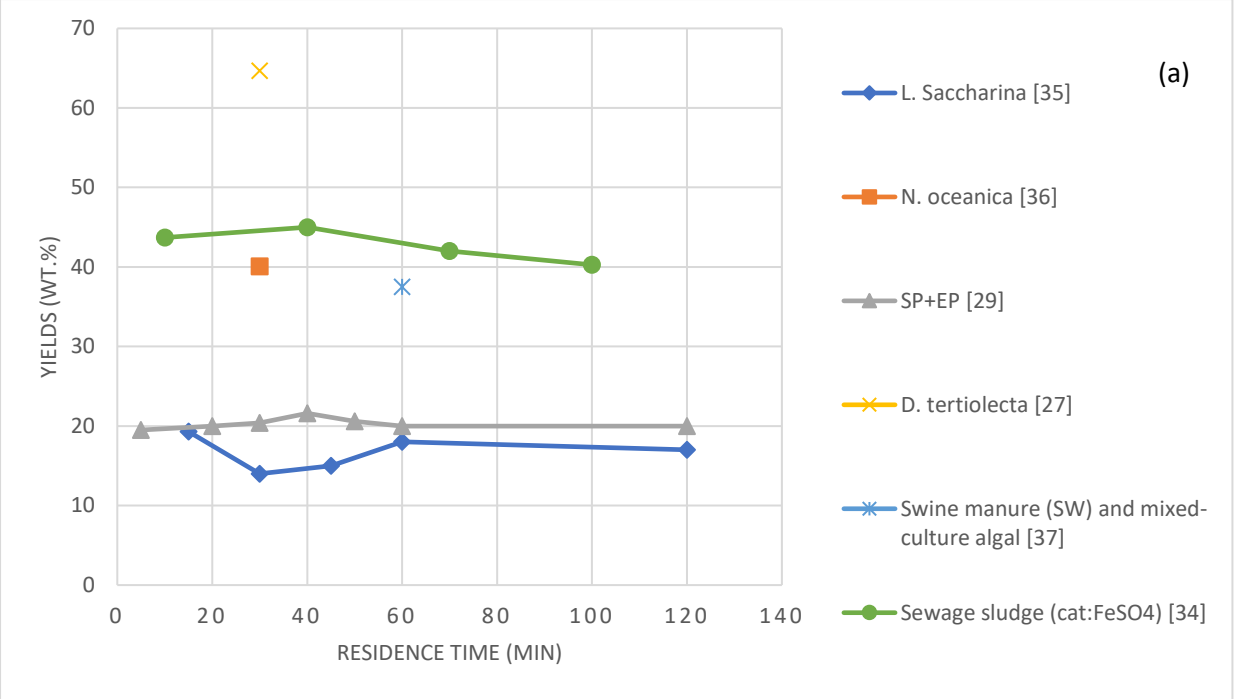
(a)
YIELDS (WT.%)
RESIDENCE TIME (MIN)
L. Saccharina [35]
N. oceanica [36]
SP+EP [29]
D. tertiolecta [27]
Swine manure (SW) and mixed-culture algal [37]
Sewage sludge (cat:FeSO4) [34]

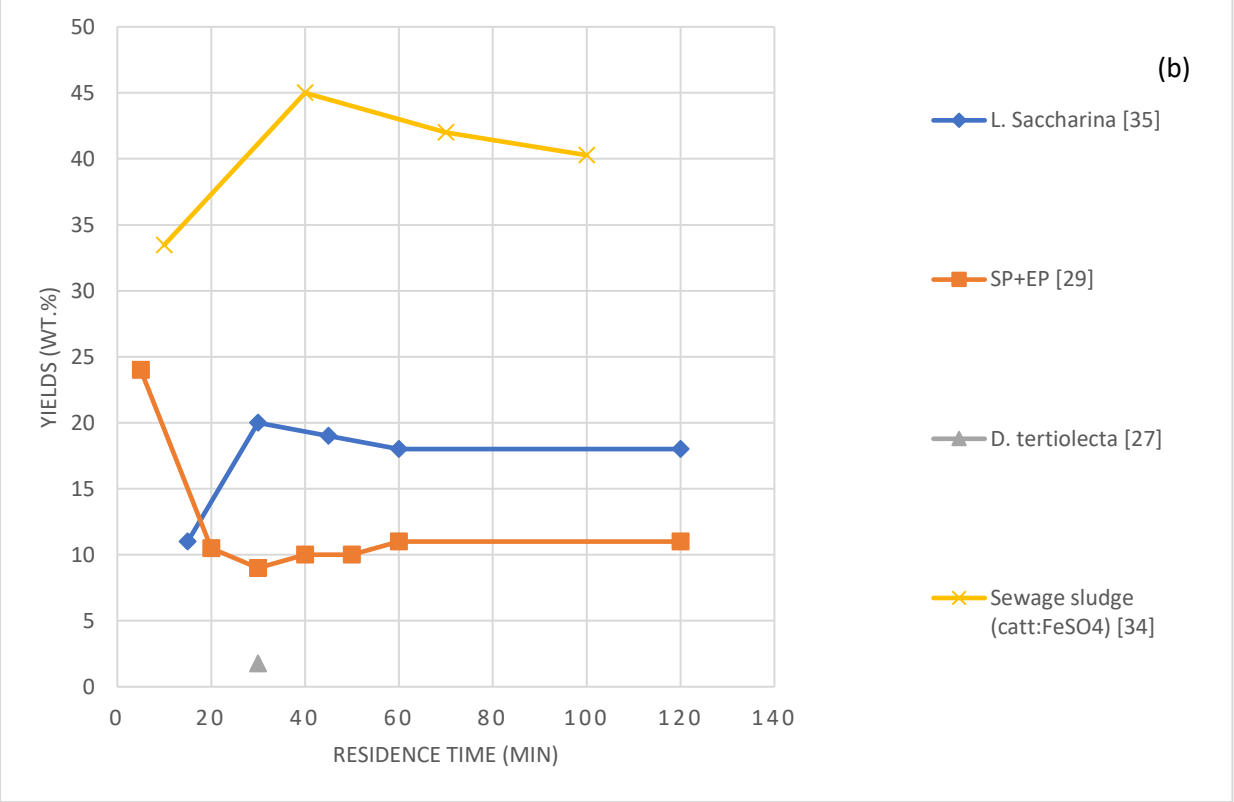
(b)
YIELDS (WT.%)
RESIDENCE TIME (MIN)
L. Saccharina [35]
SP+EP [29]
D. tertiolecta [27]
Sewage sludge (catt:FeSO4) [34]

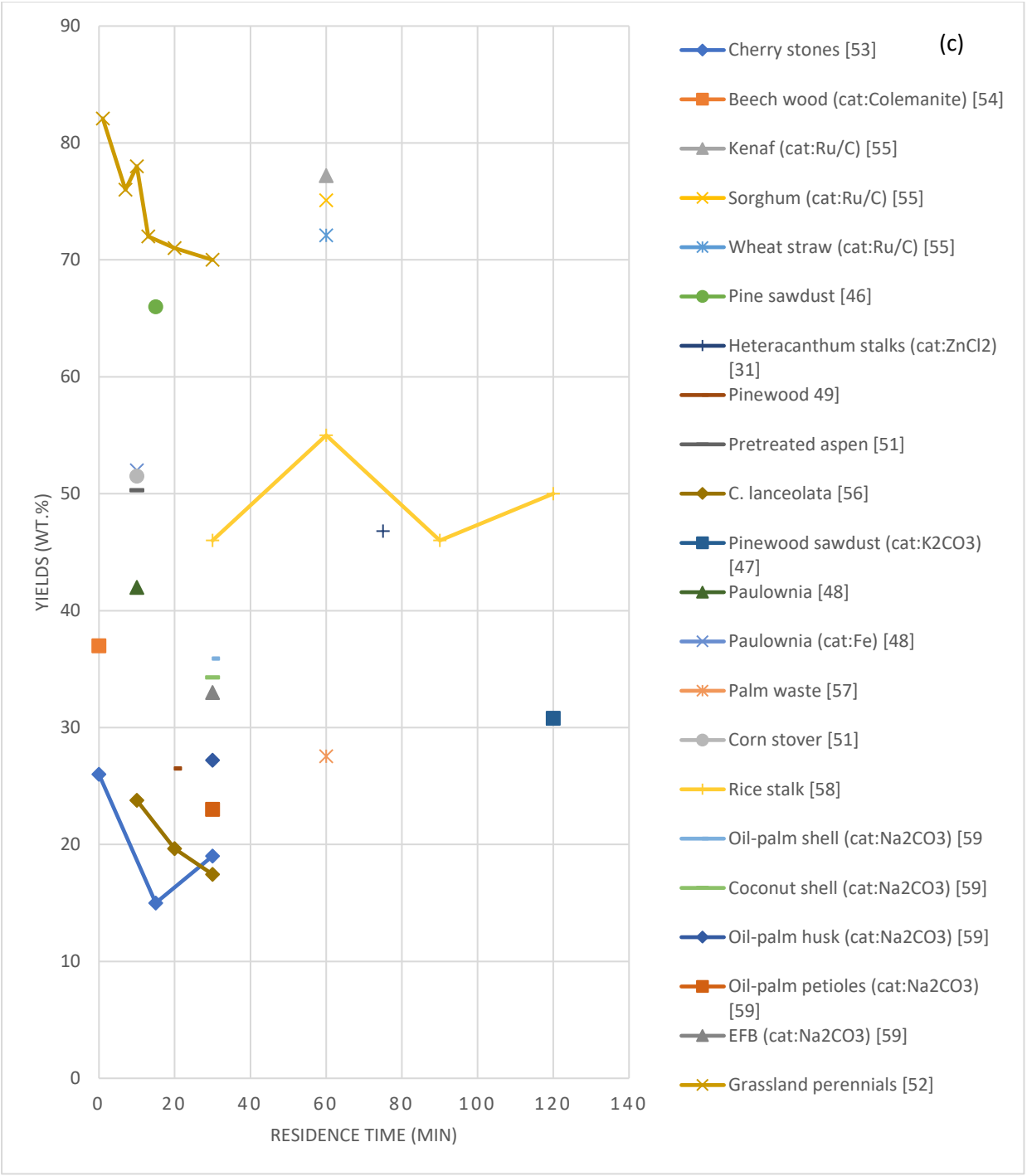
(c)
YIELDS (WT.%)
RESIDENCE TIME (MIN)
0
10
20
30
40
50
60
70
80
90
0
20
40
60
80
100
120
140
Cherry stones [53]
Beech wood (cat:Colemanite) [54]
Kenaf (cat:Ru/C) [55]
Sorghum (cat:Ru/C) [55]
Wheat straw (cat:Ru/C) [55]
Pine sawdust [46]
Heteracanthum stalks (cat:ZnCl2) [31]
Pinewood 49]
Pretreated aspen [51]
C. lanceolata [56]
Pinewood sawdust (cat:K2CO3) [47]
Paulownia [48]
Paulownia (cat:Fe) [48]
Palm waste [57]
Corn stover [51]
Rice stalk [58]
Oil-palm shell (cat:Na2CO3) [59
Coconut shell (cat:Na2CO3) [59]
Oil-palm husk (cat:Na2CO3) [59]
Oil-palm petioles (cat:Na2CO3) [59]
EFB (cat:Na2CO3) [59]
Grassland perennials [52]

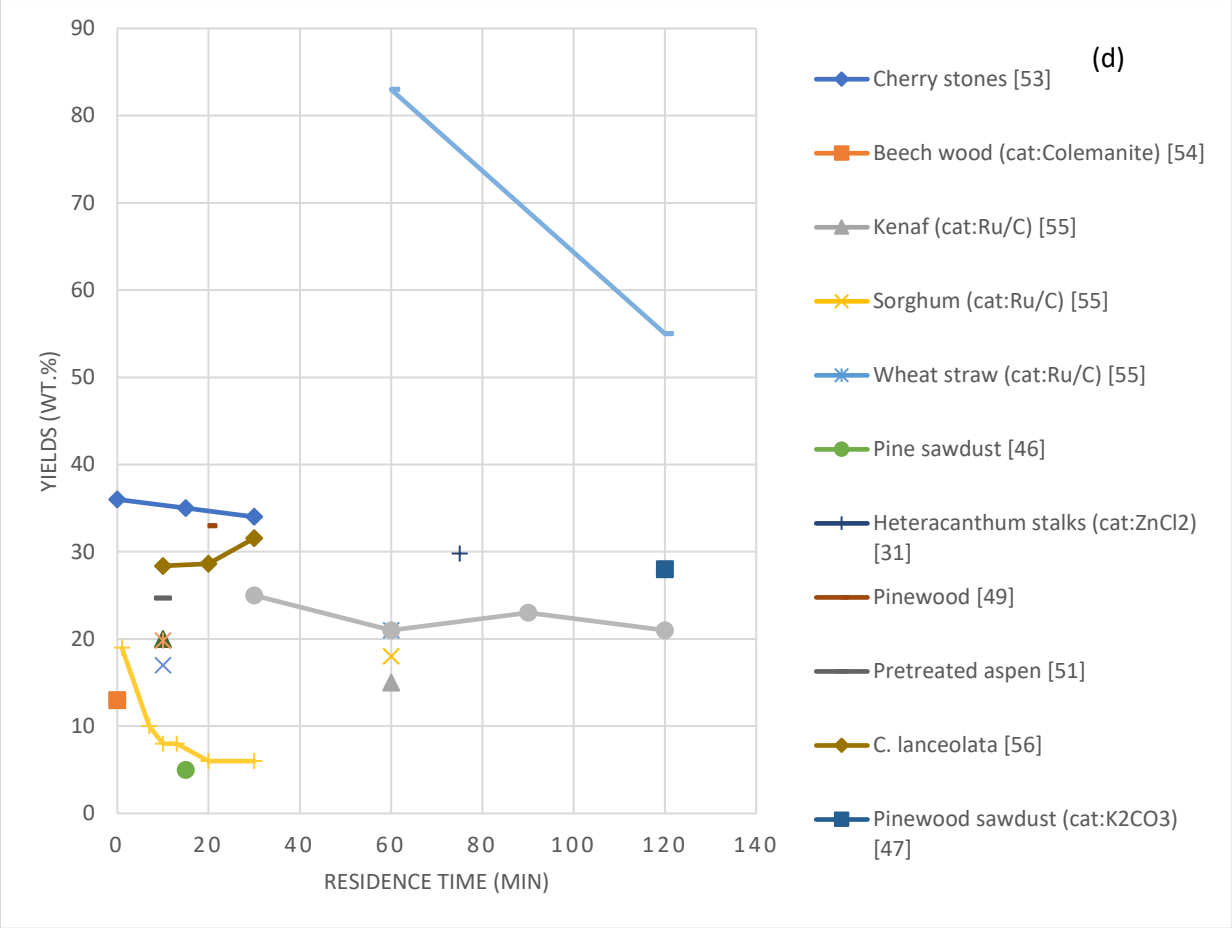


Figure 3.2: Influence of residence time for non-lignocellulosic biomass on (a) renewable crude and (b) hydrochar yields; for lignocellulosic on (c) renewable crude and (d) hydrochar yields.

### 3.3.3 Influence of the biomass/solvent ratio on product yield

Figure 3.3 presented the findings of the investigation of influence of the biomass to solvent ratio (B/S) on the HTL process for both non-lignocellulosic and lignocellulosic biomass. For non-lignocellulosic biomass, the HTL of combination of two algae species (*Spirulina platensis* + *E. prolifera*) has been conducted at varying B/S ratios (ranging from 0.17 to 1) and a temperature of 340 °C, using deionised water as the solvent [29]. The results revealed that a lower B/S ratio favoured higher yields of renewable crude, whereas a higher B/S ratio favoured greater hydrochar yields. The significant role of water in accelerating the reaction was identified as the contributing factor [10]. Reducing the water amount through an increased B/S

ratio minimised biomass decomposition, resulting in reduced yields of renewable crude. However, experiments that investigated a single B/S ratio, such as the case of *Ulra Fasciata* [41], which yielded a higher amount of renewable crude (44 wt.%) at a B/S ratio of 1.17, were unable to provide a comprehensive understanding of the reaction's nature. Conversely, *D. tertiolecta* [38] demonstrated a higher yield of renewable crude without a catalyst when the B/S ratio was 0.1. Comparing experiments involving different biomass types, such as Spirulina and *Nannochloropsis salina* [39] and *Spirulina and C. vulgaris* [40], *Nannochloropsis salina* and *C. vulgaris* produced higher yields of renewable crude. Sewage sludge [43] also yielded a considerable amount of renewable crude (30 wt.%) at a B/S ratio of 0.11. Nevertheless, in the case of the mixture of Spirulina platensis and *E. prolifera*, hydrochar yields gradually decreased due to the slower decomposition rate of biomass at higher B/S ratios. Overall, the experiments conducted on various non-lignocellulosic biomass, including *D. tertiolecta*, Spirulina, *N. salina, C.vulgaris*, and *Ulra fasciata*, indicated that a lower B/S ratio is favorable for achieving higher yields of renewable crude and lower hydrochar yields.

Regarding lignocellulosic biomass, the results showed that a lower biomass to solvent ratio (B/S) favoured higher yields of renewable crude for *C. lanceolata* [56], White pine sawdust [46] and rice stalk [63]. Conversely, a higher B/S ratio was preferred for higher yields of hydrochar for *C. lanceolata* [56], *D. latiflorus* [61], Moso bamboo [62] and White pine sawdust [46]. For instance, an experiment with a B/S ratio of 0.08 demonstrated that the HTL of Jack pine resulted in a 44 wt.% yield of renewable crude, supporting the notion that a lower B/S ratio is beneficial for renewable crude production [45]. Similarly, Rice stalk [63] indicated that the maximum yield of renewable crude (55 wt.%) was achieved at a B/S ratio of 0.1, which gradually decreased with increasing ratios, while hydrochar yields increased. Consistent findings were observed in several other investigations involving HTL of lignocellulosic biomass, such as Corn stover, Grassland perennials, Cornstalk, Pinewood, and Switchgrass, all

of which consistently reported higher renewable crude yields at lower B/S ratios. The degradation of biomass tends to be more significant in HTL reactions with lower B/S ratios, leading to increased renewable crude yields. This also results in a higher amount of aqueous solution in the final products [61].

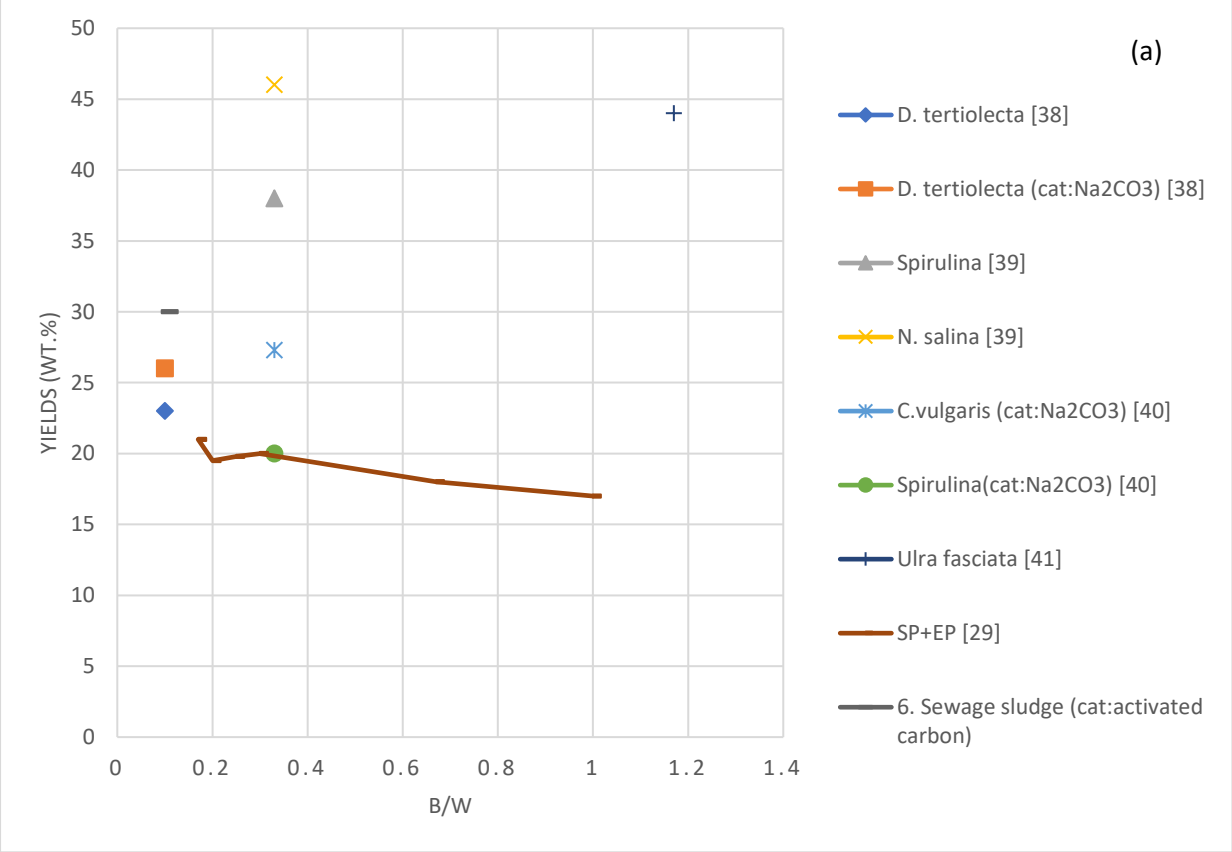


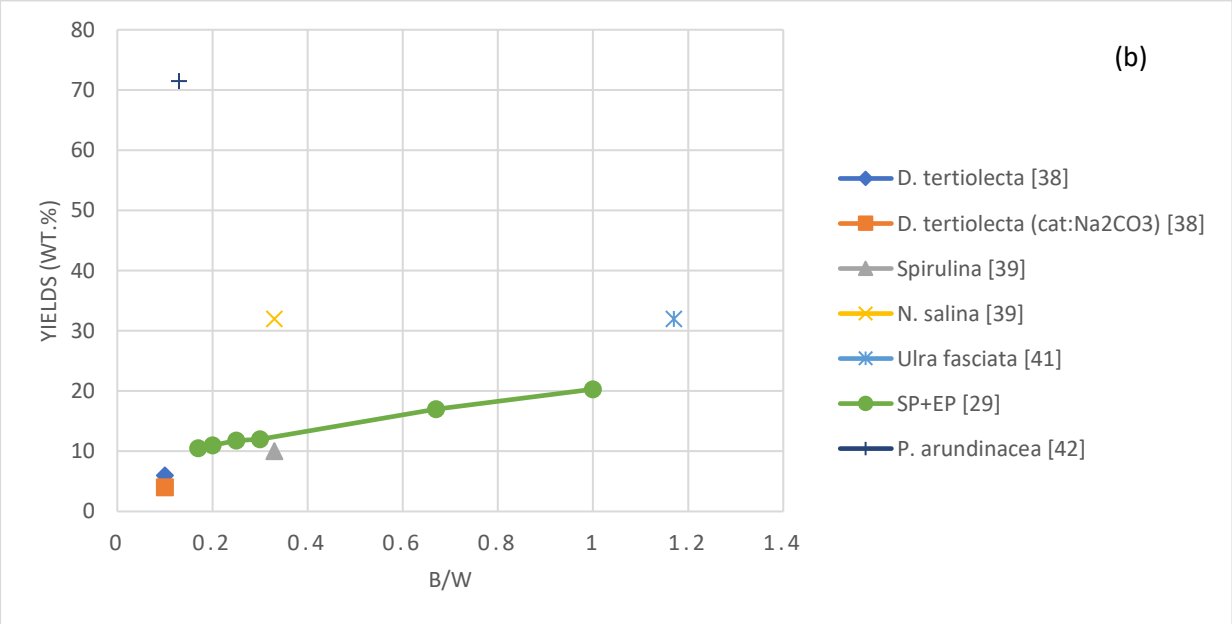

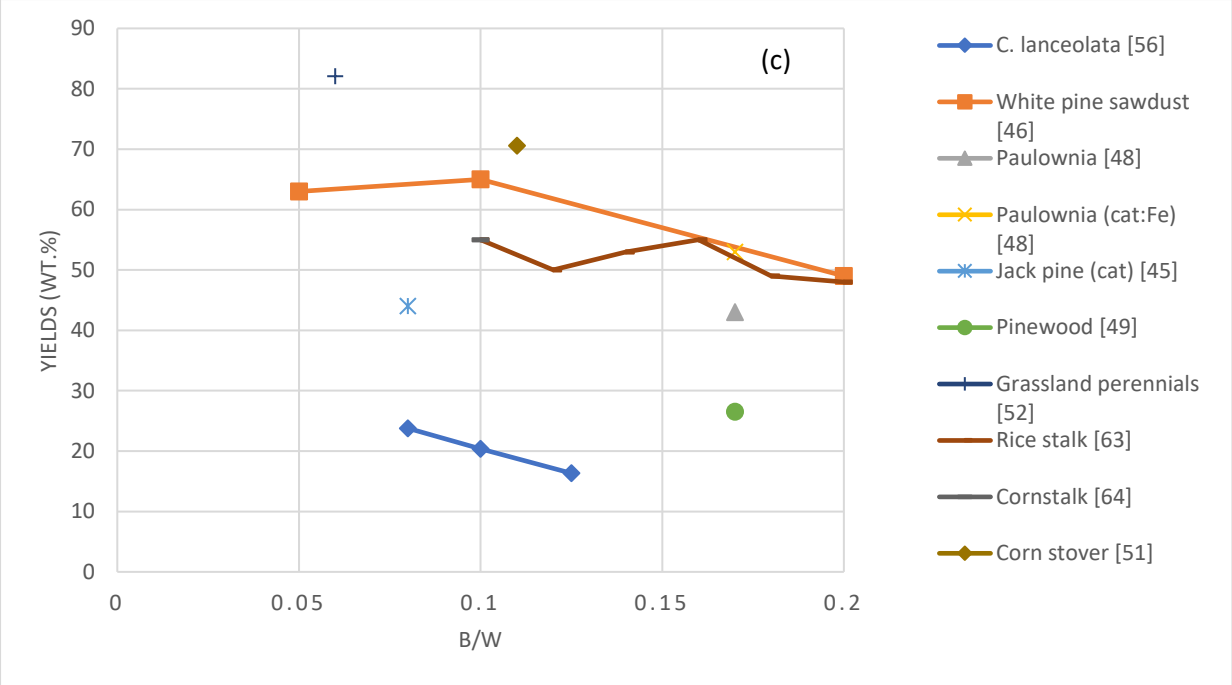


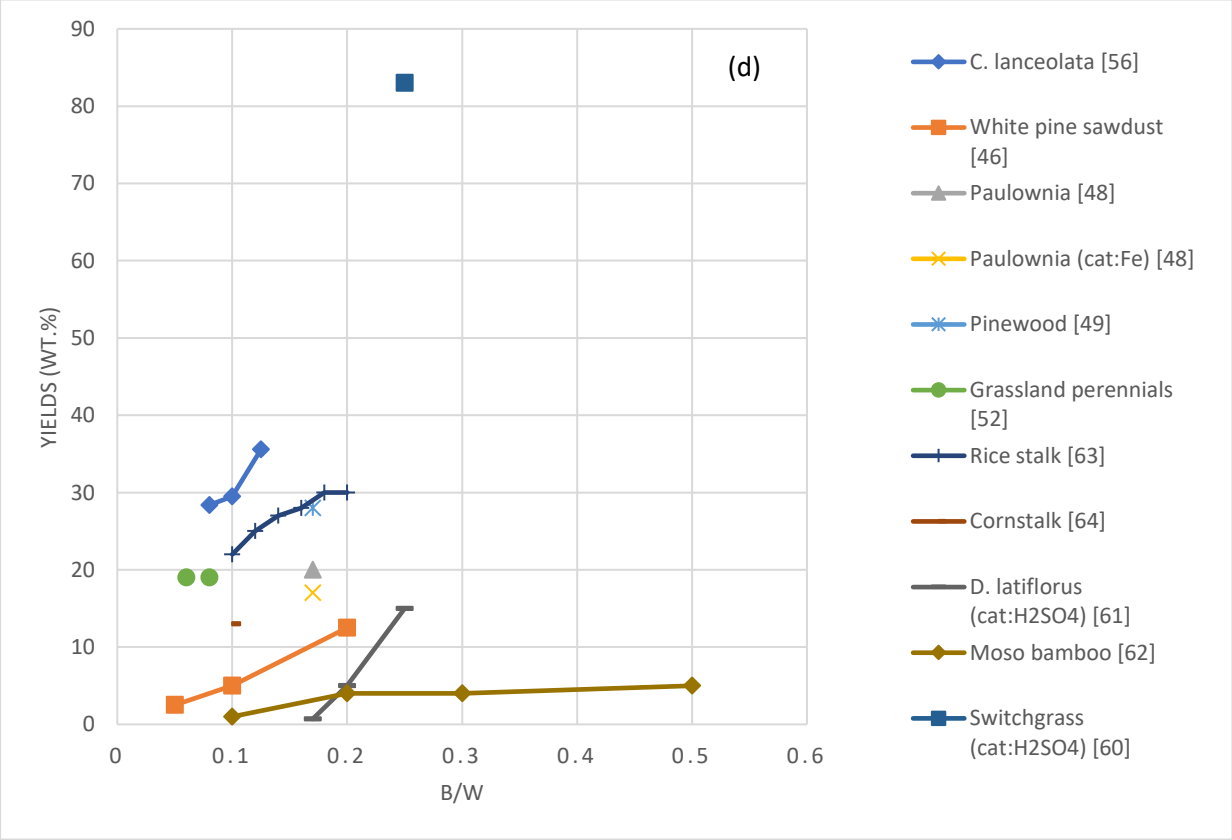


Figure 3.3: Influence of the Biomass/water ratio for non-lignocellulosic biomass on (a) renewable crude, (b) hydrochar yields; for lignocellulosic on (c) renewable crude, and (d) hydrochar yields.

### 3.3.4 Influence of catalyst on product yield

Catalysts have a significant impact on the yields of renewable crude and hydrochar in biomass HTL. Table 3.1 provides an overview of the influence of various catalysts on the HTL process. Interestingly, different types of biomass showed a preference for specific catalysts to achieve higher yields of renewable crude. In the investigation of different alkalis/salts as catalysts during the HTL of woody biomass (Birch) using 5% solution, NaOH was identified as the most effective catalyst for hydrochar production. At a temperature of 170 $^{o}$C, a maximum hydrochar yield of 71.1 wt.% was achieved [67]. Similarly, NaOH was found to be favourable for attaining higher yields of renewable crude during the HTL of a mixture of 18 perennial herbaceous grassland species [52].

An Fe based catalyst like Fe [69] for paulownia and $FeSO_4$ [45] for jack pine power were more favourable for renewable crude yields than $Na_2CO_3$ and FeS respectively [69] [45]. Although $Na_2CO_3$ did not show significant effects for renewable crude yields for paulownia, carbonate-based catalysts ($CO_3$) have shown a significant effect on the renewable crude of hydrochar yields for several biomass. During the HTL of Sawdust from pine, $RbCO_3$ was suitable for renewable crude production [68]. $Na_2CO_3$ was favoured to produce higher yields of renewable crude for *Spirulina and Chlorella* [40], *Dunaliella tertiolecta* [28], *Dunaliella tertiolecta cake* [38], Oil-palm shell [59] and Garbage (a mixture of cabbage, boiled rice, boiled and dried sardine, butter, and the shell of short-necked clams) [72]. However, the catalytic HTL of Sewage sludge showed that $FeSO_4$ gave a better performance than $Na_2CO_3$ for producing oil [34]. Use of $K_2CO_3$ as a catalyst in HTL of different woody biomass (C. lanceolate, P. massoniana Lamb and P. tomentosa Carr) showed a significant increase in renewable crude yields and a decrease in hydrochar yields from non-catalytic liquefaction [44]. *C. lanceolate* produced higher renewable crude and hydrochar yields than *P. massoniana Lamb, P. tomentosa Carr*. and *F. mandshurica.* Meryemoğlu et al. [55] investigated the two type of catalysts; i.e,

Ru/C, IMP-Ru/AC for investigation of the HTL of dried kenaf hydrolysate. Both catalysts increased the renewable crude and decreased the hydrochar from the non-catalytic reaction; however, Ru/C showed higher performance than IMP-Ru/AC. Sometimes catalysts were favoured to produce high number of aqueous fractions, such as using of $H_2SO_4$ as a catalyst, for example the HTL of *Dendrocalamus latiflorus Munro produced* 93.60% of the aqueous fraction [61].

Bamboo with an HCL catalyst produced higher amount of renewable crude (80 wt.%) at 180 $^oC$ [62]. $ZnCl_2$ was found more effective than potassium hydroxide in terms of the conversion of *Onopordum heteracanthum* stalks at 250 $^oC$ [31]. $ZnCl_2$ increased the renewable crude yields and decreased the hydrochar yields when mixed with some solvents; for instance, Methanol, Ethanol and Acetone. There was a mixed effect for KOH. KOH decreased the hydrochar and renewable crude when it was mixed with Methanol, but if it was mixed with Ethanol and Acetone, renewable crude yields were increased. There are also noticeable catalytic effects of HTL for different types of waste. $Ba(OH)_2$ as a catalyst was found more effective than $Rb_2CO_3$, $K_2CO_3$ and $Ca(OH)_2$ during the HTL of sawdust and cornstalks, as well as secondary pulp/paper sludge for renewable crude yields [70] [50], but $Ca(OH)_2$ was found favourable for hydrochar yields [50]. Lu et al. [71] found that using an $AlCl_3$ catalyst during the HTL of corn stover decreased the hydrochar yields. Hydrochar yields were decreased 36 to 30 wt.% when using 5% $AlCl_3$. They did not report any renewable crude, but it could be assumed that the decomposition rate was increased, so renewable crude may be increased by using this catalyst. Duan et al. [66] used *Chlorella p*. with several catalysts, such as HZSM-5 ($SiO_2/Al_2O_3$; 25:1, 50: 1 and 170:1), MCM-41 (50% Si and 100% Si), SAPO-11, HY (5% and 0.8% of $Na_2O$) and Hβ, but the non-catalytic HTL reaction produced more renewable crude than the catalytic reaction in this case [66]. Apart from that, MCM-41 (100 % Si) and Hβ favoured the renewable crude and hydrochar yields respectively, more than the other catalysts. Duan et al. [65]

investigated the HTL of *Nannochloropsis sp.* with several catalysts like Pd/C, Pt/C, Ru/C, CoMo/$\gamma$-$Al_2O_3$, Ni/$SiO_2$-$Al_2O_3$ and zeolite. All of the catalysts produced more oil than for the non-catalytic reactions. Among them, Pd/C showed better performance for renewable crude yields than the other catalysts.

Table 3.1: Influence of various catalysts on the yields of RNC and Hydrochar during HTL of various biomass

| Biomass | Catalyst | Renewable Crude (RNC) yields (wt%) | Hydrochar yields (wt%) |
|---|---|---|---|
| Birch [67] | NaOH | | 71.1 |
| Sawdust from pine [68] | $RbCO_3$ | 25.2 | 12 |
| Paulownia [69] | Fe | 36.34 | 9 |
| Jack pine powder [45] | $FeSO_4$ | 63 | |
| *C. lanceolata [44]* | $K_2CO_3$ | 32.21 | 10.34 |
| *P. massoniana Lamb [44]* | $K_2CO_3$ | 27.38 | 13.22 |
| *P. tomentosa Carr*. [44] | $K_2CO_3$ | 31.54 | 7.94 |
| *F. mandshurica [44]* | $K_2CO_3$ | 30.8 | 7.27 |
| Bamboo [62] | HCL | 80 | |
| Grassland [52] | NaOH | 74.4 | 13.1 |
| *O. heteracanthum* stalks [31] | $ZnCl_2$ | 46.8 | 29.8 |
| Sawdust and cornstalks [70] | $Ba(OH)_2$ | 38 | |
| Secondary pulp/paper sludge [50] | $Ba(OH)_2$ | 14.3 | 21.5 |
| Corn stover [71] | $AlCl_3$ | | 30 |
| Oil-palm shell [59] | $Na_2CO_3$ | 35.9 | |
| Garbage [72] | $Na_2CO_3$ | 27.6 | |
| Sewage sludge [34] | $FeSO_4$ | 45.58 | 31.79 |
| *Chlorella p*. [66] | Si | 54.5 | 11 |
| *Nannochloropsis sp. [65]* | Pd/C | 57 | |
| *D. tertiolecta cake [38]* | $Na_2CO_3$ | 25.8 | 7 |
| *D. tertiolecta [28]* | $Na_2CO_3$ | 42 | |
| *Chlorella [40]* | $Na_2CO_3$ | 27.3 | 5 |
| *Spirulina [40]* | $Na_2CO_3$ | 20 | 4 |

### 3.3.5 Influence of co-solvents on product yields

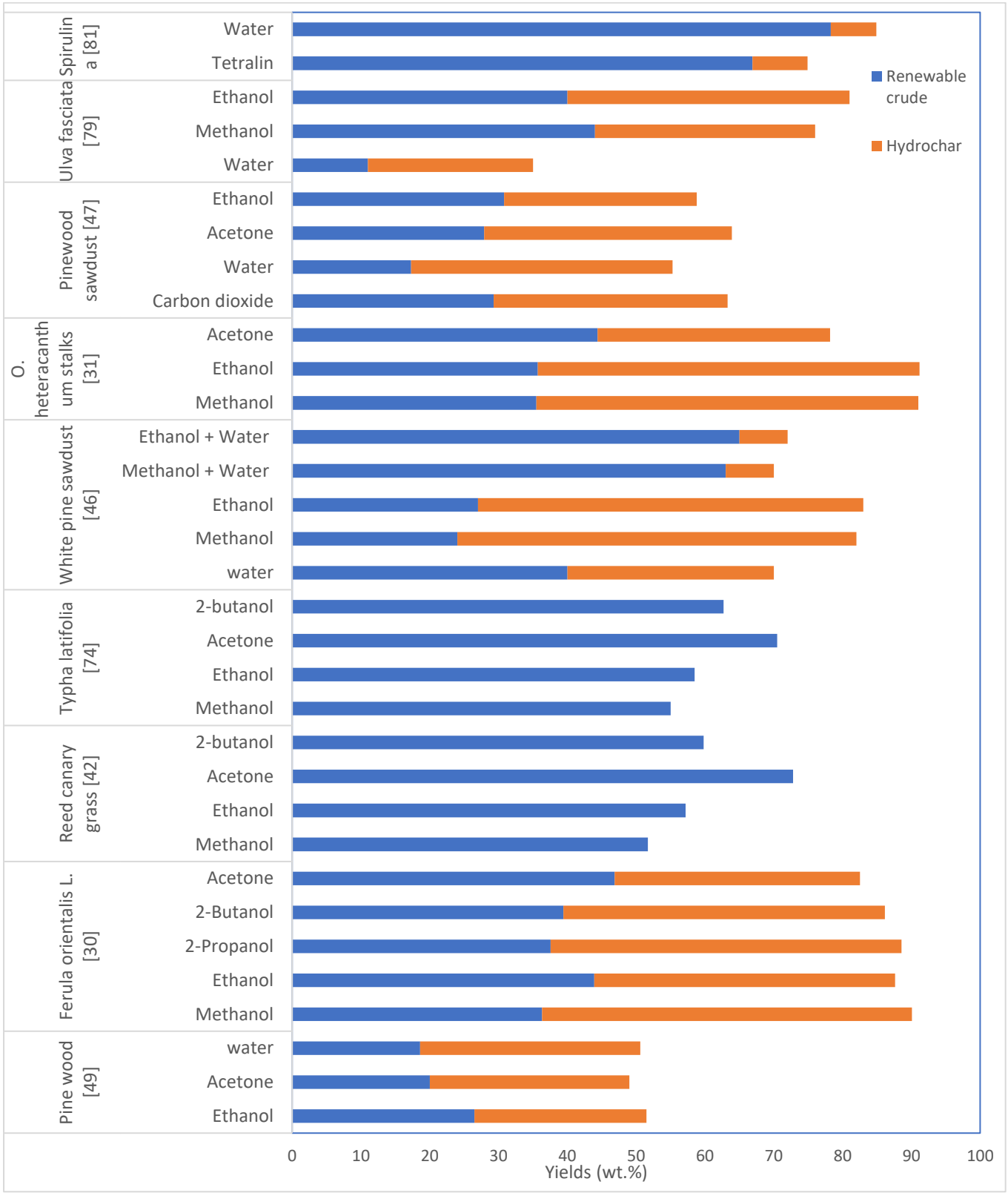


Figure 3.4: The influence of different co-solvents on renewable crude and hydrochar during the HTL of biomass.

In the HTL reaction, co-solvents can play a vital role in the product yields and separation of products. Liu et al. [49] point out that the presence of solvents can dilute the product concentration by avoiding reverse and cross linked reactions. HTL of biomass greatly depends on the use of solvents that can not only affect the products but also the content [31]. Even the properties of the products can also be changed in a positive way, which can lead the products to separate easily and effectively. For instance, some organic solvents, such as acetone, propanol, butanol, ethyl acetate and methyl ethyl ketone can lower the viscosity of the heavy oil produced from the HTL reaction [88].

Water, which is mostly used in HTL reactions, is also considered a solvent. In fact, water has several roles, i.e; as a solvent, reactant and catalyst. Though not all biomass are soluble in water, most biomass can be solubilised in water at high temperatures [89]. Figure 3.4 draws attention to the influence of several co-solvents, mixtures of two solvents and solvents with catalysts in feedstock.

However, various other organic co-solvents, i.e, ethanol and methanol, have also been investigated to examine their effects on the HTL reaction [49]. These alcoholic co-solvents can increase renewable crude yields significantly [41]. Different solvents have already been studied for HTL reactions, such as methanol, ethanol, mixtures of methanol, ethanol and water in various proportions [46], acetone [31], phenol, ethylene glycol, ethylene carbonate [62], polyethylene glycol [61], dichloromethane (DCM) [28], Chloroform [38, 90] and Tetrahydrofuran [81]. It is also noticeable that different solvents act differently for different raw materials. For instance, in case of HTL of pine wood, co-solvents' efficiency for renewable crude yields could be sequenced as ethanol > Acetone > water [49]. Nonetheless, for another raw material, like EFB, the solvents' efficiency for renewable crude could be sequenced glycol > water > ethanol > acetone > toluene [73] in terms of total oil and gas. Higher

efficiency of Acetone could be found for HTL of *Ferula orientalis L.* [30], reed canary grass [42], *Typha latifolia* [74] and milled *Onopordum heteracanthum* stalks [31].

Water was found to be an excellent solvent for overall renewable crude yields and for total conversion of corn stover [51], mixtures of native grassland perennials [52], *Cunninghamia lanceolate* [56], mixtures of *Spirulina platensis* (SP) and *Entermorpha prolifera* (EP) [29], *Nannochloropsis sp*. [78], *Chlorella* [40], *Nannochloropsis salina* and *Spirulina platensis* [39], *Dunaliella tertiolecta* [38] [28], Sewage sludge [43], Swine manure [80], oil palm shell [59], Spirulina [81] and arbitrary microalgae paste [32]. It seems that water can be a suitable co-solvent for HTL of all kinds for biomass. When water is mixed with another co-solvent, it also showed a significant effect on renewable crude products. For example, Ethanol–water (60%+40%) [27] in HTL of *Dunaliella tertiolecta* produces higher yields (64.68 wt.%). Further investigations of several co-solvents and solvents mixed with water also showed higher performance; for instance, during the HTL of white pine sawdust, co-solvent efficiency can be sequenced as Ethanol-Water (50%+50%) > Methanol-Water (50%+50%) > water > Ethanol > Methanol [46]. Water showed a good performance (40 wt.% oil) but Ethanol-Water (50%+50%) and Methanol-Water (50%+50%) produced 65 wt.% and 63 wt.% of renewable crude respectively.

### 3.4 Solid-Renewable crude interaction

Though HTL is focused on renewable crude production, there are significant amounts of solids (hydrochar) that are found from the reaction as deoxygenation and dehydration reactions makes the hydrochar more hydrophobic [91]. In the hydrophobic condition, the solid surfaces attach to the oil more strongly. There may have various reasons to make the hydrochar surface more hydrophobic during the HTL and HTC reactions. Some properties of renewable crude can give a sticky nature, which can cause more attachments with the solids. The solid renewable crude

interactions in the mixture make product extraction difficult. During the formation of renewable crude and hydrochar at high temperatures and under pressure, the series of chemical reactions can easily affect several properties of products, such as the wettability or contact angle, pH, viscosity, pores, surface area, and composition of products. Interactions between the solids and renewable crude can depend on the following properties.

### 3.4.1 Types of functional groups on solids

Functional groups are parts of the organic compounds. These have very specific types of function and property. The properties and type of attraction of solid renewable crude may depend on various factors; i.e, the type of functional groups. For example, non-polar functional groups are referred to as oil wet (hydrophobic) groups. This type of functional group has carbon, hydrogen and electronegative molecules such as $N_2$, $O_2$ and S. The oil-wet nature of nonpolar-functional groups frequently affects the shape of atoms holding these groups. For instance, proteins may fold, so that nonpolar-groups are clustered together and are not in contact with water.

Polar-functional groups also contain electronegative molecules such as $N_2$, $O_2$ and S. The existence of these electronegative atoms in any functional group produces an uneven distribution of electrical charges on the atoms that causes the bonds to become polar.

As polar bonds attract favourably with water, their properties can show a hydrophilic or water wet nature. The charged-functional group are the acids, which means they can form ions by releasing $H_2$ ions (H+), which can also be referred to as protons [92]. Existing non-polar functional groups in hydrochar found from HTL and HTC can cause the hydrochar surface to be oil-wet nature. Common types of non-polar functional groups, such as C-H stretching, C=C stretching, C=C bending, C-H bending, C=C-C stretching, C-H, C=C, and C-C are found in hydrochar after the HTL and HTC reaction. In some cases, more than one or two non-polar

functional groups can found in hydrochar produced from sweet potato waste [93], cellulose, lignin, d-xylose, Pine wood meal [94], orange peel [95], Palm empty fruit bunches [96*], Salix psammophila* [97], fish waste [98], Palm shell [99], sawdust, wheat straw, or corn stalk [100], Grape pomace [101], Cellulose [102, 103], water hyacinth [104], agricultural waste [105], sugar beet, bark [106], shrimp waste [107], oil palm shell [108], corncob and Miscanthus [109], Bamboo [110], walnut shells [111], sewage sludge [112], mixture of 7 agricultural wastes [113] and Kraft Lignin [114]; therefore, they can attract oil, which makes oil extraction difficult.

### 3.4.2 Wettability of hydrochar surfaces

In Figure 3.5, the different wettability conditions of a solid surface are illustrated, highlighting their specific effects on the attachment of liquids to the surface. Wettability plays a crucial role in determining how well a liquid (oil and water) adheres to a solid surface, influenced by both the properties of the solid surface and interfacial forces [115]. The three observed types of wettability are water-wet (favouring lower solid-oil interaction), oil-wet, and neutral wettability [116]. There is some uncertainty about the cut-off values, but usually a water droplet in a water-wet, or a hydrophilic condition will form a contact angle of less than 90°, while an angle greater than 90° will happen in an oil-wet, or hydrophobic system. Angles near 90° indicate neutral wetting [117] [118]

.

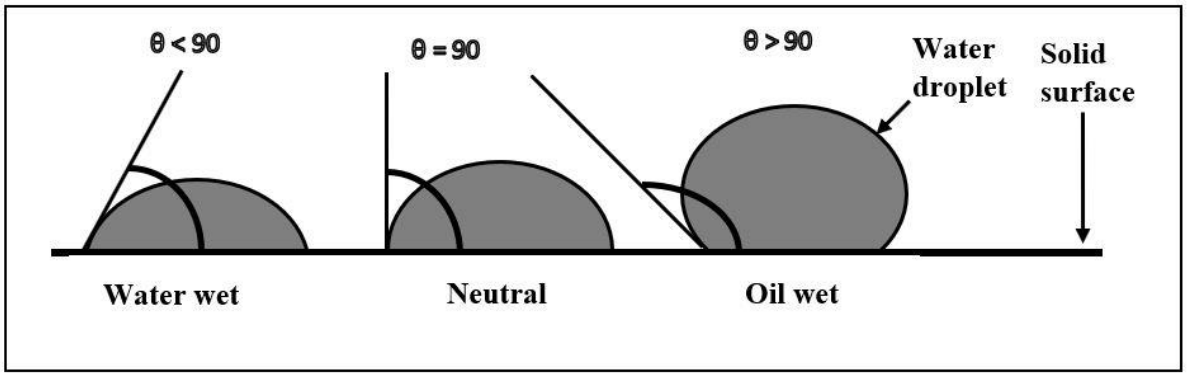


Figure 3.5: Interactions of a water droplet on a rock surface for three conditions. Adapted from Zhu et al. [119] and Formentin et al. [120].

Wettability is an important factor to explain the interactions of solids and liquids. In the case of a water wet condition, water normally covers the solid surface, making a continuous film that spreads into the small pores. Oil normally forms droplets on the top of this layout. On the other hand, in oil-wet conditions, oil normally covers the solid surface [121]. Some researchers focused on enhancing the hydrophobic (oil wet) characteristics of hydrochar because this property facilitates water removal during transportation and storage [115]. However, a water-wet (hydrophilic) condition is preferred for effective solid oil separation.

### 3.4.3 Influence of water in hydrophobicity

In the HTL process, $H_2O$ simultaneously performs as a reactant and a catalyst, which makes the procedure significantly different from pyrolysis. In a condition near to critical point, $H_2O$ has some very interesting properties: for instance, low viscosity and high solubility of organic substances. This makes subcritical water an outstanding medium for fast, homogeneous and also efficient reactions [122-124]. Subcritical water acts very differently from supercritical water. The dielectric constant reduces from 78 $Fm^{-1}$ at 25 °C and 0.1 MPa to 14.07 $Fm^{-1}$ at 350 °C and 20 MPa [125]. This can cause an increased solubility of the organic hydrophobic compounds, for example free fatty acids [126, 127].

### 3.4.4 pH

pH is the important factor which has an influence not only in solid-liquid formation, but also solid renewable crude interaction [20]. High pH can change the surface of hydrochar from a hydrophobic condition to a hydrophilic condition. This can release more residual oil from the pores. This release occurs due to a change in capillary pressure [117]. Therefore, it seems that a feedstock mixture with low pH can have more interactions with solids than a feedstock mixture with a high pH.

The change of pH in the HTL reaction also has an obvious impact on the products' formation and yield. For example, during the conversion of protein in HTL, protein is freely converted to renewable crude, via a series of chemical reactions, into amino acids and finally ammonium, which increases the pH further and also promotes a greater renewable crude yield [20]. Certain types of biomass, like *Anabaena cylindrica*, have a lot of protein content (43-56%) [128]. This high protein content can increase the pH, leading to more production of renewable crude and less interaction between solid oil during the HTL reaction.

### 3.4.5 Viscosity of renewable crude

Higher viscosity of the renewable crude (RNC) can cause multiphase flow and clogging or blocking of flow [129]; therefore, it cannot pass out easily if there is insufficient space. So, high viscous oil can easily be trapped inside the pores of the hydrochar surface. Thus, the viscosity of the RNC can be one of the reasons for solid-oil attachment or interaction.

### 3.4.6 Porosity and surface area of hydrochar

Solids with higher amounts of porous holes and a hydrophobic nature can obviously have more interactions with the renewable crude (RNC). The hydrophobic nature of the solids allows more oil to attach and porous holes can hold the oil. Therefore, a strong attachment between the soil and oil can be observed. On the other hand, higher amounts of porosity can increase the surface

area of solids. The formation of pores in hydrochar has been noticed during the hydrothermal conversion of biomass. As HTC is focused on hydrochar production, the majority of researchers analysed SEM for hydrochar produced from HTC. Gao et al. [130] found pores with diameters ranging from 5–25 μm in hydrochar produced from HTC of eucalyptus bark. Nizamuddin et al. [131] reported few pores on raw palm shell surfaces, but after HTC, the porosity was increased on the hydrochar surface. They reported that the surface structure was influenced by the reaction time. A similar influence for reaction time has been reported by Geo et al. [104], who stated that cellulose and hemicellulose decomposed at considerably higher reaction times, causing porosity on the hydrochar surface. Liu et al. [132] showed that hydrochar pellets from woody biomass and agro-residues had increased the surface area and porosity. HTC of oil palm shell resulted in surface porosity of the hydrochar, as well as a large surface area [133]. They noticed that raw materials (oil palm shell) represented 0.3106 $m^2/g$ of the surface area, 0.00129 $cm^3/g$ of total pore volume and 45.1133 nm of average pore diameter; however, after the HTC reaction, the surface area, total pore volume and average pore diameter significantly increased to 12.5996 $m^2/g$, 0.0357 $cm^3/g$ and 113.4120 nm, respectively.

Table 3.2 shows the type of porosity of hydrochar produced from different biomass feedstock. Beyond 250°C, the pore structure of hydrochar undergoes collapse and contraction as a result of biopolymer reformation, leading to a reduction in both porosity and surface area. The choice of feedstock significantly influences the surface areas of hydrochar. Hydrochar produced from lignocellulosic materials such as canola straw, wheat straw, hickory, peanut hull, and rice straw exhibit higher surface areas compared to non-lignocellulosic materials like sewage sludge and animal manure [134].

A greater surface area or pore structure facilitates increased contact with oil, developing stronger attachment between solids and oil. Therefore, it is certain that the attachment of RNC or oil to hydrochar varies due to the surface structure of hydrochar.

Table 3.2: Morphological structure of hydrochar derived from different biomass feedstocks.

| Biomass feedstock | Heating rate (ºC) | Residence time (h) | biomass/water ratio | Morphology of hydrochar | Ref. |
|---|---|---|---|---|---|
| Wood sawdust | 220 | 1.5 | 1:04 | Slightly porous | [135] |
| Tea stalk | 220 | 1.5 | 1:04 | Thick-wall pores | [134] |
| Apricot seed | 220 | 1.5 | 1:04 | Presence of microspheres | [134] |
| Spent coffee | 180, 200, 220 | 1, 3, 5 | 1:10 | enlarged pores | [136] |
| Corncobs | 230 | 0.5 | 1:06 | fine pores, microspheres | [137] |
| Maize straw | 220, 340 | 0.25, 0.33 | 1:03 | highly porous | [138] |
| Sewage sludge | 270 | 2 | 1:09 | honeycomb shaped porous structure | [139] |
| Walnut shell | 220 | 1.5 | 1:04 | Circular pores | [134] |

### 3.5 Recommendation to measure the renewable crude and solid attachment

The attachment between hydrochar and renewable crude (RNC) results from various factors. Conducting a property analysis of the hydrochar surface and RNC can help uncover the true cause of their attachment. It is crucial to examine surface properties of hydrochar, such as morphology and hydrophobicity. Similarly, for RNC, factors like viscosity and acidity are also significant considerations.

As the RNC and hydrochar stays as a mixture and there are pores in the hydrochar, the RNC can be trapped inside the pores of the hydrochar. It can be assumed that the more porosity the hydrochar has, the more RNC can be trapped inside. During the decomposition of biomass, the volatiles inside the biomass make some cavities or holes during their release, which increases the porosity in the surface of the hydrochar. Depending on the decomposition rate, the depth of porosity and the surface area of the pores varies. Therefore, porosity can hold RNC. Because of the high viscosity of RNC, it can easily be trapped inside the hydrochar.

If there are pores in the hydrochar, along with the properties of hydrophobicity, the trapping of oil can be strong. The degree of trapping can be a measurement that indicates how much renewable crude is trapped inside the hydrochar.

$$\text{So, Degree of trapping} = \frac{\text{Oil trapped inside the hydrochar}}{\text{Total renewable crude}}$$

The instrument Source Rock Analyser (SRA) can provide the value of the total trapped oil and the solid percentage from the hydrochar sample. A higher ratio indicates that a higher amount of renewable crude is trapped inside the hydrochar. The degree of trapping can be explained by changing the experimental parameters so that suitable experimental conditions for less oil trapping can be found.

### 3.6 Conclusions

The re-evaluation and re-analysis of HTL across a diverse range of biomass have provided valuable insights into the yields of hydrochar and renewable crude (RNC), as well as their interactions. HTL is a promising method for generating renewable crude from biomass, which serves as a viable alternative to fossil fuels. Understanding how processing parameters affect the yields and properties of hydrochar and renewable crude is therefore crucial, making this field of study highly significant. Based on the re-evaluation and re-analysis of HTL of biomass, the following conclusions can be drawn.

Higher temperatures, particularly within the range of 300 to 350 $^{o}$C, are favourable for obtaining higher yields of renewable crude due to enhanced biomass decomposition. Temperatures below 300 $^{o}$C, on the other hand, are more suitable for higher hydrochar yields. However, it is important to note that renewable crude yields may decrease at temperatures exceeding 350 $^{o}$C. This decline can be attributed to the re-polymerisation or further reactions of renewable crude at elevated temperatures, leading to the formation of other byproducts.

Suitable residence times differ for renewable crude and hydrochar yields. Lower residence times are preferred for higher renewable crude yields and lower hydrochar yields, especially when the temperature falls within the 300 to 350 $^{o}$C range. Conversely, higher residence times, coupled with elevated temperatures, can trigger secondary cracking or re-polymerisation of renewable crude, resulting in the generation of additional gas or solid products.

The higher the amount of solvent put into the HTL reaction, the greater the acceleration of the decomposition rate of biomass can be noticed, which also can lead to the production of more renewable crude yields and lower the hydrochar yields.

Some catalysts like $RbCO_3$, Fe, $FeSO_4$, $K_2CO_3$, HCL, $ZnCl_2$, $Na_2CO_3$ and caustic solutions can increase the renewable crude yields and decrease the hydrochar yield. Caustic solutions can also increase hydrochar for some biomass. For example, NaOH produces 71.1 wt.% hydrochar for HTL of Birch. Fe, $CsCO_3$, $H_2SO_4$, $AlCl_3$ can also be used for higher hydrochar yields.

The effectiveness of co-solvents varies depending on the biomass type. For instance, for pine wood, the sequence of solvent efficiency for RNC yields is as follows: ethanol > acetone > water. Conversely, for Oil palm empty fruit bunches, the sequence is as follows: ethylene glycol > water > ethanol > acetone > toluene. Solvents combined with catalysts demonstrate greater efficacy in producing renewable crude. Water is found to be suitable for various biomass types, including algae, wood, and waste materials. Ethanol-water (60%+40%) and methanol-water (50%+50%) mixtures have also been identified as significant solvents for renewable crude production. It should be noted that even after solvent extraction, some renewable crude may still remain trapped naturally within the hydrochar.

Viscous renewable crude can easily be trapped in the porous holes in solids. Therefore, porosity and viscosity are also related to interactions of solid-renewable crude. Hydrochar properties such as hydrophobicity (the oil-wet condition) facilitate the attraction of oil into solids. Non-

polar functional groups in solids, such as C-H stretching, C-H bending, and C=C stretching, exhibit an attraction for oil. Hydrochar's porosity plays a role in trapping oil within pores, and longer reaction times can result in increased porosity across surface areas.

**References**


1. Gollakota, A.R.K., N. Kishore, and S. Gu, *A review on hydrothermal liquefaction of biomass.* Renewable and Sustainable Energy Reviews, 2017.
2. Wang, W., Y. Kuang, and N. Huang, *Study on the decomposition of factors affecting energy-related carbon emissions in Guangdong province, China.* Energies, 2011. **4**(12): p. 2249-2272.
3. Hossain, M.A., J. Jewaratnam, and P. Ganesan, *Prospect of hydrogen production from oil palm biomass by thermochemical process – A review.* International Journal of Hydrogen Energy, 2016. **41**(38): p. 16637-16655.
4. Goswami, D.Y. and F. Kreith, *Handbook of energy efficiency and renewable energy*. 2007: Crc Press.
5. Hirel, B., et al., *Improving nitrogen use efficiency in crops for sustainable agriculture.* Sustainability, 2011. **3**(9): p. 1452-1485.
6. Robbins, M.P., et al., *New opportunities for the exploitation of energy crops by thermochemical conversion in Northern Europe and the UK.* Progress in Energy and Combustion Science, 2012. **38**(2): p. 138-155.
7. Biller, P., et al., *Nutrient recycling of aqueous phase for microalgae cultivation from the hydrothermal liquefaction process.* Algal Research, 2012. **1**(1): p. 70-76.
8. Kambo, H.S. and A. Dutta, *A comparative review of biochar and hydrochar in terms of production, physico-chemical properties and applications.* Renewable and Sustainable Energy Reviews, 2015. **45**(Supplement C): p. 359-378.
9. Jin, F., *Application of hydrothermal reactions to biomass conversion*. 2014: Springer Science & Business Media.
10. Dimitriadis, A. and S. Bezergianni, *Hydrothermal liquefaction of various biomass and waste feedstocks for biocrude production: A state of the art review.* Renewable and Sustainable Energy Reviews, 2017. **68**(Part 1): p. 113-125.
11. Bensaid, S., R. Conti, and D. Fino, *Direct liquefaction of ligno-cellulosic residues for liquid fuel production.* Fuel, 2012. **94**: p. 324-332.
12. Gao, Y., et al., *Effect of residence time on chemical and structural properties of hydrochar obtained by hydrothermal carbonization of water hyacinth.* Energy, 2013. **58**(Supplement C): p. 376-383.
13. Kumar, S., et al., *Hydrothermal pretreatment of switchgrass and corn stover for production of ethanol and carbon microspheres.* Biomass and Bioenergy, 2011. **35**(2): p. 956-968.
14. Toor, S.S., *Modeling and Optimization of Catliq Liquid Bioful Process*. 2010: Department of Energy Technology, Aalborg University.

15. Funke, A. and F. Ziegler, *Hydrothermal carbonization of biomass: a summary and discussion of chemical mechanisms for process engineering.* Biofuels, Bioproducts and Biorefining, 2010. **4**(2): p. 160-177.
16. Mumme, J., et al., *Hydrothermal carbonization of anaerobically digested maize silage.* Bioresource Technology, 2011. **102**(19): p. 9255-9260.
17. Kean, C.W., J.N. Sahu, and W.W. Daud, *Hydrothermal gasification of palm shell biomass for synthesis of hydrogen fuel.* BioResources, 2013. **8**(2): p. 1831-1840.
18. Fang, J., et al., *Minireview of potential applications of hydrochar derived from hydrothermal carbonization of biomass.* Journal of Industrial and Engineering Chemistry, 2018. **57**(Supplement C): p. 15-21.
19. He, C., A. Giannis, and J.-Y. Wang, *Conversion of sewage sludge to clean solid fuel using hydrothermal carbonization: Hydrochar fuel characteristics and combustion behavior.* Applied Energy, 2013. **111**(Supplement C): p. 257-266.
20. Biller, P. and A. Ross, *Production of biofuels via hydrothermal conversion*, in *Handbook of biofuels production*. 2016, Woodhead Publishing. p. 509-547.
21. Shah, Y.T., *Energy and fuel systems integration*. 2015: CRC Press.
22. Toor, S.S., L. Rosendahl, and A. Rudolf, *Hydrothermal liquefaction of biomass: A review of subcritical water technologies.* Energy, 2011. **36**(5): p. 2328-2342.
23. Zein, M. and R. Winter, *Effect of temperature, pressure and lipid acyl chain length on the structure and phase behaviour of phospholipid–gramicidin bilayers.* Physical Chemistry Chemical Physics, 2000. **2**(20): p. 4545-4551.
24. Jae, J., et al., *Depolymerization of lignocellulosic biomass to fuel precursors: maximizing carbon efficiency by combining hydrolysis with pyrolysis.* Energy & Environmental Science, 2010. **3**(3): p. 358-365.
25. Jena, U., et al., *Oleaginous yeast platform for producing biofuels via co-solvent hydrothermal liquefaction.* Biotechnology for biofuels, 2015. **8**(1): p. 167.
26. Akhtar, J. and N.A.S. Amin, *A review on process conditions for optimum bio-oil yield in hydrothermal liquefaction of biomass.* Renewable and Sustainable Energy Reviews, 2011. **15**(3): p. 1615-1624.
27. Chen, Y., et al., *Direct liquefaction of Dunaliella tertiolecta for bio-oil in sub/supercritical ethanol–water.* Bioresource Technology, 2012. **124**(Supplement C): p. 190-198.
28. Minowa, T., et al., *Oil production from algal cells of Dunaliella tertiolecta by direct thermochemical liquefaction.* Fuel, 1995. **74**(12): p. 1735-1738.
29. Jin, B., et al., *Co-liquefaction of micro- and macroalgae in subcritical water.* Bioresource Technology, 2013. **149**(Supplement C): p. 103-110.
30. Aysu, T. and M.M. Küçük, *Liquefaction of giant fennel (Ferula orientalis L.) in supercritical organic solvents: Effects of liquefaction parameters on product yields and character.* The Journal of Supercritical Fluids, 2013. **83**(Supplement C): p. 104-123.
31. Durak, H. and T. Aysu, *Effects of catalysts and solvents on liquefaction of Onopordum heteracanthum for production of bio-oils.* Bioresource Technology, 2014. **166**(Supplement C): p. 309-317.
32. Brown, T.M., P. Duan, and P.E. Savage, *Hydrothermal liquefaction and gasification of Nannochloropsis sp.* Energy Fuels, 2010. **24**(6): p. 3639-3646.

33. Dote, Y., et al., *Recovery of liquid fuel from hydrocarbon-rich microalgae by thermochemical liquefaction.* Fuel, 1994. **73**(12): p. 1855-1857.
34. Malins, K., et al., *Bio-oil from thermo-chemical hydro-liquefaction of wet sewage sludge.* Bioresource Technology, 2015. **187**(Supplement C): p. 23-29.
35. Anastasakis, K. and A.B. Ross, *Hydrothermal liquefaction of the brown macro-alga Laminaria Saccharina: Effect of reaction conditions on product distribution and composition.* Bioresource Technology, 2011. **102**(7): p. 4876-4883.
36. Cheng, J., et al., *Biodiesel production from lipids in wet microalgae with microwave irradiation and bio-crude production from algal residue through hydrothermal liquefaction.* Bioresource Technology, 2014. **151**(Supplement C): p. 415-418.
37. Chen, W.-T., et al., *Co-liquefaction of swine manure and mixed-culture algal biomass from a wastewater treatment system to produce bio-crude oil.* Applied Energy, 2014. **128**(Supplement C): p. 209-216.
38. Shuping, Z., et al., *Production and characterization of bio-oil from hydrothermal liquefaction of microalgae Dunaliella tertiolecta cake.* Energy, 2010. **35**(12): p. 5406-5411.
39. Toor, S.S., et al., *Hydrothermal liquefaction of Spirulina and Nannochloropsis salina under subcritical and supercritical water conditions.* Bioresource Technology, 2013. **131**(Supplement C): p. 413-419.
40. Ross, A.B., et al., *Hydrothermal processing of microalgae using alkali and organic acids.* Fuel, 2010. **89**(9): p. 2234-2243.
41. Singh, R., T. Bhaskar, and B. Balagurumurthy, *Effect of solvent on the hydrothermal liquefaction of macro algae Ulva fasciata.* Process Safety and Environmental Protection, 2015. **93**: p. 154-160.
42. Aysu, T., *Supercritical fluid extraction of reed canary grass (Phalaris arundinacea).* Biomass and Bioenergy, 2012. **41**(Supplement C): p. 139-144.
43. Zhai, Y., et al., *Influence of sewage sludge-based activated carbon and temperature on the liquefaction of sewage sludge: Yield and composition of bio-oil, immobilization and risk assessment of heavy metals.* Bioresource Technology, 2014. **159**: p. 72-79.
44. Zhong, C. and X. Wei, *A comparative experimental study on the liquefaction of wood.* Energy, 2004. **29**(11): p. 1731-1741.
45. Xu, C. and T. Etcheverry, *Hydro-liquefaction of woody biomass in sub- and super-critical ethanol with iron-based catalysts.* Fuel, 2008. **87**(3): p. 335-345.
46. Cheng, S., et al., *Highly efficient liquefaction of woody biomass in hot-compressed alcohol− water co-solvents.* Energy & Fuels, 2010. **24**(9): p. 4659-4667.
47. Wang, Y., et al., *Effects of solvents and catalysts in liquefaction of pinewood sawdust for the production of bio-oils.* Biomass and Bioenergy, 2013. **59**(Supplement C): p. 158-167.
48. Sun, P., et al., *Analysis of liquid and solid products from liquefaction of paulownia in hot-compressed water.* Energy Conversion and Management, 2011. **52**(2): p. 924-933.
49. Liu, Z. and F.-S. Zhang, *Effects of various solvents on the liquefaction of biomass to produce fuels and chemical feedstocks.* Energy Conversion and Management, 2008. **49**(12): p. 3498-3504.

50. Xu, C. and J. Lancaster, *Conversion of secondary pulp/paper sludge powder to liquid oil products for energy recovery by direct liquefaction in hot-compressed water.* Water Research, 2008. **42**(6): p. 1571-1582.
51. Zhang, B., M. von Keitz, and K. Valentas, *Thermal effects on hydrothermal biomass liquefaction.* Applied Biochemistry and Biotechnology, 2008. **147**(1-3): p. 143-150.
52. Zhang, B., M. von Keitz, and K. Valentas, *Thermochemical liquefaction of high-diversity grassland perennials.* Journal of Analytical and Applied Pyrolysis, 2009. **84**(1): p. 18-24.
53. Akalın, M.K., K. Tekin, and S. Karagöz, *Hydrothermal liquefaction of cornelian cherry stones for bio-oil production.* Bioresource Technology, 2012. **110**(Supplement C): p. 682-687.
54. Tekin, K., S. Karagöz, and S. Bektaş, *Hydrothermal liquefaction of beech wood using a natural calcium borate mineral.* The Journal of Supercritical Fluids, 2012. **72**(Supplement C): p. 134-139.
55. Meryemoğlu, B., et al., *Biofuel production by liquefaction of kenaf (Hibiscus cannabinus L.) biomass.* Bioresource Technology, 2014. **151**(Supplement C): p. 278-283.
56. Qu, Y., X. Wei, and C. Zhong, *Experimental study on the direct liquefaction of Cunninghamia lanceolata in water.* Energy, 2003. **28**(7): p. 597-606.
57. Chan, Y.H., et al., *Bio-oil production from oil palm biomass via subcritical and supercritical hydrothermal liquefaction.* The Journal of Supercritical Fluids, 2014. **95**(Supplement C): p. 407-412.
58. LI, R.-d., et al., *Liquefaction of rice stalk in sub-and supercritical ethanol.* Journal of Fuel Chemistry and Technology, 2013. **41**(12): p. 1459-1465.
59. Minowa, T., T. Kondo, and S.T. Sudirjo, *Thermochemical liquefaction of indonesian biomass residues.* Biomass and Bioenergy, 1998. **14**(5): p. 517-524.
60. Wei, N., et al., *Liquefaction and substitution of switchgrass (Panicum virgatum) based bio-oil into epoxy resins.* Industrial Crops and Products, 2014. **57**(Supplement C): p. 116-123.
61. Ye, L., et al., *Liquefaction of bamboo shoot shell for the production of polyols.* Bioresource Technology, 2014. **153**(Supplement C): p. 147-153.
62. Yip, J., et al., *Comparative study of liquefaction process and liquefied products from bamboo using different organic solvents.* Bioresource Technology, 2009. **100**(24): p. 6674-6678.
63. Li, R.-d., et al., *Liquefaction of rice stalk in sub- and supercritical ethanol.* Journal of Fuel Chemistry and Technology, 2013. **41**(12): p. 1459-1465.
64. Zhu, W.-W., et al., *Cornstalk liquefaction in methanol/water mixed solvents.* Fuel Processing Technology, 2014. **117**: p. 1-7.
65. Duan, P. and P.E. Savage, *Hydrothermal liquefaction of a microalga with heterogeneous catalysts.* Industrial & Engineering Chemistry Research, 2010. **50**(1): p. 52-61.
66. Duan, P., et al., *Catalytic upgrading of pretreated algal bio-oil over zeolite catalysts in supercritical water.* Biochemical Engineering Journal, 2016. **116**(Supplement C): p. 105-112.

67. Maldas, D. and N. Shiraishi, *Liquefaction of biomass in the presence of phenol and H2O using alkalies and salts as the catalyst.* Biomass and Bioenergy, 1997. **12**(4): p. 273-279.
68. Karagöz, S., et al., *Effect of Rb and Cs carbonates for production of phenols from liquefaction of wood biomass.* Fuel, 2004. **83**(17): p. 2293-2299.
69. Sun, P., et al., *Direct liquefaction of paulownia in hot compressed water: Influence of catalysts.* Energy, 2010. **35**(12): p. 5421-5429.
70. Tymchyshyn, M. and C. Xu, *Liquefaction of bio-mass in hot-compressed water for the production of phenolic compounds.* Bioresource Technology, 2010. **101**(7): p. 2483-2490.
71. Lu, J., et al., *Liquefaction of fermentation residue of reed- and corn stover-pretreated with liquid hot water in the presence of ethanol with aluminum chloride as the catalyst.* Chemical Engineering Journal, 2014. **247**(Supplement C): p. 142-151.
72. Minowa, T., et al., *Oil production from garbage by thermochemical liquefaction.* Biomass and Bioenergy, 1995. **8**(2): p. 117-120.
73. Fan, S.-P., et al., *Comparative studies of products obtained from solvolysis liquefaction of oil palm empty fruit bunch fibres using different solvents.* Bioresource Technology, 2011. **102**(3): p. 3521-3526.
74. Aysu, T., M. Turhan, and M.M. Küçük, *Liquefaction of Typha latifolia by supercritical fluid extraction.* Bioresource Technology, 2012. **107**(Supplement C): p. 464-470.
75. Küçük, M.M. and S. Ağırtaş, *Liquefaction of Prangmites australis by supercritical gas extraction.* Bioresource Technology, 1999. **69**(2): p. 141-143.
76. Cemek, M. and M.M. Küçük, *Liquid products from Verbascum stalk by supercritical fluid extraction.* Energy Conversion and Management, 2001. **42**(2): p. 125-130.
77. Erzengin, M. and M.M. Küçük, *Liquefaction of sunflower stalk by using supercritical extraction.* Energy Conversion and Management, 1998. **39**(11): p. 1203-1206.
78. Valdez, P.J., et al., *Hydrothermal liquefaction of Nannochloropsis sp.: Systematic study of process variables and analysis of the product fractions.* Biomass and Bioenergy, 2012. **46**(Supplement C): p. 317-331.
79. Singh, R., T. Bhaskar, and B. Balagurumurthy, *Effect of solvent on the hydrothermal liquefaction of macro algae Ulva fasciata.* Process Safety and Environmental Protection, 2015. **93**(Supplement C): p. 154-160.
80. Xiu, S., et al., *Hydrothermal pyrolysis of swine manure to bio-oil: Effects of operating parameters on products yield and characterization of bio-oil.* Journal of Analytical and Applied Pyrolysis, 2010. **88**(1): p. 73-79.
81. Matsui, T.-o., et al., *Liquefaction of micro-algae with iron catalyst.* Fuel, 1997. **76**(11): p. 1043-1048.
82. Pisupati, S.V. and A.H. Tchapda, *Thermochemical Processing of Biomass*, in *Advances in Bioprocess Technology*. 2015, Springer. p. 277-314.
83. Nasir Uddin, M., W.M.A.W. Daud, and H.F. Abbas, *Potential hydrogen and non-condensable gases production from biomass pyrolysis: Insights into the process variables.* Renewable and Sustainable Energy Reviews, 2013. **27**: p. 204-224.

84. Morf, P., P. Hasler, and T. Nussbaumer, *Mechanisms and kinetics of homogeneous secondary reactions of tar from continuous pyrolysis of wood chips.* Fuel, 2002. **81**(7): p. 843-853.
85. Yang, H., et al., *Pyrolysis of palm oil wastes for enhanced production of hydrogen rich gases.* Fuel Processing Technology, 2006. **87**(10): p. 935-942.
86. Lam, S.S., et al., *Microwave-heated pyrolysis of waste automotive engine oil: Influence of operation parameters on the yield, composition, and fuel properties of pyrolysis oil.* Fuel, 2012. **92**(1): p. 327-339.
87. Yin, S., et al., *Subcritical hydrothermal liquefaction of cattle manure to bio-oil: Effects of conversion parameters on bio-oil yield and characterization of bio-oil.* Bioresource Technology, 2010. **101**(10): p. 3657-3664.
88. Demirbaş, A., *Mechanisms of liquefaction and pyrolysis reactions of biomass.* Energy Conversion and Management, 2000. **41**(6): p. 633-646.
89. Chornet, E. and R.P. Overend, *Biomass liquefaction: an overview*, in *Fundamentals of thermochemical biomass conversion*. 1985, Springer. p. 967-1002.
90. Yang, Y.F., et al., *Analysis of energy conversion characteristics in liquefaction of algae.* Resources, Conservation and Recycling, 2004. **43**(1): p. 21-33.
91. Liu, Z., et al., *Production of solid biochar fuel from waste biomass by hydrothermal carbonization.* Fuel, 2013. **103**: p. 943-949.
92. *An Overview of the Zeta Potential*. [cited 2018 2 February]; Available from: http://www.particlesciences.com/news/technical-briefs/2012/overview-of-zeta-potential.html.
93. Chen, X., et al., *Conversion of sweet potato waste to solid fuel via hydrothermal carbonization.* Bioresource Technology, 2018. **249**: p. 900-907.
94. Kang, S., et al., *Characterization of hydrochars produced by hydrothermal carbonization of lignin, cellulose, D-xylose, and wood meal.* Industrial & engineering chemistry research, 2012. **51**(26): p. 9023-9031.
95. Fernandez, M.E., et al., *Development and characterization of activated hydrochars from orange peels as potential adsorbents for emerging organic contaminants.* Bioresource Technology, 2015. **183**: p. 221-228.
96. Parshetti, G.K., S. Kent Hoekman, and R. Balasubramanian, *Chemical, structural and combustion characteristics of carbonaceous products obtained by hydrothermal carbonization of palm empty fruit bunches.* Bioresource Technology, 2013. **135**: p. 683-689.
97. Zhu, X., et al., *Preparation of magnetic porous carbon from waste hydrochar by simultaneous activation and magnetization for tetracycline removal.* Bioresource Technology, 2014. **154**: p. 209-214.
98. Kannan, S., Y. Gariepy, and G.S.V. Raghavan, *Optimization and characterization of hydrochar produced from microwave hydrothermal carbonization of fish waste.* Waste Management, 2017. **65**: p. 159-168.
99. Nizamuddin, S., et al., *Chemical, dielectric and structural characterization of optimized hydrochar produced from hydrothermal carbonization of palm shell.* Fuel, 2016. **163**: p. 88-97.

100. Sun, K., et al., *Characterization of potassium hydroxide (KOH) modified hydrochars from different feedstocks for enhanced removal of heavy metals from water.* Environmental Science and Pollution Research, 2015. **22**(21): p. 16640-16651.
101. PetroviĿ, J., et al., *Hydrothermal conversion of grape pomace: Detailed characterization of obtained hydrochar and liquid phase.* Journal of Analytical and Applied Pyrolysis, 2016. **118**: p. 267-277.
102. Reza, M.T., et al., *Production, characterization, and biogas application of magnetic hydrochar from cellulose.* Bioresource Technology, 2015. **186**: p. 34-43.
103. Diakité, M., et al., *Chemical and morphological changes in hydrochars derived from microcrystalline cellulose and investigated by chromatographic, spectroscopic and adsorption techniques.* Bioresource technology, 2013. **150**: p. 98-105.
104. Gao, Y., et al., *Effect of residence time on chemical and structural properties of hydrochar obtained by hydrothermal carbonization of water hyacinth.* Energy, 2013. **58**: p. 376-383.
105. Donar, Y.O., E. Çağlar, and A. Sınağ, *Preparation and characterization of agricultural waste biomass based hydrochars.* Fuel, 2016. **183**: p. 366-372.
106. Cao, X., et al., *Effects of biomass types and carbonization conditions on the chemical characteristics of hydrochars.* Journal of agricultural and food chemistry, 2013. **61**(39): p. 9401-9411.
107. Kannan, S., Y. Gariepy, and G.V. Raghavan, *Optimization and characterization of hydrochar derived from shrimp waste.* Energy & Fuels, 2017. **31**(4): p. 4068-4077.
108. Nizamuddin, S., et al., *Synthesis and characterization of hydrochars produced by hydrothermal carbonization of oil palm shell.* The Canadian Journal of Chemical Engineering, 2015. **93**(11): p. 1916-1921.
109. Calucci, L., D.P. Rasse, and C. Forte, *Solid-state nuclear magnetic resonance characterization of chars obtained from hydrothermal carbonization of corncob and miscanthus.* Energy & Fuels, 2012. **27**(1): p. 303-309.
110. Li, Y., et al., *Production and optimization of bamboo hydrochars for adsorption of Congo red and 2-naphthol.* Bioresource Technology, 2016. **207**: p. 379-386.
111. Li, Y. and X. Liu, *Activated carbon/ZnO composites prepared using hydrochars as intermediate and their electrochemical performance in supercapacitor.* Materials Chemistry and Physics, 2014. **148**(1): p. 380-386.
112. He, C., et al., *Multiscale characteristics dynamics of hydrochar from hydrothermal conversion of sewage sludge under sub- and near-critical water.* Bioresource Technology, 2016. **211**: p. 486-493.
113. Zhu, X., et al., *Investigation on the physical and chemical properties of hydrochar and its derived pyrolysis char for their potential application: influence of hydrothermal carbonization conditions.* Energy & Fuels, 2015. **29**(8): p. 5222-5230.
114. Wikberg, H., et al., *Structural and morphological changes in kraft lignin during hydrothermal carbonization.* ACS Sustainable Chemistry & Engineering, 2015. **3**(11): p. 2737-2745.
115. Islam, M.T., et al., *Blending hydrochar improves hydrophobic properties of corn stover pellets.* 2022: p. 1-12.

116. Hirasaki, G., *Wettability: fundamentals and surface forces.* SPE Formation Evaluation, 1991. **6**(02): p. 217-226.
117. Donaldson, E. and W. Alam, *Wettability. Houston.* TX: Gulf Publishing Company, 2008.
118. Yuan, Y. and T.R. Lee, *Contact angle and wetting properties*, in *Surface science techniques*. 2013, Springer. p. 3-34.
119. Zhu, Y., et al., *Prediction of Contact Angle for Oriented Hydrophobic Surface and Experimental Verification by Micro-Milling.* 2023. **13**(8): p. 1305.
120. Formentín, P., et al., *Hydrophobic-oleophilic surfaces based on chemical modification of nanoporous alumina.* 2023. **302**: p. 127686.
121. Abdallah, W., Buckley, J. S., Carnegie, A., Edwards, J., Herold, B., Fordham, E., Graue, A., Habashy, T., Seleznev, N., Signer, C., Hussain, H., Montaron, B. and Ziauddin, M, *Fundamentals of Wettability.* Oilfield Review, 2007. **19**(2): p. 44-61.
122. Kruse, A. and E. Dinjus, *Hot compressed water as reaction medium and reactant: Properties and synthesis reactions.* The Journal of Supercritical Fluids, 2007. **39**(3): p. 362-380.
123. Krammer, P. and H. Vogel, *Hydrolysis of esters in subcritical and supercritical water.* The Journal of Supercritical Fluids, 2000. **16**(3): p. 189-206.
124. de Caprariis, B., et al., *Hydrothermal liquefaction of biomass: Influence of temperature and biomass composition on the bio-oil production.* Fuel, 2017. **208**: p. 618-625.
125. Uematsu, M. and E. Frank, *Static dielectric constant of water and steam.* Journal of Physical and Chemical Reference Data, 1980. **9**(4): p. 1291-1306.
126. King, J., R. Holliday, and G. List, *Hydrolysis of soybean oil. in a subcritical water flow reactor.* Green Chemistry, 1999. **1**(6): p. 261-264.
127. Biswas, B., et al., *Valorization of Sargassum tenerrimum: Value addition using hydrothermal liquefaction.* Fuel, 2018. **222**: p. 394-401.
128. Sharma, N., et al., *Effect of catalyst and temperature on the quality and productivity of HTL bio-oil from microalgae: A review.* 2021. **174**: p. 810-822.
129. Martínez-Palou, R., et al., *Transportation of heavy and extra-heavy crude oil by pipeline: A review.* Journal of Petroleum Science and Engineering, 2011. **75**(3): p. 274-282.
130. Gao, P., et al., *Preparation and characterization of hydrochar from waste eucalyptus bark by hydrothermal carbonization.* Energy, 2016. **97**: p. 238-245.
131. Nizamuddin, S., et al., *Chemical, dielectric and structural characterization of optimized hydrochar produced from hydrothermal carbonization of palm shell.* Fuel, 2016. **163**: p. 88-97.
132. Liu, Z., A. Quek, and R. Balasubramanian, *Preparation and characterization of fuel pellets from woody biomass, agro-residues and their corresponding hydrochars.* Applied Energy, 2014. **113**: p. 1315-1322.
133. Nizamuddin, S., et al., *Synthesis and characterization of hydrochars produced by hydrothermal carbonization of oil palm shell.* The Canadian Journal of Chemical Engineering, 2015. **93**(11): p. 1916-1921.
134. Khosravi, A., et al., *Production and characterization of hydrochars and their application in soil improvement and environmental remediation.* 2022. **430**: p. 133142.

135. Kabakcı, S.B. and S.S.J.W.M. Baran, *Hydrothermal carbonization of various lignocellulosics: Fuel characteristics of hydrochars and surface characteristics of activated hydrochars.* 2019. **100**: p. 259-268.
136. Afolabi, O.O., M. Sohail, and Y.-L.J.R.E. Cheng, *Optimisation and characterisation of hydrochar production from spent coffee grounds by hydrothermal carbonisation.* 2020. **147**: p. 1380-1391.
137. Zhang, T., et al., *Ammonium nitrogen recovery from digestate by hydrothermal pretreatment followed by activated hydrochar sorption.* 2020. **379**: p. 122254.
138. Wang, G., et al., *Hydrothermal carbonization of maize straw for hydrochar production and its injection for blast furnace.* 2020. **266**: p. 114818.
139. Liu, X., et al., *Hydrothermal carbonization of sewage sludge: Effect of feed-water pH on hydrochar's physicochemical properties, organic component and thermal behavior.* 2020. **388**: p. 122084.

# Chapter 4: Influence of HTL processing parameters on solid-renewable crude formation and interaction during the HTL of relevant feed focusing on carbohydrate.

# Statement of Authorship

| | |
|---|---|
| Title of Paper | Influence of HTL processing parameters on solid-renewable crude formation and interaction during the HTL of relevant feed focusing on carbohydrate. |
| Publication Status | ☐ Published ☐ Accepted for Publication<br>☐ Submitted for Publication ☑ Unpublished and Unsubmitted work written in manuscript style |
| Publication Details | |

## Principal Author

| | |
|---|---|
| Name of Principal Author (Candidate) | Md Arafat Hossain |
| Contribution to the Paper | HTL Experimental design and method<br>Concept developments<br>Raw materials preparations and HTL batch experiments<br>Method developments for analysis<br>Characterizations of the HTL products<br>Drafting the manuscript |
| Overall percentage (%) | 80% |
| Certification: | This paper reports on original research I conducted during the period of my Higher Degree by Research candidature and is not subject to any obligations or contractual agreements with a third party that would constrain its inclusion in this thesis. I am the primary author of this paper. |
| Signature | Date 14/07/2023 |

## Co-Author Contributions

By signing the Statement of Authorship, each author certifies that:

i. the candidate's stated contribution to the publication is accurate (as detailed above);

ii. permission is granted for the candidate in include the publication in the thesis; and

iii. the sum of all co-author contributions is equal to 100% less the candidate's stated contribution.

| | |
|---|---|
| Name of Co-Author | David Lewis |
| Contribution to the Paper | Concept developments<br>Assistance with analysis and interpretation of data<br>Reviewing the manuscript<br>Supervise the overall work |
| Signature | Date 19/07/2023 |

| | |
|---|---|
| Name of Co-Author | Tony Hall |
| Contribution to the Paper | Method design and analysis of Source Rock Analyser (SRA) |
| Signature | Date 29/08/2022 |

Please cut and paste additional co-author panels here as required.

| | | | |
|---|---|---|---|
| Name of Co-Author | Philip van Eyk | | |
| Contribution to the Paper | HTL reactor design and method<br>Concept developments<br>Assistance with analysis interpretation of data<br>Drafting and the reviewing manuscript<br>Supervise the overall work | | |
| Signature | | Date | 18/7/2023 |

# Influence of HTL processing parameters on solid-renewable crude formation and interaction during the HTL of relevant feed focusing on carbohydrate.

[a]Md Arafat Hossain, [a]David Lewis, [b]Tony Hall, [a]Philip van Eyk

[a]School of Chemical Engineering, The University of Adelaide, Adelaide, South Australia 5005, Australia

[b]School of Physics, Chemistry and Earth Sciences, The University of Adelaide, Adelaide, South Australia 5005, Australia

## Abstract

HTL of biomass is a promising thermochemical process for generating renewable crude as an alternative to fossil fuels. However, the trapping of renewable crude in solids during HTL poses a challenge for efficient extraction. This study aims to investigate the influence of key process parameters, including temperature (260-350 $^{o}$C), residence time (10-25 minutes), and biomass/water ratio (0.25-1), on product yields and the trapping of renewable crude in solids. Solvent extraction method (using dichloromethane (DCM)) has been employed to identify the recovered renewable crude from solid and trapped crude in solid. Source rock analyser (SRA) has been used to identify the light oil and heavy oil that are trapped in solids before and after solvent extraction. The results show that increasing the temperature from 260 to 350 $^{o}$C leads to a significant 67% increase in renewable crude yields. However, longer residence times and higher biomass/water ratios decrease the overall renewable crude yields by approximately 37% and 7 wt.%, respectively. Solvent (Dichloromethane) can extract maximum 58% of total renewable crude at 350 $^{o}$C, 10 min residence time and 0.5 of B/W ratio. Maximum degree of renewable crude trapping has been observed at the hydrochar produced at temperature 320 $^{o}$C. It is also noticeable that, the solvent (DCM) can extract more light oil than heavy oil from solids.

**Keywords:** Hydrothermal liquefaction, Renewable crude, solvent extraction, Source rock analysis, cellulose

## 4.1 Introduction

As an abundant source of renewable energy, biomass can be considered one of the promising sources and will be a significant part of sustainable energy systems for the future [1]. The Carbon (C), which makes a significant contribution to the overall heating value, forms a hydrocarbon group (C-H) to build up the biomass block [2]. Hydrogen (H), which is another important constituent of any biomass, has the highest energy value (120 MJ/kg) compared with other conventional fuels [3]. At the point of thermal conversion, $H_2$ is converted into water ($H_2O$), which plays a vital role in the overall heating value [4]. Nitrogen (N), Sulphur (S) and Oxygen (O) are other key elements of the biomass. Herbaceous biomass species obtain a higher amount of nitrogen (0.4 to 1.0 wt% ) and sulphur compared with any woody biomass [5, 6]. Nitrogen present in the biomass does not oxidise during thermal conversion and therefore it contributes to the overall heating values. During the HTL of biomass, all these elements go through depolymerisation, decomposition and recombination and produce the renewable crude that can be considered an alternative to fossil fuel [1]. HTL happens at the subcritical condition (temperature 250 – 370 $^{o}$C, pressure 4 – 20 MPa) and produce renewable crude (RNC), together with hydrochar, gaseous and aqueous phase as by-products [7]. The produced renewable crude from the HTL technique can be upgraded using typical refining methods to obtain gasoline, diesel oil or naphtha [8]. There are several advantages to the HTL reaction over other, popular biomass conversion techniques, like pyrolysis. Dry biomass is needed for the pyrolysis process, but drying the biomass is not necessary for an HTL reaction. Therefore, it holds great economic value for fuel production because of the wet nature of various feedstock of biomass, including low quality feedstock [9, 10]. Furthermore, sometimes the pyrolysis process requires catalysts, but the solvent (water) used in HTL, can perform as a catalyst in subcritical conditions. Lower oxygen and moisture contents and higher heating values can be observed in HTL products in comparison with pyrolysis products [11]. Furthermore, it has been found that the operating

pressure is high in HTL reactions, which can increase the biomass conversion rate during the reaction.

Yin et. al. [12] investigated the HTL of cellulose under acidic, neutral and alkaline conditions and reported the renewable crude yields. They reported the influence of temperature (275 to 330 $^{o}$C) and time (0 to 30 min) without showing the effect of the biomass/solvent ratio in feedstock, which is also an important factor in HTL reactions. Jin et al. [13] proved that the biomass/solvent ratio has a significant effect on renewable crude yields. Moller et. al. [14] also investigated the HTL of cellulose to understand the role of crystallinity in reactivity. They mainly focused on the products of total organic Carbon (TOC), glucose and 5-(hydroxymethyl)furfural (5-HMF) without reporting any other products like overall renewable crude, hydrochar and flue gas. Some researchers have focused on the characterisation of the renewable crude from cellulose. Gao et al. [15] mainly reported the characterisation of products from the hydrothermal reactions of cellulose. Although they reported the renewable crude and solids yields, other HTL products were not reported. They also did not consider the other processing parameters like the biomass/solvent ratio. On the other hand, Karagöz et. al. [16] reported comparative studies of oil compositions from different biomass like cellulose, sawdust, rice husk and lignin without showing the overall product yields. They found 70% conversion of cellulose at higher temperatures, which is higher than sawdust, rice husk and lignin. The influence of different processing parameters in HTL for real biomass were also investigated by different researchers. The influence of temperature for *D. tertiolecta* [17, 18], Spirulina [19], *C. vulgaris* [19], *Spirulina platensis* (SP)+ *Entermorpha prolifera* (EP) [13] and *C. lanceolate* [20] has shown that a higher temperature is favourable for higher yields of renewable crude. The influence of residence time for *L. Saccharina* [21], *Spirulina platensis, Entermorpha prolifera* [13], cherry stones [22] and grassland perennials [23] showed that residence time had little impact on renewable crude yields. It can even reduce the renewable

crude yield at higher temperatures. The influence of the biomass and solvent ratio in the feedstock of *Spirulina platensis + E. prolifera* [13] and *C. lanceolate* [24] showed that a lower biomass/solvent ratio led to a higher yield of renewable crude. As cellulose is a model compound and important component of many real biomass, it is important to understand the influence of the processing parameters of HTL on the product yields of cellulose. Though some researchers considered cellulose for their investigation, there are some gaps, such as not considering the influence of important process parameters like temperature, residence time and biomass/solvent ratio altogether for the yields of all the major products (renewable crude, hydrochar, flue gas and aqueous) of the HTL of cellulose.

Different type of solvents has been used for renewable crude extraction from the solid oil mixtures found after HTL of biomass. Fan et. al. [25] used Tetrahydrofuran as a solvent for renewable crude extraction during the HTL of oil palm empty fruit bunch (EFB). They reported a maximum of 76 wt.% oil and gas at 275 $^{o}$C. Zhou et. al. [26] used Dichloromethane as a solvent to extract renewable crude during the HTL of macroalgae (*E. prolifera)*. Dichloromethane was also used by Jin et. al. [27] during the HTL of *Spirulina platensis* (SP) *and Entermorpha prolifera* (EP). During the HTL of cellulose, Yin et. al. [12] and Gao et. al. [15] used Dichloromethane and acetone respectively. Dichloromethane is highly volatile, so, after extraction of the renewable crude, it can easily be vaporised at lower temperatures. Acetone [20, 24, 28], ethanol [29-31], and chloroform [32] were also used by different researchers during the solvent extraction process; however, the researchers did not consider oil extraction without solvents. Therefore, a comparative study between oil extraction with and without solvents will be helpful. As cellulose is a model compound, this study will isolate cellulose without the complications that arise from other compounds that exist in real biomass.

HTL of biomass produces four products: i.e., gaseous, hydrochar (solid), renewable crude (oil) and the aqueous phase. Although the aqueous phase remains separate after the HTL reaction,

the solids and oils remain mixed together. The destruction of polar groups in the biomass (generally –OH and –COO–) during the HTL reaction reduces the ability of products to attract $H_2O$ by hydrogen bonding, making it hydrophobic [33]. The hydrophobic nature of solids attracts the renewable crude or oil. Therefore, there is a strong interaction between solids and renewable crude, which makes renewable crude extraction difficult. This solid and oil attachment can vary, depending on the HTL processing parameters but there are no particular studies which focus on the influence of HTL processing parameters on solid-oil attachments.

Based on the above limitations, the objectives are firstly, to investigate the influence of temperature, residence time and biomass/solvent ratio together for the yields of all major products (renewable crude, hydrochar, flue gas and aqueous) of HTL of cellulose. Secondly, the objective is focused on the solvent extraction method, which has been considered for the extraction of renewable crude without solvent and compare it with the solvent extracted renewable crudes in terms of the processing parameters of HTL. The final objective is to focus on the influence of HTL process parameters on renewable crude trapping in solids, which have been investigated to estimate suitable operating conditions to obtain the highest yield of renewable crude.

## 4.2 Materials and method

### 4.2.1 Materials

Cellulose, which is a model compound of the biomass structure, is considered for this investigation. Cellulose is a very common organic material on Earth and is the main part that makes up the walls of cells in higher plants. It's a big part of cotton (95%), flax (80%), jute (60–70%), and wood (40–50%). The sample has an extra pure microcrystalline structure with an average particle size of 90 μm and a maximum impurity level of 10 ppm heavy metals, bought from Acros Organics. Normally, Cellulose in biomass consists of glucose units that are

connected by β-(1→4)-glycosidic bonds. The formation of a glucose unit is in straight chains of cellulose that makes strong intra-and inter-molecule hydrogen bonds [34]. This cellulose crystallinity causes it to be insoluble in water and resistant to attack by enzymes. However, at subcritical conditions cellulose is rapidly solubilised and hydrolysed into its constituents. Due to its widespread availability and substantial presence in the biomass block of cellulose, examining the HTL of cellulose can offer general insights into its behaviour in terms of HTL yields and the interaction between hydrochar and renewable crude.

### 4.2.2 Experimental setup

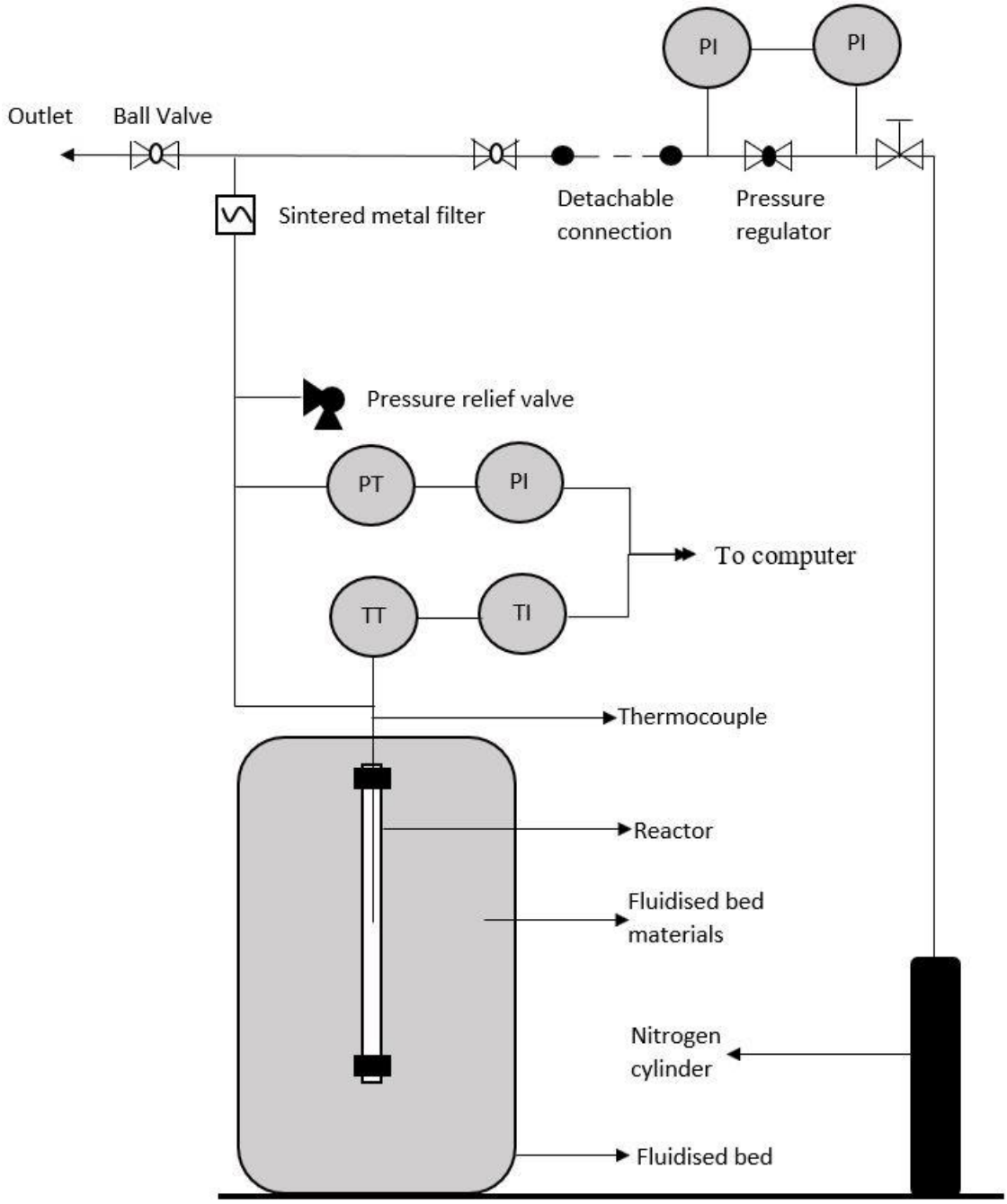


Figure 4.1: Schematic diagram of an HTL batch reactor.

Hydrothermal liquefaction of cellulose was carried out in an 11 ml stainless steel HTL batch reactor [35]. Figure 4.1 shows the schematic diagram of the batch reactor. The batch reactor consisted of a 20 cm long tube, which was made of 316 stainless steel. The outer diameter and thickness of the tube were 12.5 mm and 2 mm respectively. A 12.5 mm Swagelok port

connector and fittings were attached to each end of the reactor. One side of the reactor was covered and the other end was connected to a Type K mineral insulated thermocouple. The upper end of the reactor was attached to a tube with a diameter of 3.2 mm to prevent the inside contents of the reactor from entering the top half of the reactor. A part of the reactor tube was connected to a pressure transducer (PT) and pressure relief valve. The pressure transducer (PT) and thermocouple were also attached to a pressure indicator (PI) and temperature indicator (TI), respectively, from where the reaction temperature and pressure could be recorded by a computer. A ball valve was connected to one side of the upper section of the reactor, which was used to purge the oxygen and pressurised with $N_2$ before the HTL reaction. The flue gas was also released from the reactor via this ball valve after the HTL reaction. A $N_2$ cylinder system, which was part of the batch system, was used to put the $N_2$ pressure in the reactor. The reactor is capable of taking 400 bar pressure. The reactor was placed on a fluidised bed for further reactions. The maximum temperature capacity of the reactor is around 400 $^{o}$C.

### 4.2.3 Batch HTL experimental procedure

HTL of cellulose with different reaction parameters, i.e., temperature (260 to 350 $^{o}$C), time (10 to 25 min) and biomass/water (B/W) ratio (0.25 to 1), were carried out to see the influence of these parameters on product yields, renewable crude yields by solvent extraction, and renewable crude trapping on solids. During the changing of one parameter, all the other parameters remained fixed to observe the influence of that particular parameter (Table: 4.1). For every experiment, the reactor was filled to 50% of the total capacity at room temperature.

During the investigation of temperature, 260 to 350 $^{o}$C have been considered with a 10 min reaction time and 0.5 biomass/water ratio (1.84g/3.66g). 10 to 25 minutes reaction time has been considered for investigation of time at 350 $^{o}$C and 0.5 biomass/water ratio (1.84g/3.66g). The biomass/water ratio varies from 0.25 (1.10/4.40), 0.5 (1.84/3.66), 0.75 (2.35/3.15) and 1 (2.75/2.75) to examine the B/W ratio with 10 minutes reaction time and 350 $^{o}$C temperature.

After filling the reactor, it was charged with nitrogen ($N_2$) to 100 bar from a high pressure nitrogen gas cylinder (Figure 4.1) and left for 3 min to check for leaks. The pressure was then released and charged to the starting pressure required to achieve 200 bar at the reaction condition. The starting pressure was measured by a trial and error method, tested through preliminary experiments. The starting pressure was selected to fall between 85 and 120 bars.

Table 4.1: Experimental plan for different parameters.

| Parametric investigation | Ranges | Fixed parameter and its value |
|---|---|---|
| Investigation of temperature | 260 to 350 °C | Residence time: 10 min, biomass/water ratio: 0.5 |
| Investigation of residence time | 10 to 25 minutes | Temperature: 350 ºC, biomass/water ratio: 0.5 |
| Investigation of Biomass/water ratio | 0.25 to 1 | Residence time: 10 min, Temperature: 350 ºC |

The reactor was placed inside a Techne SBL-2D fluidised bed to be heated. A Techne 9D temperature controller was connected to vary the temperature set point and air flow rate throughout the bed. This provides uniform heating of the reactor at the required reaction temperature. The fluidised bed was pre-heated to the required temperature before placing the reactor inside the bed.

Once the reactor was placed in the fluidised bed, the reactor contents started to heat at a rate of approximately 125 °C per minute. After reaching the desired reaction temperature, the timer was set. When the timer reached the desired residence time, the reactor was removed from the bed and cooled to 70 °C, before opening the reactor. The reactor was then wiped down with a cloth to remove any bed materials (sand) from the outside of the reactor. Every experiment

been repeated two times and the standard deviation for small sample size (two repetition) has been calculated [36].

### 4.2.4 Product recovery

The reactor was weighted before and after releasing the gas to find the mass of the gas. The mass of $N_2$ added before the reaction was deducted from the total mass of gas released after the reaction to know the mass of the gas produced from HTL. The reactor top was then detached to pour the liquid and solid products. The reactor was washed three times with water to remove all the products from reactor wall and put the mixer of products in centrifuge tube. For the solvent extraction process, the reactor was washed with Dichloromethane and put the mixer of products with Dichloromethane in the centrifuge tube. The product mixture and product mixture with solvent were centrifuged from 15 minutes at 2000 rpm. The normal product mixture produced two distinct layers of aqueous and solid-oil mixtures. It would appear that all the renewable crude is attached to solids if no solvent is used. The solid phase was pipetted from the centrifuge tube, dried in an oven at 40 $^{o}$C to remove additional moisture and stored separately for Source Rock Analysis (SRA) analysis. SRA gave the value of the total trapped oil and the solid percentage from the sample. Therefore, the total oil, solid and gas were subtracted from 100 to find the percentage of aqueous phase produced.

Previous researchers have extracted the renewable crude using various solvents during HTL, such as Dichloromethane (DCM) [37-39], Acetone [23], Methanol [40] and Chloroform [32], but DCM gives higher yields of renewable crude [41]. Therefore, DCM was used for the solvent extraction method. However, the product mixture with solvent produced three distinct layers of solid, renewable crude-solvent mixture and aqueous after the centrifuged. All the phases were pipetted from the centrifuge tube and stored separately. The renewable crude-solvent mixture was dried at ambient temperature by applying a stream of nitrogen to a Büchner flask holding the mixture and venting the evaporated solvent until there was no mass change

of renewable crude observed. The renewable crude found through this method was reported as solvent extracted renewable crude. The solid phase was first dried in an oven at 40 °C to remove the moisture and then analysed using SRA to find the trapped oil and solid percentage.

A source rock analyser (SRA) is an advanced instrument that can analyse the rock or solid to provide accurate data about the oil content (S1 and S2) for rock and total organic Carbon (TOC). Therefore, it can tell us about the trapped oil inside the solid phase. A source rock analyser uses the pyrolysis process to analyse the solids. Pyrolysis has been carried out using a Weatherfords Source Rock Analyser™. Helium gas was used as the carrier gas. Crucibles were loaded into a carousel and heated under inert helium. The pyrolysis oven was first held at 300°C for 5 minutes and then ramped at 25°C per minute from 300°C to 650°C. Subsequently, the oven was reduced to 220°C and held for 5 minutes with the carrier gas converted to inert air (CO & $CO_2$ free) and also purged, then ramped at maximum heating to 580°C and held for 20 minutes. The flame ionisation detector (FID) was calibrated by running Weatherford Laboratories Instruments Division Standard 533. The IR Analysers were calibrated against standard gas with a known concentration of $CO_2$ and CO. This gave us the S1 (the amount of free hydrocarbon generated through thermal cracking at 350 °C), S2 (the amount of hydrocarbon generated through thermal cracking at higher temperatures up to 600 °C). The S1 and S2 in the solid is the trapped oil, which is considered to be normal renewable crude and heavy renewable crude.

### 4.3. Results and discussion

#### 4.3.1 Influence of process parameters on product yields

The HTL products of the reactions, i.e., renewable crude (RNC), hydrochar, gases and aqueous for different reaction parameters, are shown in Figure 4.2. Figure 4.2a demonstrates the influence of temperature on HTL product yields. The initial renewable crude yield at a

temperature of 260 °C was 8.12 wt.% and continued to increase the yields with increasing temperature. The final yield of renewable crude was 13.56 wt.%, which was 67 % higher than the initial yield. This is because of the higher decomposition of biomass at higher temperatures [17]. Yu et al. [17] investigated *D. tertiolecta* and reported that the higher temperature is responsible for higher yields of renewable crude. Jin et al. [13], Aysu et al. [42], Durak et al. [43] and Brown et al. [44] obtained comparable temperature influences, where higher temperatures were favourable for higher yields of RNC even after using a mixture of two different types of algae; i.e., *Spirulina platensis* + *Entermorpha prolifera* (EP) [13].

Though many researchers have reported lower hydrochar yields at relatively higher temperatures, HTL of cellulose showed slightly higher yields of hydrochar from 35.62 to 47.60 wt.%, at temperatures between 260 - 320 °C and slightly lower yields (43.26 wt%) at a temperature of 350 °C. This initial increase of hydrochar could be caused by additional thermal cracking [17] of the other products, which can lead to an increase in hydrochar. After a temperature of 320 °C, the decomposition of the biomass was high enough. Therefore, the hydrochar yields slightly decreased. Chen et al. [45] reported a similar temperature effect on hydrochar such that the HTL of mixed cultural algal biomass produced a higher yield of hydrochar from 260 to 280 °C and then decreased with further increase in temperature. The initial gaseous yield was 8.75 wt.%, which decreased to 5.42 wt.% at a temperature of 290 °C because of repolarisation or further thermal cracking. Further gas yields increased because of the higher decomposition of biomass at higher temperatures, which was supported by the reported results of Li et al [46]. The aqueous phase continued to decrease from 47.49 to 32.35 wt.% with rising temperatures from 260 to 350 °C, which indicated that re-polymerisation and decomposition at higher temperatures led to an increase in renewable crude and gases by decreasing the aqueous phase.

Figure 4.2b shows the influence of residence time on the product yields, i.e., renewable crude, hydrochar, gases and aqueous. The renewable crude and hydrochar yields gradually decreased with rising residence times from 10 to 25 min. The initial renewable crude yields were 13.55 wt.% at 10 minutes' residence time. At time 25 minutes, the renewable crude yields were 8.48 wt.%, which is around 37.49% lower than the initial yield of renewable crude. Anastasakis et al. [21], Jena et al. [47] and Yin et al. [48] also found that a lower residence time was suitable for higher yields of renewable crude because higher residence time may result in cracking, re-condensation and re-polymerisation of newly formed compounds [49]. The initial hydrochar yield was 43.66 wt.% at 10 minutes, which was the highest hydrochar yield. With rising residence time, hydrochar yields decreased and the minimum hydrochar yield was found to be 33.37 wt.%, which was 23.56 % lower than the maximum yield of hydrochar. A similar temperature effect on hydrochar yields was reported by Akalın et al. [22] and Tekin et al. [50]. Even Tekin et al. [50] reported a significant yield of hydrochar at 0 minute residence time. At higher temperatures, a longer residence time can lead to an increase in the decomposition of biomass in such a way that it can go further reaction of renewable crude and hydrochar to produce higher amount of gases. Therefore, gas yields and aqueous phases were increased significantly with longer residence time. The initial gas yield was 10.85 wt.% at 10 minutes, increasing to 17.12 wt.%, which was 57.88 % higher than the initial gas yields. The maximum aqueous yield was 42.91 wt.%, which was around 33.53% higher than the minimum gas yield (31.49 wt.%) found with a 15 minutes residence time.

Figure 4.2c shows the influence of the B/W ratio on product yields during the HTL of cellulose. The maximum renewable crude yield was found at a lower B/W ratio, which indicates that increasing the amount of water in the feed leads to an increase in renewable crude yields. Therefore, the maximum renewable crude yield was 15.18 wt.% at a B/W ratio of 0.25. The increasing B/W ratio leads to a significant decrease in the renewable crude yield. The minimum

renewable crude yield was 9.43 wt.% at B/W ratio 1, which was 37.88 % lower than the maximum renewable crude yield. Qu et al. [24] also reported that a higher B/W ratio could decrease the renewable crude yield during HTL, with a similar influence from the B/W ratio on the renewable crude yields for *C. lanceolate.* Even during the mixture of two algae (*Spirulina platensis* + *E. prolifera*), a lower B/S ratio was found favourable for higher renewable crude yields [13]. This can happen because of the higher decomposition rate of biomass at lower B/W ratios. Whilst the biomass amount decreases, the decomposition of biomass particles can go higher considering the level of water was also increasing. This is reasonable because the water serves as a solvent, catalyst and as a reactant for hydrolysing the cellulose, which can lead to an increase in renewable crude yields [13, 51]. On the other hand, the hydrochar and gases yields show interesting results with increasing B/W ratios. The initial hydrochar yield was 32.99 wt.% at B/W 0.25. At B/W 0.5, the renewable crude yield increased by 31%. It was then decreased with an increase in B/W ratio. Jin et al. [13] found similar movements of hydrochar yields, i.e., a sudden escalation in hydrochar yield when increasing the biomass amount. It can happen because of further reactions in the Biomass, which lead to depolymerisation or decomposition and it leads to an increase in other products. The nature of gaseous yields was also not constant. With changing volumes of water, the nature of the reactions greatly affected the depolymerisation or further reaction of gas, which can lead to the production of other products by decreasing or increasing the gas yields due to depolymerisation or further reactions of other products. The initial gas yields were 23.15 wt.% at B/W 0.25. At B/W 0.5, the gas yield (10.85 wt.%) decreased and the hydrochar yield increased. At B/W 0.75, the gas yield was at its maximum (24.48 wt.%) and the hydrochar yield was at its minimum. It can be assumed that depolymerisation occurs between the gas and hydrochar state in this case.

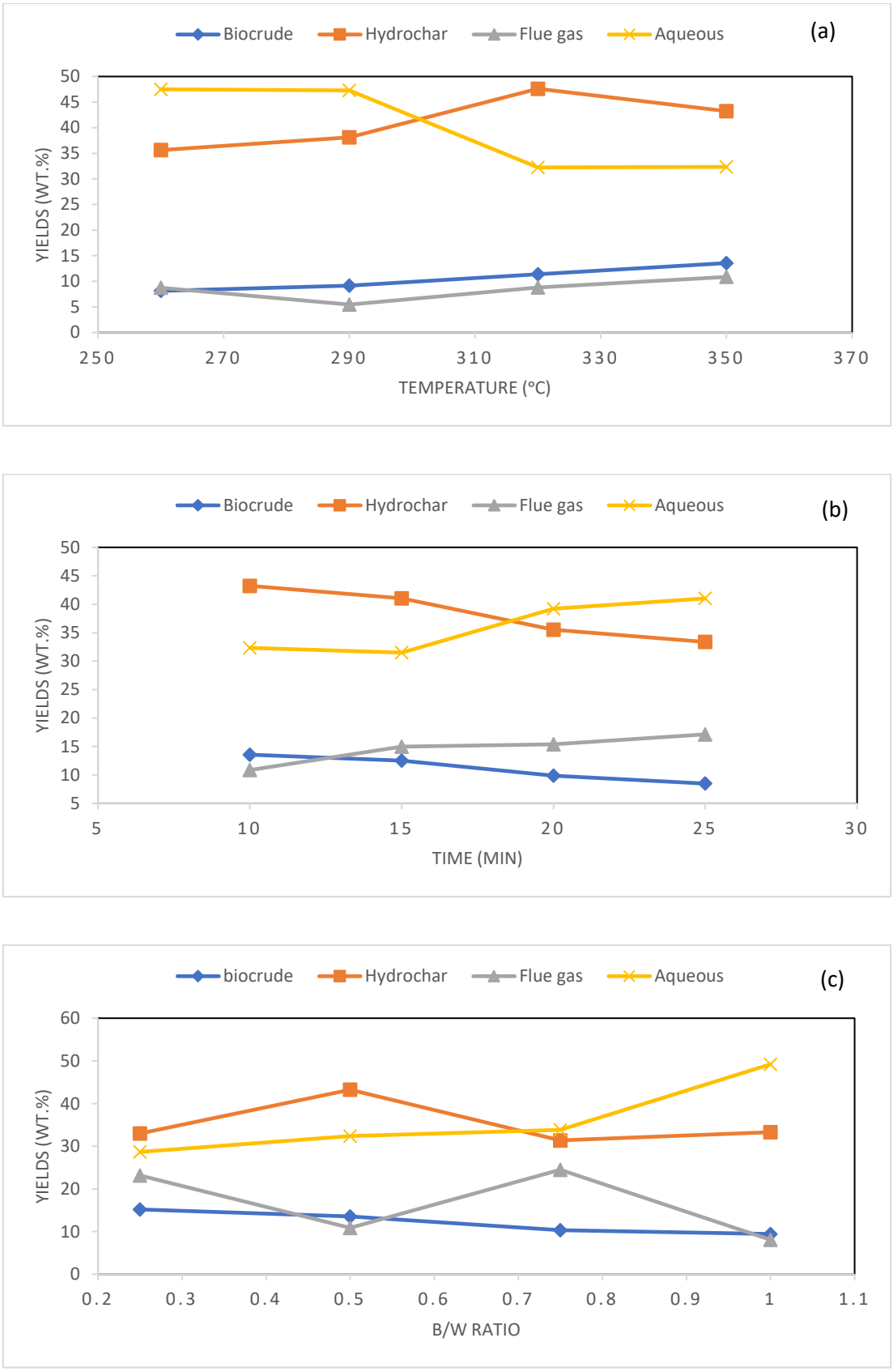


Figure 4.2: Influence of (a) temperature, (b) residence time and (c) B/W ratio on product yields.

The minimum aqueous yield was 28.66 wt.% at B/W 0.25. The aqueous yields gradually increased with the increase in B/W ratio and the maximum yield was found to be 49.21 wt.%, which is 71.7 % higher from the initial yield. Similar findings have been reported by Anastasakis et al. [21]. They found a higher aqueous yield when the B/W ratio was increased to between 0.16 - 0.2. The increasing nature of aqueous can be caused by further cracking and depolymerisation of other products of HTL.

### 4.3.2 Solvent extraction method

Dichloromethane (DCM) was used for the solvent extraction method. Figure 4.3a shows the influence of temperature on the total and solvent-extracted renewable crude yields and their relationships. As mentioned before, total renewable crude yields have increased from 7.99 to 13.17 wt.% with increases in temperature from 260 to 350 $^{o}$C. At 260 $^{o}$C, only 2.89 wt.% renewable crude can be extracted, which is 35.57 % of the total renewable crude (8.12 wt.%). Therefore, 64.43 % of the renewable crude remains trapped in the solid material, even after solvent extraction. It is also noticeable that increasing the total renewable crude yields with temperature also increases the solvent-extracted renewable crudes. Thus, the maximum solvent-extracted renewable crude is found to be 7.83 wt.%, which is extracted from 350 $^{o}$C of HTL reaction. At 350 $^{o}$C, 57.67% of the total renewable crude has been extracted but 42.32 % remains trapped in the solids. Hence, solvents alone cannot extract all the renewable crude from solids during changing the temperature. The influence of residence time on the total and solvent-extracted renewable crude yields has also shown interesting results (Figure 4.3b). As discussed earlier, the renewable crude yields were decreased gradually from 13.56 to 8.48 wt.% with increasing time from 10 to 25 minutes. At 10 minutes' residence time, the solvent-extracted renewable crude yield was 7.83 wt.%, which is around 57.67 % of the total renewable crude (13.56 wt.%).

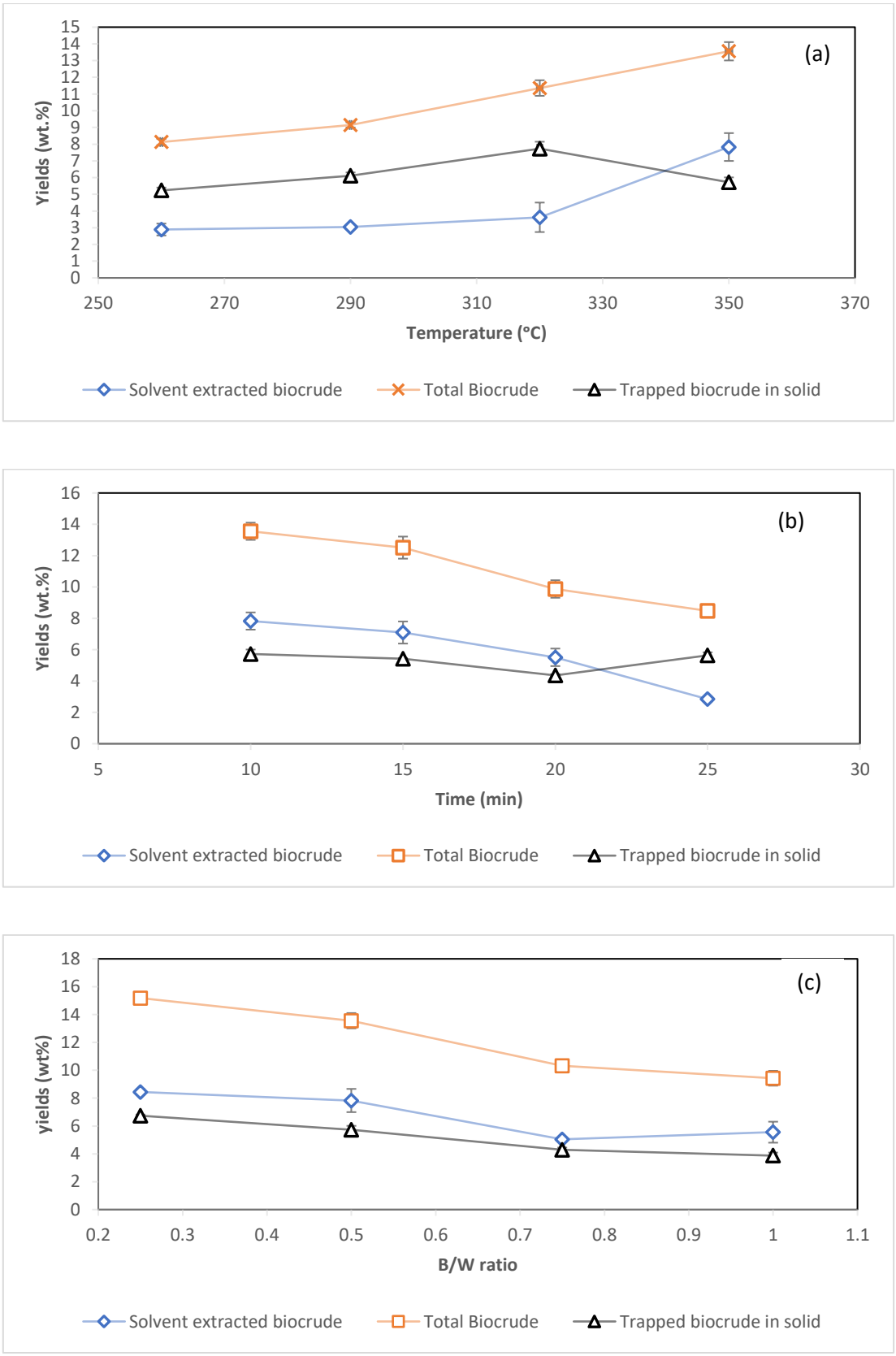


Figure 4.3: Renewable crude trapping in solids after solvent extraction; i.e., the effect of (a) temperature, (b) time and (c) B/W ratio.

With decreasing of the total renewable crude whilst increasing the residence time, solvent-extracted renewable crudes also decreased. The solvent-extracted renewable crudes were 7.09 wt.%, 5.51 wt.% and 2.85 wt% at 15, 20 and 25 minutes of residence time respectively, which equates to 56.63%, 55.79% and 33.57% of the total renewable crude. Therefore, 42.32%, 43.37%, 44.21% and 66.42% of renewable crude have been trapped in solids during residence times of 10, 15, 20, 25 minutes respectively, even after solvent extraction. The influence of biomass/water ratio also shows a significant difference between total and solvent-extracted renewable crude yields (Figure 4.3c).

It was found that total renewable crude yields decreased gradually from 9.43 wt.% to 15.18 wt.%, with an increasing B/W ratio from 0.25 to 1. Solvent can only extract 8.344 wt.% of the total renewable crude at B/W 0.25, which is around 58.79 % of the total renewable crude. With decreasing the total renewable crude, the solvent-extracted renewable crude also decreased. The solvent-extracted renewable crudes were recorded as having 7.83 wt.%, 5.04 wt.% and 5.55 wt% at a B/W ratio of 0.5, 0.75 and 1 respectively, which represent 57.67%, 58.49% and 58.79% of the total renewable crude. Therefore, 44.39%, 42.25%, 41.50% and 41.07% of the renewable crude have been trapped in solids at 0.25, 0.5, 0.75 and 1 B/W ratio respectively, even after solvent extraction.

As DCM gives higher yields of renewable crude yields [41], several researchers, such as Brown et al. [52], Vardon et al. [53], Xu et. al. [54], Tian et al. [55] and Biller et al. [56] have considered DCM for renewable crude extraction during the HTL of biomass. They did not observe that DCM cannot extract all the renewable crude from solids. Some renewable crude can remain trapped in solids. Other solvents may have similar effects on renewable crude yields.

### 4.3.3 The influence of process parameters on renewable crude trapping in solids

Comparison of the total renewable crude and solvent-extracted renewable crude clearly shows that some renewable crude can be trapped inside solids, even after the solvent extraction process. This trapped renewable crude can be explained by the degree of renewable crude trapping (DBT). The term "degree of renewable crude trapping" refers to the ratio of "trapped renewable crude in solids" and "total renewable crude". Therefore, the lower degree of trapping refers to the lower amount of trapped renewable crude in solids. The amount of trapped renewable crude has been calculated from the difference between the total and solvent-extracted renewable crude. Figure 4.4 shows the influence of temperature, residence time and B/W ratio on the degree of renewable crude trapping. Increasing the temperature from 260 to 350 °C shows a clear trend in the degree of renewable crude trapping (Figure 4.4a). With rising reaction temperatures from 260 to 320 °C, the DBT were slightly increased from 0.64 to 0.68, which can be considered a negligible change. But at 350 °C, the DBT was decreased to 0.42, which suggests that the minimum amount of renewable crude would be trapped in solids at the 350 °C reaction time. Figure 4.4b also shows the influence of residence time on DBT. The DBT increased with increasing residence time. With a rising residence time of 10 to 20 minutes, the DBT only increased from 0.42 to 0.44, which could be considered negligible; but the DBT was 0.66 at 25 minutes residence time. So, a lower residence time is preferable for lower DBT or lower volumes of trapped oil in the solids. Figure 4.4c shows the influence of the B/W ratio on the degree of renewable crude trapping. The DBT did not change significantly with changing the B/W ratio. With a rising B/W ratio from 0.25 to 1, the DBT very slightly decreased from 0.44 to 0.41, which could be considered a negligible change in the nature of renewable crude trapping. Therefore, temperature and residence time have a more significant effect on DBT than the B/W ratio.

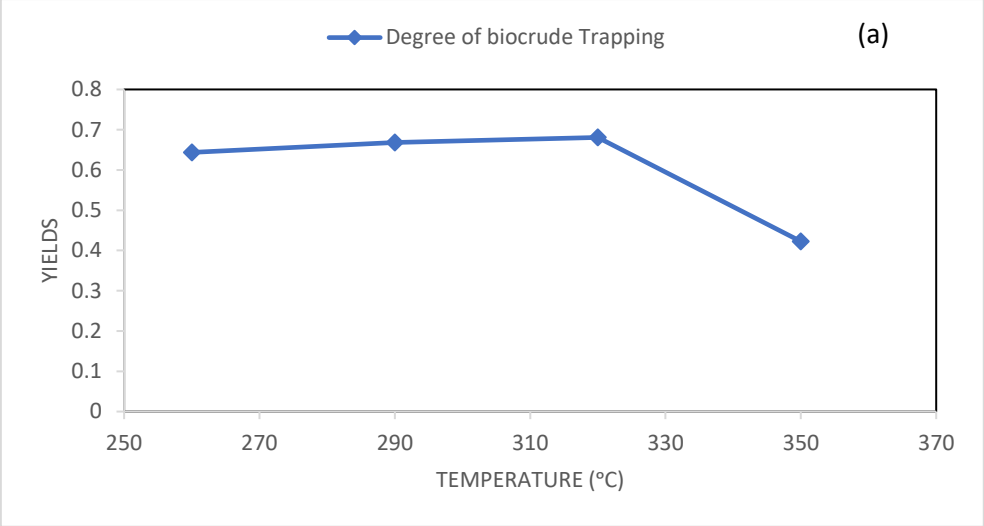


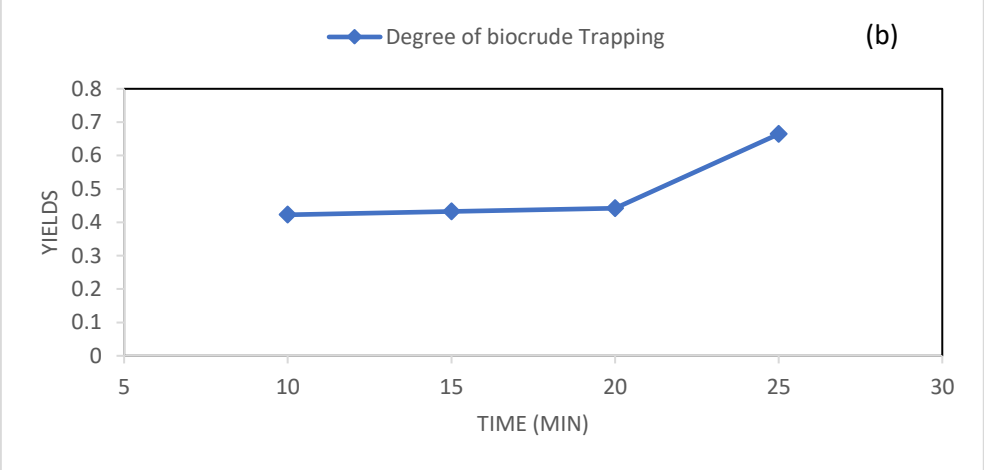


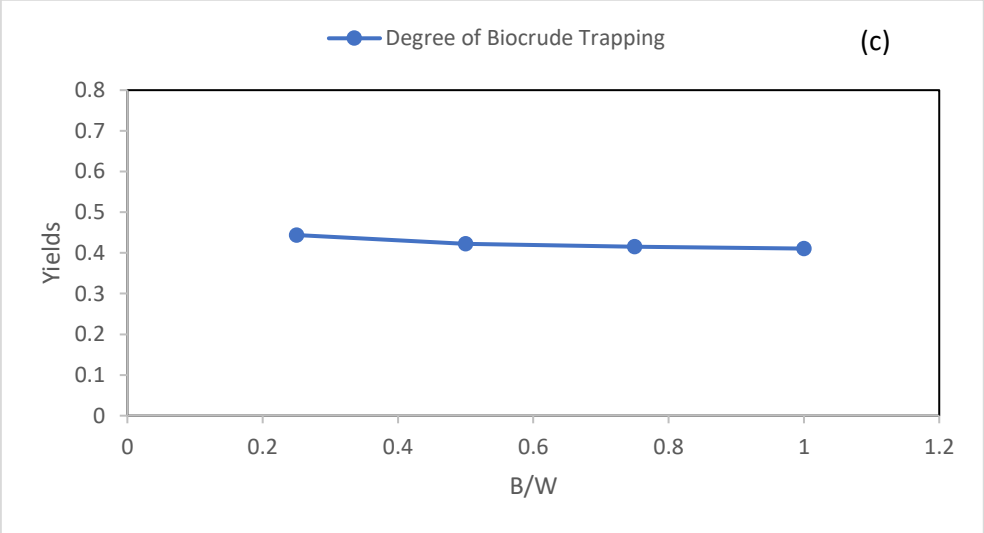


Figure 4.4: Influence of (a) temperature, (b) time and (c) B/W ratio on the degree of renewable crude trapping in solids.

Source rock analysis (SRA) can basically identify the amount of oil that can be recovered from source rock. Source rock is capable of generating petroleum oil that is trapped inside the rock [57]. Therefore, SRA characterises the source rock through pyrolysis and can show its potential by representing the amount of free hydrocarbon generated through thermal cracking at 350 °C (S1) and the amount of hydrocarbon generated through thermal cracking at higher temperatures up to 600 °C (S2) [58]. S1 and S2 can be defined as light and heavy oils that are trapped inside the rock. Therefore, SRA was used to characterise the solids found from HTL of cellulose to see the influence of HTL parameters on S1 and S2.

Figure 4.5a shows the influence of temperature on S1 and S2 in terms of using or not using the solvent extraction method. Without considering the solvent extraction method and with a rising temperature from 260 to 350 °C, the light oil (S1) seemed increase gradually from 3.41 to 6.40 wt.% and the yields of heavy oil (S2) were also increased from 4.71 to 7.16 wt.%. In this case, the rise in S1 and S2 yields indicated that higher temperatures favoured the biomass decomposition rate and increased the light oil yields. However, after using the solvent extraction method, the S1 yields were limited to 1.01 to 1.16 wt.% for all reaction temperatures. The results indicate that the solvent (DCM) could not extract a certain amount of light oil (S1) (~1 wt%) even when the actual yields of S1 were rising. Therefore, around 1 wt.% of free oil (S1) remains trapped after solvent extraction for all reaction temperatures. On the other hand, yields of heavy oil (S2) after solvent extraction were found to be slightly lower than the yields of actual heavy oil (S2). After solvent extraction, yields of heavy oil (S2) were increased from 4.07 to 6.35 wt.% when temperatures were rising from 260 to 320 °C. At 350 °C, it was noticeable that the solvent can extract a high amount 83 % of free oil and 35 % of heavy oil. Therefore, heavy oil was again decreased to 4.63 wt.% after the solvent extraction method. This outcome can happen because higher temperatures can influence the hydrochar properties

such that that the hydrochar cannot hold the higher amount of oil, even when the actual yields of oil are high. Another noticeable point was that solvent can extract more S1 than S2.

Figure 4.5b shows the influence of time (10 to 25 minutes) on the S1 and S2 both before and after the solvent extraction method is used. Without using any solvent extraction method, the light oil (S1) seems to decrease slightly from 6.39 to 3.87 wt.% and the heavy oils (S2) also decreases from 7.16 to 4.61 wt.% when the residence time increases from 10 to 25 minutes. It can happen because of the repolarisation of oil to other products at higher residence times. After the solvent extraction method, the light oil (S1) seemed to remain around 1 wt.% for all residence times. This indicates that the solvent (DCM) could not extract around 1 wt.% of light oil, even when the actual light oil might be high in yield. After the solvent extraction method, the yields of heavy oil (S2) were found to be 3.16 to 4.63 wt.%, which is very close. It was also noticeable that at 10 minutes reaction time, the maximum amount of S2 (35%) can be extracted. With rising time, yields of heavy oil might decrease significantly, but this does not affect the solvent extraction method to any great extent. A certain amount of heavy oil (S2) (3.16 to 4.63 wt.%) remains trapped inside the hydrochar.

Figure 4.5c shows the influence of the B/W ratio on the actual and trapped light oil (S1) and heavy oil (S2). The yields of actual light oil (S1) decreased from 6.63 to 4.48 wt.% and the heavy oil (S2) decreased from 8.54 to 4.95 wt.% after changing the B/W from 0.25 to 1. After the solvent extraction, the maximum trapped light oil (S1) (2.61 wt.%) was found at 0.25 B/W, even though it was noticed that the maximum renewable crude yield was 15.18 wt.% under this condition. The light oils then decreased and remained at around 1 wt.% for all other B/W ratios. Therefore, Hydrochar at 0.25 B/W can hold the maximum volume of light oil as the maximum renewable crude yield was noticed for this condition.

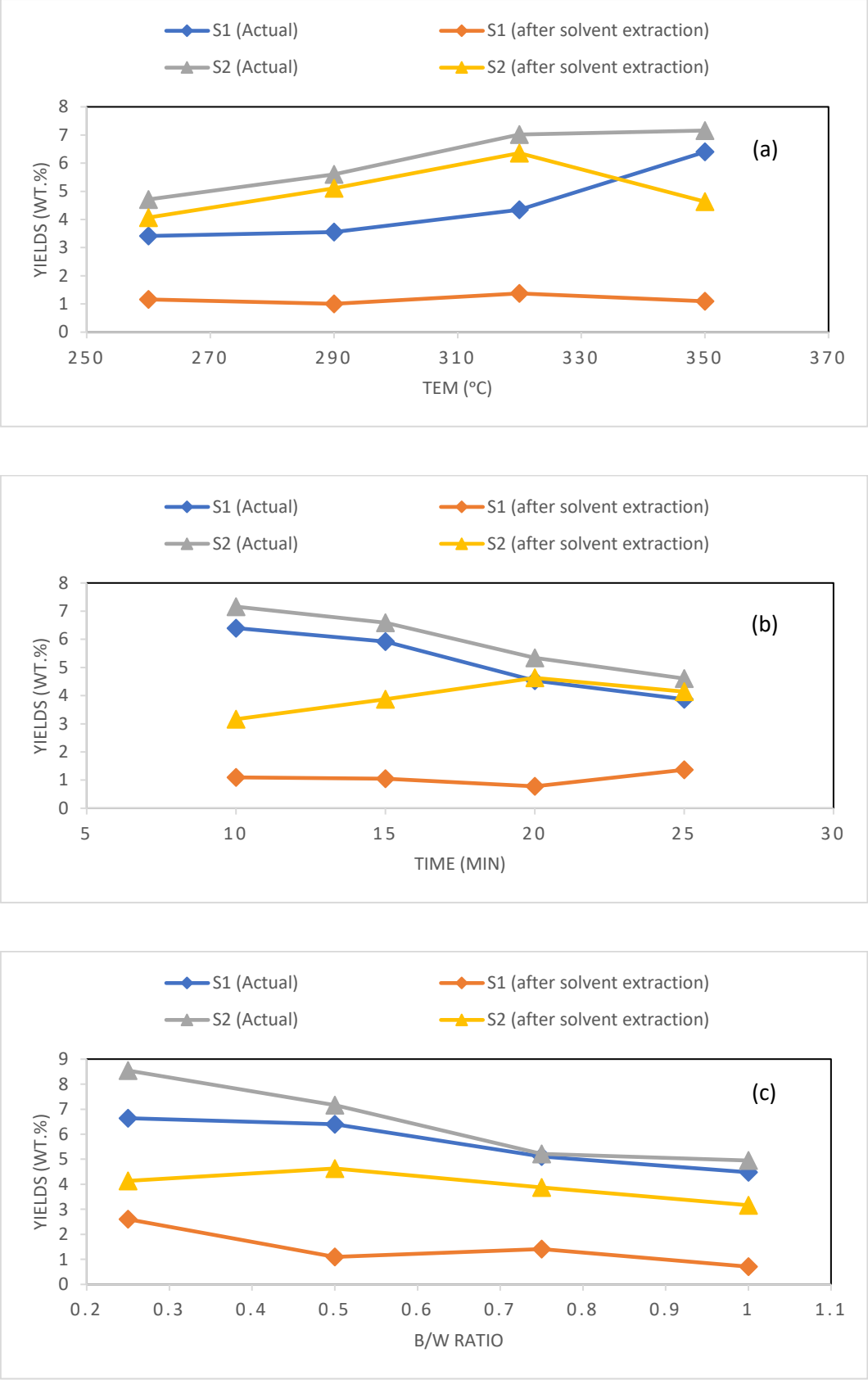


Figure 4.5: Influence of (a) temperature, (b) time and (c) B/W ratio on light oil (S1) and heavy oil (S2).

For this reaction condition, hydrochar may have some properties that can hold more free oil and the solvent cannot extract them. The yields of trapped heavy oil (S2) did not scatter much and the yields only varied from 3.16 to 4.63 wt.%. Therefore, even the actual heavy oil might have high yields, suggesting a certain amount of heavy oils might be trapped in the hydrochar. It is also noticeable that the solvent (DCM) can extract more light oil (S1) than heavy oil (S2) for all conditions. As S2 generates at high temperatures (around 600 °C), it can remain in a state or trapped in such a way that the solvent cannot reach them properly. Therefore, lower amounts of S2 have been extracted through HTL of cellulose.

### 4.4. Conclusion

In conclusion, this study investigated the influence of various processing parameters on the HTL of cellulose, specifically temperature (260-350 $^{o}$C), residence time (10-25 minutes), and biomass/water ratio (0.25-1).

The results showed that increasing the temperature enhanced the renewable crude yields, with the maximum yield of 13 wt.% observed at 350 $^{o}$C compared to 8 wt.% at 260 $^{o}$C. Hydrochar yields exhibited an increase from 35 to 47 wt.% between temperatures of 260 to 320 $^{o}$C, contrary to the expected decrease due to higher biomass decomposition rates. Further thermal cracking of other products favoured repolymerisation and condensation processes, resulting in increased hydrochar yields with rising temperature.

Increasing the residence time gradually reduced the renewable crude yields. Increasing the residence time from 10 to 25 minutes caused a 37% reduction in renewable crude yields and a corresponding decline in hydrochar yields due to cracking, re-condensation, and re-polymerisation of newly-formed compounds. Likewise, raising the biomass/water ratio from 0.25 to 1 significantly decreased the renewable crude yield.

The solvent (DCM) was capable of extracting 31% to 58% of the total oil, with a maximum extraction of 58% achieved from hydrochar produced at 350 °C. Varying the residence time and biomass/water ratio affected the oil extraction efficiency. The optimal HTL conditions for renewable crude from cellulose were found to be a temperature of 350 °C, residence time of 10 minutes, and a biomass/water ratio of 0.5.

The degree of renewable crude trapping slightly increases from 0.64 to 0.68 with increasing temperature from 260 to 320 ºC but decreases to 0.42 at 350 ºC. The degree of trapping also increases from 0.42 to 0.66 with increasing residence time from 10 to 25 minutes. Changing the B/W ratio from 0.25 to 1 does not significantly affect the degree of trapping.

Additionally, approximately 1 wt.% of light oil (S1) and 3 to 6 wt.% of heavy oil (S2) remained trapped even after solvent extraction, indicating that heavy oil possesses properties that attract hydrochar more than light oil.

**References**


1. Toor, S.S., L. Rosendahl, and A. Rudolf, *Hydrothermal liquefaction of biomass: A review of subcritical water technologies.* Energy, 2011. **36**(5): p. 2328-2342.
2. Gollakota, A.R.K., N. Kishore, and S. Gu, *A review on hydrothermal liquefaction of biomass.* Renewable and Sustainable Energy Reviews, 2017.
3. Hossain, M.A., J. Jewaratnam, and P. Ganesan, *Prospect of hydrogen production from oil palm biomass by thermochemical process – A review.* International Journal of Hydrogen Energy, 2016. **41**(38): p. 16637-16655.
4. Goswami, D.Y. and F. Kreith, *Handbook of energy efficiency and renewable energy*. 2007: Crc Press.
5. Hirel, B., et al., *Improving nitrogen use efficiency in crops for sustainable agriculture.* Sustainability, 2011. **3**(9): p. 1452-1485.
6. Robbins, M.P., et al., *New opportunities for the exploitation of energy crops by thermochemical conversion in Northern Europe and the UK.* Progress in Energy and Combustion Science, 2012. **38**(2): p. 138-155.
7. Toor, S.S., *Modeling and Optimization of Catliq Liquid Bioful Process*. 2010: Department of Energy Technology, Aalborg University.
8. Shah, Y.T., *Energy and fuel systems integration*. 2015: CRC Press.
9. Biller, P., et al., *Nutrient recycling of aqueous phase for microalgae cultivation from the hydrothermal liquefaction process.* Algal Research, 2012. **1**(1): p. 70-76.

10. Jin, F., *Application of hydrothermal reactions to biomass conversion*. 2014: Springer Science & Business Media.
11. Dimitriadis, A. and S. Bezergianni, *Hydrothermal liquefaction of various biomass and waste feedstocks for biocrude production: A state of the art review.* Renewable and Sustainable Energy Reviews, 2017. **68**(Part 1): p. 113-125.
12. Yin, S. and Z. Tan, *Hydrothermal liquefaction of cellulose to bio-oil under acidic, neutral and alkaline conditions.* Applied Energy, 2012. **92**: p. 234-239.
13. Jin, B., et al., *Co-liquefaction of micro- and macroalgae in subcritical water.* Bioresource Technology, 2013. **149**(Supplement C): p. 103-110.
14. Möller, M., F. Harnisch, and U. Schröder, *Hydrothermal liquefaction of cellulose in subcritical water—the role of crystallinity on the cellulose reactivity.* Rsc Advances, 2013. **3**(27): p. 11035-11044.
15. Gao, Y., et al., *Characterization of products from hydrothermal treatments of cellulose.* Energy, 2012. **42**(1): p. 457-465.
16. Karagöz, S., et al., *Comparative studies of oil compositions produced from sawdust, rice husk, lignin and cellulose by hydrothermal treatment.* Fuel, 2005. **84**(7-8): p. 875-884.
17. Chen, Y., et al., *Direct liquefaction of Dunaliella tertiolecta for bio-oil in sub/supercritical ethanol–water.* Bioresource Technology, 2012. **124**(Supplement C): p. 190-198.
18. Minowa, T., et al., *Oil production from algal cells of Dunaliella tertiolecta by direct thermochemical liquefaction.* Fuel, 1995. **74**(12): p. 1735-1738.
19. Ross, A.B., et al., *Hydrothermal processing of microalgae using alkali and organic acids.* Fuel, 2010. **89**(9): p. 2234-2243.
20. Zhong, C. and X. Wei, *A comparative experimental study on the liquefaction of wood.* Energy, 2004. **29**(11): p. 1731-1741.
21. Anastasakis, K. and A.B. Ross, *Hydrothermal liquefaction of the brown macro-alga Laminaria Saccharina: Effect of reaction conditions on product distribution and composition.* Bioresource Technology, 2011. **102**(7): p. 4876-4883.
22. Akalın, M.K., K. Tekin, and S. Karagöz, *Hydrothermal liquefaction of cornelian cherry stones for bio-oil production.* Bioresource Technology, 2012. **110**(Supplement C): p. 682-687.
23. Zhang, B., M. von Keitz, and K. Valentas, *Thermochemical liquefaction of high-diversity grassland perennials.* Journal of Analytical and Applied Pyrolysis, 2009. **84**(1): p. 18-24.
24. Qu, Y., X. Wei, and C. Zhong, *Experimental study on the direct liquefaction of Cunninghamia lanceolata in water.* Energy, 2003. **28**(7): p. 597-606.
25. Fan, S.-P., et al., *Comparative studies of products obtained from solvolysis liquefaction of oil palm empty fruit bunch fibres using different solvents.* Bioresource Technology, 2011. **102**(3): p. 3521-3526.
26. Zhou, D., et al., *Hydrothermal liquefaction of macroalgae Enteromorpha prolifera to bio-oil.* Energy & Fuels, 2010. **24**(7): p. 4054-4061.
27. Jin, B., et al., *Co-liquefaction of micro- and macroalgae in subcritical water.* Bioresource Technology, 2013. **149**: p. 103-110.

28. Sun, P., et al., *Analysis of liquid and solid products from liquefaction of paulownia in hot-compressed water*. Energy Conversion and Management, 2011. **52**(2): p. 924-933.
29. Xu, C. and T. Etcheverry, *Hydro-liquefaction of woody biomass in sub- and super-critical ethanol with iron-based catalysts.* Fuel, 2008. **87**(3): p. 335-345.
30. Sun, P., et al., *Direct liquefaction of paulownia in hot compressed water: Influence of catalysts.* Energy, 2010. **35**(12): p. 5421-5429.
31. Xu, C. and J. Lancaster, *Conversion of secondary pulp/paper sludge powder to liquid oil products for energy recovery by direct liquefaction in hot-compressed water.* Water Research, 2008. **42**(6): p. 1571-1582.
32. Shuping, Z., et al., *Production and characterization of bio-oil from hydrothermal liquefaction of microalgae Dunaliella tertiolecta cake.* Energy, 2010. **35**(12): p. 5406-5411.
33. Pisupati, S.V. and A.H. Tchapda, *Thermochemical Processing of Biomass*, in *Advances in Bioprocess Technology*. 2015, Springer. p. 277-314.
34. Delmer, D.P. and Y. Amor, *Cellulose biosynthesis.* The Plant Cell, 1995. **7**(7): p. 987.
35. Obeid, R., et al., *The elucidation of reaction kinetics for hydrothermal liquefaction of model macromolecules.* Chemical Engineering Journal, 2019. **370**: p. 637-645.
36. Singh, A.S., M.B.J.I.J.o.e. Masuku, commerce, and management, *Sampling techniques & determination of sample size in applied statistics research: An overview*. 2014. **2**(11): p. 1-22.
37. Xu, D. and P.E. Savage, *Effect of reaction time and algae loading on water-soluble and insoluble biocrude fractions from hydrothermal liquefaction of algae.* Algal research, 2015. **12**: p. 60-67.
38. Alhassan, Y., N. Kumar, and I.M. Bugaje, *Hydrothermal liquefaction of de-oiled Jatropha curcas cake using Deep Eutectic Solvents (DESs) as catalysts and co-solvents.* Bioresource Technology, 2016. **199**: p. 375-381.
39. Anastasakis, K. and A.B. Ross, *Hydrothermal liquefaction of four brown macro-algae commonly found on the UK coasts: An energetic analysis of the process and comparison with bio-chemical conversion methods.* Fuel, 2015. **139**: p. 546-553.
40. Yip, J., et al., *Comparative study of liquefaction process and liquefied products from bamboo using different organic solvents.* Bioresource Technology, 2009. **100**(24): p. 6674-6678.
41. Villadsen, S.R., et al., *Development and application of chemical analysis methods for investigation of bio-oils and aqueous phase from hydrothermal liquefaction of biomass.* Energy & Fuels, 2012. **26**(11): p. 6988-6998.
42. Aysu, T. and M.M. Küçük, *Liquefaction of giant fennel (Ferula orientalis L.) in supercritical organic solvents: Effects of liquefaction parameters on product yields and character.* The Journal of Supercritical Fluids, 2013. **83**(Supplement C): p. 104-123.
43. Durak, H. and T. Aysu, *Effects of catalysts and solvents on liquefaction of Onopordum heteracanthum for production of bio-oils.* Bioresource Technology, 2014. **166**(Supplement C): p. 309-317.
44. Brown, T.M., P. Duan, and P.E. Savage, *Hydrothermal liquefaction and gasification of Nannochloropsis sp.* Energy Fuels, 2010. **24**(6): p. 3639-3646.

45. Chen, W.-T., et al., *Hydrothermal liquefaction of mixed-culture algal biomass from wastewater treatment system into bio-crude oil.* Bioresource Technology, 2014. **152**: p. 130-139.
46. Li, D., et al., *Preparation and characteristics of bio-oil from the marine brown alga Sargassum patens C. Agardh.* Bioresource Technology, 2012. **104**: p. 737-742.
47. Jena, U., K.C. Das, and J.R. Kastner, *Effect of operating conditions of thermochemical liquefaction on biocrude production from Spirulina platensis.* Bioresource Technology, 2011. **102**(10): p. 6221-6229.
48. Yin, S., et al., *Subcritical hydrothermal liquefaction of cattle manure to bio-oil: Effects of conversion parameters on bio-oil yield and characterization of bio-oil.* Bioresource Technology, 2010. **101**(10): p. 3657-3664.
49. Xue, Y., et al., *A review on the operating conditions of producing bio-oil from hydrothermal liquefaction of biomass.* International Journal of Energy Research, 2016. **40**(7): p. 865-877.
50. Tekin, K., S. Karagöz, and S. Bektaş, *Hydrothermal liquefaction of beech wood using a natural calcium borate mineral.* The Journal of Supercritical Fluids, 2012. **72**(Supplement C): p. 134-139.
51. Savage, P.E., *A perspective on catalysis in sub- and supercritical water.* The Journal of Supercritical Fluids, 2009. **47**(3): p. 407-414.
52. Brown, T.M., P. Duan, and P.E. Savage, *Hydrothermal liquefaction and gasification of Nannochloropsis sp.* Energy & Fuels, 2010. **24**(6): p. 3639-3646.
53. Vardon, D.R., et al., *Thermochemical conversion of raw and defatted algal biomass via hydrothermal liquefaction and slow pyrolysis.* Bioresource Technology, 2012. **109**: p. 178-187.
54. Xu, D. and P.E. Savage, *Characterization of biocrudes recovered with and without solvent after hydrothermal liquefaction of algae.* Algal Research, 2014. **6**: p. 1-7.
55. Tian, C., et al., *Hydrothermal liquefaction of harvested high-ash low-lipid algal biomass from Dianchi Lake: Effects of operational parameters and relations of products.* Bioresource Technology, 2015. **184**: p. 336-343.
56. Biller, P., et al., *Hydroprocessing of bio-crude from continuous hydrothermal liquefaction of microalgae.* Fuel, 2015. **159**: p. 197-205.
57. McCarthy, K., et al., *Basic petroleum geochemistry for source rock evaluation.* Oilfield Review, 2011. **23**(2): p. 32-43.
58. Ramachandran, K., et al., *Source rock analysis, thermal maturation and hydrocarbon generation using rock-eval pyrolysis in parts of Krishna–Godavari basin, India: a case study.* Journal of Petroleum Exploration and Production Technology, 2013. **3**(1): p. 11-20.

# Chapter 5: Investigation of the fundamental reasons for solid–renewable crude interaction during the hydrothermal liquefaction of mixtures of model compounds.

# Statement of Authorship

| | |
|---|---|
| Title of Paper | Investigation of the fundamental reasons of solid- renewable crude interaction during the hydrothermal liquefaction of mixture of model compounds. |
| Publication Status | ☐ Published ☐ Accepted for Publication<br>☐ Submitted for Publication ☑ Unpublished and Unsubmitted work written in manuscript style |
| Publication Details | |

## Principal Author

| | |
|---|---|
| Name of Principal Author (Candidate) | Md Arafat Hossain |
| Contribution to the Paper | HTL Experimental design and method<br>Concept developments<br>Raw materials preparations and HTL batch experiments<br>Method developments for analysis<br>Characterizations of the HTL products<br>Drafting the manuscript |
| Overall percentage (%) | 80% |
| Certification: | This paper reports on original research I conducted during the period of my Higher Degree by Research candidature and is not subject to any obligations or contractual agreements with a third party that would constrain its inclusion in this thesis. I am the primary author of this paper. |
| Signature | Date 14/07/2023 |

## Co-Author Contributions

By signing the Statement of Authorship, each author certifies that:

i. the candidate's stated contribution to the publication is accurate (as detailed above);

ii. permission is granted for the candidate in include the publication in the thesis; and

iii. the sum of all co-author contributions is equal to 100% less the candidate's stated contribution.

| | |
|---|---|
| Name of Co-Author | David Lewis |
| Contribution to the Paper | Concept developments<br>Assistance with analysis and interpretation of data<br>Reviewing the manuscript<br>Supervise the overall work |
| Signature | Date 19/07/2023 |

| | |
|---|---|
| Name of Co-Author | Philip van Eyk |
| Contribution to the Paper | HTL reactor design and method<br>Concept developments<br>Assistance with analysis interpretation of data<br>Reviewing manuscript<br>Supervise the overall work |
| Signature | Date 18/7/2023 |

Please cut and paste additional co-author panels here as required.

# Investigation of the fundamental reasons for solid–renewable crude interaction during the hydrothermal liquefaction of mixtures of model compounds.

[a]Md Arafat Hossain, [a]David Lewis, [a]Philip van Eyk

[a]School of Chemical Engineering, The University of Adelaide, Adelaide, South Australia 5005, Australia

## Abstract

Hydrothermal liquefaction (HTL) is a widely recognised thermochemical process used to convert biomass into renewable crude (bio-oil). HTL produces several key products, including aqueous phase, hydrochar (solid), renewable crude (RNC), and gases. However, the actual yield of RNC is often lower than anticipated due to the trapping of oil within the hydrochar, making it difficult to extract even with solvents. In general, HTL of binary mixtures of model compounds demonstrates increased RNC yields at higher temperatures, as the decomposition rate rises. Source rock analysis (SRA) technique indicates that during the HTL of model compound mixtures, a significant portion (ranging from 57% to 71%) of RNC becomes trapped within the hydrochar for cellulose-lipid (50:50) combinations, with similar trapping percentages observed for cellulose-protein (50:50) and lignin-lipid (50:50) mixtures. For lignin-protein (50:50) mixtures, the trapping range is between 60% and 66%. To investigate the underlying reasons for oil trapping in solid or hydrochar, the products resulting from the highest and lowest degrees of RNC trapping were analysed. It was discovered that the hydrochar lacks pores capable of retaining oils. The presence of non-polar functional groups on the hydrochar surface attracts the oil due to their hydrophobic (oil-wet condition) properties, and a higher number of non-polar functional groups corresponds to a greater degree of RNC trapping into solid. The acid value (AV) of RNC and the viscosity of the oil also significantly influence solid-oil entrapment. Oils with better wetting capabilities on solid surfaces (from a

lower contact angle with the solid) allow for a greater amount of RNC trapping in the hydrochar.

Keyword: Hydrothermal liquefaction; biocrude; hydrochar; solid-biocrude interaction; model compounds.

### 5.1. Introduction

Current sources of energy are greatly dependent on non-renewable fossil fuels. The biggest disadvantage of the use of fossil fuels is that they produce greenhouse gases such as $CO_2$, $CH_4$ and $N_2O$ [1]. There are some other concerns, for instance, their uncertain availability and rapid depletion. Over the years, finding a new source of fuel that is renewable and environmental friendly has become a major target for researchers. Bioenergy, i.e., energy generation from biomass, is one solution to this problem [2]. Biomass is one of the most abundant organic resources and the only renewable organic source [2, 3]. The structure of the biomass has an extensive impact on biofuel conversion and any other products derived from biomass sources [4]. Cellulose, hemicellulose and lignin are the plentiful carbohydrates in biomass. Depending on the conversion technique, all these compounds are converted to gases, renewable crude (RNC), hydrochar and aqueous phase. Different thermal conversion techniques have been employed to target the different products; for example, pyrolysis has been used to produce mainly hydrochar and HTL has been used to produce RNC. though some other by-products can also result from the both process [2].

HTL is a popular thermochemical process that is used to produce the liquid fuel known as renewable crude or bio crude [5]. There are several advantages of the HTL reaction over other popular biomass conversion techniques, such as pyrolysis. Dry biomass is needed for the pyrolysis process, but drying the biomass is not necessary for an HTL reaction. Therefore, it holds great economic value for fuel production because of the wet nature of various biomass

feedstocks, including low quality feedstock [6, 7]. The HTL reaction happens under subcritical conditions (temperature 250–370°C, pressure 4–20 MPa) and produces RNC, together with hydrochar, gasses and aqueous phase as by-products [8]. The RNC from HTL can be refined to gasoline, diesel oil or naphtha [9]. In HTL, water acts as both reactant and catalyst, which makes the reaction different from other thermochemical conversion techniques. At subcritical conditions, water has low viscosity and can dissolve organic substances. This makes subcritical water an excellent medium for fast, homogeneous and efficient reactions [10, 11]. Consequently, the use of subcritical water for biomass conversion is of great interest to many researchers.

Beckman et al. [12] compared the yields and properties of oil produced from the thermochemical liquefaction process. They concluded that changing the governing parameters such as temperature had significant impact on products yields. Jin et al. [13], Aysu et al. [14] and Brown et al. [15] found that higher temperatures favor higher yields of RNC and lower the hydrochar yields, even when a mixture of two different algae; i.e, *Spirulina platensis* + *Entermorpha prolifera* (EP) were used [13]. Sometimes very high temperature reduce the RNC yields by increasing gas formation. Products can undergo further reactions (secondary reactions), such as tar cracking and shifting reactions, which can lead to a decrease in certain products and can increase gas formation [16, 17].

Yin et al. [18] found that a lower residence time is suitable for higher yield of renewable crude during the HTL of cattle manure. HTL of *Nannochloropsis oceanica* [19], *Dunaliella tertiolecta* [20], swine manure and mixed-culture algae [21] also showed higher yields of renewable crude from lower residence times. HTL of a mixture of two algae (*Spirulina platensis* + *E. prolifera*) has been carried out for different biomass to solvent (B/S) ratios (0.17 to 1) at 340°C with deionised water as a solvent [13]. A lower B/S ratio was found to be favorable for higher renewable crude yields and hydrochar yields were favored by a higher B/S

ratio. As water plays an important role in accelerating the reaction [22], increasing the biomass to water (B/S) ratio can reduce the decomposition of the biomass, which then reduces the renewable crude yields. The investigations were not only limited to the product formation from HTL of Biomass.

Characterisation and analysis of HTL products has also been performed by several researchers, such as Arturi et al. [23] and Obeid et al. [24]. Obeid et al. also investigated the reaction kinetics for HTL of polymers. Fan et al. [25] studied the HTL of model compounds such as lactose (lac), maltose (mal), lysine (lys), and hydroxymethylfurfural (HMF) to produce RNC. They also investigated the HTL of binary mixtures and produced RNC with unfavorable nitrogen content. Madsen et al. [26] predicted the chemical composition of the aqueous phase from HTL of biomass and model compounds. HTL of cellulose [27], lignin [28], protein [29] and lipid [30] have been extensively studied for yields and characterisation of HTL products. Researchers also encountered challenges in the separation of HTL products, specially RNC separation from hydrochar.

As the attachment of hydrochar and RNC is strong, researchers have used different solvents to extract the oil. Some organic solvents, such as acetone, propanol, butanol, ethyl acetate and methyl ethyl ketone can lower the viscosity of the heavy oil produced from the HTL reaction [31]. But no solvent has been found to extract the whole amount of oil from the hydrochar. The solvent efficiency depends on the raw materials and other experimental factors. For instance, in case of the HTL of pine wood, the efficiency of co-solvents for renewable crude yields is ethanol > acetone > water [32]. However, for another raw material, empty fruit bunch (EFB), the efficiency is glycol > water > ethanol > acetone > toluene [33] in terms of total oil and gas. Acetone has a high solvent efficiency for the HTL of *Ferula orientalis L.* [14], reed canary grass [34], *Typha latifolia* [35] and milled *Onopordum heteracanthum* stalks [36].

The destruction of polar groups (generally –OH and –COO–) during the HTL reaction reduces the ability of products to attract water by hydrogen bonding, making the resulting solids hydrophobic (attract to oil) [37]. The solid-oil interaction of the hydrochar and RNC oil varies depending on different factors and properties. To the authors' knowledge, no study to-date has focused on an investigation of the fundamental reason for the solid-oil interaction during the HTL of biomass.

The breakdown of cellulose and lignin produces mostly solids and lipids, and HTL of protein produces mostly oil. Therefore, we have performed HTL on several different mixtures, including cellulose, protein, lipid and lignin, to produce both hydrochar (solid) and RNC (oil). We reported yields of products, including the trapped RNC in the hydrochar and the extracted RNC, and our investigation into how different experimental parameters affect the yields and the degree of biocrude trapping in the hydrochar. In addition, we investigated the fundamental reasons for the solid-oil interaction.

## 2. Materials and Methods

### 2.1 Materials

As this investigation focuses on the solid-renewable crude (RNC) interaction, raw materials were selected to produce high levels of hydrochar and RNC during HTL. HTL of cellulose and lignin produces mostly solids, and that of proteins and lipids produces mostly RNC. Therefore, the following binary mixtures have been selected for this investigation: 50% cellulose + 50% lipid (CL50%), 50% cellulose + 50% protein (CP50%), 50% lignin + 50% lipid (LL50%) and 50% lignin + 50% protein (LP50%).

Cellulose is a carbohydrate model compound. The selected cellulose sample (Acros Organics) has an extra pure microcrystalline structure with an average particle size of 90 μm and a maximum impurity level of 10 ppm heavy metals. The alkaline lignin selected for this

investigation (Tokyo Chemical Industries) contains maximum of 10% moisture. Crisco 100% premium sunflower oil was used as a lipid and was bought from the supermarket. The protein used was 100% soy protein from the supermarket. In this study, no solvent was used to extract the renewable crude from the hydrochar. As half of the mixture was protein or lipid, enough RNC was produced to be easily extracted and analyzed.

### 5.2 Experimental setup

HTL of a prepared mixture of model compounds was carried out in an 11-ml stainless steel HTL batch reactor. The layout of the batch reactor and fluidised bed is shown in Figure 5.1. The reactor was a 20-cm 316 stainless steel tube of outer diameter 12.5 mm and 2-mm thickness. A 12.5 mm Swagelok port connector and fittings was attached to each end of the reactor. A Type K mineral insulated thermocouple was connected to one end of the reactor and other end was covered. A 3.2-mm tube was attached to the upper end of the reactor to stop the contents from entering the top half. A pressure transducer and pressure-relief valve were connected to the reactor and also to a pressure indicator, and the thermocouple was connected to a temperature indicator. A ball valve was used to purge the oxygen and the reactor was pressurised with $N_2$ before the HTL reaction. The flue gas was released from the reactor via this ball valve after the HTL reaction. The capacity of the reactor was 400 bar. Sand was used as the fluidised bed material. The maximum rise temperature was around 400°C.

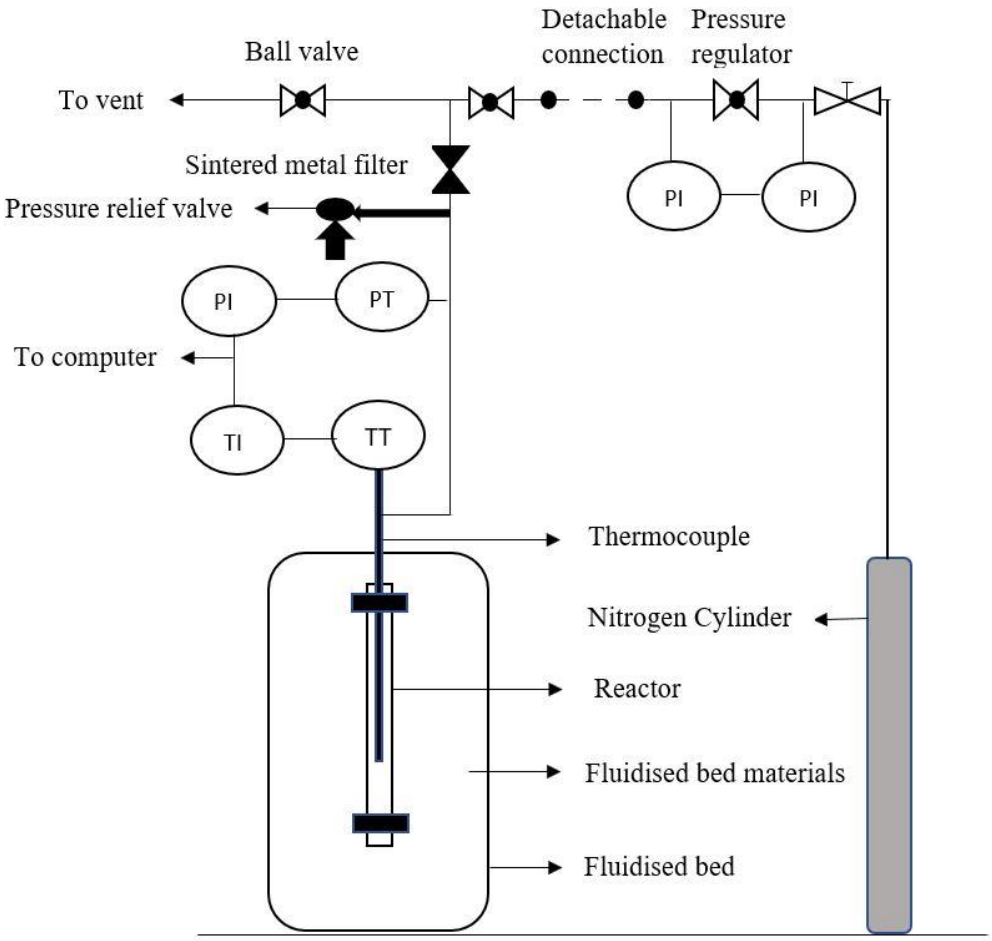


Figure 5.1: Schematic diagram of an HTL batch reactor. PT – pressure transducer, PI – pressure indicator, TI – temperature indicator

### 5.2.1 Batch HTL experimental procedure

HTL of mixtures of model compounds was carried out under varying reaction parameters. Previous work has suggested a lower residence time (10 min) and 0.5 B/W ratio is suitable. Reaction temperatures ranged from 260–350°C.

For every experiment, the reactor was filled to 50% of the total capacity at room temperature. After filling the reactor, it was charged with nitrogen ($N_2$) to 100 bar from a high pressure nitrogen gas cylinder (Figure 5.1) and left for 3 min to check for leaks. The pressure was then released and charged to the starting pressure (between 85 and 120 bar) required to achieve 200 bar under the reaction conditions.

After the reactor was filled with feedstock and at the required pressure, it was positioned inside a Techne SBL-2D fluidised bed to be heated. A Techne 9D temperature controller was connected to vary the temperature set point and air flow rate throughout the bed. This provides uniform heating of the reactor at the required reaction temperature. The fluidised bed was pre-heated to the required temperature before the reactor was placed inside the bed. After positioning the reactor in the fluidised bed, the feed in the reactor was heated at a rate of approximately 125°C per minute. The reaction was held at the desired reaction temperature for 10 minutes, then cooled to 70°C.

### 5.3 Product recovery and analysis

The reactor was weighed before and after filling to record the feedstock weight. It was also weighed before and after releasing the gas to find the mass of the $N_2$ gas. The mass of the added $N_2$ in the reaction was deducted from the mass of gas released after the reaction to give the mass of the gas produced from the HTL. The reactor was washed with water carefully three times and the mixture was centrifuged at 2000 rpm for 15 minutes. The normal product mixture produced three distinct layers: aqueous, RNC and the solid-RNC mixture. The solid and RNC phase was pipetted from the centrifuge tube, dried at 40°C to remove additional moisture and stored separately for Source Rock analyser (SRA). No solvent was used to extract additional (trapped) oil from the hydrochar. The remaining oil is called the extracted RNC. SRA gives the percentages of the total trapped oil in the solid. The total RNC, Hydrochar (solid) and gas values were subtracted from 100 to find the percentage of aqueous compounds produced. Every experiment been repeated two times and the standard deviation for small sample size (two repetition) has been calculated [38].

#### 5.3.1 Renewable crude recovery with Source Rock Analyser (SRA)

Source Rock Analyser (SRA) uses pyrolysis to provide accurate data about the NC and total organic carbon (TOC) in a solid. A Weatherfords Source Rock Analyser™ was used, with

helium as the carrier gas. The pyrolysis oven was first held at 300°C for 5 minutes and then ramped (at 25°C per minute) from 300°C to 650°C. Subsequently, the oven was reduced to 220°C and held for five minutes, purged with inert air (CO & $CO_2$ free), then ramped at maximum heating to 580°C and held for 20 minutes under helium. The flame ionisation detector (FID) was calibrated with Weatherford Laboratories Instruments Division Standard 533. The IR analysers were calibrated against standard gas with a known concentration of $CO_2$ and CO. This gave the amount of free hydrocarbon generated through thermal cracking at 350°C (S1) and the amount of hydrocarbon generated through thermal cracking at higher temperatures up to 600°C (S2). The total of S1 and S2 in the solid is the total trapped oil.

### 5.3.2 Acid value (AV) of renewable crude

The acid value (AV) of an oil refers to the number of milligrams of potassium hydroxide (KOH) required to neutralise the free fatty acids in a 1 g sample [39-41]. The AV influences the attachment of the oil to hydrochar. The American Society for Testing and Materials (ASTM) standard D974 method was used to determine the AV of the RNC. In this method, the oil sample was dissolved in a mixture of isopropyl alcohol and a small amount of water. The subsequent single-phase solution was titrated at normal temperature with a standard alcoholic base solution to the end point indicated by the color change of the added p-naphtholbenzein solution (orange in acid and green-brown in base). To determine the strong acid number, a separate portion of the sample was extracted with hot water and the aqueous extract was titrated with potassium hydroxide solution, using methyl orange as an indicator.

### 5.3.3 Contact angle measurement

The contact angle (tangent) of the oil with respect to glass was measured to determine how much oil is inclined to attach to the hydrochar [42]. A lower oil contact angle means that that the oil covers a greater surface area of the glass. A Theta Optical tensiometer was used to measure the contact angle of the oil. The tensiometer was placed on a vibration-free table where

air flows were at a minimum. A high-resolution camera lens was used to capture the angle between the 5-µl droplet and the glass film at room temperature. The contact angles of oil droplets were measured by means of contact angle goniometry.

### 5.3.4 Fourier transform infrared (FTIR) analysis

The functional groups of hydrochar impact oil attraction. Therefore, FTIR analysis was performed using a Nicolet 6700 Thermo Fisher Fourier transform infrared (FTIR) spectrometer over the wavelength range of 4000–400 $cm^{-1}$. The hydrochar was washed with ethanol to remove as much oil as possible, then dried in oven at 40°C for 48 hours before FTIR analysis.

### 5.3.5 Brunauer-Emmett-Teller (BET) analysis

The hydrochar was washed with ethanol as above, then $N_2$ adsorption isotherms were measured using a Micromeritics 3 Flex analyser (Micromeritics Instrument Corporation, Norcross, GA) at 77 K.

### 5.3.6 Viscosity analysis

The batch reactor could only produce a small amount of RNC, which was not enough for the viscosity measurement. Therefore, using the same feedstocks and same reaction conditions, a 1L Parr batch reactor was used to produce higher amount of RNC. A Universal Stress Rheometer SR5 (TA Instruments) with a cone and plate configuration was used to obtain rate-shear stress data, which was then used to calculate the viscosity.

## 5.4 Results and Discussion

### 5.4.1 HTL of mixture of cellulose and Lipid

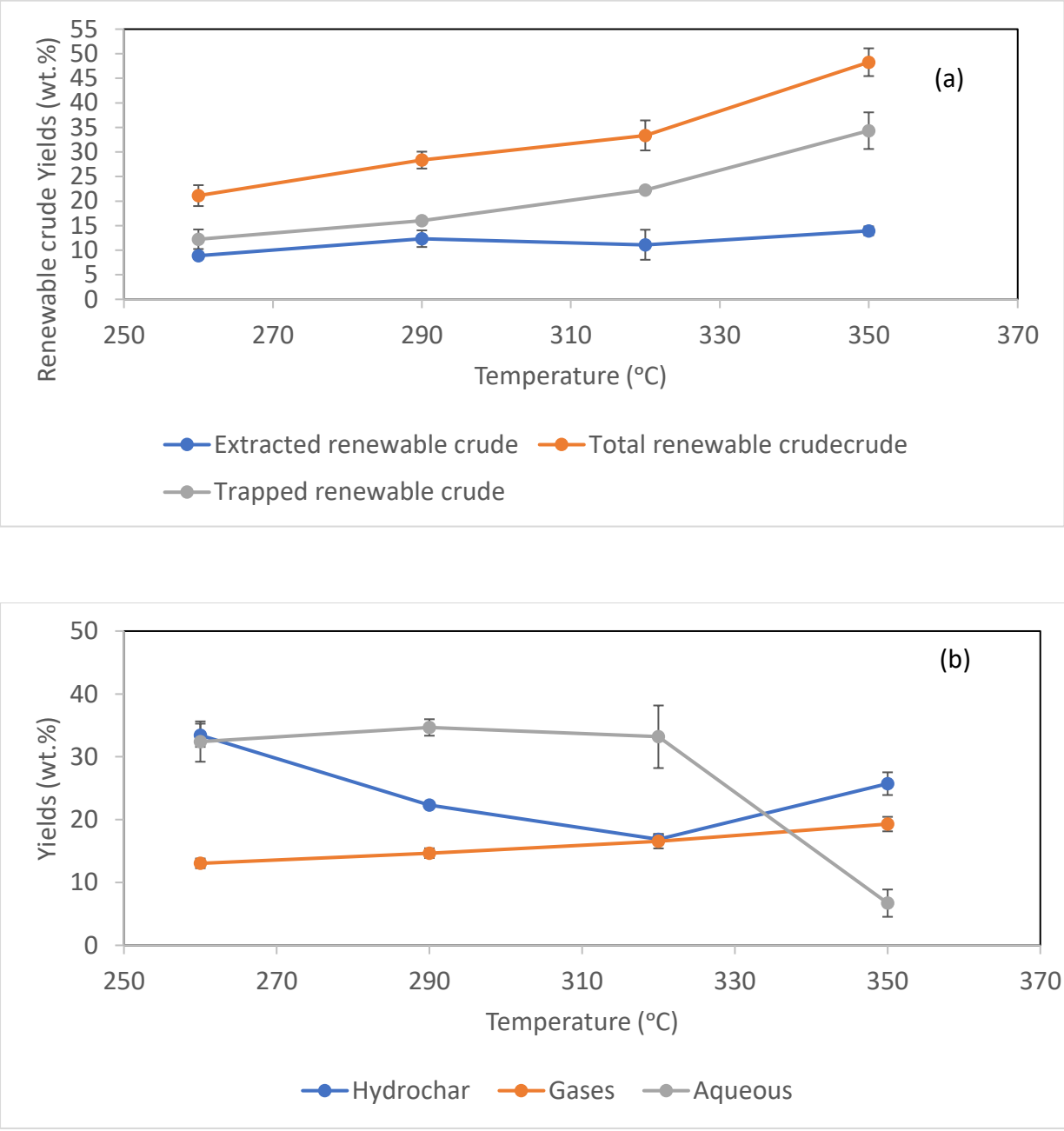


Figure 5.2: Yields of (a) RNC (b) other products for CL50%

The HTL products obtained from the CL50% mixture i.e, hydrochar, gases, aqueous and RNC, are presented in Figure 5.2. Figure 5.2a shows the influence of temperature on the RNC yields, including both the trapped (analyzed by SRA) and extracted RNC. The graph demonstrated

that total RNC increased from 21–48 wt.% when the temperature changed from 260–350°C. At the same time, extracted RNCs were also increased from 8–13 wt.% when changing temperature from 260–350°C. Yu et al. [20] observed a similar temperature effect during the HTL of *D. tertiolecta,* and Feng et al. [43] also report an increased yields with increased temperature from the HTL of α-cellulose.

The amount of RNC trapped in hydrochar was at a minimum (12 wt.%) at a temperature of 260°C and was at a maximum (34 wt.%) at 350°C. It is obvious that most of the produced RNC is trapped in hydrochar and that higher yields of total RNC lead to higher trapping of RNC.

Figure 5.2b shows the influence of temperature on product yields from the HTL of CL50%. The maximum hydrochar yield was 33 wt.% at 260°C. It then declined to 16.86 wt.% at 320°C and then increased again to 25 wt.%. The higher yield of hydrochar at the lower temperature was because of the lower decomposition of biomass [43]. Secondary cracking of one product at very high temperature can led the increase of another product [43]. This may be the one of the reasons hydrochar yield was further increased again at a higher temperature. The yield of aqueous was steady (13–16 wt.%) from 260–320°C. But after 320°C there was a sudden decrease and at 350°C the aqueous yield was only 6 wt.%. Therefore, we can conclude that the secondary cracking of the aqueous phase at 350°C led to the increase in the hydrochar yield. The gas yields gradually increased from 13–19 wt.% as the temperature increased from 260–350°C. It is obvious that decomposition of biomass leading to an increase in gas yields occurs at higher temperatures [44]. Caprariis et al. [44] investigated the HTL of cellulose and found a similar increase of gas yield with high temperature.

### 5.4.2 HTL of the mixture of cellulose and protein

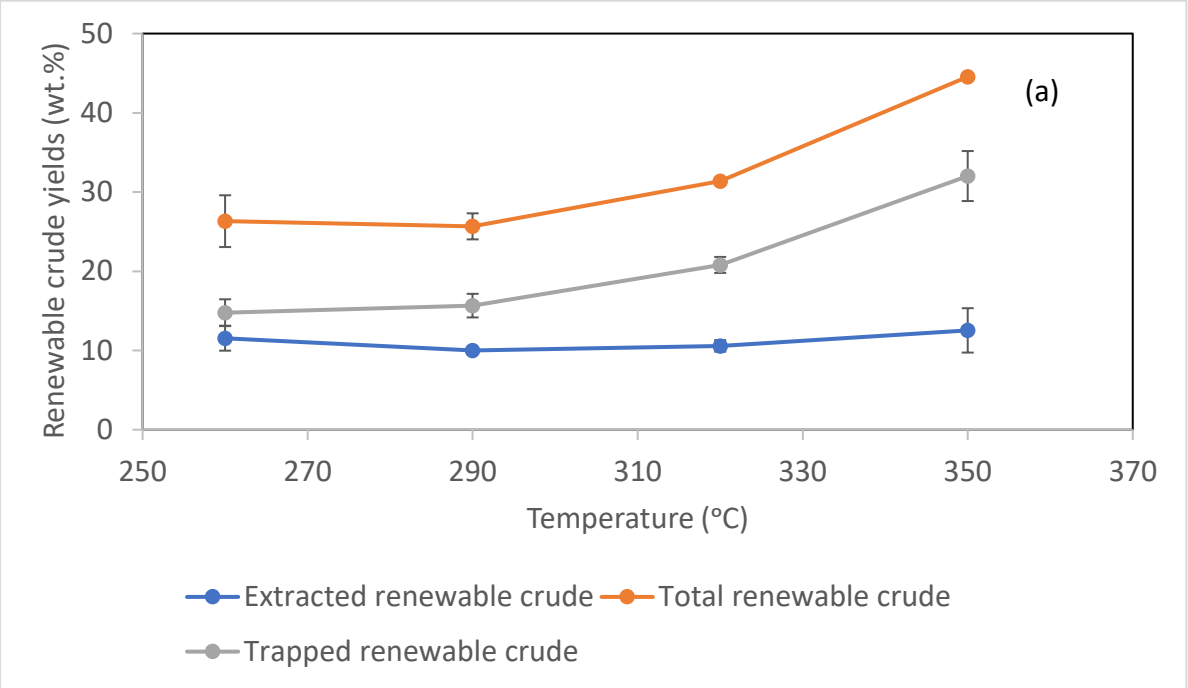


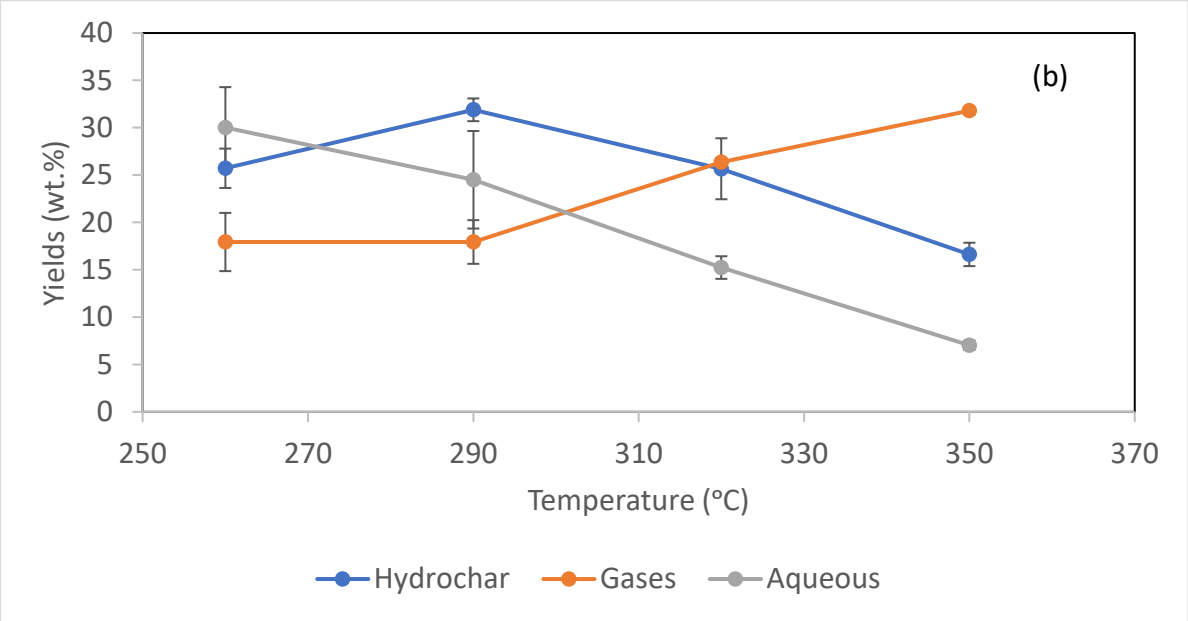


Figure 5.3: Yields of (a) RNC (b) other products for CP50%

Products obtained from the HTL of CP50%, are presented in Figure 5.3. Figure 5.3a shows the influence of temperature on the RNC yield including trapped and extracted RNC. At 260°C, total RNC was 26 wt.% which was slightly decreased to 25 wt.% at 290°C. This could be due

to secondary cracking occurring earlier than expected [27] as well as higher temperatures leading to the higher decomposition of biomass which could produce more RNC [20]. Increasing the temperature from 290°C to 350°C increased the total RNC to 44 wt.%. Though total RNC was gradually increased, extracted RNC was limited to 10–12 wt.%. As the HTL of protein produces amino acids, it lowers the pH. A low pH mixture (acidic mixture) interacts with the oil, therefore there was a low yield of extracted RNC [25] [45] [46]. As a result, most of the RNC was trapped inside the hydrochar and the trapping increased (14–32 wt.%) with increasing temperature (260–350°C).

Figure 5.3b shows the influence of temperature on product yields from the HTL of CP50%. The hydrochar yield increases from 25–31 wt.% when the temperature rises from 260–290°C. It then gradually decreases to 16 wt.% at 350°C. Secondary cracking of the hydrochar started after 290°C, which reduced the yield of hydrochar, but dramatically increased the gas yield. The gas yield was around 17 wt.% at 260–290°C, it then gradually increased to 31 wt.% at 350°C. The aqueous phase gradually decreased from 30–7 wt.% with rising temperature.

### 5.4.3 HTL of mixture of Lignin and Lipid

Products from the HTL of LL50%, are presented in Figure 5.4. The total RNC increased from 37–52 wt.% when the temperature increased 260–320°C due to the higher decomposition of biomass [20]. But the RNC yield then decreased to 40 wt.% when the temperature rose further to 350°C due to secondary cracking [43]. Feng et al. [47] found a similar temperature effect during the catalyst-supported HTL of lignin.

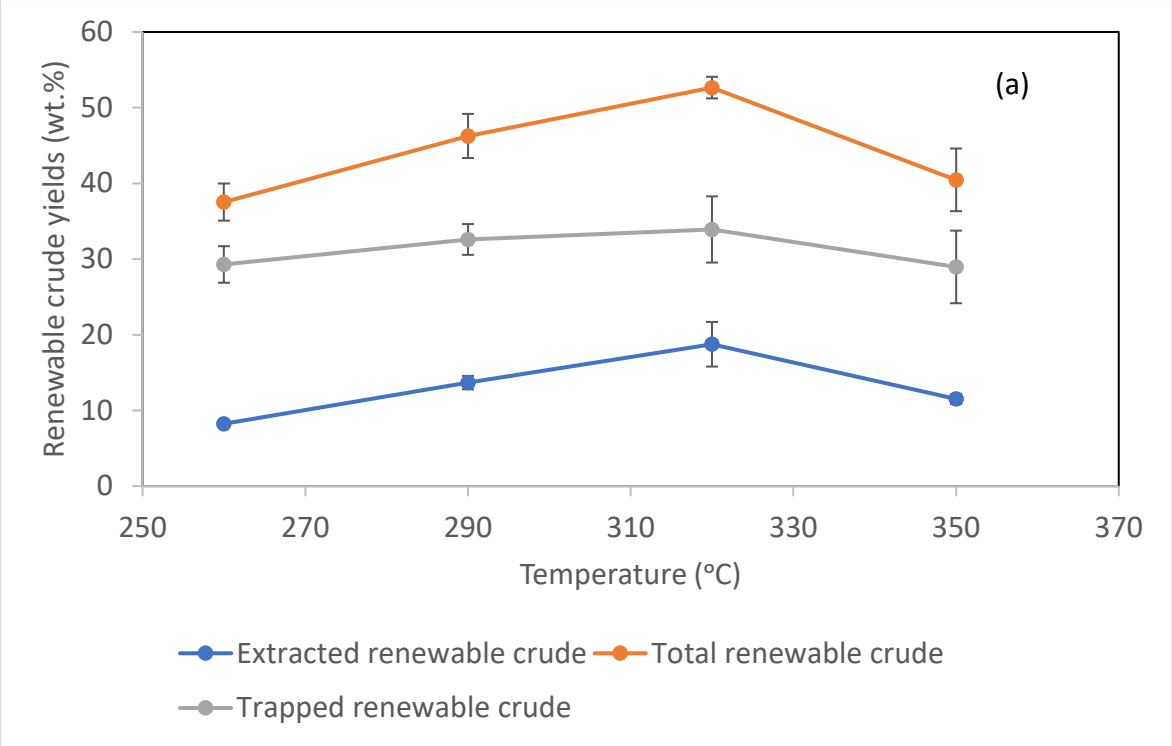


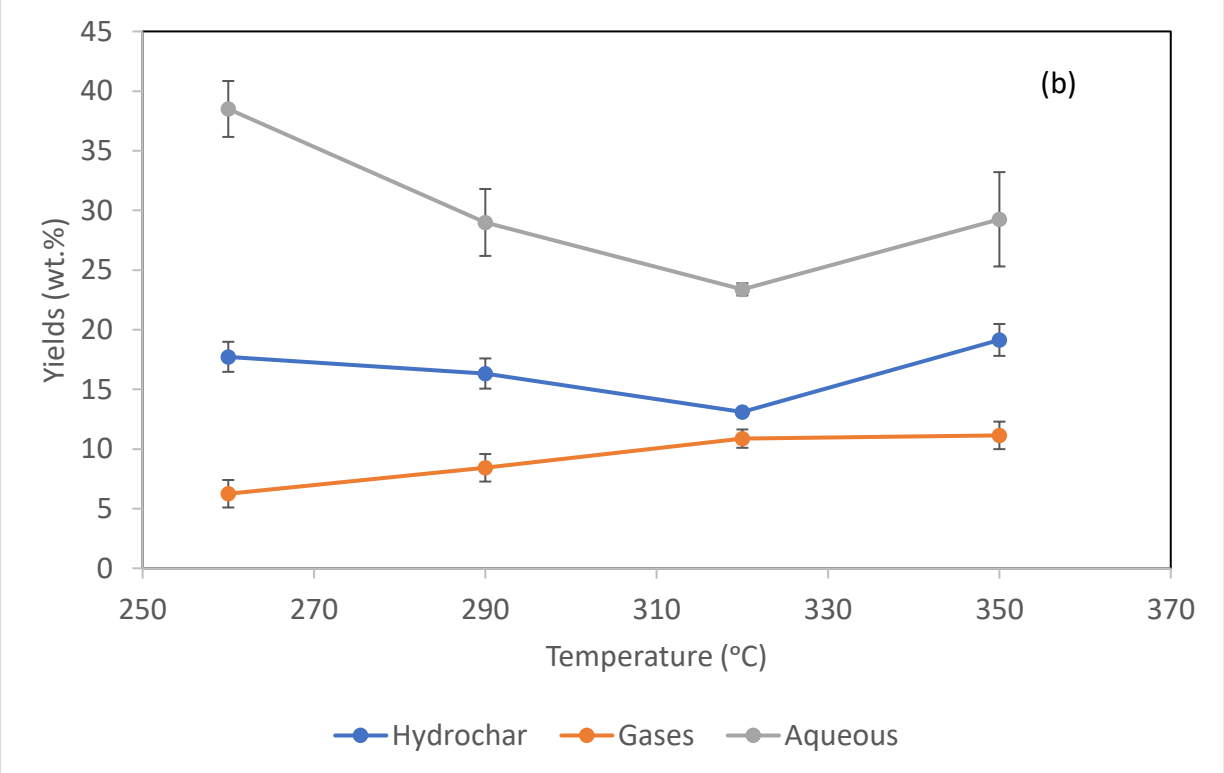


Figure 5.4: Yields of (a) RNC (b) other products for LL50%

Extracted RNC also increased from 8–18 wt.% with a rise in temperature from 260–320°C and decreased at 250°C. The maximum and minimum trapping of RNC, 33 wt.% and 29 wt.%, occurred at 320°C and 260°C, respectively. As the total RNC increased, the extracted and trapped RNC also increased (Figure 5.4a).

Figure 5.4b shows that decomposition at higher temperatures led to a decrease in hydrochar yields (17–13 wt.% from 260–320°C); however, the yields increased again to 19 wt.% at 350°C. Like the hydrochar, the aqueous phase also decreased from 38–23 wt.% as the temperature rose from 260–350°C and increased to 29 wt.% at 350°C. Re-polymerisation and condensation from other products such as RNC 320°C could lead to more hydrochar and aqueous phase at 350°C [43]. Decomposition of biomass increased with temperature; gas yields also increased from 260°C to 350°C.

### 5.4.4 HTL of mixture of lignin and protein

Figure 5.5a shows the influence of temperature on RNC yields for LP50%. Total RNC increased gradually from 21–48 wt.% and extracted RNC increased from 8–13 wt.% with a rise in temperature from 260–350°C. There was no secondary cracking found in the reaction of this mixture. Biswas et al. [48] investigated the catalyst-supported HTL of lignin and found a similar temperature effect on RNC yield, in solvents such as water, ethanol and methanol.

Minimum and maximum yields of trapped RNC were 12 wt.% and 34 wt.% at temperatures of 260°C and 350°C, respectively (Figure 5.5a). Decomposition at higher temperatures led to a decrease in hydrochar yields (from 27–18 wt.% at 260°C and 350°C, Figure 5.5b). The gas production gradually increased from 7–13 wt.% with rising temperatures from 260–350°C. The decrease of hydrochar with rising temperature can lead to increased yields of gas or other products. Repolymerisation, condensation, hydrolysis and polymerisation reactions are parts of the HTL reaction can produce gas when hydrochar decomposes with temperature [43].

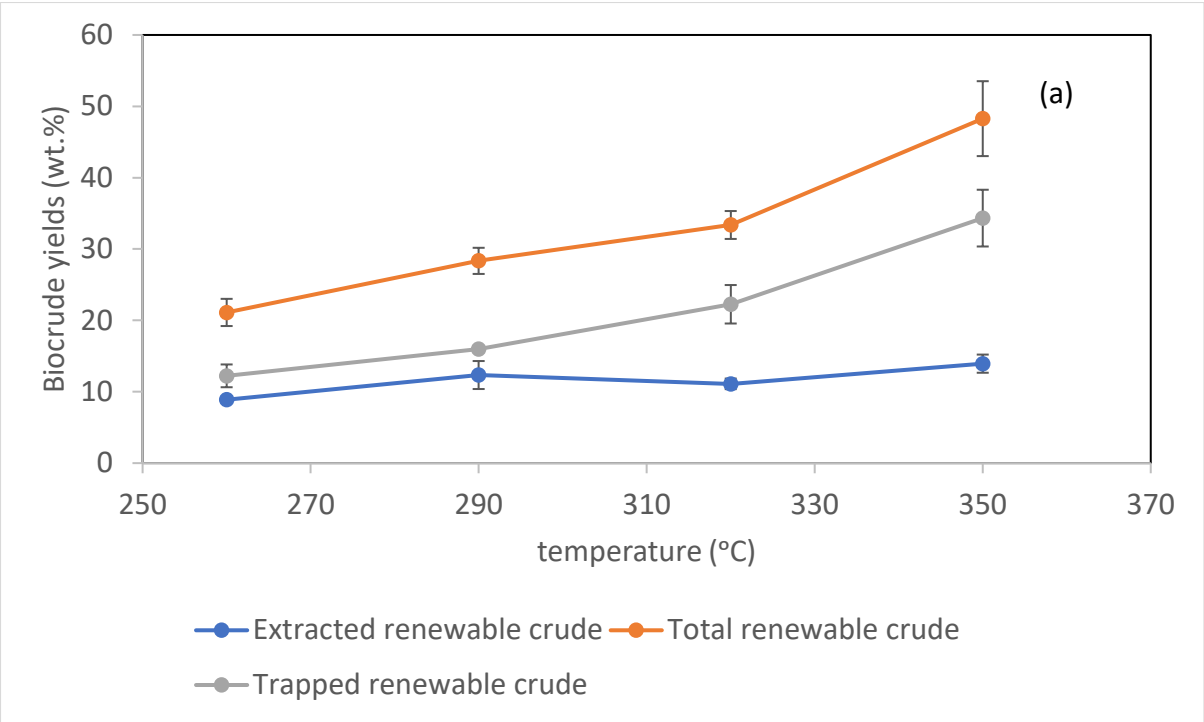


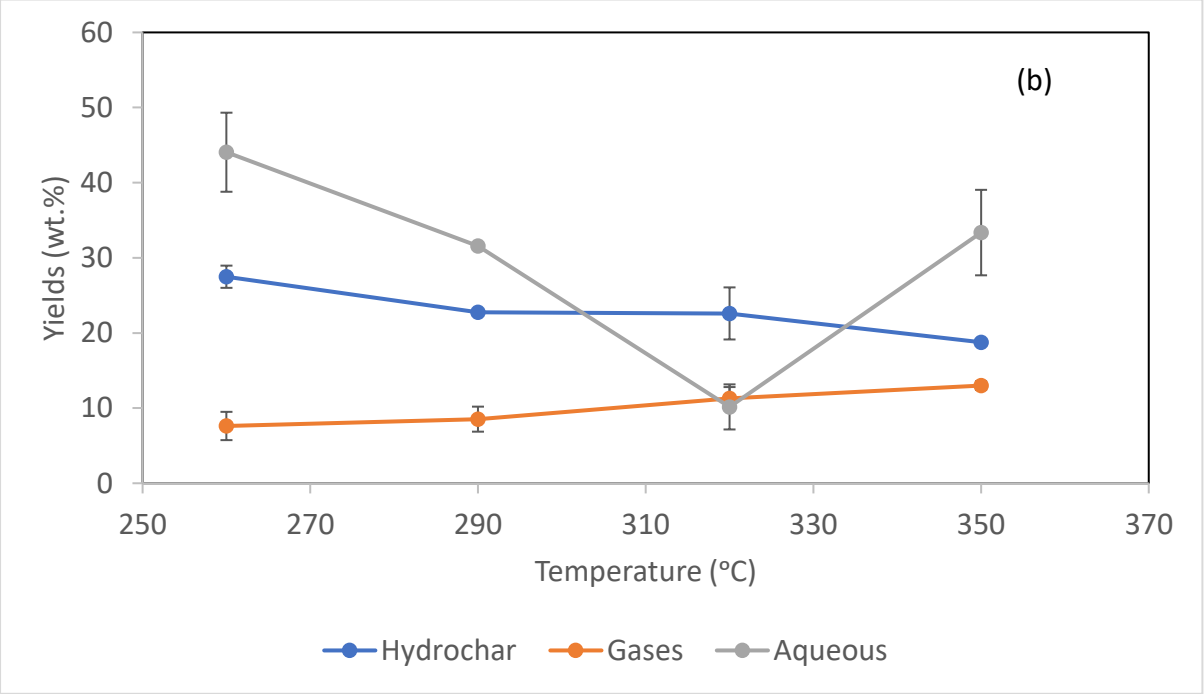


Figure 5.5: Yields of (a) RNC (b) other products for LP50%

### 5.4.5 Degree of trapping (DOT)

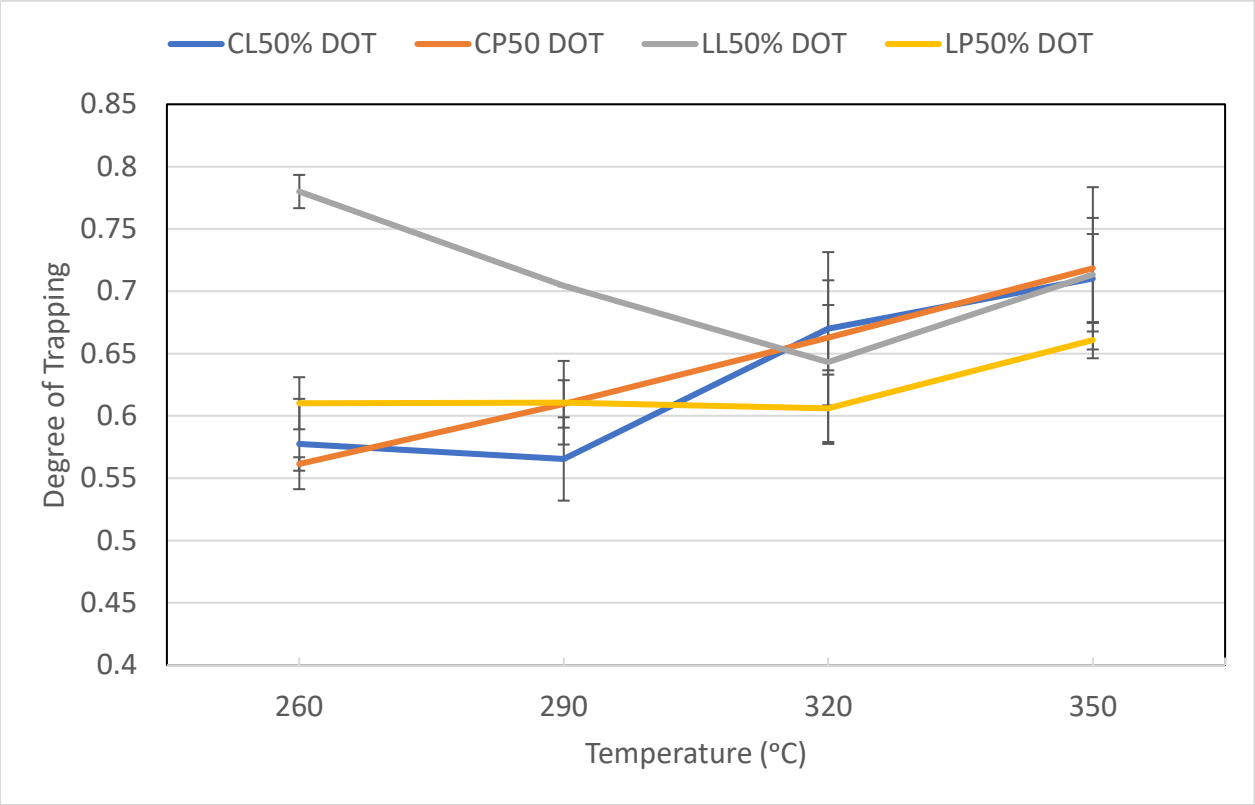


Figure 5.6: DOT of RNC in hydrochar

Table 5.1: Lowest and highest DOT of RNC in hydrochar

| | CL50% | CP50% | LL50% | LP50% |
|---|---|---|---|---|
| Lowest Trapping | 290°C | 260°C | 320°C | 260°C |
| Highest Trapping | 350°C | 350°C | 260°C | 350°C |

The DOT is defined as the ratio of trapped RNC to total RNC. For the HTL of both CL50% and CP50% the lowest DOT (0.56) occurred at 290°C and the maximum DOT (0.71) at 350°C (Figure 5.6). For CP50%, higher yields of total RNC increased the DOT. For LL50% the minimum DOT (0.64) was found at 320°C though the total RNC yield was highest, and the maximum DOT (0.78) occurred at 260°C though the total yield of RNC was lowest at that temperature. For LP50%, at 260°C, 290°C and 320°C, the DOTs were similar, at around 0.61,

even though the total RNC yields increased with rising temperature. The minimum DOT (0.60) was recorded at 320°C. The DOT then increased to a maximum of 0.66 at 350°C (Figure 5.6).

Factors affecting DOT include the AV of the RNC, the contact angle of oil with respect to the solid, the functional groups on the solid, the porosity of solid, and the viscosity of the RNC. Therefore, the products (RNC and hydrochar) from the experiments with the highest and lowest DOT were selected for further investigation. Table 5.1 shows the parameters of the selected products.

### 5.4.6 Characterisation

#### 5.4.6.1 Effect of Acid value (AV) on RNC trapping

Figure 5.7a shows the acid value (AV) of the RNC from the HTL of the different model mixtures. The AV for lowest and highest trapping of CP50% are 49 mg KOH/g and 65 mg KOH/g, and for CL50% are 13 mg KOH/g and 27 mg KOH/g, respectively. The AV for lowest and highest trapping are 38 mg KOH/g and 49 mg KOH/g for LP50% and are 11 mg KOH/g and 32 mg KOH/g for LL50%, respectively. A lower AV resulted in a lower amount of trapping. It was also observed that the mixtures containing protein gave higher AV than the non-protein mixtures.

During the conversion of protein in HTL, protein is converted to RNC via a series of chemical reactions, which first result in amino acids [45]. Therefore, HTL of a protein mixture could result in a higher AV.

Acidity is an important factor that has an influence not only in the solid-liquid formation, but also the interaction of the RNC with the solid [45, 49]. The alkaline oil (lower AV) can change the surface of hydrochar from hydrophobic (oil wet) to hydrophilic (water wet). This can release more residual oil that is trapped in the solid. This release occurs due to a change in

capillary pressure [46]. Therefore, the lowest RNC trapping in hydrochar occurred in cases where the AV was the lowest.

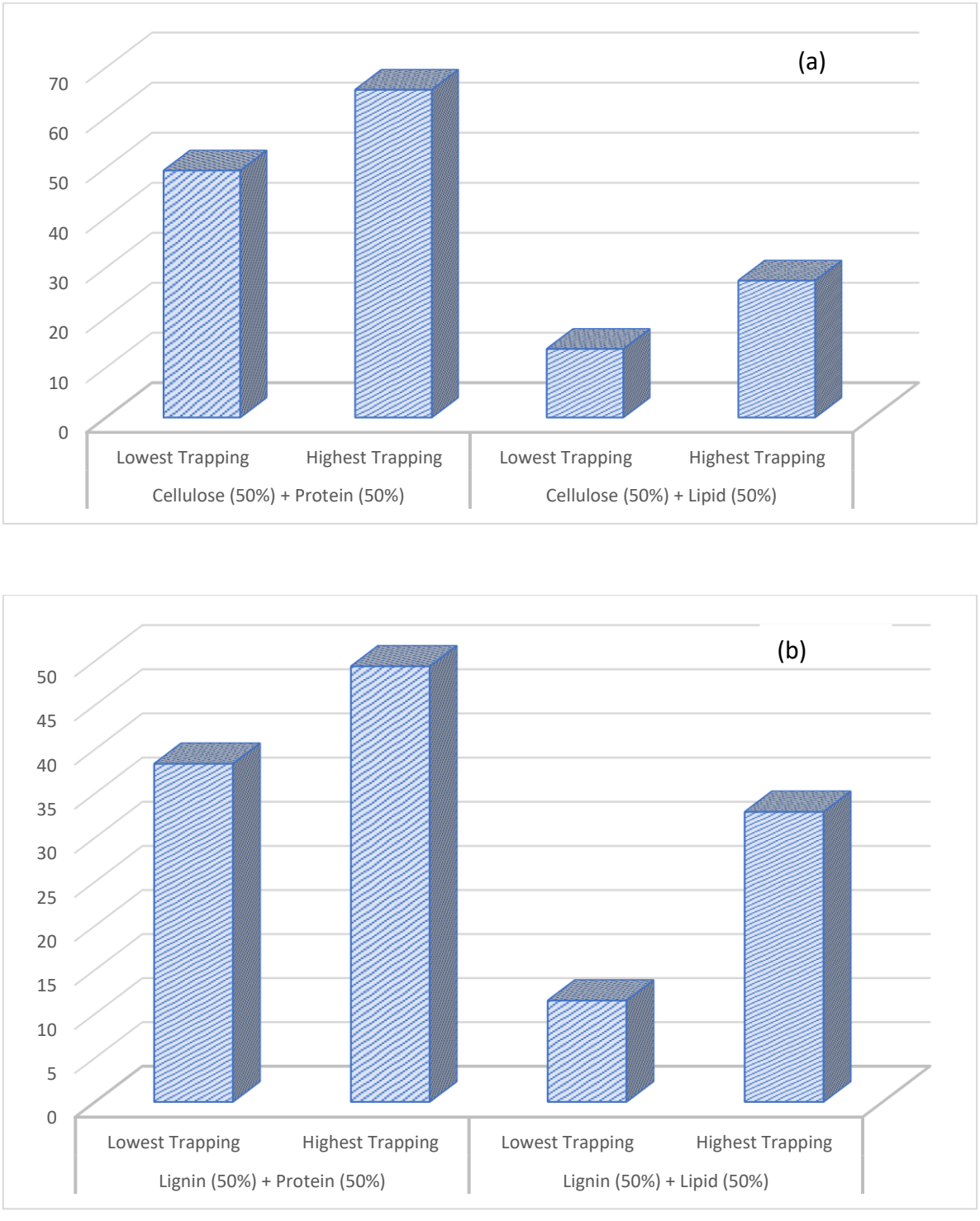


Figure 5.7: AV of the RNC from mixture of (a) CL50% and CP50%and (b) LL50% and LP50%

#### 5.4.6.2 Contact angle for higher trapping of RNC

The contact angle is a quantitative measure of the wetting of a solid surface. It is the angle formed by a liquid at the three-phase boundary where a liquid, gas, and solid interact [50]. The wettability of an oil can be calculated from the contact angle formed in an oil-solid interface and the wettability of solid can be calculate from the contact angle with water-solid interface [51]. A smaller contact angle shows that the oil spreads on the surface and covers a higher surface area. A larger contact angle shows that the oil beads on the surface and covers less surface area [51].

A glass plate was used as a reference surface. Figure 5.8 shows the contact angle of lower trapping (28°) and higher trapping (15°) of RNC produced from CL50% as well as lower trapping (25°) and higher trapping (16°) of RNC produced from CP50%. Figure 5.9 shows the contact angle of lower trapping (28°) and higher trapping (16°) of RNC produced from LL50% as well as that of the lower trapping (28°) and higher trapping (18°) of RNC produced from LP50%. The higher trappings always showed a lower contact angle with the glass surface; hence, a higher wetting of the surface leads to higher trapping of the oil.

If water forms a contact angle of less than 90º with a solid surface, the solid has a hydrophobic nature and if the contact angle is more than 90º, the solid has a hydrophilic nature [52]. However, there are limitations when measuring the contact angle of the HTL hydrochar and water interface. As the hydrochar holds some oil, it might provide the wrong contact angle. Additionally, the hydrochar has a small particle size and is not the plain surface needed for measurement. Therefore, only the wettability of the RNC was measured.

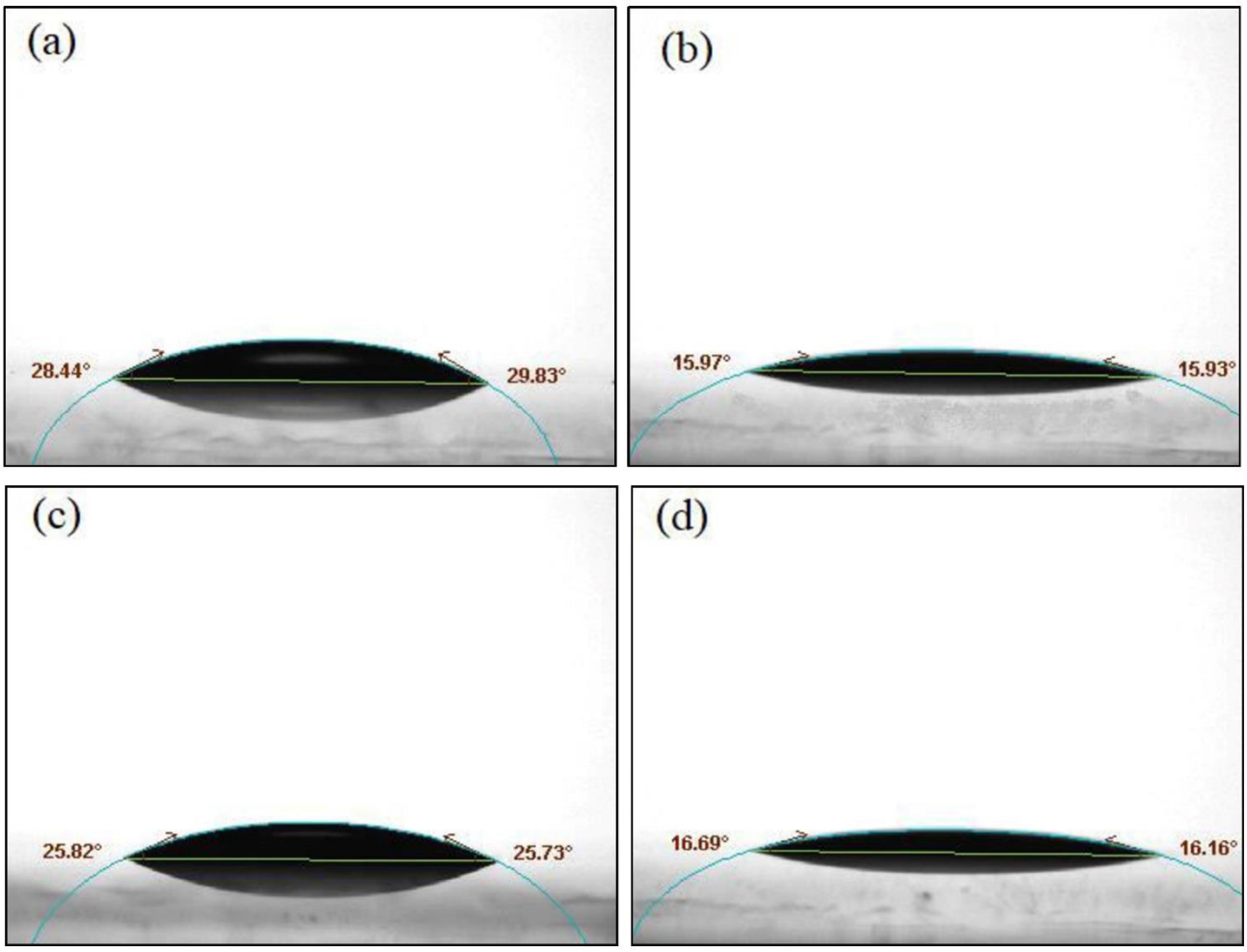


Figure 5.8: Contact angle measurement with respect to glass for (a) lower trapping (b) higher trapping of RNC produced from CL50% and (c) lower trapping (d) higher trapping of RNC produced from CP50%.

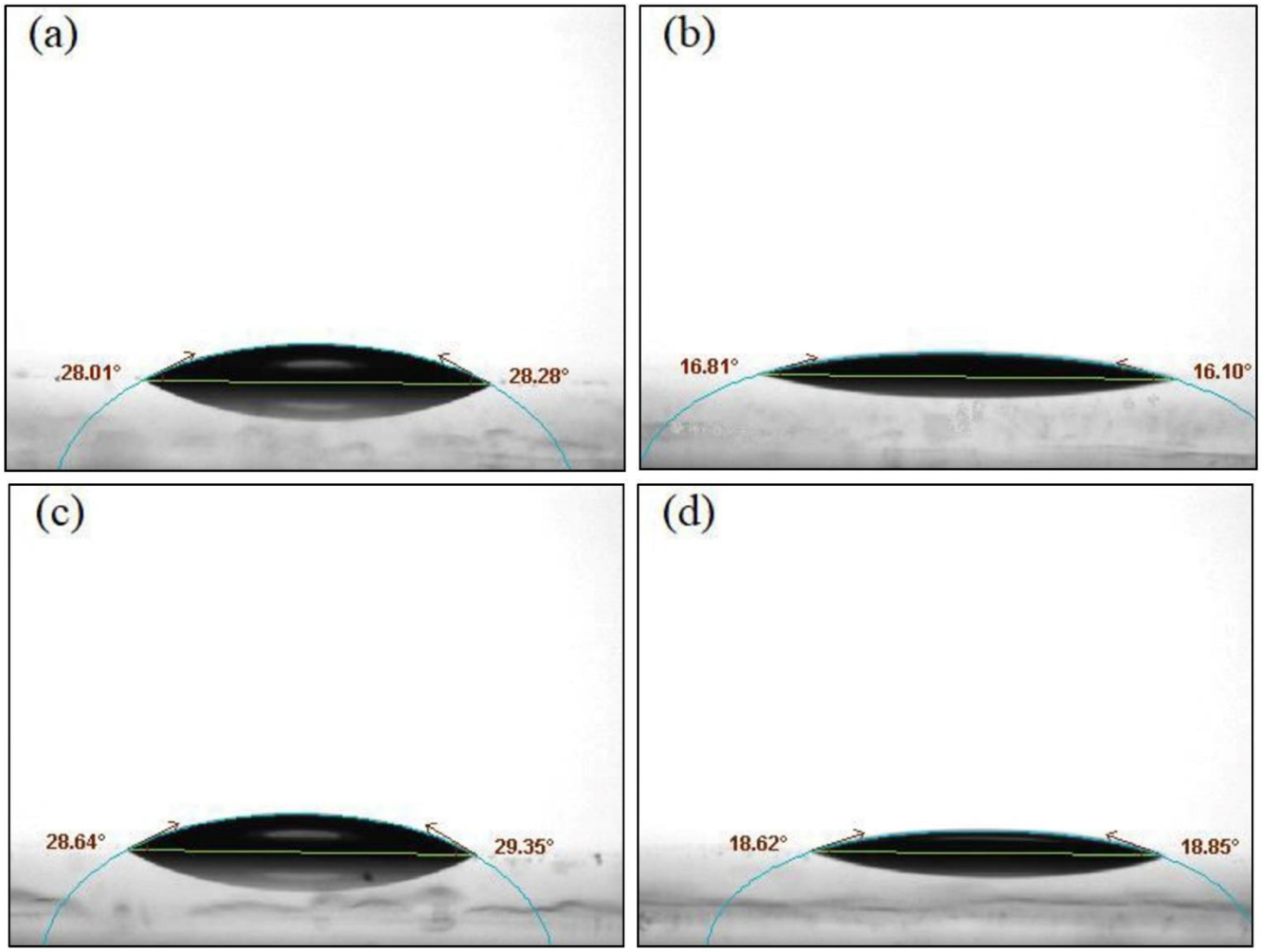


Figure 5.9: Contact angle measurement with respect to glass for (a) lower trapping (b) higher trapping of RNC produced from LL50% and (c) lower trapping (d) higher trapping of RNC produced from LP50%.

### 5.4.6.3 Influence of Non-polar functional groups on RNC trapping

Polar and non-polar functional group have characteristics that can alter the wettability of the surface [53]. The functional groups of the hydrochar were investigated with FTIR analysis (Figures 5.10). The peak for the non polar functional group has been found from figure 5.10 and listed at Table 5.2. Table 5.2 lists the functional groups present in hydrochar for the highest and lowest trapping of RNC. The table clearly shows that the highest trapping hydrochar has the higher number of non-polar functional groups, for instance, for CP50%, the high-trapping hydrochar has 13 non-polar functional groups and low-trapping hydrochar has only five non-

polar functional groups (Table 5.2). A higher number of non-polar functional groups results in a higher solid-oil attachment [54]. Therefore, altering the functional groups on the hydrochar from nonpolar to polar will allow more oil to be recovered during the HTL of biomass. This technique has been used for oil recovery [55].

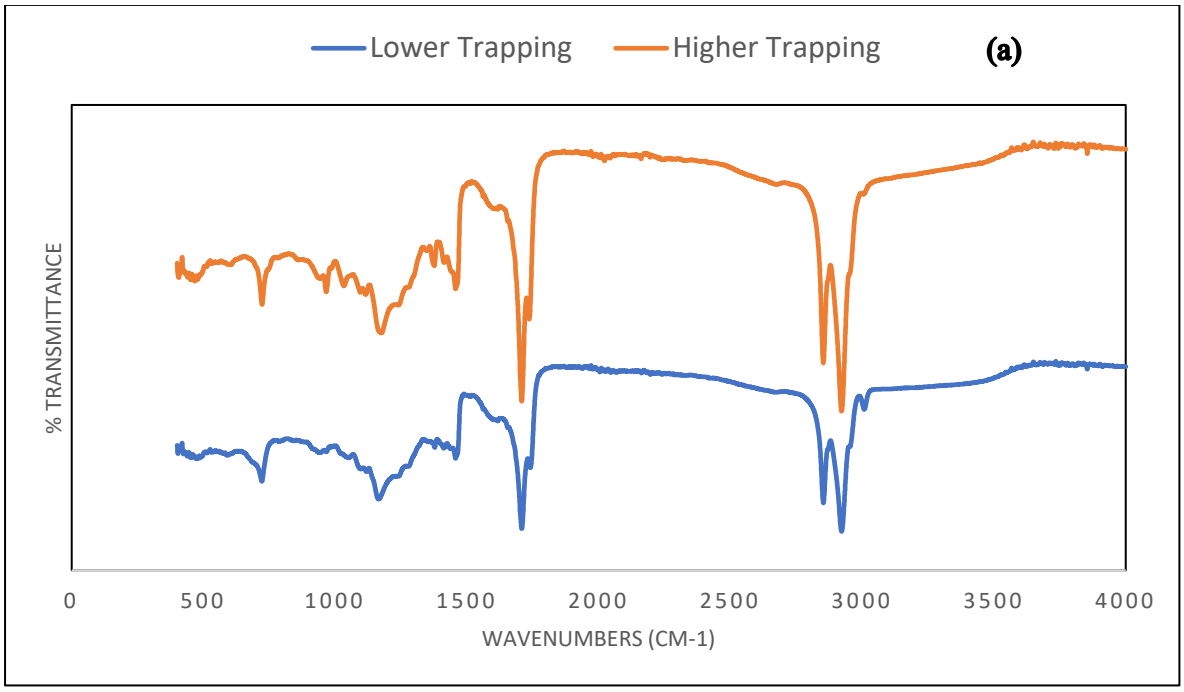


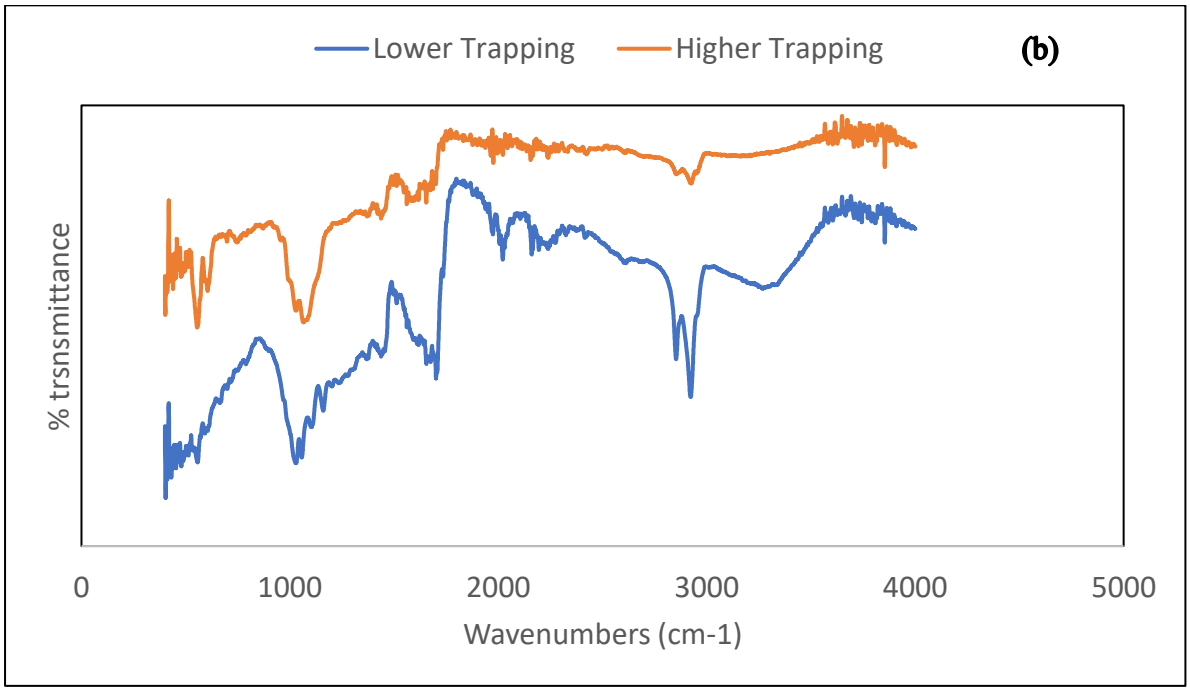

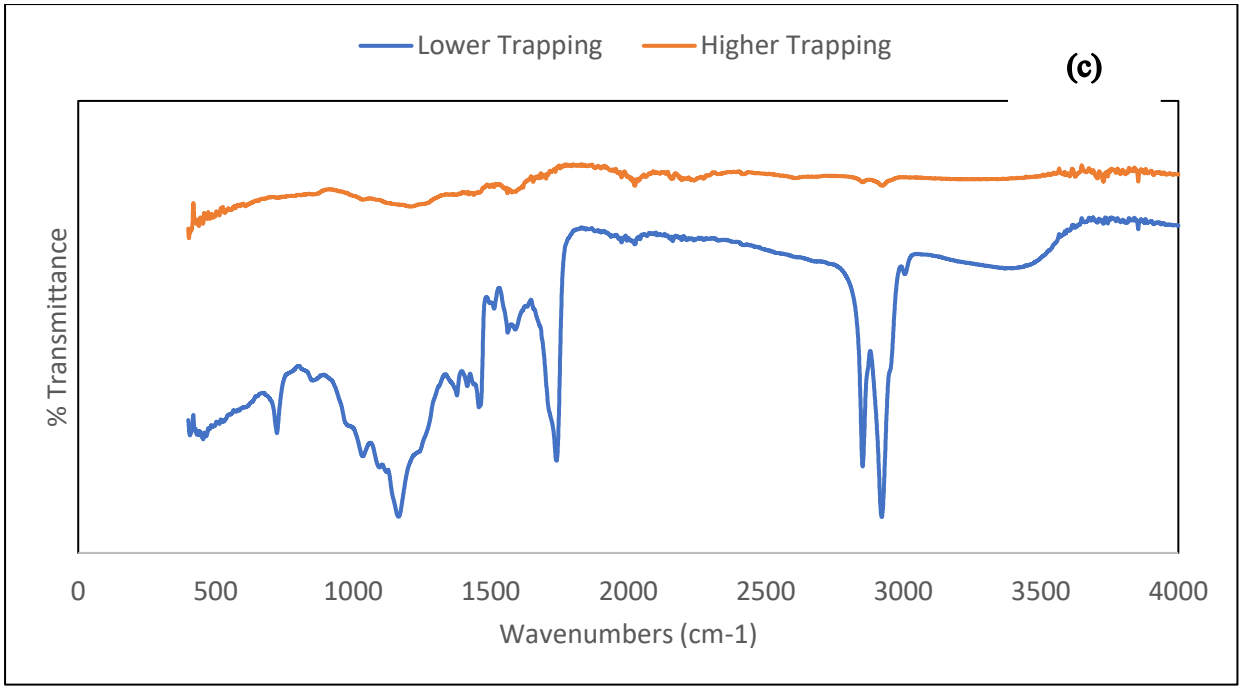


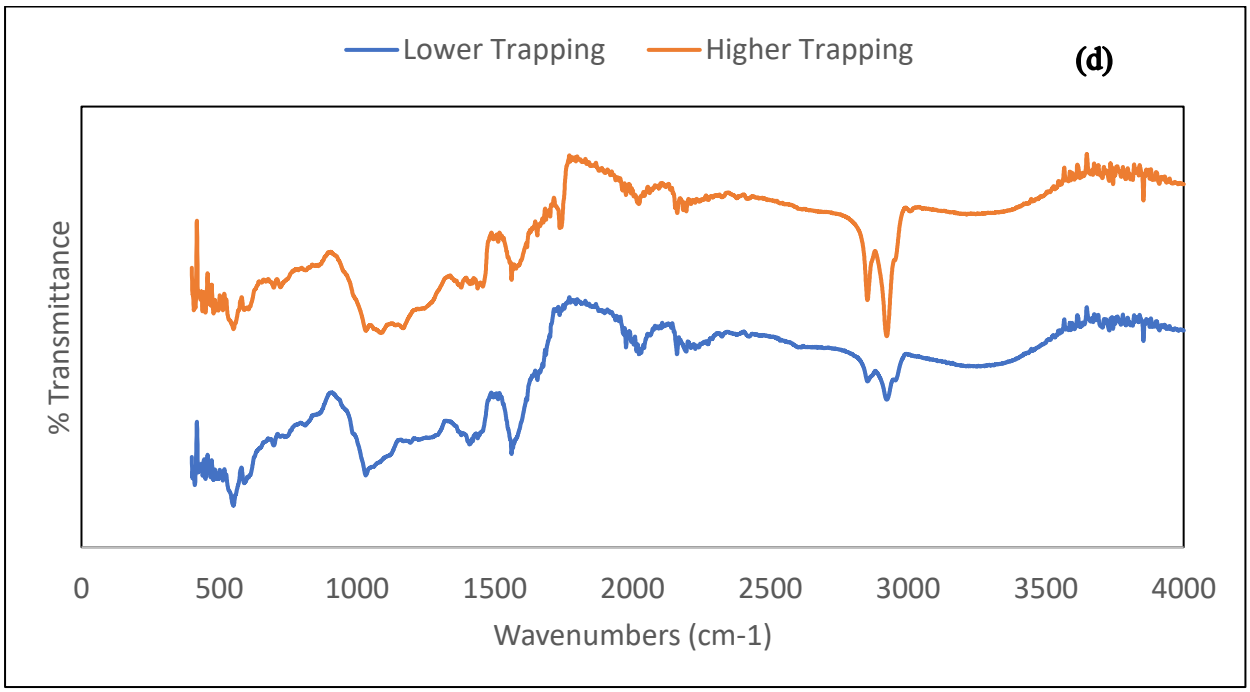


Figure 5.10: FTIR analysis for hydrochar obtained from (a) CL50% (b) CP50%, (c) LL50% and (d) LP50%

Table 5.2: List of non-polar functional groups and their wavenumbers (cm-1)

| Materials | Trapping type | Wavenumbers (cm-1) and non-polar functional groups |
|---|---|---|
| CL50% | Lower Trapping | 2921 (C-H), 2852 (C-H), 1456 (C=C) |
| | Higher Trapping | 2921 (C-H), 2852 (C-H), 1456 (C=C), 695 (C=H) 467 (C=H), |
| CP50% | Lower Trapping | 2922 (C-H), 2852 (C-H), 1974 (C-H), 1701 (C-H), 1605 (C-H), |
| | Higher Trapping | 2926 (C-H), 1994 (C-H), 1976 (C-H), 1963(C-H), 1937(C-H), 1752(C-H), 1735(C-H), 1700 (C-H), 1685 (C-H), 1654 (C-C), 1617 (C-C, 1496 (C-C) 745 (C-H) |
| LL50% | Lower Trapping | 2921 (C-H), 2852(C-H), 1739(C-H), 722 (C=C) |
| | Higher Trapping | 2924 (C-H), 2852 (C-H), 1975 (C-H), 1949 (C-H), 1752 (C-H), 1434 (C-H), 1701 (C-H), 1685 (C-H), 1654 (C-C) |
| LP50% | Lower Trapping | 2922 (C-H), 2852 (C-H), 2023 (C≡C), 1976 (C-H), 1735 (C-H), 1654 (C-H), |
| | Higher Trapping | 2922 (C-H), 2852 (C-H), 2102 (C≡C), 1975 (C-H), 1963 (C-H), 1735 (C-H), 1701 (C-H), 1685 (C-H), 1654 (C-H), 721 (C-H), |

#### 5.4.6.4 BET analysis for investigation of hydrochar surface

$N_2$ adsorption/desorption isothermal curves of hydrochar for the HTL of mixtures of model compounds have been investigated. Figure 5.11 is a representative isothermal adsorption-desorption curve for hydrochar from the HTL of CL50%, showing that the hydrochar is not porous. The isothermal $N_2$ adsorption-desorption curves clearly show that 1.25 $cm^3/g$ STP was the maximum $N_2$ quantity absorbed. The adsorption isotherms of hydrochar from cellulose and lipid mixtures were Type 1 isotherms, which can be obtained for non-porous to microporous

solids [56, 57]. The desorption hysteresis loop also indicated that there were no pores in the hydrochar. Therefore, porosity of the hydrochar is not a factor in the solid-oil interaction in HTL.

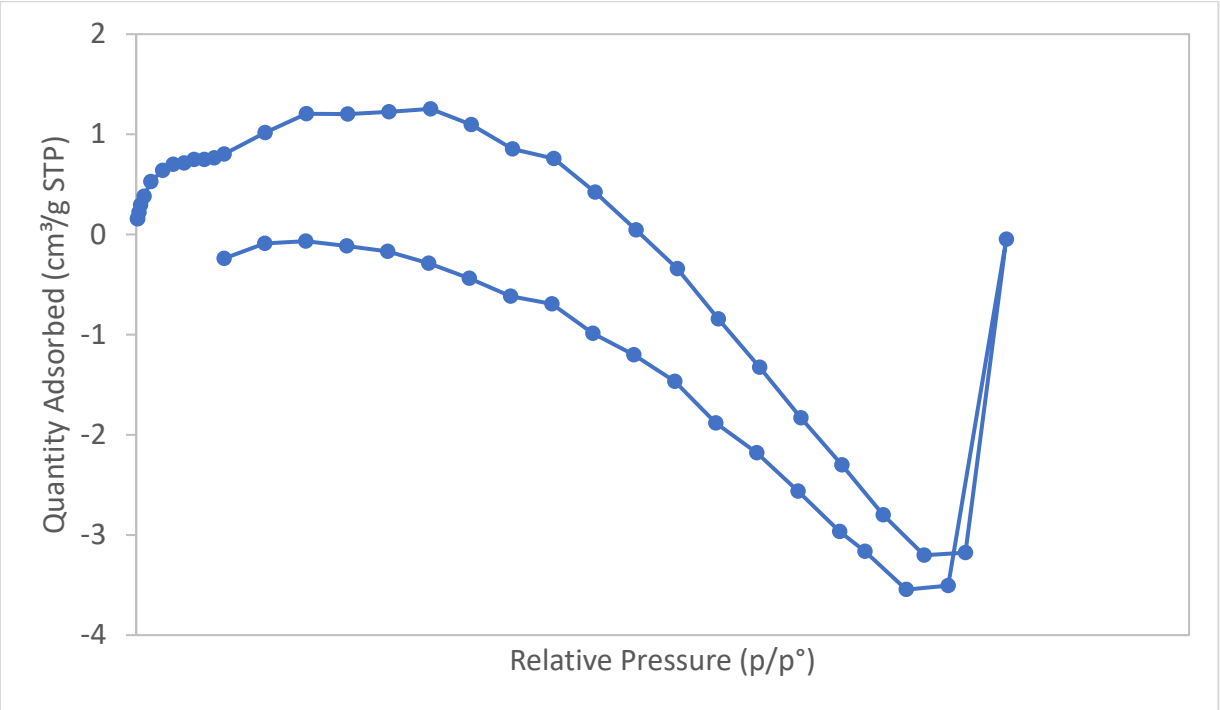


Figure 5.11: $N_2$ adsorption/desorption isotherm plot for CL50%

**5.4.6.5 Viscosity analysis of the renewable crude**

The viscosity analysis (Figure 5.12) shows that the RNC acts as a Newtonian fluid [58]. Shear rate is defined as the rate of change in velocity at which one layer of fluid moves over another adjacent layer [59]. The HTL reaction occurs at high temperature, and shear rate can increase under these reaction conditions. As all the RNC are newtonian fluids, viscosity can decrease as shear rate and temperature increase [60].

The viscosities of RNC for the lowest trapping (LT) were lower than the viscosities of RNC for higher trapping (HT) in the solids; i.e, the viscosities of RNC from CL50% were 4.28 (LT) and 7.41 $nS/m^2$ (HT), viscosities of RNC from CP50% were 3.42 (LT) and 6.94 $nS/m^2$ (HT),

viscosities of RNC from LL50% were 4.06 (LT) and 5.72 nS/m$^2$ (HT) and viscosities of RNC from LP50% were 5.83 (LT) and 7.15 nS/m$^2$ (HT).

Higher viscosity in RNC can cause multiphase flow and clogging or blocking of flow [61]. Therefore, the oil cannot pass out of the surface easily, and the highly viscous oil can easily be trapped on the hydrochar surface. Therefore, viscosity plays a vital role in the solid-oil interaction in the HTL reaction.

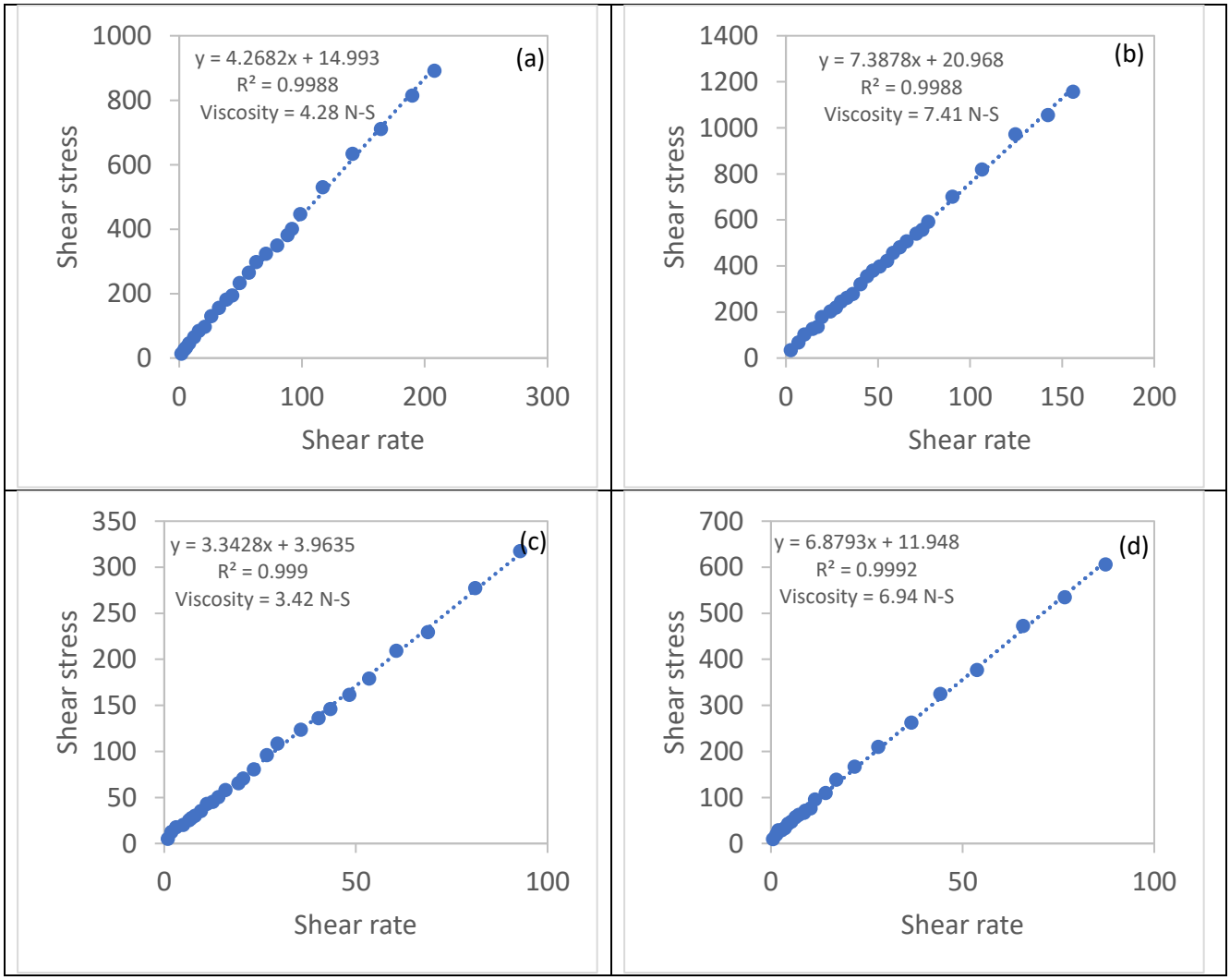

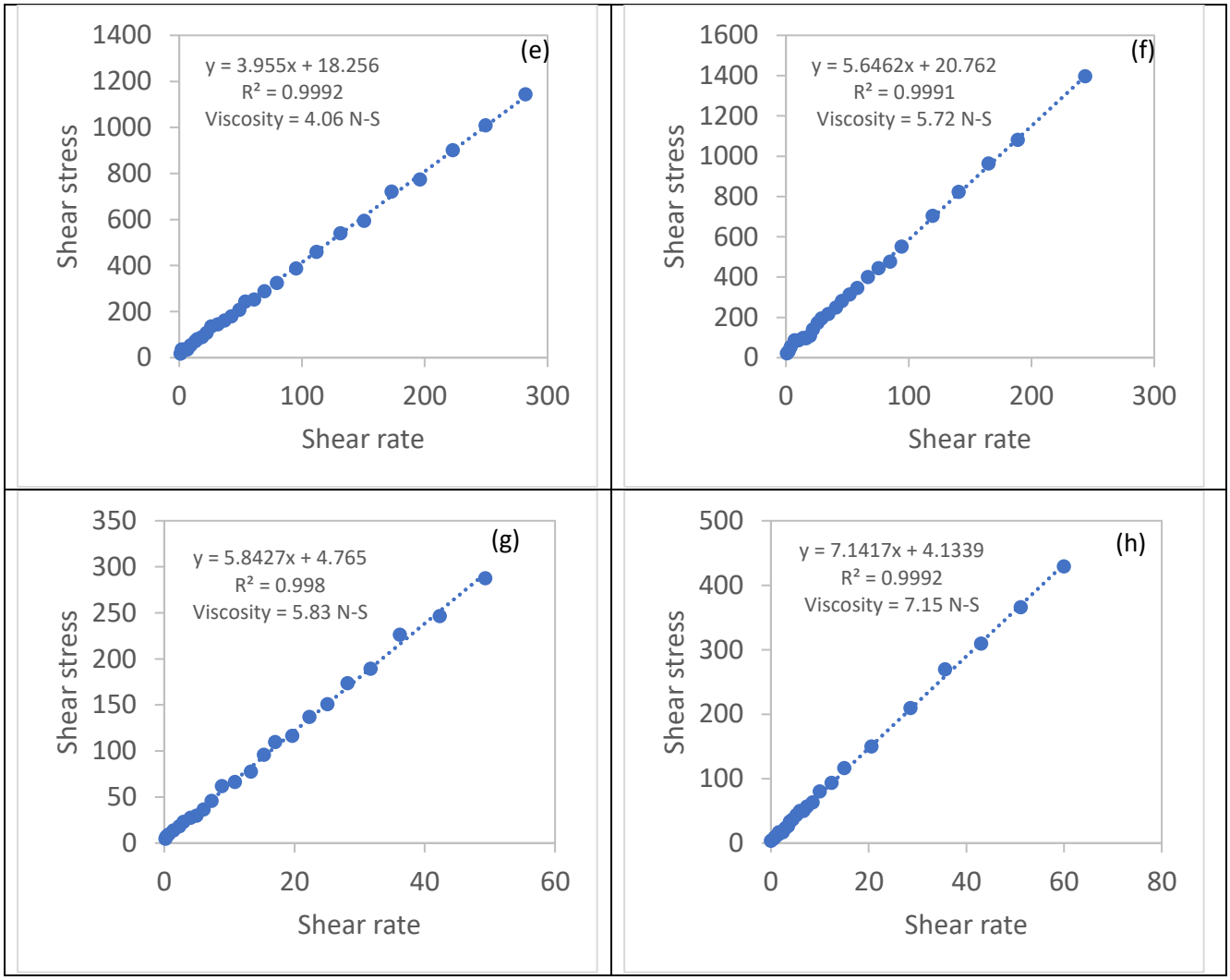


Figure 5.12: Shear rate vs. shear stress and viscosity analysis for RNC obtained from (a) CL50% LT (b) CL50% HT; (c) CP50% LT (d) CP50% HT; (e) LL50% LT (f) LL50% HT; (g) LP50% LT (h) LP50% HT.

### 5.5 Conclusion

In this study, the reasons behind the interaction between solid and have been investigated and explored suitable operating temperatures for maximum RNC yields. Four different types of raw materials, namely CL50%, CP50%, LL50%, and LP50%, were used for the HTL reaction.

The results showed that higher temperatures always led to higher RNC yields due to increased decomposition of the feedstock. It was observed that a higher degree of RNC trapping in

hydrochar resulted in higher RNC yields. For CL50%, the minimum and maximum total RNC yields were achieved at 350°C and 260°C, respectively. The lowest and highest degree of trapping (DOT) occurred at 290°C and 350°C, respectively, with 57-71% of RNC trapped in hydrochar. CP50% exhibited the lowest and highest total RNC yields at 290°C and 350°C, respectively, with 56-71% of RNC trapped in hydrochar. Lowest and highest degree of trapping (DOT) were found at 260°C and 350°C in this case. LL50% showed the maximum and minimum total RNC yields at 320°C and 260°C, respectively, with 64-77% of RNC trapped in hydrochar. Lowest and highest DOT were found at 320°C and 260°C for LL50%. LP50% had the maximum and minimum total RNC yields at 350°C and 260°C, respectively, with 60-66% of RNC trapped in hydrochar. Lowest and highest DOT were found at 260°C and 350°C. No secondary reactions were observed for LP50%.

The study also found that acidic oil had a stronger interaction with hydrochar compared to alkaline oil, leading to more RNC trapping. A lower Acid Value (AV) resulted in less trapping. Oil with alkaline behavior changed the hydrochar surface from oil-wet to water-wet, releasing more trapped oil. RNC with a higher DOT had a lower contact angle with the solid, indicating better wetting of the solid surface and increased trapping. Non-polar functional groups in the hydrochar had an obvious impact on the on solid-oil interaction. The hydrochar surface with the highest DOT had a higher number of non-polar functional groups of hydrophobic nature (oil wet), resulting in higher trapping of oil in the hydrochar. This happens because of the properties of non-polar functional group which can alter the surface of hydrochar from hydrophilic to hydrophobic. $N_2$ adsorption/desorption curves with BET analysis suggested that the hydrochar is not porous; therefore, there was no expectation that pores could hold the oil and influence the solid-oil attachment. Viscosity analysis suggests that all the RNCs are Newtonian fluids; therefore, viscosity would increase as shear rate and temperature increased in the HTL reaction. Additionally, the RNC with the highest DOT had the highest viscosity,

which could cause multiphase flow and clogging or blocking of flow resulting in a higher solid-oil interaction.

## Reference


1. Pande, M. and A.N. Bhaskarwar, *Biomass conversion to energy*, in *Biomass conversion*. 2012, Springer. p. 1-90.
2. Bridgwater, T.J.J.o.t.S.o.F. and Agriculture, *Biomass for energy*. 2006. **86**(12): p. 1755-1768.
3. Singh, J., S.J.R. Gu, and S.E. Reviews, *Biomass conversion to energy in India—A critique.* 2010. **14**(5): p. 1367-1378.
4. Irmak, S., *Challenges of biomass utilization for biofuels*, in *Biomass for bioenergy-recent trends and future challenges*. 2019, IntechOpen.
5. Toor, S.S., L. Rosendahl, and A.J.E. Rudolf, *Hydrothermal liquefaction of biomass: a review of subcritical water technologies.* 2011. **36**(5): p. 2328-2342.
6. Biller, P., et al., *Nutrient recycling of aqueous phase for microalgae cultivation from the hydrothermal liquefaction process.* Algal Research, 2012. **1**(1): p. 70-76.
7. Jin, F., *Application of hydrothermal reactions to biomass conversion*. 2014: Springer Science & Business Media.
8. Toor, S.S., *Modeling and Optimization of Catliq Liquid Bioful Process*. 2010: Department of Energy Technology, Aalborg University.
9. Shah, Y.T., *Energy and fuel systems integration*. 2015: CRC Press.
10. Franck, E.J.S., Water, and H. Systems, *Supercritical water.* 2000: p. 22-34.
11. Krammer, P. and H.J.T.J.o.S.F. Vogel, *Hydrolysis of esters in subcritical and supercritical water.* 2000. **16**(3): p. 189-206.
12. Beckman, D. and D.C.J.T.C.J.o.C.E. Elliott, *Comparisons of the yields and properties of the oil products from direct thermochemical biomass liquefaction processes.* 1985. **63**(1): p. 99-104.
13. Jin, B., et al., *Co-liquefaction of micro- and macroalgae in subcritical water.* Bioresource Technology, 2013. **149**(Supplement C): p. 103-110.
14. Aysu, T. and M.M. Küçük, *Liquefaction of giant fennel (Ferula orientalis L.) in supercritical organic solvents: Effects of liquefaction parameters on product yields and character.* The Journal of Supercritical Fluids, 2013. **83**(Supplement C): p. 104-123.
15. Brown, T.M., P. Duan, and P.E. Savage, *Hydrothermal liquefaction and gasification of Nannochloropsis sp.* Energy Fuels, 2010. **24**(6): p. 3639-3646.
16. Yang, H., et al., *Pyrolysis of palm oil wastes for enhanced production of hydrogen rich gases.* Fuel Processing Technology, 2006. **87**(10): p. 935-942.
17. Lam, S.S., et al., *Microwave-heated pyrolysis of waste automotive engine oil: Influence of operation parameters on the yield, composition, and fuel properties of pyrolysis oil.* Fuel, 2012. **92**(1): p. 327-339.
18. Yin, S., et al., *Subcritical hydrothermal liquefaction of cattle manure to bio-oil: Effects of conversion parameters on bio-oil yield and characterization of bio-oil.* Bioresource Technology, 2010. **101**(10): p. 3657-3664.

19. Cheng, J., et al., *Biodiesel production from lipids in wet microalgae with microwave irradiation and bio-crude production from algal residue through hydrothermal liquefaction.* Bioresource Technology, 2014. **151**(Supplement C): p. 415-418.
20. Chen, Y., et al., *Direct liquefaction of Dunaliella tertiolecta for bio-oil in sub/supercritical ethanol–water.* Bioresource Technology, 2012. **124**(Supplement C): p. 190-198.
21. Chen, W.-T., et al., *Co-liquefaction of swine manure and mixed-culture algal biomass from a wastewater treatment system to produce bio-crude oil.* Applied Energy, 2014. **128**(Supplement C): p. 209-216.
22. Dimitriadis, A. and S. Bezergianni, *Hydrothermal liquefaction of various biomass and waste feedstocks for biocrude production: A state of the art review.* Renewable and Sustainable Energy Reviews, 2017. **68**(Part 1): p. 113-125.
23. Arturi, K.R., et al., *Characterization of liquid products from hydrothermal liquefaction (HTL) of biomass via solid-phase microextraction (SPME).* Biomass and Bioenergy, 2016. **88**: p. 116-125.
24. Obeid, R., et al., *Reaction kinetics and characterization of species in renewable crude from hydrothermal liquefaction of mixtures of polymer compounds to represent organic fractions of biomass feedstocks.* 2019. **34**(1): p. 419-429.
25. Fan, Y., et al., *Hydrothermal liquefaction of protein-containing biomass: Study of model compounds for Maillard reactions.* 2018. **8**(4): p. 909-923.
26. Madsen, R.B., et al., *Predicting the chemical composition of aqueous phase from hydrothermal liquefaction of model compounds and biomasses.* 2016. **30**(12): p. 10470-10483.
27. Yin, S. and Z. Tan, *Hydrothermal liquefaction of cellulose to bio-oil under acidic, neutral and alkaline conditions.* Applied Energy, 2012. **92**: p. 234-239.
28. Cao, Y., et al., *Hydrothermal liquefaction of lignin to aromatic chemicals: impact of lignin structure.* 2020. **59**(39): p. 16957-16969.
29. Lu, J., et al., *Synergistic and antagonistic interactions during hydrothermal liquefaction of soybean oil, soy protein, cellulose, xylose, and lignin.* 2018. **6**(11): p. 14501-14509.
30. Tang, S., et al., *Hydrotreatment of biocrudes derived from hydrothermal liquefaction and lipid extraction of the high-lipid Scenedesmus.* 2019. **21**(12): p. 3413-3423.
31. Demirbaş, A., *Mechanisms of liquefaction and pyrolysis reactions of biomass.* Energy Conversion and Management, 2000. **41**(6): p. 633-646.
32. Liu, Z. and F.-S. Zhang, *Effects of various solvents on the liquefaction of biomass to produce fuels and chemical feedstocks.* Energy Conversion and Management, 2008. **49**(12): p. 3498-3504.
33. Fan, S.-P., et al., *Comparative studies of products obtained from solvolysis liquefaction of oil palm empty fruit bunch fibres using different solvents.* Bioresource Technology, 2011. **102**(3): p. 3521-3526.
34. Aysu, T., *Supercritical fluid extraction of reed canary grass (Phalaris arundinacea).* Biomass and Bioenergy, 2012. **41**(Supplement C): p. 139-144.
35. Aysu, T., M. Turhan, and M.M. Küçük, *Liquefaction of Typha latifolia by supercritical fluid extraction.* Bioresource Technology, 2012. **107**(Supplement C): p. 464-470.

36. Durak, H. and T. Aysu, *Effects of catalysts and solvents on liquefaction of Onopordum heteracanthum for production of bio-oils.* Bioresource Technology, 2014. **166**(Supplement C): p. 309-317.
37. Pisupati, S.V. and A.H. Tchapda, *Thermochemical Processing of Biomass*, in *Advances in Bioprocess Technology*. 2015, Springer. p. 277-314.
38. Singh, A.S., M.B.J.I.J.o.e. Masuku, commerce, and management, *Sampling techniques & determination of sample size in applied statistics research: An overview*. 2014. **2**(11): p. 1-22.
39. Spitz, L., *12 - Glossary*, in *Soap Manufacturing Technology (Second Edition)*, L. Spitz, Editor. 2016, AOCS Press. p. 267-280.
40. Patterson, H.B.W., *Chapter 12 - Quality and Control*, in *Hydrogenation of Fats and Oils (Second Edition)*, G.R. List and J.W. King, Editors. 2011, AOCS Press. p. 329-350.
41. Onu, P. and C. Mbohwa, *Chapter 6 - New approach and prospects of agrowaste resources conversion for energy systems performance and development*, in *Agricultural Waste Diversity and Sustainability Issues*, P. Onu and C. Mbohwa, Editors. 2021, Academic Press. p. 97-118.
42. Kwok, D.Y. and A.W. Neumann, *Contact angle measurement and contact angle interpretation.* Advances in colloid and interface science, 1999. **81**(3): p. 167-249.
43. Feng, H., et al., *Synergistic bio-oil production from hydrothermal co-liquefaction of Spirulina platensis and α-Cellulose.* Energy, 2019. **174**: p. 1283-1291.
44. de Caprariis, B., et al., *Effect of Ni, Zn and Fe on hydrothermal liquefaction of cellulose: Impact on bio-crude yield and composition.* 2021. **157**: p. 105225.
45. Biller, P. and A. Ross, *Production of biofuels via hydrothermal conversion*, in *Handbook of biofuels production*. 2016, Woodhead Publishing. p. 509-547.
46. Donaldson, E. and W. Alam, *Wettability. Houston.* TX: Gulf Publishing Company, 2008.
47. Feng, L., et al., *Catalytic hydrothermal liquefaction of lignin for production of aromatic hydrocarbon over metal supported mesoporous catalyst.* Bioresource Technology, 2021. **323**: p. 124569.
48. Biswas, B., et al., *Catalytic hydrothermal liquefaction of alkali lignin over activated bio-char supported bimetallic catalyst.* Bioresource Technology, 2021. **337**: p. 125439.
49. Cantero-Tubilla, B., et al., *Characterization of the solid products from hydrothermal liquefaction of waste feedstocks from food and agricultural industries.* The Journal of Supercritical Fluids, 2018. **133**: p. 665-673.
50. Hashemi, L., et al., *Contact angle measurement for hydrogen/brine/sandstone system using captive-bubble method relevant for underground hydrogen storage.* Advances in Water Resources, 2021. **154**: p. 103964.
51. Yuan, Y. and T.R. Lee, *Contact angle and wetting properties*, in *Surface science techniques*. 2013, Springer. p. 3-34.
52. Eral, H., J.J.C. Oh, and p. science, *Contact angle hysteresis: a review of fundamentals and applications.* Colloid and polymer science, 2013. **291**(2): p. 247-260.

53. Jarrahian, K., et al., *Wettability alteration of carbonate rocks by surfactants: A mechanistic study.* Colloids and Surfaces A: Physicochemical and Engineering Aspects, 2012. **410**: p. 1-10.
54. *Module 11 /Functional Groups*. [cited 2022 23 January]; Available from: https://oli.cmu.edu/jcourse/workbook/activity/page?context=90d3ff9080020ca601040285a20dd2c4.
55. Wu, J., et al., *Effect of specific functional groups on oil adhesion from mica substrate: Implications for low salinity effect.* Journal of Industrial and Engineering Chemistry, 2017. **56**: p. 342-349.
56. Zhang, S., et al., *Green synthesis of aluminum-hydrochar for the selective isomerization of glucose to fructose.* Science of The Total Environment, 2020. **727**: p. 138743.
57. Zhang, P. *Adsorption and Desorption Isotherms*. 2016 [cited 2022 24 January]; Available from: http://www.keresearchgroup.com/uploads/4/8/4/5/48456521/160903_introduction_to_bet_isotherms.pdf.
58. Chhabra, R.P., *Non-Newtonian fluids: an introduction*, in *Rheology of complex fluids*. 2010, Springer. p. 3-34.
59. Krishna, K.V., et al., *Chapter 1.6 - Bioelectrocatalyst in Microbial Electrochemical Systems and Extracellular Electron Transport*, in *Microbial Electrochemical Technology*, S.V. Mohan, S. Varjani, and A. Pandey, Editors. 2019, Elsevier. p. 117-141.
60. Sakthipriya, N., M. Doble, and J.S. Sangwai, *Performance of thermophilic strain on the reduction of viscosity of crude oil under high pressure and high temperature conditions: Experiments and modeling.* Journal of Petroleum Science and Engineering, 2022. **210**: p. 110016.
61. Martínez-Palou, R., et al., *Transportation of heavy and extra-heavy crude oil by pipeline: A review.* Journal of Petroleum Science and Engineering, 2011. **75**(3): p. 274-282.

# Chapter 6: Study of the fundamental causes of solid-renewable crude interaction during the hydrothermal liquefaction of actual biomass

# Statement of Authorship

| | |
|---|---|
| Title of Paper | Study of the fundamental causes of solid-renewable crude interaction during hydrothermal liquefaction of actual biomass |
| Publication Status | ☐ Published ☐ Accepted for Publication<br>☐ Submitted for Publication ☑ Unpublished and Unsubmitted work written in manuscript style |
| Publication Details | |

## Principal Author

| | |
|---|---|
| Name of Principal Author (Candidate) | Md Arafat Hossain |
| Contribution to the Paper | HTL Experimental design and method<br>Concept developments<br>Raw materials preparations<br>HTL batch experiments<br>Method developments for analysis<br>Characterizations of the HTL products |
| Overall percentage (%) | 80% |
| Certification: | This paper reports on original research I conducted during the period of my Higher Degree by Research candidature and is not subject to any obligations or contractual agreements with a third party that would constrain its inclusion in this thesis. I am the primary author of this paper. |
| Signature | Date 14/07/2023 |

## Co-Author Contributions

By signing the Statement of Authorship, each author certifies that:

i. the candidate's stated contribution to the publication is accurate (as detailed above);

ii. permission is granted for the candidate in include the publication in the thesis; and

iii. the sum of all co-author contributions is equal to 100% less the candidate's stated contribution.

| | |
|---|---|
| Name of Co-Author | David Lewis |
| Contribution to the Paper | Concept developments<br>Assistance with analysis and interpretation of data<br>Drafting the manuscript<br>Supervise the overall work |
| Signature | Date 19/7/2023 |

| | |
|---|---|
| Name of Co-Author | Philip van Eyk |
| Contribution to the Paper | HTL Experimental design and method<br>Concept developments<br>Assistance with analysis interpretation of data<br>Drafting the reviewing manuscript<br>Supervise the overall work |
| Signature | Date 18/7/2023 |

Please cut and paste additional co-author panels here as required.

# Study of the fundamental causes of solid-renewable crude interaction during the hydrothermal liquefaction of actual biomass

[a]Md Arafat Hossain, [a]David Lewis, [a]Philip van Eyk

[a]School of Chemical Engineering, The University of Adelaide, Adelaide, South Australia 5005, Australia

**Abstract**

This study investigates the challenges associated with the extraction of renewable crude (RNC) from hydrochar during hydrothermal liquefaction (HTL) of different biomass. Despite using various solvents, achieving complete RNC extraction from hydrochar has proven to be difficult. Therefore, the objective of this research is to identify the underlying factors responsible for RNC trapped in hydrochar and evaluate the resulting product yields using different biomass feedstocks such as pine wood, sludge, and microalgae.

The investigation reveals varying RNC yields, both maximum and minimum, under different HTL conditions. For pine wood, maximum and minimum RNC yields of 14 wt.% and 8 wt.% were obtained at temperatures of 320°C and 350°C, respectively. Decreased RNC yield at 350°C was found from 320°C due to the secondary cracking of RNC. In the case of sludge, the maximum and minimum RNC yields were 20 wt.% and 14 wt.% at temperatures of 350°C and 260°C, respectively. Similarly, for microalgae, the maximum and minimum RNC yields were 21 wt.% and 12 wt.% at temperatures of 260°C and 350°C, respectively, with secondary cracking occurring even at lower temperatures, leading to reduced overall yields. Source rock analysis indicated that a significant amount of RNC was trapped in hydrochar, ranging from 42% to 61% for pine wood, 50% to 67% for sludge, and 48% to 71% for microalgae.

To determine the fundamental reasons for the attachment between hydrochar and RNC, the hydrochar and RNC found from higher and lower degrees of RNC trapping were selected for analysis. Though hydrochar did not have pores which could hold oil to contribute the solid–oil attachment, a higher number of non-polar functional groups was found on the hydrochar

surface where higher trapping of RNC occurred. The oil with a higher capability of wetting a solid surface (forming a lower contact angle with the solid) also tended to be trapped in hydrochar to a higher degree. Higher oil viscosity and higher acid values also contributed to a higher solid–oil attachment.

Keyword: Hydrothermal liquefaction; biocrude; hydrochar; solid-biocrude interaction; biomass

### 6.1 Introduction

Biomass, as an organic resource, currently accounts for 12.83% of the total renewable energy stock. [1]. It serves as the only renewable organic resource [2, 3], offering sustainability and eco-friendliness, making it a promising energy source to address the escalating demand [4]. Large amounts of biomass are generated from harvesting, cultivation, processing and consumption of agricultural resources [5]. Biomass is built of cellulose, hemicellulose and lignin, and these structures have an impact on bioenergy production [6]. In contrast to the current heavy reliance on non-renewable fossil fuels, which contribute to global warming through the emission of harmful gases [7], biomass can be converted to multiple energy forms, including renewable crude (RNC), gas, and hydrochar [8].

HTL is a promising popular thermochemical process for the production of the liquid fuel known as RNC [9, 10]. One of the major advantages of HTL compared to other biomass conversion techniques is its capability to process wet biomass [11, 12] eliminating the need for time-consuming and costly biomass drying processes. Furthermore, HTL offers the advantage of converting low-grade biomass mixtures and waste of biomass like sludge, which often consist of crop residues, into high-grade oils and valuable chemical products [13].

The HTL reaction runs under subcritical conditions (temperature 250–370°C, pressure 4–20 MPa) and produces RNC, together with hydrochar, gases and aqueous phase as by-products

[14]. Gasoline, diesel oil or naphtha can be obtained by refining the RNC from HTL [15]. In HTL, in contrast to other thermochemical conversion techniques, water plays a vital role and acts as both reactant and catalyst. Subcritical water is of great interest to researchers as it is an excellent medium for fast, homogeneous and efficient reactions [16, 17].

The product yields, characterisation of the products, solvent extraction and kinetics of HTL have been extensively studied, including yields and characterisations of products from the HTL of microalgae [18, 19]. Aysu et al. [20] and Brown et al. [21] reported that higher temperatures led to a greater decomposition of biomass, and produced higher amounts of RNC during the HTL of giant fennel and *Nannochloropsis sp*. (microalgae), respectively. Yin et al. [22] reported that during the HTL of cattle manure, lower residence times gave higher RNC yields. The HTL of *Nannochloropsis oceanica* [23], *Dunaliella tertiolecta* [24], swine manure and mixed-culture algae [25] also showed higher yields of RNC from lower residence times.

As water plays an important role in accelerating the HTL reaction, the influence of the biomass/water (B/W) ratio has also been investigated by several researchers [26]. Increasing the B/W ratio can reduce the decomposition of the biomass, which then reduces RNC and favors hydrochar yields [27]. A lower B/W ratio increased yields of RNC for the HTL of *C. lanceolata* [28], white pine sawdust [29] and rice stalk [30].

Arturi et.al. [31] has characterised the liquid products obtained from the HTL of biomass and reported the group of chemicals present in the RNC. Obeid et al. [32] investigated the HTL of a mixture of polymeric compounds and calculated the reaction kinetics as well as characterising the resulting RNC. Fan et al. [33] investigated the HTL of the model compounds lactose, maltose, lysine, and hydroxymethylfurfural as well as binary mixtures of these compounds. These experiments produced RNC with unfavorable nitrogen content. The chemical composition of the aqueous phase from the HTL of biomass and model compounds has been

investigated by Madsen et al. [34]. The HTL of cellulose [35], lignin [36], protein [37] and lipid [38] has also been extensively studied.

Most researchers struggle to extract RNC from the hydrochar-RNC mixture due to the strong attachment between the two. Researchers have used different solvents, including acetone, propanol, butanol, ethyl acetate and methyl ethyl ketone to lower the RNC viscosity and extract the oil [39], but have found it almost impossible to complete a total extraction. Therefore, RNC is being wasted even though it is being produced.

The solvent extraction efficiency depends on the raw materials and experimental factors. For instance, in the HTL of pine wood, the efficiency for RNC extraction is ethanol > acetone > water [40]. Nonetheless, for another raw material like EFB (empty fruit bunch), the efficiency is glycol > water > ethanol > acetone > toluene [41]. A higher efficiency of acetone could be found for the HTL of *Ferula orientalis L.* [20], reed canary grass [42], *Typha latifolia* [43] and milled *Onopordum heteracanthum* stalks [44].

The hydrophobic nature of the hydrochar obtained from HTL contributes to the strong solid-RNC attachment. During HTL, the polar groups of the biomass (generally –OH and –COO–) are destroyed, reducing the ability of the products to attract water by hydrogen bonding and making the biochar hydrophobic [45].

In the current study, the variation of yields from different types of biomass, i.e, pine, sludge, and microalgae, under the same set of reaction conditions is investigated. Variation in yield with different experimental parameters, as well as the variation in the degree of RNC trapping in biochar are also investigated. We then outline some fundamental reasons for the solid-RNC interaction.

## 6.2 Methodology and Experimental Procedure

### 6.2.1 Materials

The study was focused on solid-RNC interaction from the HTL of real biomass. Microalgae, sludge and pine wood have been selected for this study. All three biomass sources were dried at 40°C in an oven for 48 hours before being analyzed and used as feedstocks for the HTL experiments. The microalgae (*Tetraselmis* sp. MUR 233) was grown in a recycled culture medium with growth conditions described by Sing et al. [46]. Sewage sludge obtained from Melbourne Water was collected from the wastewater treatment process after treatment in the aerobic lagoons but prior to ultraviolet light treatment, and was ground and sieved at <1mm. Radiata pine sawdust was ground and sieved at <1mm. Ethanol was used as solvent to extract the RNC from the hydrochar. Ethanol was employed in this study, as it is commonly used by many researchers in their investigations. Additionally, it is more cost-effective than several other solvents, such as Dichloromethane (DCM) or chloroform, and poses fewer hazards.

### 6.2.2 HTL Batch Reactor System

HTL of the prepared samples was performed in a stainless steel HTL batch reactor, pressure capacity 400 bar (Figure 6.1). A 12.5-mm diameter and 2-mm thickness 316 stainless steel tube was employed to make a 20-cm long reactor tube, which can run 11 ml feedstocks at a time. A 12.5-mm Swagelok port connector and fittings was attached to each end of the reactor. A Type K mineral-insulated thermocouple was connected to one end of the reactor and other end was covered. A 3.2-mm tube was attached to the upper end of the reactor to stop the inside contents from entering the top half of the reactor. The reactor tube was connected to a pressure transducer and pressure relief valve. A thermocouple was used to measure the temperature. The pressure transducer was connected to a pressure indicator and the thermocouple was connected to a temperature indicator. $N_2$ pressure was supplied by gas from a cylinder. The reactor was placed on a sand fluidised bed (Techne SBL-2D) of maximum temperature around 400°C. The

upper section of the reactor was attached to a ball valve which was used to purge the oxygen and pressurise with $N_2$ before the HTL reaction. The flue gas was also released from the reactor via this ball valve after the HTL reaction.

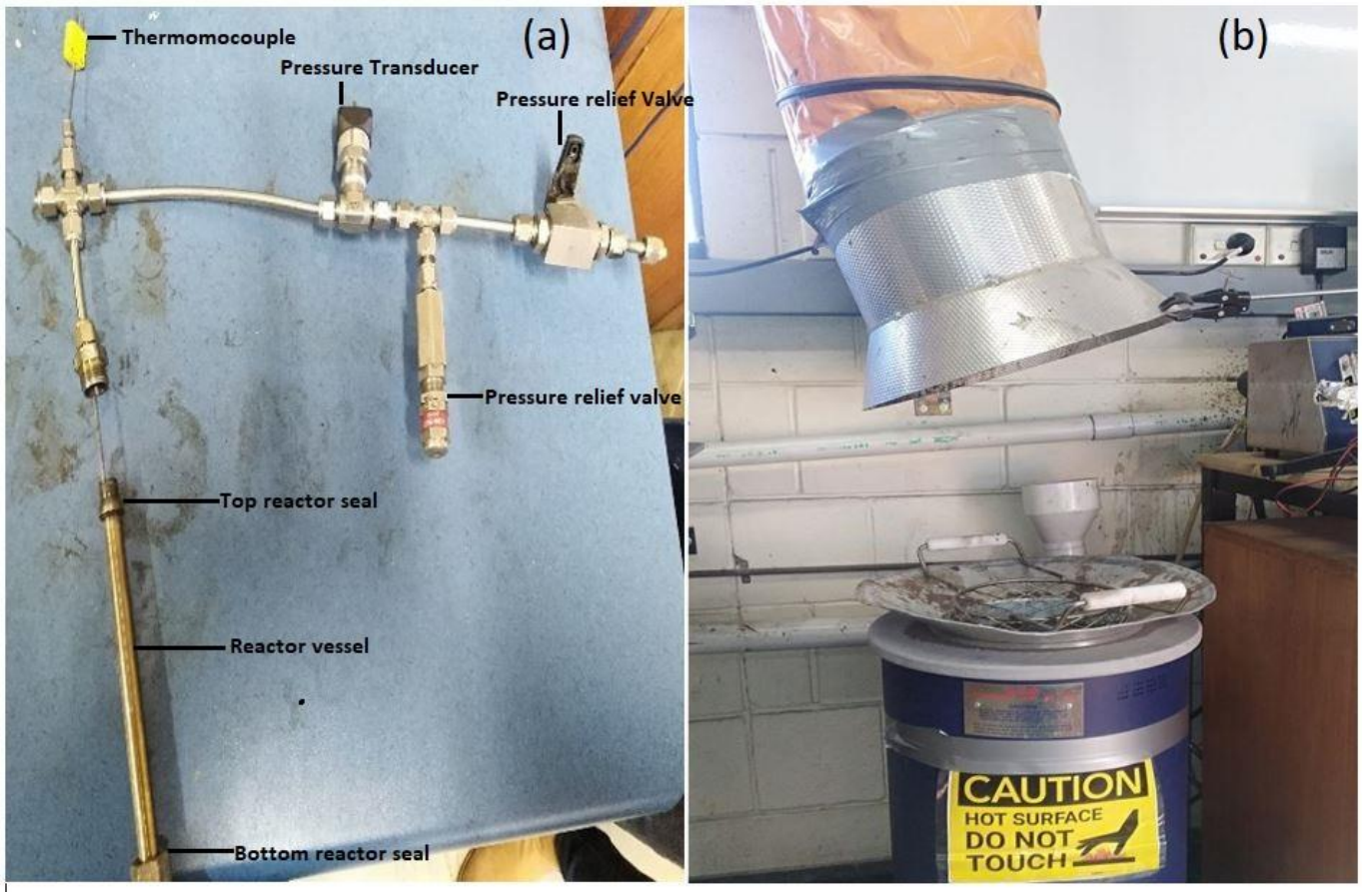


Figure 6.1: (a) HTL reactor (b) Reactor Bed

### 6.2.3 Experimental Procedure

A previous study focused on the parametric investigation of product yields and solid–oil attachment has suggested that a lower residence time (10 min) and a B/W ratio of 0.5 (1.84g/3.66g) is suitable. Reaction temperatures were set to (260–350°C). Product yields and RNC yields (both trapped and extracted oil) were reported in terms of changing temperature.

The reactor was filled to 50% of its total capacity at room temperature for every HTL reaction. To remove the oxygen and unnecessary gas from the reactor it was charged with nitrogen ($N_2$)

to 100 bar. The gas was left for 3 min to check for leaks. The nitrogen was then released slowly and charged to the starting pressure required to achieve 200 bar under the reaction conditions. The starting pressure was set between 85 and 120 bar. After the reactor was filled with the selected B/W ratio of feedstock and the required pressure, it was positioned inside a fluidised bed to be heated.

A temperature controller (Techne 9D) was connected to change the temperature set point. A flow-rate controller was also connected to change the air flow throughout the fluidised bed. This provides uniform heating of the reactor at the required reaction temperature. The fluidised bed was pre-heated to the required temperature before the reactor was placed inside the bed, after which the reactor was heated at a rate of approximately 125°C per minute. After the desired residence time of 10 minutes, the reactor was removed from the bed and cooled down. It was not opened until the temperature reached at 70°C.

### 6.2.4 Separation of the HTL Products and Analysis

The reactor weight was recorded before and after filling with the raw materials and $N_2$ gas. The mass of added $N_2$ before the reaction was deducted from the total mass of gas released after the reaction to know the mass of the gas produced from HTL.

Once emptied, the reactor was washed three times with water to remove all the products from the reactor wall and the mixture of products was centrifuged for 15 minutes at 2000 rpm. For the solvent extraction process, the reactor was washed with ethanol and washings were placed with the mixture of products in the centrifuge tube and centrifuged for 15 minutes at 2000 rpm. The normal product mixture produced three distinct layers: aqueous, solid and oil mixtures. All the phases were pipetted from the centrifuge tube and stored separately. The solid phase was dried in an oven at 40°C to remove additional moisture and stored separately for Source Rock Analysis (SRA). SRA gave the percentage of total trapped oil and solid in the sample. The

RNC-solvent mixture was dried at ambient temperature by applying a stream of nitrogen to a Büchner flask holding the mixture and venting the evaporated solvent until no mass change was observed. The RNC found through this method was reported as solvent-extracted RNC. The total RNC, solid and gas percentages were subtracted from 100 to find the percentage of aqueous produced. Every experiment been repeated two times and the standard deviation for small sample size (two repetition) has been calculated [47]

#### 6.2.4.1 Measurement of the Trapped Renewable Crude

A source rock analyser is an instrument that is capable of analyzing rock or solid by pyrolysis to provide accurate data about the oil content and the total organic carbon (TOC). A Weatherfords Source Rock Analyser™ was used for the pyrolysis and helium was used as the carrier gas. Crucibles were loaded into a carousel and heated under inert helium. The pyrolysis oven was first held at 300°C for 5 minutes and then ramped at 25°C per minute from 300°C to 650°C. Subsequently, the oven was reduced to 220°C and held for 5 minutes with the carrier gas converted to inert air (CO & $CO_2$ free), then purged, ramped at maximum heating to 580°C and held for 20 minutes. The flame ionisation detector (FID) was calibrated by running Weatherford Laboratories Instruments Division Standard 533. IR analysers were calibrated against standard gas with a known concentration of $CO_2$ and CO. This gave S1 (the amount of free hydrocarbon generated through thermal cracking at 350°C) and S2 (the amount of hydrocarbon generated through thermal cracking at higher temperatures up to 600°C). Total S1 and S2 in the solid equates to the trapped RNC.

#### 6.2.4.2 Acid Value (AV) of Renewable Crude

The acid value (AV) is the number of milligrams of potassium hydroxide (KOH) necessary to neutralise the free fatty acid in one gram of fat [48-50]. The American Society for Testing and Materials (ASTM) standards D974 method was used to measure the AV of produced RNC. In this method, the oil sample was dissolved in a mixture of isopropyl alcohol which contained

small amount of water. The subsequent single-phase solution was titrated at room temperature with standard alcoholic base to the end point indicated by the color change of the added p-naphtholbenzein solution (orange in acid and green-brown in base). To determine the AV for a strong acid, a separate portion of the sample was extracted with hot water and the aqueous extract was titrated with potassium hydroxide solution, using methyl orange as an indicator.

#### 6.2.4.3 Wettability of the RNC

Wettability refers to the ability of a liquid to spread or adhere to a solid surface. When a liquid exhibits high wettability, it tends to spread easily over the solid surface, forming a thin and uniform film. This indicates a strong attraction between the liquid molecules and the solid surface, resulting in good wetting. On the other hand, low wettability means that the liquid tends to bead up and form droplets on the surface, indicating weak interaction between the liquid and the solid. Contact angle is a measure of wettability and it is defined by the tangent (angle) of a liquid drop to a solid surface [51]. A lower contact angle of any liquid means that it can cover more surface area of the solid. The contact angle of RNC with respect to a glass plate was measured to determine how much is it inclined to attach to the hydrochar. An Attension Theta Optical tensiometer was used to measure the contact angle of RNC. The tensiometer was placed on a vibration free table where air flows were at a minimum. This instrument is capable of producing a 1–10 μL drop and a high-resolution camera lens captures the angle of the droplet to the glass plate. The contact angles of 5 μl oil (RNC) droplets were measured at room temperature by contact angle goniometry.

#### 6.2.4.4 FTIR Analysis

FTIR analysis of hydrochar was performed using a Nicolet 6700 Thermo Fisher FTIR spectrometer over the wavelength range of 4000–400 $cm^{-1}$. As the hydrochar holds RNC, it was washed with ethanol to remove as much of the oil as possible, then dried at 40°C for 48 hours before FTIR analysis.

#### 6.2.4.5 Brunauer-Emmett-Teller (BET) analysis

The hydrochar was dried at 40°C for 48 hours before BET analysis. The $N_2$ adsorption isotherms were measured using a Micromeritics 3 Flex analyser (Micromeritics Instrument Corporation, Norcross, GA) at 77 K.

#### 6.2.4.6 Viscosity analysis

A Rheometer SR5 (TA Instruments) with a cone and plate configuration was used to obtain the shear rate–shear stress data of the power law fluid. The viscosity was calculated from the shear rate and shear stress. However, a higher amount of RNC oil than could be obtained from the batch HTL reactor was required for this analysis. Therefore, experiments in a 1-L Parr batch reactor were used to obtain the required crude oil for the viscosity measurement. The reaction conditions giving the higher and lower amounts of trapped RNC were used for the Parr reactor.

## 6.3. Results and Discussion

### 6.3.1 HTL of Pine Wood

Yields of the products, i.e, hydrochar, gases, aqueous phase and RNC, from the HTL of pine wood are presented in Figure 6.2. Figure 6.2a shows the influence of temperature on the RNC yield including trapped and extracted RNC. At 260°C, total RNC was 9.2 wt.% which gradually increased to 14 wt.% at 320°C due to the greater decomposition of the biomass at higher temperatures [24]. Total RNC dramatically decreased after 320°C due to secondary cracking of the RNC [52] and a minimum yield of 8 wt.% was reached at 350°C. This is consistent with the work of Liu et al. [40] who reported that with solvents such as water, acetone and ethanol, higher temperatures favored RNC yields. The yield of extracted RNC greatly depended on the total RNC as extracted RNC also increased as temperature increased from 260–320°C (3–8 wt.%). As the total RNC yield decreased at 350°C, the extracted RNC yield also decreased to 3 wt.% at 350°C. However, at 260°C, trapped RNC was 5 wt.% and trapping was maximum

(8 wt.%) at 290°C. It then gradually decreased to 4 wt.% at 350°C. The various other factors that can influence the trapping of RNC are reported in the next section.

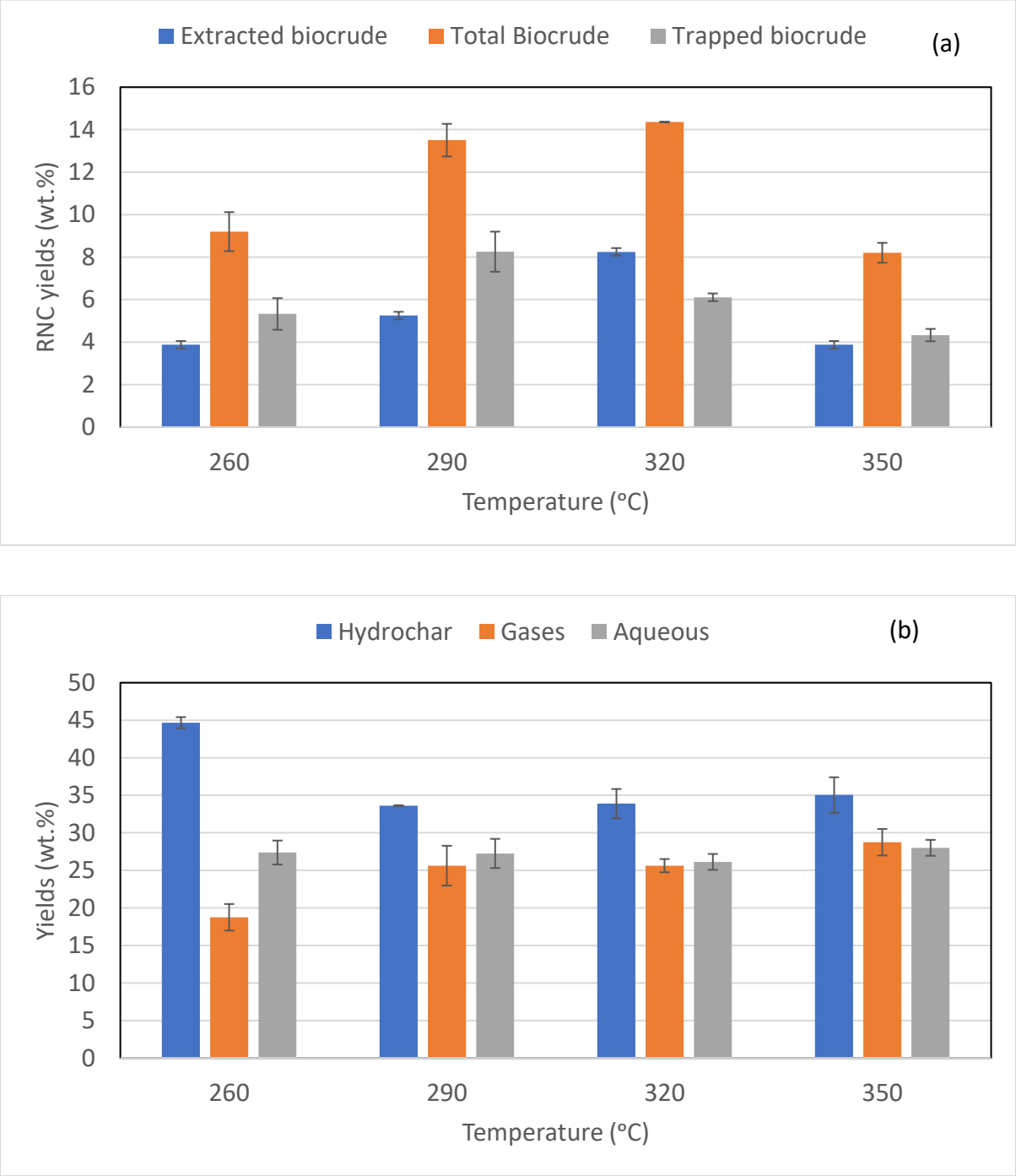


Figure 6.2: Yields of (a) RNC, and (b) other products for the HTL of pine wood

Figure 6.2b shows the influence of temperature on yields of hydrochar, aqueous phase and gases from the HTL of pine wood. The hydrochar yield was a maximum of 44 wt.% at 260°C.

It then decreased to 33 wt.% at 290°C and 320°C and slightly increased to 35 wt.% at 350°C. Decomposition of biomass increases with rising temperature; therefore, the hydrochar yield was expected to decrease gradually, but it increased slightly at 350°C. As the total RNC yield decreased at 350°C, polymerisation, repolarisation and condensation of RNC may have formed a solid residue and increased the yield of hydrochar [52]. Yields of gases increased from 18–28 wt.% with rising temperature due to the higher decomposition of the biomass at higher temperature [24]. The aqueous phase yield was almost constant (around 27 wt.%) during the HTL of pine wood.

### 6.3.2 HTL of Sludge

Products obtained from the HTL of a sludge mixture, i.e, hydrochar, gases, aqueous phase and RNC, are presented in Figure 6.3. Figure 6.3a shows the influence of temperature on the RNC yields including trapped and extracted RNC. Total RNC yield increased from 14–20 wt.% with a change in temperature from 260–350°C, due to increased biomass decomposition [24]. There was no secondary cracking of RNC observed in the HTL of sludge. The extracted RNC yield also increased from 4–10 wt.% with the change in temperature, and was greatly dependent on the yields of total RNC. Qien et al. [53] also found that higher temperature favored higher yields of RNC from the HTL of sewage sludge.

At 260°C, trapped RNC was at a minimum (9 wt.%), and it increased to a maximum of 12 wt.% at 290°C. It then gradually decreased to 10 wt.% at 350°C. As there are many other factors that influence RNC trapping in a solid, this is discussed in a separate section.

Figure 6.3b shows the yields of hydrochar, gases and aqueous phase from the HTL of sludge. The hydrochar yields were around 20 wt.% at temperatures of 260°C and 290°C, and then gradually increased with rising temperature. The gas yields increased from 13–23 wt.% when changing temperature from 260–290 ºC. The gas yields then decreased 22 wt.% at 350°C. The

aqueous phase was at a maximum (51 wt.%) at 260°C and then gradually decreased to 30 wt.% at 350°C. Higher temperatures are thought to decrease the hydrochar yields and increase the gas and aqueous phase yields because of the higher decomposition at higher temperatures [24]. Secondary reactions of the gas and aqueous phases after 290°C and 260°C, respectively, may have increased the hydrochar yields by re-polymerisation or condensation processes [52].

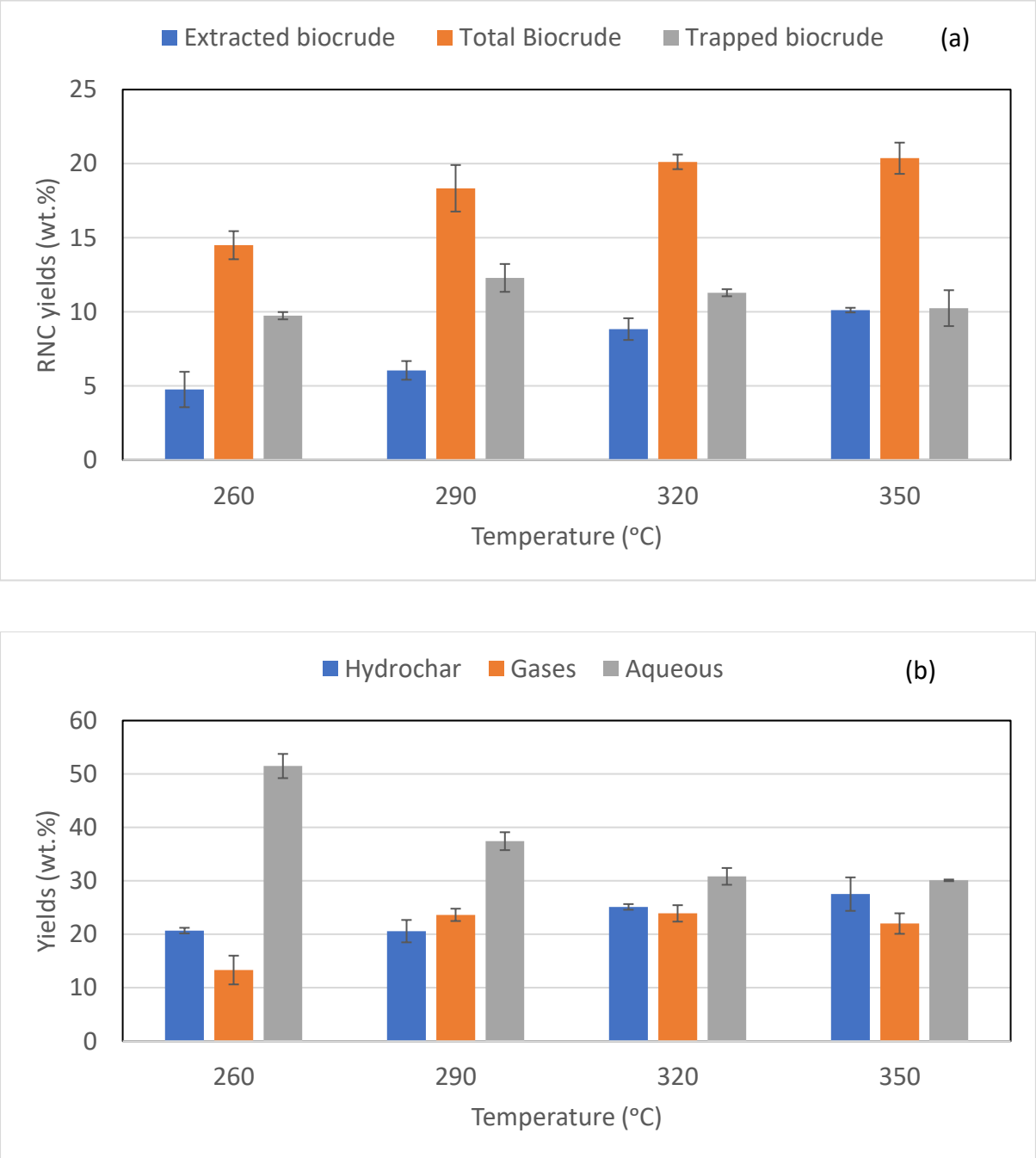


Figure 6.3: Yields of (a) RNC, and (b) other products for the HTL of sludge

### 6.3.3 HTL of Microalgae

Figure 6.4a shows the influence of temperature on the RNC yields including extracted RNC and trapped RNC for the HTL of microalgae. Total RNC unexpectedly decreased from 21–12 wt.% with a rise in temperature from 260–350°C. The extracted RNC was around 6 wt.% in all cases. Trapped RNC was 15 wt.% at 260°C and decreased gradually to a minimum of 6 wt.% at 350°C

Higher temperatures usually increase the biomass decomposition, and hence RNC yields [24]. If secondary cracking occurs, RNC can undergo further reaction, and decompose to produce gases, aqueous phase, or even solids if re-polymerisation or condensation occurs [52]. Biller et al. [54] produced RNC from the HTL of microalgae and reported similar higher temperature decreases in the yields of RNC. They ran the HTL reaction under three different conditions, i.e, no catalyst, and with NiMo and CoMO as catalysts. In every case, they found that the RNC yields decreased as temperature increased.

Figure 6.4b shows the yields of hydrochar, gases and aqueous phase from the HTL of microalgae. Hydrochar yields slowly decreased from 28–18 wt.% with a rise in temperature from 260–350°C. The decreased yields of hydrochar at higher temperature were due to biomass decomposition [24]. A higher rate of biomass decomposition at higher temperatures also increased the gas and aqueous phase. Gas yields were found to increase from 33–42 wt.% and aqueous phases from 17–26 wt.% with a rise in temperature from 260–350°C. Secondary cracking of RNC can also produce gases or aqueous phase which could be the reason for the higher yields of gas and aqueous phase at higher temperature.

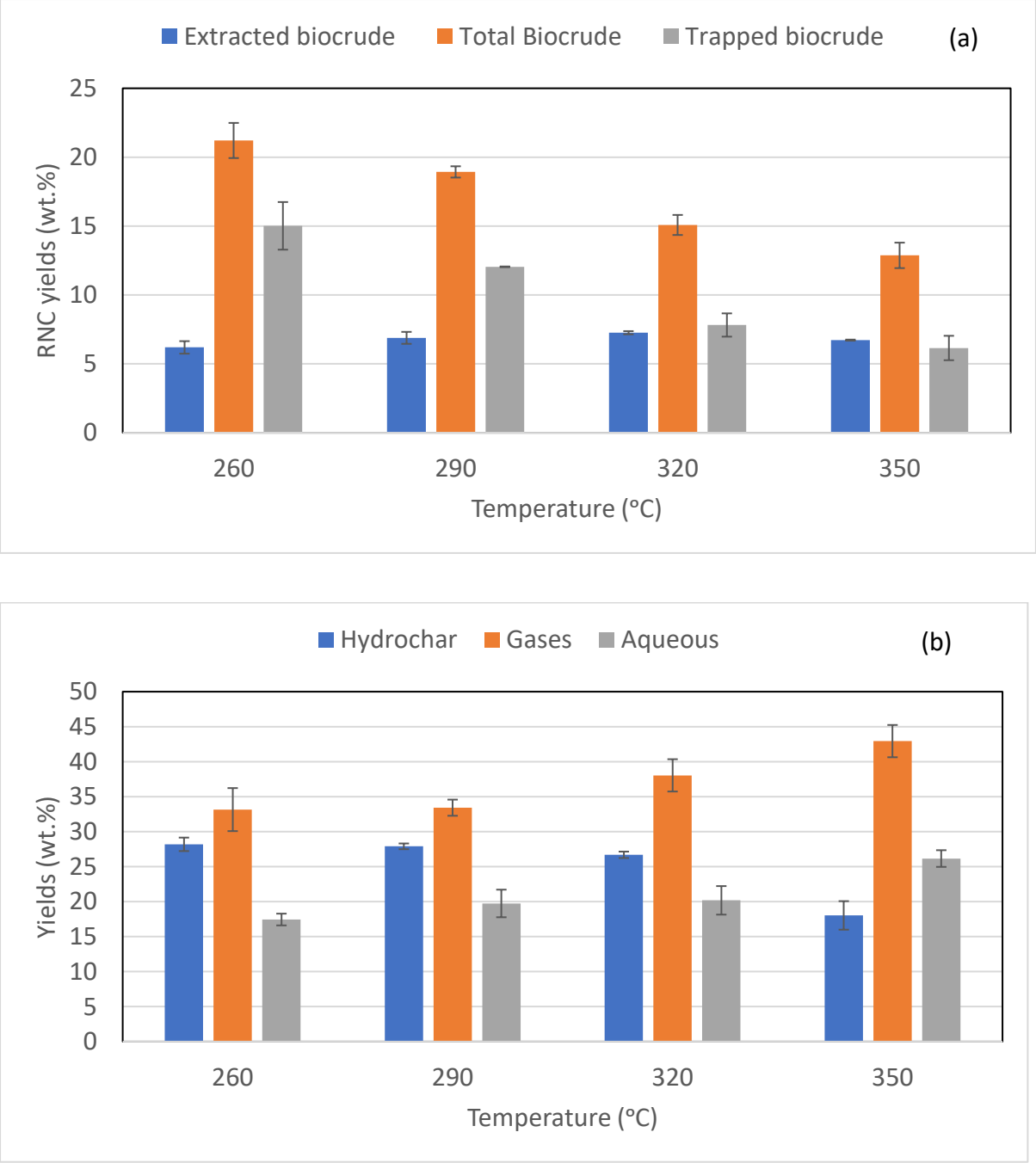


Figure 6.4: Yields of (a) biocrude, and (b) other products for the HTL of microalgae.

### 6.3.4 Degree of Trapping (DOT)

The degree of trapping (DOT) of RNC is defined as the ratio of RNC trapped in biochar to the total RNC. Figure 6.5 shows the DOT of biomass at different temperature. For the HTL of pine wood, the lowest DOT of 0.42 was found at 320°C even though the highest RNC was recorded at this temperature. The highest DOT was 0.61 at 290°C. It is therefore obvious that for pine

wood, the DOT does not depend on the total RNC yield. Similarly for sludge, though the total RNC increased with rising temperature, the DOT decreased. The minimum DOT was 0.50 at 350°C and the maximum was 0.67 at 260°C. However, in the HTL of microalgae, the DOT was 0.48 at 350°C and 0.71 at 260°C. There was a relationship between the total RNC and the DOT as decreasing the total RNC decreased the DOT.

Possible fundamental reasons for RNC trapping in biochar may include the AV of the RNC, the contact angle of the oil with respect to the solid, the functional groups in the solid, the porosity of the solid and the viscosity of the RNC. Therefore, the products (RNC and. hydrochar) for the highest and lowest DOT for each experiment were selected for further investigation. Table 6.1 shows the parameters of the products selected for further analysis.

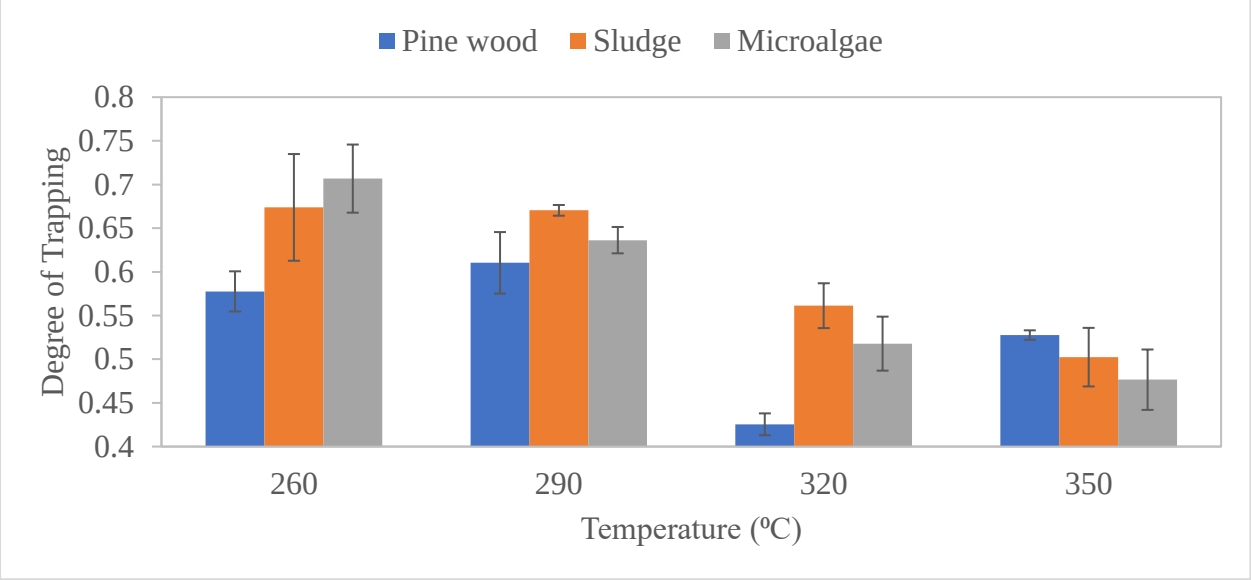


Figure 6.5: DOT at various temperatures

Table 6.1: Temperatures for the lowest and highest DOT

| | Pine wood | Sludge | Microalgae |
|---|---|---|---|
| Lowest DOT | 320ºC | 260ºC | 350ºC |
| Highest DOT | 290ºC | 350ºC | 260ºC |

### 6.3.5 Characterisation

#### 6.3.5.1 Effect of Acid value (AV) on RNC trapping

The acid number or AV indicates the number of milligrams of potassium hydroxide (KOH) required to neutralise the free fatty acids in 1 g of sample [48-50]. Table 6.2 shows the effect of the RNC AVs on the DOT for the HTL of pine wood, sludge and microalgae. The RNC AVs for the lowest and highest DOT are 98 mg KOH/g and 115 mg KOH/g for pine wood, 71 mg KOH/g and 92 mg KOH/g for sludge and 38 mg KOH/g and 54 mg KOH/g for microalgae. It was observed that AV was always lower for the lower trapping of RNC in hydrochar for all biomass.

Acidity is an important factor that has an influence not only on solid-liquid formation, but also interaction [55, 56]. A decrease in the AV of RNS can change the surface of the hydrochar from hydrophobic (oil wet) to hydrophilic (water wet). This can release more residual oil, due to a change in capillary pressure [57]. Similarly, the RNC with the lower AV was more hydrophilic; therefore, the lowest trapping occurs in cases where the AV is lower.

Table 6.2: Acid Value (AV) of RNC from different biomass

| | Lowest Trapping | Highest Trapping |
|---|---|---|
| Pine wood | 98.418 | 115.165 |
| Sludge | 71.364 | 92.49 |
| Micro algae | 38.084 | 54.731 |

#### 6.3.5.2 Contact angle for higher trapping of RNC

The contact angle is a microscopic manifestation of the interaction between a liquid and a solid surface, and it can provide information on surface chemistry and the wettability of the surface. It is an angle formed by a liquid at the three-phase boundary where a liquid, gas, and solid interact [58]. The wettability of an oil can be measured by finding the contact angle in the oil-

solid interface and the wettability of a solid can be found by measuring the contact angle of a water-solid interface [59].

A glass plate was used as a reference solid surface and the wettability of the RNC was measured with respect to the glass surface. Figure 6.6 shows the contact angles of the RNC from the various experiments. For pine wood, the RNC with a lower DOT gave an angle of 30º and that with a higher DOT gave an angle of 20º. For sludge, the angles were 29º (lower DOT) and 19º (higher DOT), and for microalgae, 29º (lower DOT) 16º (higher DOT). The higher DOT always produced a lower contact angle with the glass surface.

A large contact angle is recorded when the oil beads on the surface and covers less surface area [59]. Therefore, the RNC that formed a lower contact angle with a glass surface was more attached to the solid than the RNC that formed higher contact angle with the glass surface. Hence, the wettability properties of oil play an important role for solid–oil attachment.

The contact angle made by water-solid interface can define the wettability of solid surface. If the water forms the contact angle less than 90º with a solid surface, the solid surface has the hydrophobic nature and if the contact angle is more than 90º, the solid is hydrophilic [60]. However, there are limitations when measuring the contact angle of the HTL hydrochar and water interface. As the hydrochar holds some oil, it might provide the wrong contact angle. Additionally, the hydrochar has a small particle size and is not the plain surface needed for measurement. Therefore, only the wettability of the RNC was measured.

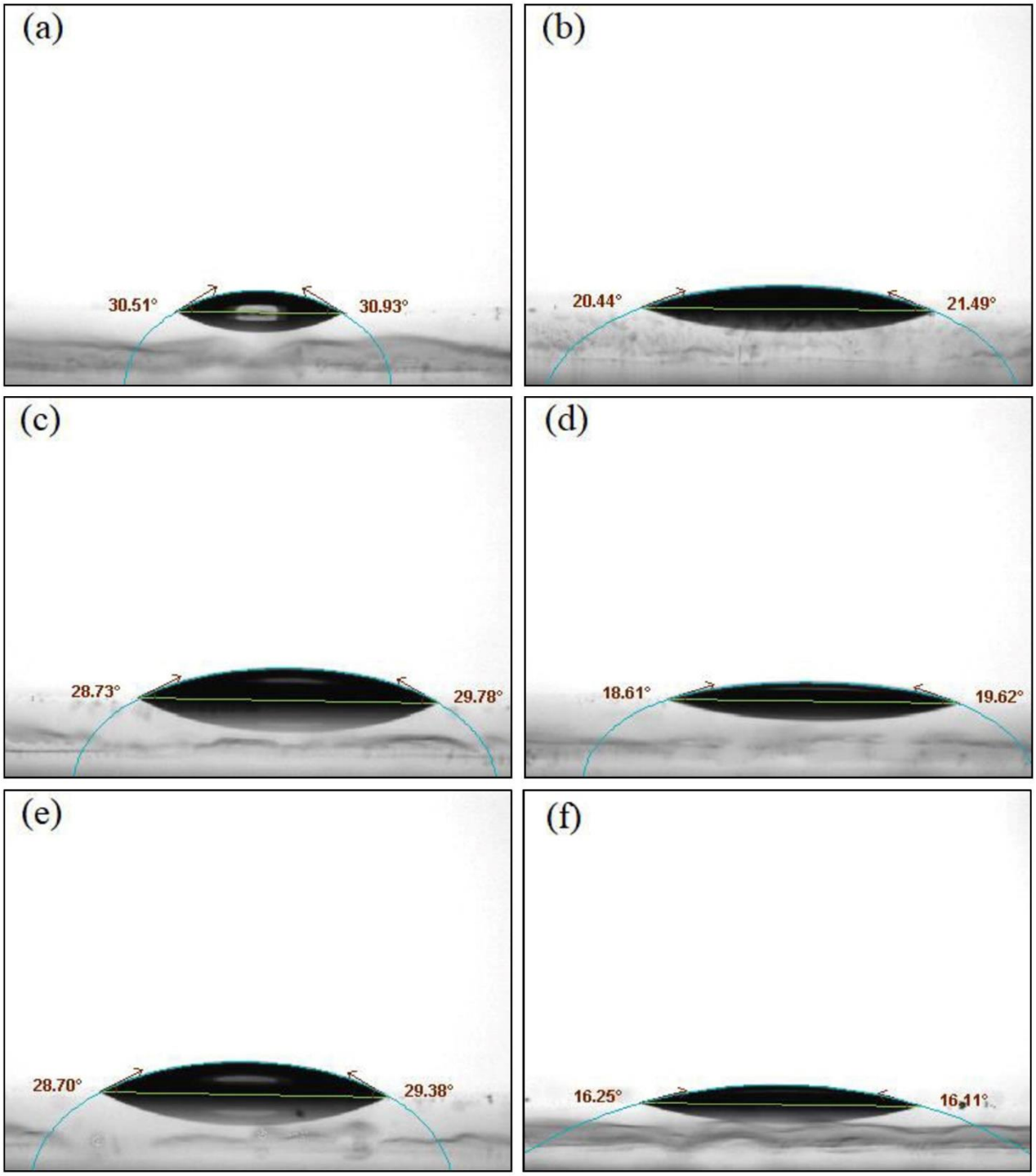


Figure 6.6: Contact angle measurement for produced RNC with respect to a glass plate for (a) lower DOT (b) higher DOT for pine wood, (c) lower DOT (d) higher DOT for sludge, and (e) lower DOT (f) higher DOT for microalgae

### 6.3.5.3 Effect of Non-polar functional groups on RNC trapping

Polar and non-polar functional groups are parts of organic compounds that can alter the wettability of the solid surface depending on the functional group available on the surface [61]. Hydrophobic surfaces have greater numbers of non-polar than polar functional groups. Non-polar functional groups are made up of mostly carbon and hydrogen, and molecules such as $N_2$, $O_2$ and S.

Figures 6.7, 6.8, and 6.9 show the FTIR analysis for pine wood, sludge and microalgae, respectively, and Table 6.3 shows the functional groups in the hydrochar. The table clearly shows that for the highest DOT of RNC in the solid, a higher number of non-polar functional groups are present. For instance, for the HTL of pine wood, the hydrochar with the highest DOT has seven non-polar functional groups and that with the lowest DOT has only five non-polar functional groups. As polar bonds favor interaction with water and non-polar bonds interact with oil, the higher number of non-polar functional group holds the oil and results in a higher solid–oil attachment [62]. Therefore, altering the functional groups from nonpolar to polar will lead to the recovery of more RNC during the HTL of biomass. Oil recovery from rock has been carried out using this technique [63].

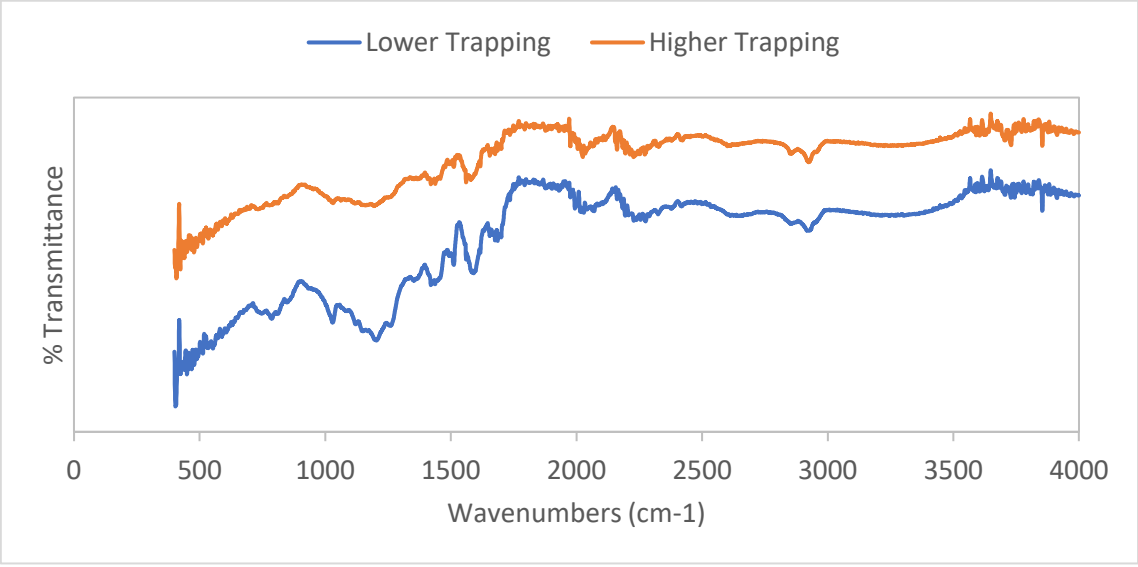


Figure 6.7: FTIR analysis for hydrochar obtained from pine wood

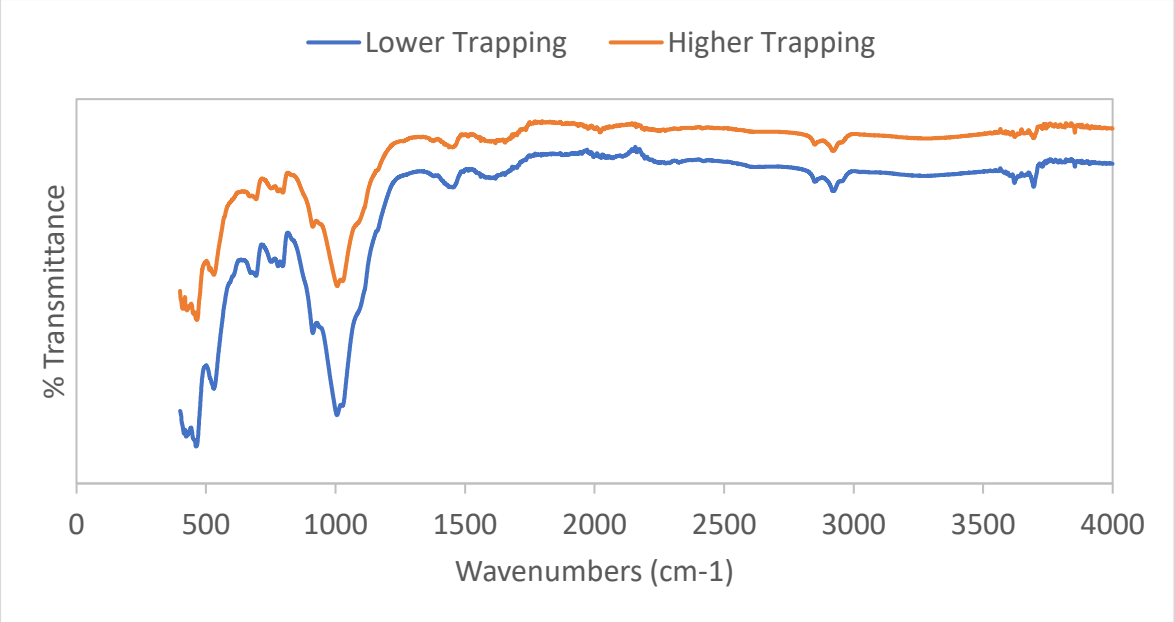


Figure 6.8: FTIR analysis for hydrochar obtained from sludge

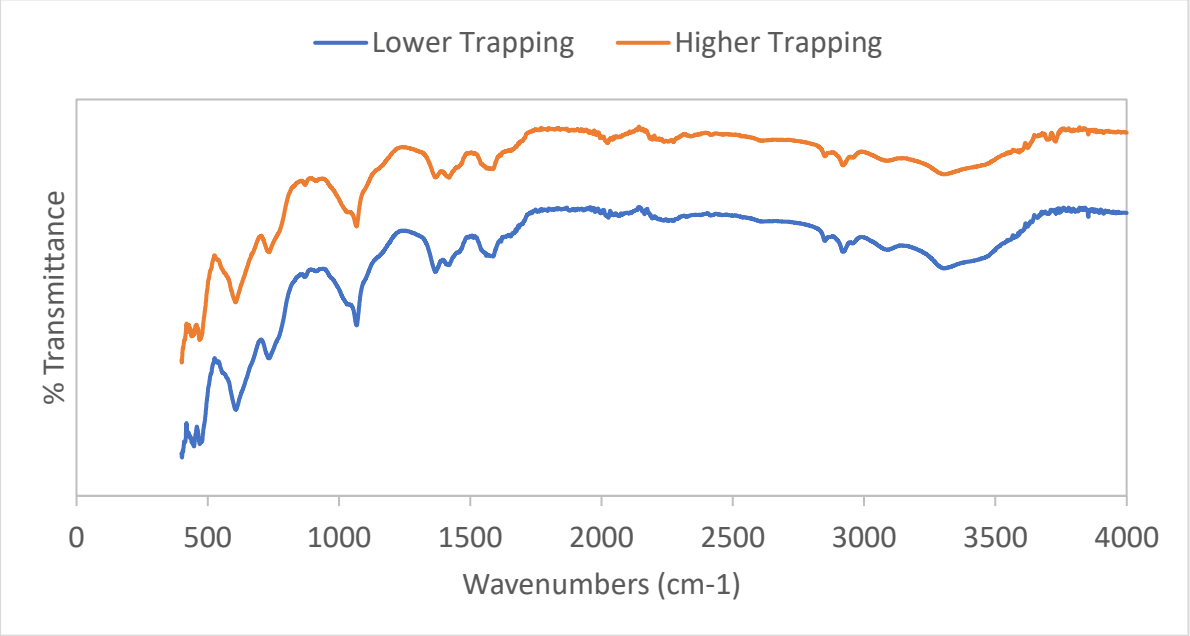


Figure 6.9: FTIR analysis for hydrochar obtained from microalgae

Table 6.3: List of non-polar functional groups on the hydrochar of pine wood, sludge, and microalgae

| Biomass | Type of DOT | Wavenumbers (cm-1) and non-polar functional groups |
|---|---|---|
| Pine Wood | Lower DOT | 2927 (C-H), 1993 (C-H), 1685 (C-H), 1676 (C-H), 1654 (C-C) |
| | Highest DOT | 2924 (C-H), 2227 (C≡C), 1975 (C-H), 1930 (C-H),1875 (C-H), 1793 (C-H), 1685 (C-H), 721 (C=C) |
| Sludge | Lower DOT | 796 (C=C), 693 (C=C) |
| | Highest DOT | 2921 (C-H), 1617 (C-H), 796 (C=C), 692 (C=C) |
| Microalgae | Lower DOT | 2919 (C-H), 733 (C=C) |
| | Highest DOT | 2919 (C-H), 2238 (C≡C), 731 (C=C) |

#### 6.3.5.4 BET for investigation hydrochar surface

A representative isothermal $N_2$ adsorption-desorption curve for the hydrochar from the HTL of pine wood is shown in Figure 6.10. A maximum of 37.04 $cm^3/g$ STP adsorption was recorded for the hydrochar of pine wood. The isotherm of the pine-wood hydrochar was a Type 2 isotherm, which is obtained for non-porous or microporous adsorbent materials [64, 65]. The desorption hysteresis loop indicates that the pores in the sample are negligible in number. Similar plots were obtained for the hydrochar from the HTL of sludge and microalgae.

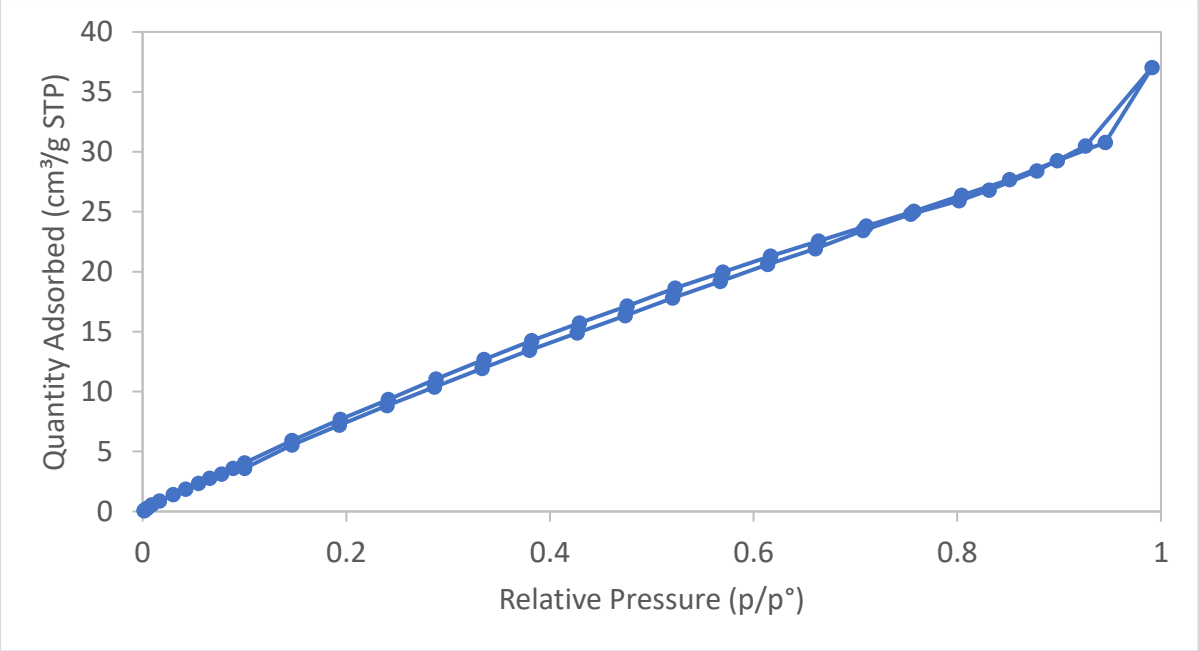


Figure 6.10: Isotherm plot for hydrochar obtained from the HTL of pine wood.

#### 6.3.5.5 RNC viscosity analysis

Figure 6.11 shows the viscosity analysis for the RNC from the experiments with the lowest and highest DOT. The shear rate vs. shear stress plot suggests that the RNC acts like a Newtonian fluid [66]. Shear rate is defined as the rate of change in velocity at which one layer of fluid moves over another adjacent layer [67]. High temperature is used in the HTL reaction, and the reaction conditions can cause an increase in the shear rate. The RNCs found from the HTL of biomass are Newtonian fluids; therefore, viscosity decreases because of the increase in shear rate with temperature [68].

The viscosity of the RNC for the lowest DOT was lower than the viscosity of the RNC of the higher DOT; i.e, the viscosity of RNC from pine wood was 3.41 $nS/m^2$ (LT) and 4.87 $nS/m^2$ (HT), the viscosity of RNC from sludge was 4.80 $nS/m^2$ (LT) and 8.29 $nS/m^2$ (HT) and the viscosity of RNC from microalgae was 2.69 $nS/m^2$ (LT) and 5.06 $nS/m^2$ (HT).

Multiphase flow and clogging or blocking of flow can be observed during the flow of higher viscosity RNC [69]. This may be the reason that RNC does not pass out of the hydrochar easily

and may have resulted in the trapping of the oil. Therefore, viscosity has an obvious impact on solid–RNC attachment.

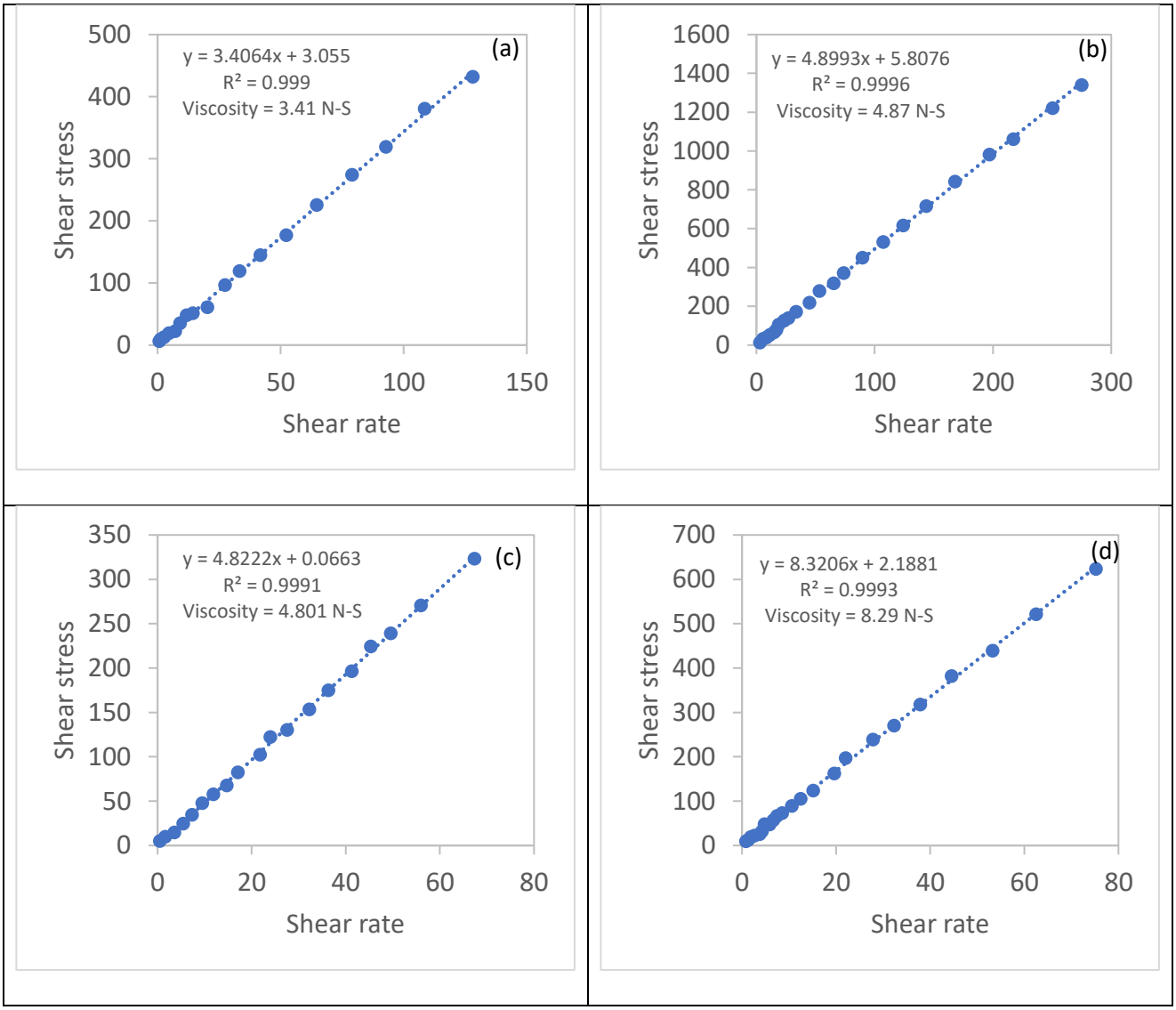

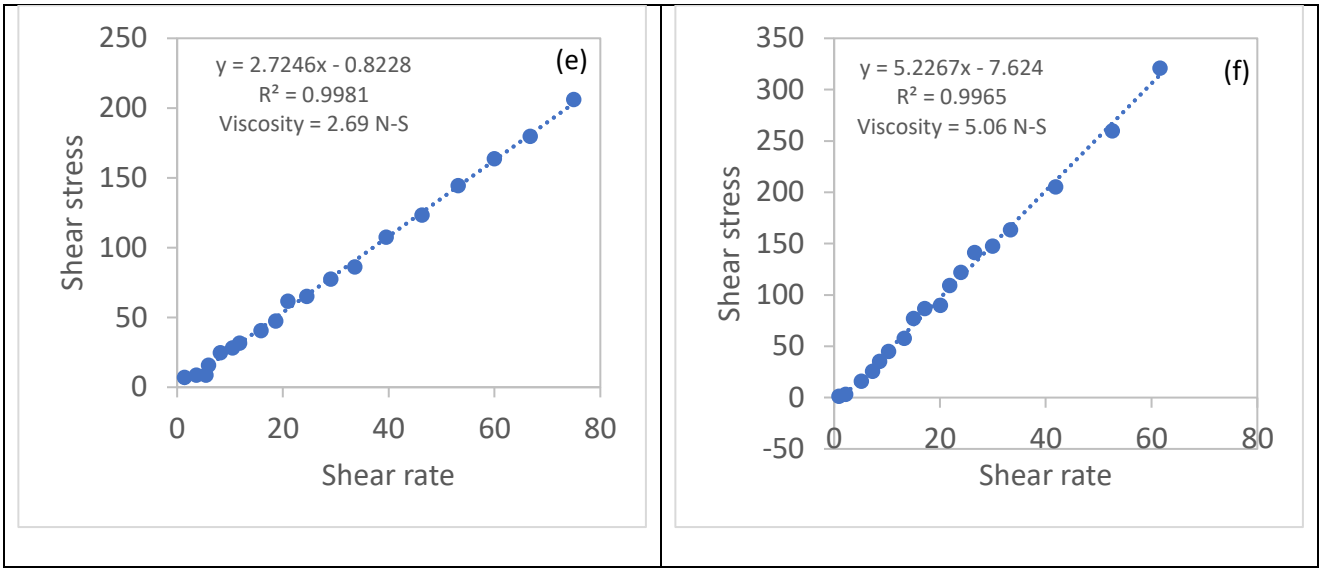


Figure 6.11: Shear rate vs. shear stress and viscosity analysis for RNC obtained from pine wood for (a) lower and (b) higher trapping, for RNC obtained from sludge for (c) lower and (d) higher trapping, and for RNC obtained from microalgae for (e) lower and (f) higher trapping.

### 6.4 Conclusion

In conclusion, this study aimed to investigate the interaction between solid-renewable crude (RNC) and determine the suitable operating conditions for biocrude yields during HTL of real biomass. The research focused on three types of biomass: pine wood, sludge, and microalgae.

The findings revealed that higher temperatures during HTL resulted in increased biomass decomposition and higher yields of RNC, leading to a greater degree of RNC trapping in hydrochar. For pine wood, the highest and lowest total RNC yields were observed at 320°C and 350°C respectively, with secondary reactions reducing RNC yield significantly beyond 320°C. In the case of sludge, the minimum and maximum total RNC yields occurred at 260°C and 350°C respectively, without any secondary cracking. As for microalgae, secondary cracking was observed from the initial stage, resulting in a decrease in total RNC yield from 260°C to 350°C. Additionally, the degrees of RNC trapping varied across temperatures: 320°C and 290°C for pine wood, 260°C and 350°C for sludge, and 350°C and 260°C for microalgae.

Furthermore, the study investigated factors influencing the solid-oil interaction during HTL of pine wood, sludge, and microalgae. Parameters such as the acid or base number of RNC, contact angle of oil with the solid, functional groups of the solid and viscosity of RNC were found to affect the solid-oil interaction. RNC with a higher degree of trapping exhibited a more acidic nature and formed a lower contact angle with the solid surface, facilitating greater wetting and trapping of RNC in the solid or hydrochar. Non-polar functional groups in the hydrochar played a role in solid-oil interaction, while higher viscosity of RNC led to multiphase flow and clogging, resulting in increased attachment of hydrochar and RNC.

## Reference


1. Adewole, B.Z., et al., *CO-pyrolysis of bituminous coal and coconut shell blends via thermogravimetric analysis.* 2020: p. 1-14.
2. Bridgwater, T.J.J.o.t.S.o.F. and Agriculture, *Biomass for energy*. 2006. **86**(12): p. 1755-1768.
3. Singh, J., S.J.R. Gu, and S.E. Reviews, *Biomass conversion to energy in India—A critique*. 2010. **14**(5): p. 1367-1378.
4. Adeniyi, A.G., et al., *Pyrolysis of different fruit peel waste via a thermodynamic model.* 2019. **2**: p. 16-24.
5. Azeta, O., et al., *A review on the sustainable energy generation from the pyrolysis of coconut biomass.* Scientific African, 2021. **13**: p. e00909.
6. Irmak, S., *Challenges of biomass utilization for biofuels*, in *Biomass for bioenergy-recent trends and future challenges*. 2019, IntechOpen.
7. Pande, M. and A.N. Bhaskarwar, *Biomass conversion to energy*, in *Biomass conversion*. 2012, Springer. p. 1-90.
8. Ahmad, R.K., et al., *Effects of Process Conditions on Calorific Value and Yield of Charcoal Produced from Pyrolysis of Coconut Shells*, in *Advances in Manufacturing Engineering*. 2020, Springer. p. 253-262.
9. Toor, S.S., L. Rosendahl, and A.J.E. Rudolf, *Hydrothermal liquefaction of biomass: a review of subcritical water technologies.* 2011. **36**(5): p. 2328-2342.
10. Zhu, Z., et al., *Hydrothermal liquefaction of barley straw to bio-crude oil: Effects of reaction temperature and aqueous phase recirculation.* 2015. **137**: p. 183-192.
11. Hammerschmidt, A., et al., *Catalytic conversion of waste biomass by hydrothermal treatment.* 2011. **90**(2): p. 555-562.
12. Yin, S., et al., *Subcritical hydrothermal liquefaction of cattle manure to bio-oil: Effects of conversion parameters on bio-oil yield and characterization of bio-oil.* 2010. **101**(10): p. 3657-3664.

13. Xue, Y., et al., *A review on the operating conditions of producing bio-oil from hydrothermal liquefaction of biomass.* 2016. **40**(7): p. 865-877.
14. Toor, S.S., *Modeling and Optimization of Catliq Liquid Bioful Process*. 2010: Department of Energy Technology, Aalborg University.
15. Shah, Y.T., *Energy and fuel systems integration*. 2015: CRC Press.
16. Franck, E.J.S., Water, and H. Systems, *Supercritical water*. 2000: p. 22-34.
17. Krammer, P. and H.J.T.J.o.S.F. Vogel, *Hydrolysis of esters in subcritical and supercritical water.* 2000. **16**(3): p. 189-206.
18. Brown, T.M., P. Duan, and P.E. Savage, *Hydrothermal liquefaction and gasification of Nannochloropsis sp.* Energy & Fuels, 2010. **24**(6): p. 3639-3646.
19. Valdez, P.J., et al., *Characterization of product fractions from hydrothermal liquefaction of Nannochloropsis sp. and the influence of solvents.* 2011. **25**(7): p. 3235-3243.
20. Aysu, T. and M.M. Küçük, *Liquefaction of giant fennel (Ferula orientalis L.) in supercritical organic solvents: Effects of liquefaction parameters on product yields and character.* The Journal of Supercritical Fluids, 2013. **83**(Supplement C): p. 104-123.
21. Brown, T.M., P. Duan, and P.E. Savage, *Hydrothermal liquefaction and gasification of Nannochloropsis sp.* Energy Fuels, 2010. **24**(6): p. 3639-3646.
22. Yin, S., et al., *Subcritical hydrothermal liquefaction of cattle manure to bio-oil: Effects of conversion parameters on bio-oil yield and characterization of bio-oil.* Bioresource Technology, 2010. **101**(10): p. 3657-3664.
23. Cheng, J., et al., *Biodiesel production from lipids in wet microalgae with microwave irradiation and bio-crude production from algal residue through hydrothermal liquefaction.* Bioresource Technology, 2014. **151**(Supplement C): p. 415-418.
24. Chen, Y., et al., *Direct liquefaction of Dunaliella tertiolecta for bio-oil in sub/supercritical ethanol–water.* Bioresource Technology, 2012. **124**(Supplement C): p. 190-198.
25. Chen, W.-T., et al., *Co-liquefaction of swine manure and mixed-culture algal biomass from a wastewater treatment system to produce bio-crude oil.* Applied Energy, 2014. **128**(Supplement C): p. 209-216.
26. Dimitriadis, A. and S. Bezergianni, *Hydrothermal liquefaction of various biomass and waste feedstocks for biocrude production: A state of the art review.* Renewable and Sustainable Energy Reviews, 2017. **68**(Part 1): p. 113-125.
27. Jin, B., et al., *Co-liquefaction of micro- and macroalgae in subcritical water.* Bioresource Technology, 2013. **149**(Supplement C): p. 103-110.
28. Qu, Y., X. Wei, and C. Zhong, *Experimental study on the direct liquefaction of Cunninghamia lanceolata in water.* Energy, 2003. **28**(7): p. 597-606.
29. Cheng, S., et al., *Highly efficient liquefaction of woody biomass in hot-compressed alcohol− water co-solvents.* Energy & Fuels, 2010. **24**(9): p. 4659-4667.
30. Li, R.-d., et al., *Liquefaction of rice stalk in sub- and supercritical ethanol.* Journal of Fuel Chemistry and Technology, 2013. **41**(12): p. 1459-1465.
31. Arturi, K.R., et al., *Characterization of liquid products from hydrothermal liquefaction (HTL) of biomass via solid-phase microextraction (SPME).* Biomass and Bioenergy, 2016. **88**: p. 116-125.

32. Obeid, R., et al., *Reaction kinetics and characterization of species in renewable crude from hydrothermal liquefaction of mixtures of polymer compounds to represent organic fractions of biomass feedstocks.* 2019. **34**(1): p. 419-429.
33. Fan, Y., et al., *Hydrothermal liquefaction of protein-containing biomass: Study of model compounds for Maillard reactions.* 2018. **8**(4): p. 909-923.
34. Madsen, R.B., et al., *Predicting the chemical composition of aqueous phase from hydrothermal liquefaction of model compounds and biomasses.* 2016. **30**(12): p. 10470-10483.
35. Yin, S. and Z.J.A.E. Tan, *Hydrothermal liquefaction of cellulose to bio-oil under acidic, neutral and alkaline conditions.* 2012. **92**: p. 234-239.
36. Cao, Y., et al., *Hydrothermal liquefaction of lignin to aromatic chemicals: impact of lignin structure.* 2020. **59**(39): p. 16957-16969.
37. Lu, J., et al., *Synergistic and antagonistic interactions during hydrothermal liquefaction of soybean oil, soy protein, cellulose, xylose, and lignin.* 2018. **6**(11): p. 14501-14509.
38. Tang, S., et al., *Hydrotreatment of biocrudes derived from hydrothermal liquefaction and lipid extraction of the high-lipid Scenedesmus.* 2019. **21**(12): p. 3413-3423.
39. Demirbaş, A., *Mechanisms of liquefaction and pyrolysis reactions of biomass.* Energy Conversion and Management, 2000. **41**(6): p. 633-646.
40. Liu, Z. and F.-S. Zhang, *Effects of various solvents on the liquefaction of biomass to produce fuels and chemical feedstocks.* Energy Conversion and Management, 2008. **49**(12): p. 3498-3504.
41. Fan, S.-P., et al., *Comparative studies of products obtained from solvolysis liquefaction of oil palm empty fruit bunch fibres using different solvents.* Bioresource Technology, 2011. **102**(3): p. 3521-3526.
42. Aysu, T., *Supercritical fluid extraction of reed canary grass (Phalaris arundinacea).* Biomass and Bioenergy, 2012. **41**(Supplement C): p. 139-144.
43. Aysu, T., M. Turhan, and M.M. Küçük, *Liquefaction of Typha latifolia by supercritical fluid extraction.* Bioresource Technology, 2012. **107**(Supplement C): p. 464-470.
44. Durak, H. and T. Aysu, *Effects of catalysts and solvents on liquefaction of Onopordum heteracanthum for production of bio-oils.* Bioresource Technology, 2014. **166**(Supplement C): p. 309-317.
45. Pisupati, S.V. and A.H. Tchapda, *Thermochemical Processing of Biomass*, in *Advances in Bioprocess Technology*. 2015, Springer. p. 277-314.
46. Sing, S.F., et al., *Pilot-scale continuous recycling of growth medium for the mass culture of a halotolerant Tetraselmis sp. in raceway ponds under increasing salinity: a novel protocol for commercial microalgal biomass production.* 2014. **161**: p. 47-54.
47. Singh, A.S., M.B.J.I.J.o.e. Masuku, commerce, and management, *Sampling techniques & determination of sample size in applied statistics research: An overview.* 2014. **2**(11): p. 1-22.
48. Patterson, H.B.W., *Chapter 12 - Quality and Control*, in *Hydrogenation of Fats and Oils (Second Edition)*, G.R. List and J.W. King, Editors. 2011, AOCS Press. p. 329-350.

49. Spitz, L., *12 - Glossary*, in *Soap Manufacturing Technology (Second Edition)*, L. Spitz, Editor. 2016, AOCS Press. p. 267-280.
50. Onu, P. and C. Mbohwa, *Chapter 6 - New approach and prospects of agrowaste resources conversion for energy systems performance and development*, in *Agricultural Waste Diversity and Sustainability Issues*, P. Onu and C. Mbohwa, Editors. 2021, Academic Press. p. 97-118.
51. Kwok, D.Y. and A.W. Neumann, *Contact angle measurement and contact angle interpretation.* Advances in colloid and interface science, 1999. **81**(3): p. 167-249.
52. Feng, H., et al., *Synergistic bio-oil production from hydrothermal co-liquefaction of Spirulina platensis and α-Cellulose.* Energy, 2019. **174**: p. 1283-1291.
53. Qian, L., S. Wang, and P.E. Savage, *Hydrothermal liquefaction of sewage sludge under isothermal and fast conditions.* Bioresource Technology, 2017. **232**: p. 27-34.
54. Biller, P., et al., *Hydroprocessing of bio-crude from continuous hydrothermal liquefaction of microalgae.* Fuel, 2015. **159**: p. 197-205.
55. Biller, P. and A. Ross, *Production of biofuels via hydrothermal conversion*, in *Handbook of biofuels production*. 2016, Woodhead Publishing. p. 509-547.
56. Posmanik, R., et al., *Acid and alkali catalyzed hydrothermal liquefaction of dairy manure digestate and food waste.* ACS Sustainable Chemistry & Engineering, 2018. **6**(2): p. 2724-2732.
57. Donaldson, E. and W. Alam, *Wettability. Houston.* TX: Gulf Publishing Company, 2008.
58. Akbari, R. and C. Antonini, *Contact angle measurements: From existing methods to an open-source tool.* Advances in Colloid and Interface Science, 2021. **294**: p. 102470.
59. Yuan, Y. and T.R. Lee, *Contact angle and wetting properties*, in *Surface science techniques*. 2013, Springer. p. 3-34.
60. Eral, H., J.J.C. Oh, and p. science, *Contact angle hysteresis: a review of fundamentals and applications.* Colloid and polymer science, 2013. **291**(2): p. 247-260.
61. Jarrahian, K., et al., *Wettability alteration of carbonate rocks by surfactants: A mechanistic study.* Colloids and Surfaces A: Physicochemical and Engineering Aspects, 2012. **410**: p. 1-10.
62. *Module 11 /Functional Groups*. [cited 2022 23 January]; Available from: https://oli.cmu.edu/jcourse/workbook/activity/page?context=90d3ff9080020ca601040285a20dd2c4.
63. Wu, J., et al., *Effect of specific functional groups on oil adhesion from mica substrate: Implications for low salinity effect.* Journal of Industrial and Engineering Chemistry, 2017. **56**: p. 342-349.
64. Zhang, S., et al., *Bamboo derived hydrochar microspheres fabricated by acid-assisted hydrothermal carbonization.* Chemosphere, 2021. **263**: p. 128093.
65. Zhang, P. *Adsorption and Desorption Isotherms*. 2016 [cited 2022 24 January]; Available from: http://www.keresearchgroup.com/uploads/4/8/4/5/48456521/160903_introduction_to_bet_isotherms.pdf.
66. Chhabra, R.P., *Non-Newtonian fluids: an introduction*, in *Rheology of complex fluids*. 2010, Springer. p. 3-34.

67. Krishna, K.V., et al., *Chapter 1.6 - Bioelectrocatalyst in Microbial Electrochemical Systems and Extracellular Electron Transport*, in *Microbial Electrochemical Technology*, S.V. Mohan, S. Varjani, and A. Pandey, Editors. 2019, Elsevier. p. 117-141.
68. Sakthipriya, N., M. Doble, and J.S. Sangwai, *Performance of thermophilic strain on the reduction of viscosity of crude oil under high pressure and high temperature conditions: Experiments and modeling.* Journal of Petroleum Science and Engineering, 2022. **210**: p. 110016.
69. Martínez-Palou, R., et al., *Transportation of heavy and extra-heavy crude oil by pipeline: A review.* Journal of Petroleum Science and Engineering, 2011. **75**(3): p. 274-282.

# Chapter 7 – Conclusion

## 7.1 Conclusion

The thesis mainly focused on how experimental parameters and the interaction between hydrochar and renewable crude make it challenging to extract renewable crude during product separation. This is due to the strong attachment between hydrochar and renewable crude, leading to lower yields than expected. The thesis made a significant contribution by re-analysing published data to better understand the conditions affecting product yields and hydrochar-RNC interaction. The re-evaluation considered both lignocellulosic and non-lignocellulosic biomass. In addition, the thesis examined how HTL processing parameters impact the formation and interaction of solid-renewable crude during the HTL of relevant feed, with a specific focus on carbohydrates. The research also looked into the fundamental reasons behind hydrochar and RNC attachment during the HTL of both model compounds and real biomass.

Initially, the thesis re-evaluated published literature regarding the interaction between hydrochar and renewable crude during HTL. The studies revealed that higher temperatures between 300 to 350 $^{o}$C resulted in higher RNC yields due to greater biomass decomposition, while temperatures below 300 $^{o}$C led to higher hydrochar yields. However, yields decreased at temperatures exceeding 350 $^{o}$C due to RNC re-polymerisation and further decomposition. Lower residence times were more favourable for higher RNC yields as longer residence times and higher temperatures can result in secondary cracking or re-polymerisation of RNC. The use of a higher amount of solvent (water) in the HTL reaction accelerates the decomposition rate of biomass, resulting in more RNC yields and lower hydrochar yields. Catalysts such as $RbCO_3$, Fe, $FeSO_4$, $K_2CO_3$, HCL, $ZnCl_2$, $Na_2CO_3$, and caustic solutions were found to increase RNC yields while decreasing hydrochar yields. However, some biomass can produce higher hydrochar yields using caustic solutions, such as NaOH which produced 71.1 wt.% hydrochar for Birch HTL. Co-solvents were also found to work differently for various biomass. For

example, for pine wood, the solvent efficiency for oil yields can be sequenced as follows: ethanol > Acetone > water. Conversely, for oil palm empty fruit bunches, the solvent efficiency can be sequenced as follows: ethylene glycol > water > ethanol > acetone > toluene. Water was suitable for all biomass, like algae, wood and waste materials. Ethanol–water (60%+40%) and methanol-Water (50%+50%) mixtures were also significant solvents for producing renewable crude. It was also noticeable that some of the RNC were trapped in the hydrochar. The study also found that some RNC were trapped in hydrochar due to the porosity and viscosity of the renewable crude. Hydrophobicity, or the oil-wet condition, of hydrochar was found to be responsible for attracting oil into solids. Non-polar functional groups in hydrochar, such as C-H stretching, C-H bending, and C=C stretching, were found to attract the most oil. Porosity also played a role in oil trapped inside the pores, with higher reaction times resulting in higher porosity across surface areas.

The second aspect of the thesis aimed to investigate how different processing parameters affect the product yields and the trapping of RNC in hydrochar during HTL of carbohydrates. These parameters included temperature (ranging from 260 to 350 °C), residence time (ranging from 10 to 25 minutes), and biomass-to-water ratio (ranging from 0.25 to 1). The study found that higher temperatures during hydrothermal liquefaction resulted in higher yields of renewable crude (RNC) due to the higher decomposition rate of cellulose, with the maximum yield at 350°C. However, hydrochar yields increased until 320°C due to thermal cracking and repolymerisation of other products. Lower residence time was also favourable for higher RNC yields, with yields decreasing at longer residence times. A lower biomass/water ratio (higher water content) was favourable for higher yields of RNC. The study found that a B/W ratio of 0.25 yielded the highest RNC, while a B/W ratio of 1 yielded the lowest RNC yield. The solvent extraction process can extract around 31.78% to 57.67% of the total RNC at temperatures ranging from 260 to 350 ºC, with a maximum of 58% extracted at 350 ºC. During 10 to 25

minutes of residence time, the maximum RNC extraction (57.67%) was reported at a residence time of 10 minutes. Changing the B/W ratio from 0.25 to 1 showed that maximum oil extraction (57.80% of total oil) was possible at a 1 B/W ratio, but this condition was not effective due to lower RNC yield. The suitable condition for HTL of cellulose would be 350 ºC temperature, 10 minutes of residence time, and a 0.5 B/W ratio. The degree of renewable crude trapping slightly increases from 0.64 to 0.68 with increasing temperature from 260 to 320 ºC but decreases to 0.42 at 350 ºC. The degree of trapping also increases from 0.42 to 0.66 with increasing residence time from 10 to 25 minutes. Changing the B/W ratio from 0.25 to 1 does not significantly affect the degree of trapping. Source rock analyser (SRA), which was employed, can measure the trapped light and heavy RNC. Around 1 wt.% of light RNC and 3 to 6 wt.% of heavy RNC remain trapped even after solvent extraction. Solvent can extract more light oil than heavy oil, indicating that heavy oil has properties that attract hydrochar more than light oil. A suitable condition for RNC extraction would be a temperature of 350 ºC, a residence time of 10 minutes, and a B/W ratio of 0.5.

The third focus of this thesis was on exploring the impact of experimental parameters, understanding the underlying factors that influence the interaction between solid and renewable crude (RNC), and determining the appropriate operating conditions for achieving maximum product yields. The study utilised four different raw materials, including a 50% cellulose and 50% lipid mixture (CL50%), 50% cellulose and 50% protein mixture (CP50%), 50% lipid and 50% lipid mixture (LL50%), and 50% lipid and 50% protein mixture (LP50%), for the HTL reaction.

Higher temperatures favour higher RNC yields due to increased feedstock decomposition. Higher RNC yields lead to increased RNC trapping in hydrochar. HTL of CL50% showed maximum and minimum total RNC yields at 350 ºC and 260 ºC respectively, with the lowest and highest degree of RNC trapping (DOT) at 290 ºC and 350 ºC. HTL of CP50% had the

highest and lowest total RNC yields at 290 ºC and 350 ºC, with the lowest and highest RNC trapping at 260 ºC and 350 ºC. HTL of LL50% resulted in maximum and minimum total RNC yields at 320 ºC and 260 ºC, respectively, with the lowest and highest RNC trapping at 320 ºC and 260 ºC. HTL of LP50% had maximum and minimum total RNC yields at 350 ºC and 260 ºC, respectively, with the lowest and highest RNC trapping at 260 ºC and 350 ºC. SRA analysis revealed that 56-77% of RNC were trapped in the hydrochar in each case.

The attachment of RNC and hydrochar is influenced by several factors such as the contact angle of oil with the solid, acid/base number of RNC, functional group of solid, porosity of solid, and viscosity of RNC. RNC's acid and base properties influence the attachment of RNC and hydrochar, and RNC with more acidic properties can interact more with hydrochar. The non-polar functional group on the hydrochar surface attracts oil and results in higher oil trapping. Viscosity also plays a vital role in hydrochar and RNC attachment, and RNC with higher viscosity can cause multiphase flow and clogging, resulting in higher hydrochar and RNC interaction. $N_2$ adsorption/desorption curves with BET analysis suggest that hydrochar is not porous, and there is no expectation that pores could hold oil and influence solid oil attachment.

Finally, the thesis was to investigate the underlying reasons for the interaction between solid-renewable crude (RNC) and to identify the appropriate operating conditions for product yields during hydrothermal liquefaction of real biomass. The study focused on three types of real biomass, namely pine wood, sludge, and microalgae.

Higher temperature led to higher decomposition of biomass and a higher yield of RNC, which also led to a higher degree of RNC trapping in hydrochar. The highest and lowest total RNC were found at 320°C and 350°C respectively for HTL of pine wood. Secondary reactions reduced RNC yield significantly after 320°C. For sludge, the maximum and minimum total

RNC were found at 350°C and 260°C, respectively, with no secondary cracking. For microalgae, secondary cracking occurred from the initial stage, resulting in a decrease in total RNC from 260 to 350°C. The highest and lowest degrees of RNC trapping were found at 320°C and 290°C for pine wood, 260°C and 350°C for sludge, and 350°C and 260°C for microalgae.

The study also investigated the factors that influence the solid-oil interaction during hydrothermal liquefaction of pine wood, sludge, and microalgae. The acid or base number of renewable crude (RNC), contact angle of oil in respect to the solid, functional group of solid, porosity of solid, and viscosity of RNC were found to affect solid-oil interaction. The RNC with the highest degree of trapping (DOT) had a more acidic nature and could form a lower contact angle with a solid surface, resulting in higher wetting and trapping of RNC in solid or hydrochar. Non-polar functional groups in the hydrochar played a role in solid-oil interaction, and RNC with higher viscosity led to multiphase flow and clogging, resulting in higher hydrochar and RNC attachment.

### 7.2 Recommendations for future work

This thesis offers an in-depth comprehension of how process parameters affect product yields and the interaction between hydrochar and renewable crude. It investigates the fundamental reasons for this interaction, including the degree of trapping and cause of renewable crude trapping in hydrochar, as well as the impact of process parameters on RNC trapping in solid. Nonetheless, more research is required to enhance the existing knowledge of hydrothermal liquefaction of biomass.

1. To address this research gap, various types of reactors with different configurations can be utilised, as the current experimental results are confined to a specific reactor configuration. In this study, an 11 mL volume batch reactor was used for all experiments. To gain a deeper understanding, a comparison of results between batch and continuous processes in HTL can be

conducted. Moreover, the results can be validated through investigations by an autoclave reactor.

2. The present HTL reaction is also limited to one heating rate and mass loading of feedstocks as the heating rate and reactor size are fixed in the employed batch reactor. Further experiments with different heating rates and mass loading can be conducted to understand renewable crude trapping in hydrochar better.

3. The research findings are confined to model compounds and some specific biomass, such as pine wood, microalgae, and sludge. However, exploring the potential of other biomass as feedstock in HTL reactions can provide a deeper understanding of hydrochar and renewable crude interaction.

4. The possibility of chemical treatment to eliminate the fundamental reasons for hydrochar and renewable crude attachment can be explored through studies. For instance, using surfactant or catalysts in the HTL reaction to remove the non-polar functional group from the hydrochar can increase the recovery of RNC. This approach can be valuable for the production of RNC on an industrial scale.

5. Further research is necessary not only to understand the fundamental reasons for solid-oil attachment but also to upgrade the renewable crude for practical applications.

## Reference


1. Pandey, A., *Foreword*, in *Emerging Technologies and Biological Systems for Biogas Upgrading*, N. Aryal, et al., Editors. 2021, Academic Press. p. xix-xx.
2. Toor, S.S., L. Rosendahl, and A. Rudolf, *Hydrothermal liquefaction of biomass: A review of subcritical water technologies.* Energy, 2011. **36**(5): p. 2328-2342.
3. Tungal, R. and R.V. Shende, *Hydrothermal liquefaction of pinewood (Pinus ponderosa) for H2, biocrude and bio-oil generation.* Applied Energy, 2014. **134**: p. 401-412.
4. Behrendt, F., et al., *Direct liquefaction of biomass.* Chemical Engineering Technology, 2008. **31**(5): p. 667-677.
5. Peterson, A.A., et al., *Kinetic Evidence of the Maillard Reaction in Hydrothermal Biomass Processing: Glucos‡ Glycine Interactions in High-Temperature, High-Pressure Water.* Industrial & Engineering Chemistry Research, 2010. **49**: p. 2107-2117.
6. Elliott, D.C., et al., *Hydrothermal liquefaction of biomass: Developments from batch to continuous process.* Bioresource Technology, 2015. **178**: p. 147-156.
7. Dimitriadis, A. and S. Bezergianni, *Hydrothermal liquefaction of various biomass and waste feedstocks for biocrude production: A state of the art review.* Renewable and Sustainable Energy Reviews, 2017. **68**: p. 113-125.
8. Duan, P., et al., *Activated carbons for the hydrothermal upgrading of crude duckweed bio-oil.* Catalysis Today, 2016. **274**: p. 73-81.
9. Castello, D., T.H. Pedersen, and L.A. Rosendahl, *Continuous Hydrothermal Liquefaction of Biomass: A Critical Review.* Thermochemical Biorefining, 2018. **11**(11): p. 3165.
10. Gao, Y., et al., *Effect of residence time on chemical and structural properties of hydrochar obtained by hydrothermal carbonization of water hyacinth.* Energy, 2013. **58**(Supplement C): p. 376-383.
11. Kumar, S., et al., *Hydrothermal pretreatment of switchgrass and corn stover for production of ethanol and carbon microspheres.* Biomass and Bioenergy, 2011. **35**(2): p. 956-968.
12. Goudriaan, F. and D.G.R. Peferoen, *Liquid fuels from biomass via a hydrothermal process.* Chemical Engineering Science, 1990. **45**(8): p. 2729-2734.
13. Brunner, G., *Near critical and supercritical water. Part I. Hydrolytic and hydrothermal processes.* The Journal of Supercritical Fluids, 2009. **47**(3): p. 373-381.
14. Tekin, K., S. Karagöz, and S. Bektaş, *A review of hydrothermal biomass processing.* Renewable and Sustainable Energy Reviews, 2014. **40**: p. 673-687.
15. Basar, I.A., et al., *A review on key design and operational parameters to optimize and develop hydrothermal liquefaction of biomass for biorefinery applications.* Green Chemistry, 2021. **23**(4): p. 1404-1446.
16. Funke, A. and F. Ziegler, *Hydrothermal carbonization of biomass: a summary and discussion of chemical mechanisms for process engineering.* Biofuels, Bioproducts and Biorefining, 2010. **4**(2): p. 160-177.
17. Mumme, J., et al., *Hydrothermal carbonization of anaerobically digested maize silage.* Bioresource Technology, 2011. **102**(19): p. 9255-9260.

18. He, C., et al., *Hydrothermal gasification of sewage sludge and model compounds for renewable hydrogen production: A review*. Renewable and Sustainable Energy Reviews, 2014. **39**(Supplement C): p. 1127-1142.
19. Peterson, A.A., et al., *Thermochemical biofuel production in hydrothermal media: a review of sub-and supercritical water technologies.* Energy & Environmental Science, 2008. **1**(1): p. 32-65.
20. Biller, P. and A. Ross, *Production of biofuels via hydrothermal conversion*, in *Handbook of biofuels production*. 2016, Woodhead Publishing. p. 509-547.
21. Fang, J., et al., *Minireview of potential applications of hydrochar derived from hydrothermal carbonization of biomass.* Journal of Industrial and Engineering Chemistry, 2018. **57**(Supplement C): p. 15-21.
22. He, C., A. Giannis, and J.-Y. Wang, *Conversion of sewage sludge to clean solid fuel using hydrothermal carbonization: Hydrochar fuel characteristics and combustion behavior.* Applied Energy, 2013. **111**(Supplement C): p. 257-266.
23. Kambo, H.S. and A. Dutta, *A comparative review of biochar and hydrochar in terms of production, physico-chemical properties and applications.* Renewable and Sustainable Energy Reviews, 2015. **45**(Supplement C): p. 359-378.
24. Kean, C.W., J.N. Sahu, and W.W. Daud, *Hydrothermal gasification of palm shell biomass for synthesis of hydrogen fuel.* BioResources, 2013. **8**(2): p. 1831-1840.
25. Matsumura, Y., *Chapter 9 - Hydrothermal Gasification of Biomass*, in *Recent Advances in Thermo-Chemical Conversion of Biomass*, A. Pandey, et al., Editors. 2015, Elsevier: Boston. p. 251-267.
26. Matsumura, Y., et al., *Biomass gasification in near- and super-critical water: Status and prospects.* Biomass and Bioenergy, 2005. **29**(4): p. 269-292.
27. Peterson, A.A., et al., *In situ visualization of the performance of a supercritical-water salt separator using neutron radiography.* The Journal of Supercritical Fluids, 2008. **43**(3): p. 490-499.
28. Matsumura, Y., et al., *Gasification rate of various biomass feedstocks in supercritical water.* Journal of the Japan Petroleum Institute, 2013. **56**(1): p. 1-10.
29. Elliott, D.C.J.B., Bioproducts and Biorefining, *Catalytic hydrothermal gasification of biomass.* 2008. **2**(3): p. 254-265.
30. Toor, S.S., *Modeling and Optimization of Catliq Liquid Bioful Process*. 2010: Department of Energy Technology, Aalborg University.
31. Akiya, N. and P.E. Savage, *Roles of water for chemical reactions in high-temperature water.* Chemical reviews, 2002. **102**(8): p. 2725-2750.
32. Kruse, A., A. Funke, and M.-M. Titirici, *Hydrothermal conversion of biomass to fuels and energetic materials.* Current Opinion in Chemical Biology, 2013. **17**(3): p. 515-521.
33. Shuping, Z., et al., *Production and characterization of bio-oil from hydrothermal liquefaction of microalgae Dunaliella tertiolecta cake.* Energy, 2010. **35**(12): p. 5406-5411.
34. Krammer, P. and H. Vogel, *Hydrolysis of esters in subcritical and supercritical water.* The Journal of Supercritical Fluids, 2000. **16**(3): p. 189-206.

35. Bröll, D., et al., *Chemistry in supercritical water.* Angewandte Chemie International Edition, 1999. **38**(20): p. 2998-3014.
36. Kruse, A. and E. Dinjus, *Hot compressed water as reaction medium and reactant: properties and synthesis reactions.* The Journal of supercritical fluids, 2007. **39**(3): p. 362-380.
37. Franck, E., *Thermophysical properties of supercritical fluids with special consideration of aqueous systems.* Fluid Phase Equilibria, 1983. **10**(2-3): p. 211-222.
38. Marshall, W.L. and E. Franck, *Ion product of water substance, 0–1000 C, 1–10,000 bars new international formulation and its background.* Journal of physical and chemical reference data, 1981. **10**(2): p. 295-304.
39. Heger, K., M. Uematsu, and E. Franck, *The static dielectric constant of water at high pressures and temperatures to 500 MPa and 550 C.* Berichte der Bunsengesellschaft für physikalische Chemie, 1980. **84**(8): p. 758-762.
40. Jin, F., *Application of hydrothermal reactions to biomass conversion*. 2014: Springer Science & Business Media.
41. Zein, M. and R. Winter, *Effect of temperature, pressure and lipid acyl chain length on the structure and phase behaviour of phospholipid–gramicidin bilayers.* Physical Chemistry Chemical Physics, 2000. **2**(20): p. 4545-4551.
42. Jae, J., et al., *Depolymerization of lignocellulosic biomass to fuel precursors: maximizing carbon efficiency by combining hydrolysis with pyrolysis.* Energy & Environmental Science, 2010. **3**(3): p. 358-365.
43. Jena, U., et al., *Oleaginous yeast platform for producing biofuels via co-solvent hydrothermal liquefaction.* Biotechnology for biofuels, 2015. **8**(1): p. 167.
44. Gollakota, A.R.K., N. Kishore, and S. Gu, *A review on hydrothermal liquefaction of biomass.* Renewable and Sustainable Energy Reviews, 2017.
45. Shah, Y.T., *Energy and fuel systems integration*. 2015: CRC Press.
46. Biller, P., et al., *Nutrient recycling of aqueous phase for microalgae cultivation from the hydrothermal liquefaction process.* Algal Research, 2012. **1**(1): p. 70-76.
47. Dimitriadis, A. and S. Bezergianni, *Hydrothermal liquefaction of various biomass and waste feedstocks for biocrude production: A state of the art review.* Renewable and Sustainable Energy Reviews, 2017. **68**(Part 1): p. 113-125.
48. Bensaid, S., R. Conti, and D. Fino, *Direct liquefaction of ligno-cellulosic residues for liquid fuel production.* Fuel, 2012. **94**: p. 324-332.
49. Bridgwater, A., D. Meier, and D. Radlein, *An overview of fast pyrolysis of biomass.* Organic geochemistry, 1999. **30**(12): p. 1479-1493.
50. Demirbaş, A., *Mechanisms of liquefaction and pyrolysis reactions of biomass.* Energy Conversion and Management, 2000. **41**(6): p. 633-646.
51. Xu, C. and J. Lancaster, *Conversion of secondary pulp/paper sludge powder to liquid oil products for energy recovery by direct liquefaction in hot-compressed water.* Water Research, 2008. **42**(6): p. 1571-1582.
52. Vassilev, S.V., et al., *An overview of the composition and application of biomass ash. Part 1. Phase–mineral and chemical composition and classification.* Fuel, 2013. **105**: p. 40-76.

53. Jenkins, B.M., et al., *Biomass combustion.* Thermochemical processing of biomass: conversion into fuels, chemicals and power, 2019: p. 49-83.
54. Tekin, K. and S.J.R.o.C.I. Karagöz, *Non-catalytic and catalytic hydrothermal liquefaction of biomass.* Research on Chemical Intermediates, 2013. **39**(2): p. 485-498.
55. Basu, P., *Chapter 2 - Biomass Characteristics*, in *Biomass Gasification and Pyrolysis*, P. Basu, Editor. 2010, Academic Press: Boston. p. 27-63.
56. Toor, S.S., et al., *Hydrothermal liquefaction of biomass*, in *Application of hydrothermal reactions to biomass conversion*. 2014, Springer. p. 189-217.
57. Klemm, D., et al., *Cellulose: fascinating biopolymer and sustainable raw material.* Angewandte chemie international edition, 2005. **44**(22): p. 3358-3393.
58. Delmer, D.P. and Y. Amor, *Cellulose biosynthesis.* The Plant Cell, 1995. **7**(7): p. 987.
59. Vassilev, S.V., et al., *An overview of the organic and inorganic phase composition of biomass.* Fuel, 2012. **94**: p. 1-33.
60. Bobleter, O., *Hydrothermal degradation of polymers derived from plants.* Progress in polymer science, 1994. **19**(5): p. 797-841.
61. Rowell, R.M., et al., *Cell wall chemistry.* Handbook of wood chemistry and wood composites, 2005. **2**.
62. Lu, F. and J. Ralph, *Chapter 6 - Lignin*, in *Cereal Straw as a Resource for Sustainable Biomaterials and Biofuels*, R.-C. Sun, Editor. 2010, Elsevier: Amsterdam. p. 169-207.
63. Khuwijitjaru, P., S. Adachi, and R. Matsuno, *Solubility of saturated fatty acids in water at elevated temperatures.* Bioscience, biotechnology, and biochemistry, 2002. **66**(8): p. 1723-1726.
64. Rogalinski, T., et al., *Hydrolysis kinetics of biopolymers in subcritical water.* The Journal of Supercritical Fluids, 2008. **46**(3): p. 335-341.
65. Wang, W., Y. Kuang, and N. Huang, *Study on the decomposition of factors affecting energy-related carbon emissions in Guangdong province, China.* Energies, 2011. **4**(12): p. 2249-2272.
66. Goswami, D.Y. and F. Kreith, *Handbook of energy efficiency and renewable energy*. 2007: Crc Press.
67. Hirel, B., et al., *Improving nitrogen use efficiency in crops for sustainable agriculture.* Sustainability, 2011. **3**(9): p. 1452-1485.
68. Robbins, M.P., et al., *New opportunities for the exploitation of energy crops by thermochemical conversion in Northern Europe and the UK.* Progress in Energy and Combustion Science, 2012. **38**(2): p. 138-155.
69. Pisupati, S.V. and A.H. Tchapda, *Thermochemical Processing of Biomass*, in *Advances in Bioprocess Technology*. 2015, Springer. p. 277-314.
70. Trimm, D.L.J.C.T., *Coke formation and minimisation during steam reforming reactions.* Catalysis Today, 1997. **37**(3): p. 233-238.
71. Kruse, A., A.J.I. Gawlik, and e.c. research, *Biomass conversion in water at 330− 410 C and 30− 50 MPa. Identification of key compounds for indicating different chemical reaction pathways.* Industrial & engineering chemistry research, 2003. **42**(2): p. 267-279.

72. Kruse, A. and E.J.T.J.o.S.F. Dinjus, *Hot compressed water as reaction medium and reactant: 2. Degradation reactions.* The Journal of Supercritical Fluids, 2007. **41**(3): p. 361-379.
73. Kumar, S. and R.B. Gupta, *Biocrude production from switchgrass using subcritical water.* Energy & Fuels, 2009. **23**(10): p. 5151-5159.
74. Yiin, C.L., et al., *Stabilization of Empty Fruit Bunch (EFB) derived Bio-oil using Antioxidants*, in *Computer Aided Chemical Engineering*, J.J. Klemeš, P.S. Varbanov, and P.Y. Liew, Editors. 2014, Elsevier. p. 223-228.
75. *Task 34: Direct Thermochemical Liquefaction*. [cited 2022 10 February]; Available from: https://task34.ieabioenergy.com/bio-crude/.
76. Huber, G.W., S. Iborra, and A.J.C.r. Corma, *Synthesis of transportation fuels from biomass: chemistry, catalysts, and engineering.* Chemical reviews, 2006. **106**(9): p. 4044-4098.
77. Brown, T.M., P. Duan, and P.E. Savage, *Hydrothermal liquefaction and gasification of Nannochloropsis sp.* Energy & Fuels, 2010. **24**(6): p. 3639-3646.
78. Xiu, S., et al., *Hydrothermal pyrolysis of swine manure to bio-oil: Effects of operating parameters on products yield and characterization of bio-oil.* Journal of Analytical and Applied Pyrolysis, 2010. **88**(1): p. 73-79.
79. Yin, S., et al., *Subcritical hydrothermal liquefaction of cattle manure to bio-oil: Effects of conversion parameters on bio-oil yield and characterization of bio-oil.* Bioresource Technology, 2010. **101**(10): p. 3657-3664.
80. Zhou, D., et al., *Hydrothermal liquefaction of macroalgae Enteromorpha prolifera to bio-oil.* Energy & Fuels, 2010. **24**(7): p. 4054-4061.
81. Biller, P. and A.B. Ross, *Potential yields and properties of oil from the hydrothermal liquefaction of microalgae with different biochemical content.* Bioresource Technology, 2011. **102**(1): p. 215-225.
82. Demirbas, M.F.J.A.e., *Biorefineries for biofuel upgrading: a critical review.* Applied energy, 2009. **86**: p. S151-S161.
83. Adjaye, J.D., R.K. Sharma, and N.N. Bakhshi, *Characterization and stability analysis of wood-derived bio-oil.* Fuel Processing Technology, 1992. **31**(3): p. 241-256.
84. Vardon, D.R., et al., *Chemical properties of biocrude oil from the hydrothermal liquefaction of Spirulina algae, swine manure, and digested anaerobic sludge.* Bioresource Technology, 2011. **102**(17): p. 8295-8303.
85. Toor, S.S., et al., *Hydrothermal liquefaction of Spirulina and Nannochloropsis salina under subcritical and supercritical water conditions.* Bioresource Technology, 2013. **131**(Supplement C): p. 413-419.
86. Lavanya, M., et al., *Hydrothermal liquefaction of freshwater and marine algal biomass: A novel approach to produce distillate fuel fractions through blending and co-processing of biocrude with petrocrude.* Bioresource Technology, 2016. **203**: p. 228-235.
87. López Barreiro, D., et al., *Hydrothermal liquefaction of microalgae: Effect on the product yields of the addition of an organic solvent to separate the aqueous phase and the biocrude oil.* Algal Research, 2015. **12**: p. 206-212.

88. Caporgno, M.P., et al., *Hydrothermal liquefaction of Nannochloropsis oceanica in different solvents.* Bioresource Technology, 2016. **214**: p. 404-410.
89. Neveux, N., et al., *Biocrude yield and productivity from the hydrothermal liquefaction of marine and freshwater green macroalgae.* Bioresource Technology, 2014. **155**: p. 334-341.
90. Pedersen, T.H., et al., *Continuous hydrothermal co-liquefaction of aspen wood and glycerol with water phase recirculation.* Applied Energy, 2016. **162**: p. 1034-1041.
91. Vardon, D.R., et al., *Thermochemical conversion of raw and defatted algal biomass via hydrothermal liquefaction and slow pyrolysis.* Bioresource Technology, 2012. **109**: p. 178-187.
92. He, Y., et al., *Continuous hydrothermal liquefaction of macroalgae in the presence of organic co-solvents.* Algal Research, 2016. **17**: p. 185-195.
93. Yang, L., et al., *Hydrothermal liquefaction of spent coffee grounds in water medium for bio-oil production.* Biomass and Bioenergy, 2016. **86**: p. 191-198.
94. Cao, L., et al., *Bio-oil production from eight selected green landscaping wastes through hydrothermal liquefaction.* 2016. **6**(18): p. 15260-15270.
95. Chen, W.-T., et al., *Hydrothermal liquefaction of mixed-culture algal biomass from wastewater treatment system into bio-crude oil.* Bioresource Technology, 2014. **152**: p. 130-139.
96. Valdez, P.J., et al., *Hydrothermal liquefaction of Nannochloropsis sp.: Systematic study of process variables and analysis of the product fractions.* Biomass and Bioenergy, 2012. **46**(Supplement C): p. 317-331.
97. Raikova, S., et al., *Assessing hydrothermal liquefaction for the production of bio-oil and enhanced metal recovery from microalgae cultivated on acid mine drainage.* Fuel Processing Technology, 2016. **142**: p. 219-227.
98. Huang, Y., et al., *Bio-oil production from hydrothermal liquefaction of high-protein high-ash microalgae including wild Cyanobacteria sp. and cultivated Bacillariophyta sp.* Fuel, 2016. **183**: p. 9-19.
99. Bach, Q.-V., et al., *Fast hydrothermal liquefaction of a Norwegian macro-alga: Screening tests.* Algal Research, 2014. **6**: p. 271-276.
100. Anastasakis, K. and A.B. Ross, *Hydrothermal liquefaction of four brown macro-algae commonly found on the UK coasts: An energetic analysis of the process and comparison with bio-chemical conversion methods.* Fuel, 2015. **139**: p. 546-553.
101. Guo, Y., et al., *A review of bio-oil production from hydrothermal liquefaction of algae.* Renewable and Sustainable Energy Reviews, 2015. **48**: p. 776-790.
102. Nautiyal, P., K.A. Subramanian, and M.G. Dastidar, *Production and characterization of biodiesel from algae.* Fuel Processing Technology, 2014. **120**: p. 79-88.
103. Díaz-Rey, M., et al., *Hydrogen-rich gas production from algae-biomass by low temperature catalytic gasification.* Catalysis Today, 2015. **257**: p. 177-184.
104. Trivedi, N., et al., *Enzymatic hydrolysis and production of bioethanol from common macrophytic green alga Ulva fasciata Delile.* Bioresource Technology, 2013. **150**: p. 106-112.

105. Louw, J., C.E. Schwarz, and A.J. Burger, *Supercritical water gasification of Eucalyptus grandis and related pyrolysis char: Effect of feedstock composition.* Bioresource Technology, 2016. **216**: p. 1030-1039.
106. Minowa, T., et al., *Oil production from algal cells of Dunaliella tertiolecta by direct thermochemical liquefaction.* Fuel, 1995. **74**(12): p. 1735-1738.
107. Ross, A.B., et al., *Classification of macroalgae as fuel and its thermochemical behaviour*. Bioresource Technology, 2008. **99**(14): p. 6494-6504.
108. Wagner, J., et al., *Co-production of bio-oil and propylene through the hydrothermal liquefaction of polyhydroxybutyrate producing cyanobacteria.* Bioresource Technology, 2016. **207**: p. 166-174.
109. Phukan, M.M., et al., *Microalgae Chlorella as a potential bio-energy feedstock.* Applied Energy, 2011. **88**(10): p. 3307-3312.
110. Yang, W., et al., *Direct hydrothermal liquefaction of undried macroalgae Enteromorpha prolifera using acid catalysts.* Energy Conversion and Management, 2014. **87**: p. 938-945.
111. Aysu, T. and H. Durak, *Thermochemical conversion of Datura stramonium L. by supercritical liquefaction and pyrolysis processes.* The Journal of Supercritical Fluids, 2015. **102**: p. 98-114.
112. Aysu, T., et al., *Evaluation of Eremurus spectabilis for production of bio-oils with supercritical solvents.* Process Safety and Environmental Protection, 2015. **94**: p. 339-349.
113. Watson, J., et al., *Effects of the extraction solvents in hydrothermal liquefaction processes: Biocrude oil quality and energy conversion efficiency.* Energy, 2019. **167**: p. 189-197.
114. Yan, W.-H., et al., *Composition of the bio-oil from the hydrothermal liquefaction of duckweed and the influence of the extraction solvents.* Fuel, 2016. **185**: p. 229-235.
115. Singh, A.S., M.B.J.I.J.o.e. Masuku, commerce, and management, *Sampling techniques & determination of sample size in applied statistics research: An overview*. 2014. **2**(11): p. 1-22.